ICRAA'4

4th International Conference on Radiations And Applications

Algiers, 13-15, April 2025

https://icraa-dz.com

BOOK OF ABSTRACTS

The Fourth International Conference on Radiation And Application

ICRAA'4

https://icraa-dz.com

April 13-15, 2025

Jointly Organized by

*The University of Sciences and Technologies Houari-Boumediene - **USTHB***
and
*The Algerian Atomic Energy Commission - **COMENA***

Sponsored by

Table of Contents

Conference topics

Topic 1: Radiation Matter Interaction

- Nuclear reaction
- Nuclear structure
- Nuclear astrophysics
- Atomic spectroscopy
- Ion surface interaction

Topic 2: Nuclear Techniques and Detection

- Ion beam analysis
- Characterization of materials
- Detectors and data analysis
- Novel detectors and materials

Topic 3: Radiological and Medical Physics

- Radiation dosimetry
- Radiology & imaging with ionizing radiation
- Radiation oncology physics, radiotherapy, radiopharmaceuticals and nuclear medicine
- Radiobiology and radiation protection of patients and workers
- Computational codes, machine learning and artificial intelligence in medical physics
- Beam standardization in medical physics
- Ionizing radiation metrology in medical physics

Topic 4: Nuclear Reactor Physics

- Neutronic and core analysis
- Nuclear reactor safety analysis
- Multi-physics reactor modeling and simulation
- Research reactors utilization
- SMRs and new trends in nuclear reactors technology

Topic 5: Radiation in Industry, Life and Environment

- Radioisotope and radiotracers
- Irradiation of Materials
- Nanotechnology and Material Modification
- Natural radioactivity
- Radiations for resources prospection

Organizing committee

- **Mohamed BELGAID,** FP, USTHB, Chairman
- **Layachi BOUKERDJA**, CRNB, COMENA, Deputy Chairman
- **Nassima ADIMI**, FP, USTHB, Scientific Secretary
- **Tarek AZLI**, CRND, COMENA, Member
- **Salah-Eddine BENTRIDI**, FST, Khemis-Miliana University, Member
- **Boualem BOUZID**, FP, USTHB, Member
- **Azzedine CHAFA**, FP, USTHB, Member
- **Said DJAROUM**, CRNB, COMENA, Member
- **Mohamed Reda OUDIH**, FP, USTHB, Member
- **Djamel TAIEBERRAHMANI**, CRNA, COMENA, Member
- **Said TERNICHE**, FP, USTHB, Member

Scientific committee

- **ADIMI Nassima**, FP-USTHB, ALGERIA.
- **AIT ABDERRAHIM Hamid**, MYRRHA, Brussels, BELGIUM.
- **ALGORA Alejandro**, IFIC, UV, SPAIN.
- **ALLAL H. Nassima**, FP-USTHB, ALGERIA.
- **AMRANI Naima**, Université Ferhat Abbas, ALGERIA.
- **ARIB Mehenna**, King Faisal Specialist Hospital and Research Centre, KSA.
- **ATTALLAH Réda**, Univ. de Annaba, ALGERIA.
- **AYDIN Abdullah**, KIRIKKALE-UNIV., TURKEY.
- **AZBOUCHE Ahmed**, CRNA-COMENA, ALGERIA.
- **AZLI Tarik**, CRND-COMENA, ALGERIA.
- **BELGAID Mohamed**, FP-USTHB, ALGERIA.
- **BENCHOUK CHAFIK**, FP-USTHB, ALGERIA.
- **BENKHARFIA Hocine**, CRNB-COMENA, ALGERIA.
- **BENRACHI FATIMA**, UMC1, Constantine, ALGERIA.
- **BENTRIDI Salah-Eddine**, LESI, KHEMIS MILIANA-UNIV., ALGERIA.
- **BLANK BERTRAM**, LP2I, Bordeaux, FRANCE.
- **BORGE J. Maria**, IEM, CSIC, SPAIN.
- **BOUCHAREB Yassine**, COM & HS, SQU, OMAN.
- **BOUKERDJA Layachi**, CRNB-COMENA, ALGERIA.
- **BOUKHENFOUF Wassila** , Université Ferhat Abbas, Setif, ALGERIA.
- **BOULDJEDRI Abdelhamid**, BATNA-UNIV., ALGERIA.
- **BOUSBIA-SALAH Anis**, BEL-V, BELGIUM.
- **BOUYOUCEF Salaheddine**, CHU de Bab El Oued, ALGERIA.
- **BOUZID Boualem**, FP-USTHB, ALGERIA.
- **CHAFA Azeddine**, FP-USTHB, ALGERIA.
- **CLOETE Karen J**, University of South Africa, SOUTH AFRICA.
- **DIAZ José**, IFIC, University of Valencia, SPAIN.
- **DJAROUM Saïd**, CRNB-COMENA, ALGERIA.
- **DJOUIDER Fathi**, King Abdelaziz-Univ, KSA.
- **DOKHANE Abdelhamid**, Paul Scherrer institute, SWITZERLAND.
- **GALL Benoit**, IPHC, FRANCE.
- **GUERBOUS Lakhdar**, CRNA-COMENA, ALGERIA.
- **GUITTOUM Abderrahim**, CRNA-COMENA, ALGERIA.
- **HAMIDATOU Lylia**, CRNB-COMENA, ALGERIA.
- **HAMIDOUCHE Tewfik**, SCK/MOL, BELGIUM.
- **HIDAKA Hiroshi**, Nagoya-Univ., JAPAN.
- **HOCINE Nora**, Institut de Radioprotection et de Sûreté Nucléaire (IRSN), FRANCE.
- **IZERROUKEN Mahmoud**, CRND-COMENA, ALGERIA.
- **KHARFI Fayçal**, Université Ferhat Abbas, ALGERIA.
- **KHELASSI-TOUTAOUI Nadia**, CRNA-COMENA, ALGERIA.
- **KURTUKİAN Teresa**, CENBG, FRANCE.
- **LOUNIS-MOKRANI Zohra**, CRNA-COMENA, ALGERIA.
- **MAMMERI Ster**, CRNA-COMENA, ALGERIA.
- **MAZROU Hakim**, CRNA-COMENA, ALGERIA.
- **MENEZES M. Angela**, CDTN, CNEN., BRAZIL.

- **MOUSSAOUI Noureddine**, FP-USTHB, ALGERIA.
- **MSIMANGA Mandla**, Ithemba-Labs., SOUTH AFRICA.
- **NAOUN Lilia**, Service de Radiothérapie - CHU Annaba, ALGERIA.
- **OUDIH Mohamed Reda**, FP-USTHB, ALGERIA.
- **OUICHAOUI Saad**, FP-USTHB, ALGERIA.
- **PAGE Robert**, University of Liverpool, UNITED KINGDOM.
- **PASCHALIDIS Ioannis**, University of Cyprus, CYPRUS.
- **PIETRI Stephane**, GSI, GERMANY.
- **QUERAL César**, UTM, SPAIN.
- **REGAN Patrick Henry**, UNIV. SURREY & NPL, UNITED KINGDOM.
- **SANCHEZ ESPINOZA Victor Hugo**, KARLSRUHE Institute Of Technology, GERMANY.
- **SARPUN Ismail**, ANTALYA-UNIV., TURKEY.
- **SAVERIO Altieri**, University of Pavia , ITALY.
- **SEGHOUR Abdeslam**, CRNA-COMENA, ALGERIA.
- **SERKAN Akkoyun**, Univ. Syvas, TURKEY.
- **SIDI ALI Kamel**, CRND-COMENA, ALGERIA.
- **SOUGA Chedly**, ENAU/ Carthage University, TUNISIA.
- **SOUIDI Maamar**, IRSN, FRANCE.
- **TAIEB ERRAHMANI Djamel**, CRNA-COMENA, ALGERIA.
- **TALAI Med Cherif**, Univ. de Annaba, ALGERIA.
- **TASKAEV Sergey**, Budker Institute of Nuclear Physics, RUSSIA.
- **THOMAS Jean Charles**, GANIL, FRANCE.
- **TOUTAOUI Abdelkader**, HCM, Tizi-Ouzou, ALGERIA.
- **WALRAND Stephan**, Clinique Universitaire Saint Luc, BELGIUM.
- **YAHLALI Nadia**, IFIC, UV, SPAIN.
- **YLLI Fatos**, Institute of Applied Nuclear Physics, University of Tirana, ALBANIA.
- **ZAIDI Habib**, GENEVA UNIV., SWITZERLAND.
- **ZENNINE NADJAH**, CRNA-COMENA, ALGERIA.
- **ZIDI Tahar**, COMENA, ALGERIA.

PLENARY TALKS

PL1: Quantitative Molecular Imaging in the Era of Precision Medicine

Habib Zaidi, Fieee, Faimbe, Faapm, Fiomp, Faaia, Fbir [1,2,3,4]

[1]*Division of Nuclear Medicine and Molecular Imaging, Geneva University Hospital, Switzerland*

[2]*Department of Nuclear Medicine and Molecular Imaging, University of Groningen, The Netherlands*

[3]*Department of Nuclear Medicine, University of Southern Denmark, Odense, Denmark*

[4]*University Research and Innovation Center, Óbuda University, Budapest, Hungary*

Email: habib.zaidi@hug.ch

Web: http://www.pinlab.ch/

Early diagnosis and therapy increasingly operate at the cellular, molecular or even at the genetic level. As diagnostic techniques transition from the systems to the molecular level, the role of multimodality molecular imaging becomes increasingly important. Positron emission tomography (PET), x-ray computed tomography (CT) and magnetic resonance imaging (MRI) and their combinations (PET/CT and PET/MRI) provide powerful multimodality techniques for *in vivo* imaging. Quantitative image analysis has deep roots in the usage of molecular imaging in clinical and research settings to address a wide variety of diseases. It has been extensively employed to assess molecular and physiological biomarkers *in vivo* in healthy and disease states, in oncology, cardiology, neurology, and psychiatry. This talk reflects the tremendous increase in multimodality molecular imaging as both clinical and research imaging modalities in the past decade. An overview of advanced medial image instrumentation technologies and PET image quantification and related image processing issues with special emphasis on radiomics analysis will be presented. This talk aims to bring the medical physics community a review on the state-of-the-art algorithms used and under development for accurate quantitative analysis in multimodality and multiparametric molecular imaging and their validation mainly from the developer's perspective. It will inform the audience about a series of advanced development carried out recently at the PET instrumentation & Neuroimaging Lab of Geneva University Hospital and other active research groups. Current and prospective future applications of quantitative molecular imaging are also addressed especially its use prior to therapy for dose distribution modeling and optimization of treatment volumes in external radiation therapy and patient-specific 3D dosimetry in targeted therapy towards the concept of image-guided radiation therapy. In this regard, the promising role of artificial intelligence (AI), in particular deep learning approaches, will be emphasized. To this end, example applications of deep learning in five generic fields of multimodality medical image analysis, including imaging instrumentation design, image denoising (low-dose imaging), image reconstruction quantification and segmentation, radiation dosimetry and computer-aided diagnosis and outcome prediction will be discussed. Future opportunities and the challenges facing the adoption of quantitative imaging biomarkers in the clinic and their role in basic research will also be addressed.

PL2: KIT Multi-physics/-scale Methods and Tools for Advanced Core Analysis of LWR and Water-cooled SMRs

Victor Hugo Sanchez-Espinoza

Institute of Neutron Physics and Reactor technology (INR), Karlsruhe Institute of Technology (KLIT) Hermann-vom-Helmholtz-Platz-1, 76344 Eggenstein-Leopoldshafen, Germany

victor.sanchez@kit.edu

The deployment of nuclear power plants worldwide is advancing for the CO_2-free to provide electricity and heat, etc. Among the most reactor designs being built are the VVER-1200, APR-1400, AP-1000, and EPR. In addition, the deployment of Small Modular Reactors (SMR), and in special water-cooled SMRs have experienced a considerable progress [1]. Among the nine SRM-design selected by the European Industrial Partnership for the deployment of SMRs, five concepts are water-cooled SMRs. European designs such as the NUWARD and the LDR-50 are in the advanced design phase. Both designs rely on boron-free cores built of shorter standard Fuel Assemblies (FA) of type FA 17x17-25. The Roll Royce SMR will be built in Czech Republic. NuScale and SMART use the same FA-design but they consider boron in the coolant. In general, SMRs are designed for electricity generation, water desalination, industrial heat production, hydrogen production, etc. The BWR-X-300 is going to be built in Canada, Poland, and Sweden. It works without pumps based on natural convection as the larger ESBWR unit. The CAREM, ACP-100 and the RITM-200N are under construction in Argentina, China, and Russia. In Canada, the BWR-X-300 was selected for new-build and demonstration by 2028. In the EU, different research projects such as ELSMOR [2], McSAFER [3], are focused on the licensing, experiments for thermal-hydraulic phenomena (cross-flow, performance of helical heat exchanger, CHF), and safety evaluation methods for the core and plant behaviour and on advanced Multiphysics analysis of core transients including diffusion, transport and Monte Carlo methods coupled with thermal hydraulic solvers.

KIT is involved in McSAFER and in German SMR-projects with focus on the development of new core analysis tools (neutronics and thermal hydraulics) as well as multi-physics and -scale methods for the improved analysis of core and plant transients [4]. This lecture will describe the KIT computational chains under development and validation for large reactors and SMRs. It will start with the discussion of the challenges for reactor physics and thermal hydraulics. Then, the different tools will be shortly described including the coupling approaches. Finally, selected applications to large PWR and water- cooled SMRs will be presented. An outlook about further development directions ends the presentation.

References:

[1] OECD, "Small Modular Reactors: Challenges and Opportunities. NEA Nr. 7560," OECD, Paris, 2021.

[2] ELSMOR, "Towards European Licencing of Small Modular Reactors," EU, 1 September 2019. [Online] Available: https://cordis.europa.eu/project/id/847553/reporting/fr. [Accessed 25 Mai 2022].

[3] V. H. Sanchez-Espinoza, S. Gabriel, H. Suikkanen, J. Telkkä, V. Valtavirta, M. Bencik, S. Kliem, C. Queral, A. Farda, F. Abéguilé, P. Smith, P. V. Uffelen, L. Ammirabile, M. Seidl, C. Schneidesch, D. Grishchenko and H. Lestani, "The H2020 McSAFER Project: Main Goals, Technical Work, Program, and Status," *Energies,* vol. 6348, p. 14, 2021.

[4] V. H. Sanchez-Espinoza, U. Imke, K. Zhang, J. Duran-Gonzalez, A. Campos-Muñoz and G. Huaccho-Zavala, "KIT Numerical Simulation Tools for the Transient Analysis of Water-Cooled Small Modular Reactors," in *ICAPP 2024*, Las Vegas, 2024

PL3: Exploring the limits of observable nuclei

Robert Page

University of Liverpool

A long-standing question in nuclear physics is where are the limits of nuclear existence? On earth there are around 300 nuclear species that occur naturally, many of which are stable, but a few undergo alpha decay, beta decay or spontaneous fission.

Much of our knowledge of the strong force that binds atomic nuclei is based on measurements of these nuclides and their neighbours. Over many years, this understanding has been tested and refined by extending experimental studies to nuclides away from the valley of beta stability, where other decay modes including beta-delayed particle emission and the spontaneous emission of nucleons become important. Around 3300 nuclides have been studied to date, with many more being discovered every year. Their properties can be of interest beyond pure nuclear physics because of applications in medicine and nuclear-related sectors, as well as the ramifications for the synthesis of heavy elements in various astrophysical scenarios that involve nuclear reactions of unstable species. In this talk I will review recent progress in extending the boundaries of our knowledge of nuclear properties and exploring the limits of observable nuclei.

PL4: Applications within particle accelerators

Sergey Taskaev

Budker Institute of Nuclear Physics, , RUSSIA

Particle accelerators are used for fundamental scientific research aimed at expanding our understanding of matter, for a variety of socio-economic applications related to human health, environmental monitoring, food quality, energy and aerospace technologies, and other areas. We will consider applications of a particle accelerator using the example of accelerator VITA developed at BINP (Russia). This accelerator is an electrostatic tandem accelerator of charged particles of an original to produce beam of protons or deuterons with energy up to 2.3 MeV and with current up to 10 mA.

This accelerator is actively used for the development of boron neutron capture therapy (BNCT), including the development of methods and instruments of dosimetry, testing of new boron delivery drugs, and treatment of domestic animals. The second neutron source was made for the treatment of patients in clinic in Xiamen (China) and China became the second country in the world to begin treating patients with BNCT. The third neutron source made for Oncology Center in Moscow to begin clinical trials in Russia from 2025. The fourth neutron source is currently being developed for Biological Center in Moscow.

The facility VITA in BINP produces powerful neutron fluxes of various energy ranges (from cold to fast), and powerful fluxes of monoenergetic α-particles and photons. For this purpose, a thin lithium target and a number of beam shaping assemblies are used. The facility is used for applications such as radiation testing of promising materials, including for ITER and CERN, measurement of the cross-section of nuclear reactions, development of lithium-neutron capture therapy; creation of quantum dots in crystals, determination of elemental composition of thin films, study of the luminescence of substances under the influence of neutrons; seed modifications; neutron diffraction, etc.

The report describes the created facilities, presents the results of the conducted research and declares plans.

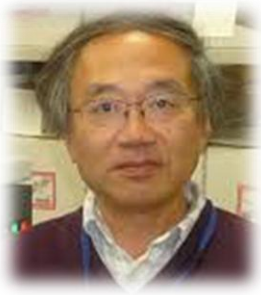

PL5: Isotopic variations of solar planetary materials caused by neutron capture reactions in space

Hiroshi Hidaka

Nagoya University, Japan
hidaka@eps.nagoya-u.ac.jp

The surficial parts of solar planetary materials without the atmospheric layers have been exposed to cosmic rays consisting mainly of high-energy protons, and have occurred nuclear reactions such as spallation and neutron-capture by the interactions of cosmic-ray irradiation. Then, the accumulation of thus nuclear reactions produces the variations of isotopic compositions of several elements. Here in this talk, I would like to introduce my recent topics about the isotopic work to characterize the extraterrestrial materials from the cosmic-ray irradiation conditions.

The samples used in this study were lunar surface materials returned by the Apollo mission [1,2]. The samples weighting about 40-50 mg were digested by acid and made solutions. Rare earth elements (REEs) and Hf in each solution were chemically separated by conventional resin chemistry [3]. The isotopic compositions of these elements were measured by mass spectrometric techniques.

Our recent techniques make possible to collect most isotopic data within 0.01 % of analytical precisions. In particular, the detection of depletion degrees of ^{168}Yb caused by ^{168}Yb(n,$\gamma\beta^{+}$)^{169}Tm using a sensitive amplifier board connected with Faraday cup detector [3].

^{149}Sm, ^{155}Gd and ^{157}Gd react sensitively with thermal neutrons (E<0.1 eV) rather than epithermal neutrons (0.1 eV <E< 0.5 MeV), whereas ^{167}Er, ^{168}Yb, ^{177}Hf and ^{178}Hf react with thermal as well as epi-thermal neutrons because of their large principal resonance peaks in the epi-thermal energy regions. Systematic isotopic analyses of Sm, Gd, Er, Yb and Hf collected from a single material can be practically used to reconstruct neutron energy spectra in a wide energy range from thermal to epithermal regions.

References:

[1]. Hidaka H., Ebihara M. and Yoneda S. Neutron capture effects on Sm, Eu and Gd in Apollo 15 deep drill core samples. *Meteoritics & Planetary Science*. 2000;35:5581-589. doi:10.1111/j.1945- 5100.2000.tb01438x

[2]. Hidaka H. and Yoneda S. Sm and Gd isotopic shifts of the Apollo 16 and 17 drill stem samples and their implication for regolith history. *Geochimica et Cosmochimica Acta*. 2007;71:1074-1086. doi:10.1016/j.gca.2006.10.015

[3]. Hidaka H. Isotopic variations of Sm, Gd, Er and Yb found in planetary materials caused by neutron capture reactions in nature. *Journal of Analytical Science and Technology*. 2024;15:14(10pp). doi:10.1186/s40543-024-00424-6

ORAL SESSIONS

T1-O1: Deep learning algorithms to predict the production cross sections of bromine-77 radionuclide

A. Aydin[1], R.G Türeci[2], I.H. Sarpün[3,4,5], H. Özdoğan[6]

[1]Kırıkkale University, Department of Physics, Kırıkkale, Türkiye [2]Kırıkkale University, Kırıkkale Vocational School, Kırıkkale, Türkiye [3]Akdeniz University, Physics Department, Antalya, Türkiye [4]Akdeniz University, Faculty of Medicine, Radiation Oncology, Antalya,Türkiye [5]Akdeniz University, Nuclear Research and Application Centre, Antalya,Türkiye [6]Antalya Bilim University, Vocational School of Health Services, Department of Medical Imaging Techniques, Antalya, Türkiye

Background/Purpose: Bromine-77 has a half-life of 56 h and decays nearly exclusively (99.3%) by electron capture, with prominent gamma rays at 239.0 and 520.7 keV. Once considered primarily for SPECT imaging, this nuclide is now increasingly being evaluated for its potential in Auger electron therapy. In this study, deep learning algorithms with Python programming language are improved to predict the production cross sections of bromine-77 radionuclide.

Material & Method: Experimental cross sections data used in artificial neural network (ANN) were taken from the EXFOR nuclear reactions database. These data were used to train an artificial neural network (ANN) implemented in Python with deep learning techniques. The deep learning results obtained for the 77Se(p,n)77Br, 78Se(p,2n)77Br, 80Se(p,4n)77Br and 75As(□,2n)77Br reactions were compared with the calculation results obtained from the TALYS code.

Results: The deep learning model provided highly accurate predictions of cross-section values for the studied reactions. Compared to the theoretical results obtained from TALYS, the ANN predictions exhibited a significantly better agreement with the experimental data. The results indicate that deep learning-based models can effectively capture complex nuclear reaction mechanisms and provide reliable cross-section estimations.

Conclusion: The neural network was optimized to enhance prediction accuracy, and its outputs were compared with theoretical cross-section calculations obtained from the TALYS nuclear reaction code. The performance of the ANN model was evaluated based on its agreement with experimental data and its generalization capability for predicting unknown cross-section values. These findings highlight the potential of machine learning in nuclear physics applications, particularly for cases where experimental data are scarce or unavailable.

T1-O2: Investigation of Crater Formation Induced by Gold Cluster Ions: Experimental and Theoretical Approaches

S. Gouasmia Boussahoul[1,2*], F. Boussahoul[1], M. Benguerba[2], S. Della Negra[3], D. Jacquet[3], I. Ribaud[3].

[1] *Laboratory for Ion Beam Interactions, Division of Experimental Physics, Ruđer Bošković Institute, Bijenička 54, 10000 Zagreb, Croatia.*

[2] *U.S.T.H.B University, Faculty of Physics, BP 32, Bab-Ezzouar, Algiers 16111, Algeria.*

[3] *CNRS/IN2P3, IJCLab, Universite Paris-Saclay, 91405 Orsay, France.*

Corresponding Author: gouasmia@irb.hr

Background/Purpose: The impact of energetic particle clusters on solid surfaces is of significant interest due to its effects on surface erosion (sputtering, crater formation), implantation, and material modifications. Crater formation, in particular, plays a crucial role in applications such as space science, surface analysis, and material engineering. This study aims to validate a theoretical model by experimentally investigating crater formation induced by gold cluster impacts (1.5 and 3 MV) at the Andromede facility (IJCLab, Orsay, France).

Materials & Methods: To analyze the effects of high-velocity gold cluster impacts (Au_n, Gold films of 4 nm, 20 nm, and 40 nm thicknesses were irradiated by gold clusters (Aun, n = 150, 400, 700). Atomic Force Microscopy (AFM, NX20 Park System) was employed to analyze surface modifications. The study specifically focused on two types of craters: simple and complex (with centrally or laterally positioned hillocks).

Results: AFM analysis revealed that crater formation is strongly influenced by cluster size and impact energy. Larger clusters and higher impact energies led to more pronounced crater structures. The experimental data show excellent agreement with theoretical predictions, supporting the role of shock waves in crater formation.

Conclusion: This study provides experimental validation of theoretical models concerning crater formation due to high-velocity cluster impacts. The results offer valuable insights into shock wave dynamics in material erosion and have potential applications in space research, nanotechnology, and surface modification techniques. Future work will explore different materials and impact conditions.

References

[1]. S. Gouasmia, M. Benguerba, Nucl. Inst. Meth. Phys. Res. B 447 (2019) 43–49. doi.org/10.1016/j.nimb.2019.03.025

[2] . Thanh Loan Lai, Dominique Jacquet, Isabelle Ribaud, Michael John Eller, Dmitriy Verkhoturov, Emile Albert Schweikert, Luiz Henrique Galvão Tizei, Fuhui Shao, Suheyla Bilgen, Bruno Mercier, Gael Sattonnay, and Serge Della Negra, J. Vac. Sci. Technol. B 38, 044008 (2020); doi.org/10.1116/6.0000173

Keywords: **Cluster ion, Crater, High-velocity cluster impact, Theoretical approach, Shock wave**

T1-O3: Spectral Line Shape Broadening under Oscillating Electric and static Magnetic Fields

I. Hannachi[a@], R. Stamm[b]

[a]*University of Batna 1, PRIMALAB, Department of Physics, Batna, Algeria*
[b]*Aix-Marseille Univ. and CNRS, PIIM, 13397 Marseille, France*
[@]*Corresponding author ibtissam.hannachi@univ-batna.dz*

Background/Purpose: In plasma environments, atoms and ions frequently interact with oscillating electric fields, leading to alterations in the shapes of emitted spectral lines. This phenomenon is particularly prevalent in non-equilibrium plasmas, where ion sound and Langmuir waves are commonly observed. Understanding these interactions is crucial for advancing our knowledge of wave-plasma dynamics [1], especially in contexts such as laboratory experiments and magnetic fusion devices that utilize radio frequency (RF) waves for heating and current drive.

Materials & Methods: This research employs computer simulations to investigate the effects of particle microfields and simultaneous periodic electric fields on spectral line shapes [2]. By numerically solving the Schrödinger equation for a hydrogen emitter, we aim to capture the intricate dynamics of these interactions. The study builds on a long history of oscillating electric field research, which has produced numerous models to explain variations in line shapes, often focusing on a monochromatic, linearly polarized wave represented by $E_w cos(\omega t + \phi)$, where ϕ denotes a random phase.

Results: Our simulations reveal significant insights into how the magnitude of the wave E_w and its frequency ω influence spectral line shapes. We will summarize recent comparisons from various research groups regarding hydrogen lines in a periodic electric field [3], highlighting the consistency and discrepancies observed across different simulations.

Conclusion: The findings from this study underscore the importance of computer simulations in understanding the complex interactions between oscillating electric fields and plasma particles. These insights can be applied to various laboratory and fusion plasma settings, enhancing our comprehension of wave-plasma interactions and their implications for future research in the field.

References:

[1]. Klepper C et al.. Dynamic Stark Spectroscopic Measurements of Microwave Electric Fields Inside the plasma Near a High-Power Antenna. *Phys. Rev. Lett.*. 2013;110:215005. doi:10.1103/PhysRevLett.110.215005

[2]. Baranger M and Mozer B.. Light as a Plasma Probe. Phys. Rev.. 1961;123:25. doi: 10.1103/PhysRev.123.25

[3]. Hannachi I., Alexiou S. and Stamm R..Line Shape Comparison of the Effect of Periodic Field on Hydrogen Lines. atoms. 2024;12:5-19. doi: 10.3390/atoms12040019

Keywords: **Stark broadening; oscillating electric field; Spectral line shape.**

T1-O4: Simulating Atmospheric Neutrino Oscillations for Neutrino Mass Hierarchy Discovery

M. Fouka [1@], S. Slimateni[1,2]

[1] *Centre de Recherche en Astronomie, Astrophysique et Géophysique, Observatoire de Bouzaréah, Alger, Algérie*
[2] *Faculté de Physique, Université des Sciences et Technologies Houari Boumediene, Alger, Algérie*
[@] *Corresponding author m.fouka@craag.dz*

Background/Purpose: Neutrino oscillations, confirmed by experiments like Super-Kamiokande [1], are described by the three-flavor standard model. In this model, neutrinos oscillate between flavors via the PMNS matrix [2]. However, the neutrino mass hierarchy and CP-violating phase remain unresolved at 5σ confidence. This study evaluates underwater detectors, such as KM3NeT and IceCube/DeepCore, to determine the mass hierarchy using simulated atmospheric neutrino data.

Materials & Methods: We developed a C++ particle transport code incorporating neutrino oscillation with the MSW effect [3]. Atmospheric neutrinos, produced from pion and kaon decays, are propagated through the Earth and simulated for both normal (NH) and inverted (IH) hierarchies.

Results: Simulations show the energy range E ~ 3–10 GeV is optimal for distinguishing the mass hierarchy, with sufficient event statistics for robust analysis.

Conclusion: Our findings align with KM3NeT collaboration tools. Further details will be shared in our upcoming contribution.

References:

[1]. Y. Fukuda et al. (Super-Kamiokande Collaboration), Evidence for Oscillation of Atmospheric Neutrinos, Physical Review Letters, Vol. 81, No. 8, pp. 1562-1567, 1998. doi: 10.1103/PhysRevLett.81.1562.

[2]. Z. Maki, M. Nakagawa, and S. Sakata, Remarks on the Unified Model of Elementary Particles, *Progress of Theoretical Physics*, Vol. 28, No. 5, pp. 870–880, 1962. doi: 10.1143/PTP.28.870.

[3]. L. Wolfenstein, Neutrino Oscillations in Matter, Physical Review D, Vol. 17, No. 9, pp. 2369–2374, 1978. doi: 10.1103/PhysRevD.17.2369.

Keywords: **Atmospheric Neutrino Oscillation, PMNS mixing Matrix, KM3NeT, Mass Hierarchy, MSW Matter Effect**

T1-O5: Single Folding Potential Calculations in 127I

I.H. Sarpün[1,2,3], F. Akdeniz[1] , A. Aydın[4]

[1]Akdeniz University, Physics Department, Antalya Turkiye
[2]Akdeniz University, Faculty of Medicine, Radiation Oncology, Antalya Turkiye
[3]Akdeniz University, Nuclear Research and Application Centre, Antalya Turkiye
[4]Kirikkale Uni., Fac. of Eng. and Nat. Sci, Dept. of Physics, Kirikkale, Turkiye

Background/Purpose: In this study, an optical model based elastic scattering (n,el) was investigated in which neutron was used as a projectile particle. The nucleon densities of the ^{127}I were calculated to use in single folding method to obtain interaction potential of ^{127}I(n,el) reaction depending on the projectile energy.

Material & Method: In this study, SHF-WS method in which Skyrme Hartree Fock (SHF) approach is used together with Woods-Saxon (WS) potential are used in the calculation of nucleon densities. The HARTREE-FOCK code was used for the SHF method is used to calculate nucleon densities. The obtained densities were used in the Single Folding model to calculate nucleon-nucleus interaction potentials for the neutron incident energies of 0.8893 MeV, 2 MeV and 16.1 MeV. The angle-dependent differential cross sections were obtained using Talys nuclear reaction code via using these interaction potential values as input keyword. The evaluated cross sections compared with existing experimental results and other theoretical studies in the literature.

Results: The nucleon densities calculated with the SHF-WS method to obtain the nucleon-nucleus interaction potential. The single folding method used to calculate nucleon-nucleus interaction potential, and the results are quite compatible with other theoretical values which was found in the literature. The angular dependent cross section values are also compatible with experimental results which was found in the EXFOR library.

Conclusion: The obtained results and previous studies have shown that the nucleon-nucleus interaction potentials obtained by using the nucleon densities in the single folding method give results that are compatible with the values in the literature and are quite successful especially in the nuclei above the fp shell.

T1-O6: Temperature Dependent Pure Isoscalar Neutron-Proton Pairing Gap Equations

D. Mokhtari[@], N-H. Allal and M Fellah

Laboratoire de Physique Théorique, Faculté de Physique, USTHB BP 32, El-Alia, 16111 Bab-Ezzouar, Algiers, Algeria
[@] Corresponding author djmokhtari@yahoo.fr, dmokhtari@usthb.dz

Background/Purpose: It is well known that in nuclei away from the N=Z line, like-particles pairing dominates. In N≈Z nuclei, protons and neutrons occupy neighbouring levels, so the neutron and proton Fermi levels are close to each other and therefore the neutron-proton (n-p) pairing correlations are expected to play a significant role in their structure. These correlations can either correspond to isovector (T = 1) or isoscalar (T = 0) pairing, where T is the isospin quantum number. Recently, renewed interest in the study of these correlations occurred [1-3] due to the development of the radioactive beam facilities that made the experimental study of medium mass nuclei such as N ≈ Z possible.

On the other hand, the study of the temperature effect on pairing correlations have been the subject of many efforts since the sixties and is still a relevant subject.

Materials & Methods: In the present work, temperature effect on the pure isoscalar n-p pairing gap parameter is studied. The gap equations are deduced using the path integral approach. The model is numerically applied within the schematic one-level model.

Results: It is shown that the pure isoscalar n-p gap parameter $\Delta_{np}^{T=0}$ of the present work behaves, as a function of the temperature, like its homologues Δ_{pp} and Δ_{nn} in the conventional FTBCS approach. This behavior is also the same as those of $\Delta_{np}^{T=0}$ in the isovector plus isoscalar pairing case [2] and $\Delta_{np}^{T=1}$ in the pure isovector pairing case [3]. However, one observes a shift of the critical temperatures values.

Conclusion: The lack of experimental data doesn't allow us to judge the quality of our results. However, the present work results could be improved by taking into account the thermal and quantal fluctuations.

References:

[1] Negrea D et al. (Proton-neutron pairing and binding energies of nuclei close to the N=Z line): *Physical Review C*. 2022;105:034325. DOI :10.1103/PhysRevC.105.034325

[2] Mokhtari D et al. (Isovector plus isoscalar neutron–proton pairing effect on nuclear statistical quantities using a path integral approach) : *International Journal of Modern Physics E*. 2018; 27: 850054. DOI: 10.1142/S0218301318500544.

[3] Fellah M et al. (Temperature-dependent isovector pairing gap equations using a path integral approach): *Physical Review C*. 2007; 76:047306. DOI: 10.1103/PhysRevC.76.047306.

Keywords: pure isoscalar pairing, temperature, path integral, gap equations.

T2-O1: Lanthanide Targets for Cutting-Edge Nuclear Research

R. Rahali@, C. Stodel, G. Frémont, M. Bourges, F. Pérocheau

GANIL, Grand Accélérateur National d'Ions Lourds, CEA/DRF-CNRS/IN2P3, B.P. 55027, 14076 Caen, France @ Corresponding author radia.rahali@ganil.fr

Background/Purpose: GANIL (Grand Accélérateur National d'Ions Lourds) is a research infrastructure using ion beams in various fields such as nuclear physics, astrophysics, and materials science. The target laboratory at GANIL produces tailored targets for diverse experimental applications. High-quality targets are an essential element of the experimental set-up as they play a key role in ensuring the accuracy of the obtained observables.
With the new facility SPIRAL2 at GANIL, including high intensity beams from the superconducting linear accelerator (LINAG), the Neutrons for Science experimental area (NFS)
[1] and the "Super Separator Spectrometer" (S3) [2], cutting edge research in fundamental nuclear physics, and applications is being pursued. To achieve the envisaged extensive experimental program- such as the study of heavy and super-heavy elements (SHE with Z>103)- specific research and developments on targets is being conducted [3].
As part of ongoing efforts to expand the capabilities of GANIL, the target laboratory is undergoing an upgrade, including the development of isotopically enriched targets designed to withstand high beam intensities. In this context, emphasis is placed on lanthanide targets, alongside the development of other target types essential for exploring nuclear reactions and the study of exotic nuclei.

Materials & Methods: Techniques such as physical vapor deposition (PVD), electrodeposition [4], and mechanical rolling are used to fabricate targets in various forms and thicknesses to meet experimental requirements. In this work, we focused on the fabrication of stable lanthanide targets using the PVD method. The process was optimized to deposit ytterbium directly onto carbon foil backings which, due to their thickness (≈ 35 µg/cm²), require careful handling to prevent damage. This preliminary work serves as a foundation for future applications involving isotopic materials, where cost and scarcity demand high efficiency. The high melting point of ytterbium oxide, combined with the need for uniform deposition over large surfaces (11 cm x 2 cm), presents significant challenges. A rotation system was integrated into the deposition chamber to ensure uniform deposition. Elemental analyses, including XRF and SEM-EDX, are planned to confirm the uniformity of the deposition and the absence of contamination, ensuring the quality and reproducibility of the fabricated targets.

Results: Early development of lanthanides targets, especially ytterbium, showed promising results in terms of homogeneity and quality, with thicknesses ranging from a few µg/cm² to mg/cm². The deposition demonstrated excellent adhesion, which is critical for target stability during experiments.

Conclusion: The development of nuclear targets at the GANIL target laboratory represents a significant advancement in producing materials for fundamental nuclear research. The results obtained for ytterbium targets pave the way for expanded and optimized production of nuclear targets, including other lanthanides, for future scientific projects.

References:

[1]. X. Ledoux et al., First beams at neutrons for science. Eur. Phys. J. A, 2021;57: 25. doi: 10.1140/epja/s10050-021-00565-x

[2]. H. Savajols et al., S^3 : The Super Separator Spectrometer for SPIRAL2 stable beams. AIP Conf. Proc.

2010; 1238: 251-256. doi: 10.1063/1.3455944

[3]. Ch. Stodel et al., Targets for S3 at SPIRAL2. Nucl. Instrum. Methods Phys. Res. Sect. A. 2010; 613: 480-485. doi: 10.1016/j.nima.2009.10.008.

[4]. G. Fremont et al., Preparation of osmium targets with carbon backing. AIP Conf. Proc. 2018; 1962: 030002. doi: 10.1063/1.5035519.

Keywords: **Nuclear target; nuclear physics, PVD, Lanthanides.**

T2-O2: SYSCADE project: Combining X-Ray Inspection and Radiologic Characterization for a better evaluation of total radioactivity content in nuclear wastes

T. Delvigne[a@], B. Hennebert[b]

[a]*Deltabeam SRL*
[b]*SYSCADE SA*

[@]*Corresponding author* thierry.delvigne@deltabeam.net

Background/Purpose: "SYSCADE" (SYStème de CAractérisation de DEchets) is a mobile equipment developed by Delta Industrial Services (DSi) Belgium for automatic assay of nuclear waste drums. It consists in a 40-feet container equipped with an X-Ray Inspection system associated to a sophisticated spectroscopic characterization equipment. It allows determining the isotopic content, the presence and localization of hot spots of radioactivity in a drum, and the level of radioactivity for each isotope. This paper presents the technical solutions selected during this ambitious R&D project, and valuable results obtained when superimposing X-Ray radiographs and gamma spectroscopy data.

Materials & Methods: SYSCADE solution combines in a 40-feet container a 320 kV X- Ray inspection cabin and a high-resolution radiologic characterization unit with High Purity Germanium (HPGe) detector. The equipment was developed to inspect Low Level radioactive Wastes (LLW), including NORMs. Both assay systems are installed in a 40-feet container equipped with a lead shielded cabin. The main technical challenge of this project was to minimize both dimensions and weight (less than 25 tons) of the container. Another challenge is the integration of a high-resolution spectroscopy system in a limited space where intense X-Ray beams are generated. A 3-axis, retractable, HPGe detection arm was developed. The unit allows inspecting wastes in 2 steps: 2D or 3D X-ray scans followed by Segmented Gamma Scans (SGS) or Angular-SGS to detect hot spots of radioactivity in each drum, and determine the activity distribution of each isotope.

Results: The equipment is now fully operational, and it offers the following benefits: the X-Ray unit is self-shielded and does not require any additional shield outside the container; due to the internal shield, background radiation is significantly reduced when activity measurement are performed, leading to improved Minimum Detectable Activities (MDAs) and shorter measuring times. The latest development of this project concerns the superimposition of X-Ray imaging information with gamma-ray characterization results. Software routines have also been developed to determine gamma-ray attenuation factors associated to each segment and each part of segment (angular resolution), allowing to minimize "type B" errors due to non-homogeneous distribution of the materials (matrix) contained in the waste drums. A new software was also developed according to ASTM C1133 standard to determine uncertainties on activity measurement results when the SGS mode is used.

Conclusion: Developed within a short 3 years, SYSCADE solution is fully operational. It combines an inspection (X-ray) to visualize the inner content of waste drums, and a characterization (HPGe) equipment to determine the isotopic content, to detect hot spots, and calculate the activity levels. As next step, we are developing a new version of the A-SGS gamma station that will integrate a new, very compact detector technology that offers several advantages compared to HPGe technology. To be revealed during the presentation…

References: (TBC)

1. Strulab D et al.. GATE (geant4 application for tomographic emission): a PET/SPECT general-purpose simulation platform. *Nuclear Physics B - Proceedings Supplements*. 2003;125:75-79. doi:10.1016/S0920-5632(03)90969-8

2. Strulab D et al.. GATE (geant4 application for tomographic emission): a PET/SPECT general-purpose simulation platform. *Nuclear Physics B - Proceedings Supplements*. 2003;125:75-79. doi:10.1016/S0920-5632(03)90969-8

T2-O3: Actions within the framework of the radiological emergencies program of Valencia Region

M. Simeó[a@], T. Cámara[a], V. Delgado[a] , J. Díaz[a] , N. Yahlali[a]

[a]*Ins%tuto de Física Corpuscular (IFIC), Centro Mixto Universitat de València (UV) - CSIC*
[@]*Corresponding author: mireia.simeo@ific.uv.es*

Background/Purpose: The increasing global use of radioac2ve isotopes in different sectors - including industry, energy produc2on and medical applica2ons - has led to widespread distribu2on of these materials in society. This situa2on has raised significant concerns among governments and organiza2ons regarding the poten2al accidental release of radioac2vity into the environment, which could result in a radiological emergency. To address these concerns, it is crucial to implement effec2ve safeguards and monitoring systems to prevent accidental radioac2ve releases and ensure public protec2on in the event of a radiological incident[1]. In this context, the Laboratory of Environmental Radioac2vity of the University of Valencia (LARAM) has signed an agreement with the Valencia's Regional Government to develop an environmental monitoring plan specifically designed for radiological emergencies.

Materials & Methods: In order to meet the objec2ves of the comprehensive monitoring plan for radiological emergencies, a portable measurement and analysis system was designed and built in the laboratory. It features two gamma portable NaI and HPGe detectors mounted on a mobile plaQorm equipped with a stabiliza2on system. Each gamma detector was calibrated and characterized. This setup enables swiS gamma radia2on measurements in the field during a radiological emergency.

Results: In-situ measurements offer reduced sensi2vity to local soil sampling varia2ons, allowing for swiS coverage of extensive areas to iden2fy present isotopes and hotspots. In contrast, laboratory measurements allow large sta2s2cs to be taken for detec2ng small peaks. Addi2onally, it is essen2al to conduct background radia2on measurements in the vicinity of radioac2ve facili2es before any incident. These pre-accident measurements help characterize the environment and assess the extent of recovery in the area following a radiological event.

Conclusion: A protocol for radiological emergencies was established, which enables rapid in-situ measurements using the emergency detec2on system developed at LARAM. With these reference measurements, background radia2on maps of key radiological facili2es in the Valencia Region. This protocol has been successfully tested during emergency drills organized by local authori2es.

References:

1. S. Apikyan, D. Diamond y R. Way, Preven2on, Detec2on and Response to Nuclear and Radiological Threats, Springer 2008.

Keywords: radiological protec2on, gamma detectors, radiological emergency.

T2-O4: Development of Noble element detectors for neutrino experiments at IFIC and application prospects to medicine and environmental radioprotection

N. Yahlali[a]

[a]*Instituto de Física Corpuscular (IFIC), Centro Mixto Universitat de València (UV) - CSIC*
[@]*Corresponding author: nadia.yahlali@ific.uv.es*

Background/Purpose: Noble element detectors based on Time Projection Chamber (TPC) technology operated with gaseous xenon and liquid argon are being developed at IFIC for neutrinoless double beta decay ($\beta\beta0\upsilon$) and neutrino oscillation experiments in underground laboratories. Noble elements, mainly Xe and Ar have outstanding detection properties as scintillators with high light-yield, transparent to their own scintillation, and high Z favoring energy deposition of charged particles. Interaction of charged particles with Xe and Ar media produces ionization and scintillation signals which can be both recorded for energy, tracking and particle identification. However, the scintillation light, which is emitted in the deep ultra-violet (VUV) spectrum, ~128 nm for Ar and ~172 nm for Xe, poses a serious challenge for its detection, as standard photodetectors are insensitive to wavelengths < 200 nm. An intense R&D on light conversion, transmission and detection is being held at IFIC to overcome this detection limit. Possible applications of noble element detectors to societal challenges in medicine and environmental radioprotection are being explored.

Materials & Methods: An intense R&D funded by the Valencian regional government (*Generalitat Valenciana - GVA*) and the European Community through the project IFIC-NuLIGHT ASFAE/2022/029 is being held at IFIC for the development of VUV light detection systems for noble element experiments: NEXT for $\beta\beta0\upsilon$ search and DUNE for long-baseline neutrino oscillation experiment [1]. An optic laboratory enclosed in a clean room, was equipped with VUV and UV-Visible light sources, vacuum monochromator, calibrated VUV photodetectors, sample holders, rotary stages and dark test chambers, for the optical characterization of light collectors, detector materials and new generation photodetectors in different environmental conditions: vacuum, gaseous and liquid argon.

Results: A description of the IFIC Optics Laboratory and the current R&D held in it, funded by the GVA through the IFIC-NuLIGHT project, will be described along with some preliminary results of measurements in the VUV spectral range. Application prospects of these investigations to medicine (PET scan with LXe technology) and environmental radioactivity (gamma-spectroscopy with gaseous portable TPC) will be outlined.

Conclusion: An Optics facility for the development of noble element detectors has been recently set up at IFIC, allowing a thorough R&D on light detection systems in noble element detectors for neutrino experiments and possible applications to societal challenges.

References:

1. https://next-experiment.org/, https://www.dunescience.org/

Keywords: Noble element detectors, xenon, liquid argon, VUV light detection

T2-O5: Enhanced Micro-RBS Sensitivity for Spatial Distribution Analysis of Heavy Elements.

F. Boussahoul[1@], M. Jakšić[1], G. Provatas[1]

[1] *Ruđer Bošković Institute, Zagreb, Croatia.*
[@] *Corresponding author fboussah@irb.hr*

Background/Purpose: This study presents a novel experimental concept that integrates heavy ion Rutherford Backscattering Spectrometry (RBS) with microbeam technology to measure the spatial distribution of heavy trace elements in various materials. The primary objective is to enhance the sensitivity and precision of trace element analysis by employing a heavier probing beam than the major substrate elements. This approach not only increases the backscattering cross-section but also mitigates pileup effects caused by substrate backscattering, which is crucial for sensitive analysis. The proposed method aims to achieve high-resolution measurements of both areal concentrations and depth profiles of heavy elements in materials.

Materials & Methods: A focused 2.4 MeV Si^{2+} ion beam was utilized as the probing beam, selected for its optimal mass and energy characteristics. The beam was focused to a spot size of approximately 10 µm, with beam currents reaching up to 1 nA. The detection system employed a solid angle of approximately 1 sr in an unconventional geometry, allowing ions to enter the detector at different angles. This geometry required the development of a spectral analysis model to correct kinematic spread effects. The system was tested on silicon and silicon carbide (SiC) samples containing Au and Pt elements at concentrations ranging from 10^{12} to 10^{14} at/cm³. Additionally, Au-implanted silicon samples were used to determine the detection limit of the system.

Results: The experimental setup demonstrated the capability to accurately measure both areal concentrations and depth profiles of heavy elements. The spectral analysis model effectively corrected kinematic spread distortions, improving the overall measurement precision. The detection sensitivity reached 10^{10} at/cm², with clear detection of Au and Pt elements at very low concentrations. The unconventional detector geometry showed a measurable impact on detector resolution, which was successfully addressed through the developed correction model [1].

Conclusion: The combination of heavy ion RBS with microbeam technology significantly improves the sensitivity and precision of heavy trace element analysis. The use of a heavier probing beam minimizes substrate pileup and enhances detection capabilities, making the method particularly suitable for low-concentration trace elements. This approach opens new possibilities for high-resolution mapping of heavy elements in materials, with potential applications in materials science and microelectronics. Future work will focus on further improving spatial resolution and extending the method to other heavy elements.

References:

[1]. F. Boussahoul, M. Jaksic, G. Provatas, D. Maouche, A high sensitivity microbeam RBS setup for heavy elements implantation profiles analysis. https://doi.org/10.1016/j.nimb.2023.165152

Keywords: Sensitive RBS; Micro-RBS; Trace elements analysis; Depth profile.

T2-O6: Estimated radon concentration in the air of a room with marble walls

W. Boukhenfouf@, A. BOUAZIZ, S.N. CHOUGUI, G MELLAK

Dosage Analysis and Characterization laboratory, physics department, faculty of Sciences, Setif-1 University
@ Corresponding author ouassila.boukhenfouf@univ-setif.dz

Background/Purpose: The natural radioactivity in marble primarily originates from primordial radionuclides governed by ^{238}U, ^{232}Th and ^{235}U and their decay products, and are considered major contributors to external irradiation sources for the human body. Among the decay products of ^{238}U is ^{222}Rn, a rare radioactive gas that is colorless, odorless, and predominantly of natural origin. The inhalation of radon (^{222}Rn) is recognized as a potential health risk. Since ^{222}Rn can accumulate in confined spaces such as homes and workplaces, it accounts for one- third of the total radiological exposure of the population to ionizing radiation and is one of the leading causes of lung cancer.

The objective of this work is to estimate the radon level released in a closed room with marble walls. Is all the radon emitted by the marble released into the room?

Materials & Methods: Six marble samples (three local types and three imported ones) were collected to determine the activity of ^{222}Rn. The technique used was gamma spectrometry with a NaI (Tl) scintillation detector, operating at 680 volts. The prepared samples were completely sealed for over 2 months before measurement to achieve radioactive equilibrium in the ^{238}U and ^{232}Th decay chains.

Results: Formula adopted by UNSCEAR are used to estimate the rate of ^{222}Rn activity found inside samples and the rate emitted into the air. The radon level emitted by a 2 cm thick layer of marble in a $14m^3$ room was estimated. The values obtained range from 0.05 to 0.36 Bq/m^3. The International Commission on Radiological Protection (ICRP) recommends that radon levels should not exceed 200 Bq/m^3 in older homes and confined spaces.

Conclusion: The portion of radon emitted in the volume of the room represents 0.03% of the total value amount released from the marble. On the basis of the results, the types of marble studied can be classified as products exempt from any restrictions on use. Consequently, they present no health risk to the public and can be used effectively in a variety of construction activities.

References:

[1]. Ngachin M et al.. Assessment of natural radioactivity and associated radiation hazards in some Cameroonian building materials. *Radiation Measurements*. 2007; 42:61-67. doi: https://doi.org/10.1016/j.radmeas.2006.07.007

[2]. International Commission On Radiological Protection (ICRP), Protection against radon at home and at work, ICRP Publication 65, Annals of the ICRP, 1993; 23(4)

Keywords: Radon; marbles; gamma spectrometry; dose rate.

T2-O7: Investigation of Neutron irradiation-induced defects in BCF12 plastic scintillators

M. Izerrouken[1], N. R. Idourane[2]

[1]*Nuclear research center of Draria, Bp43, Sebbala street, Draria, Algiers, Algeriz*
[2]*Faculy of physic, university of science and technology Houari Boumedien, Bp 32 El-Alia, Bab-ezzouar, Algiers, Algeria*

Background/Purpose: Detection of nuclear radiation (-rays, neutron, charged particle, …) remains a research field that attracts more and more researchers given the various applications (medicine: PET scanners, aerospace, high energy physics, etc.) which require high-performance detectors with better efficiency, high resolution and the lowest possible detection limit [1]. Plastic scintillators are among the detectors that are currently under development [2]. The latter are known for their excellent optical property (fast scintillation decay, high detection efficiency, and high light yield) [3] and hardness [4]. Detectors used in high energy physics (accelerators, LHC experiments and nuclear reactors) and in aerospace are subjected to a very severe irradiation environment altering its performance. Therefore, the study of the radiation tolerance of such a detector is crucial before its use. Thus, since their introduction, many papers have been published exploring the effect of several parameters including dose and dose rate on their scintillation properties [5]. In this communication, the irradiation tolerance tests of the BCF12 plastic scintillators were carried out in the core of a nuclear reactor where it is subjected to a broad spectrum of neutrons and gamma rays. Several characterization techniques were used to evaluate the changes of some parameters namely, crystallinity, transmittance, hardness and fluorescence after irradiation. Our aim is to elucidate the behavior of the BCF12 plastic scintillator under a mixed irradiation field (neutron-gamma).

Materials & Methods: Plastic scintillator used in this study are BCF12 model from Saint-Gobain Crystals, purchased from Valencia University, Spain. The samples are 30 mm long and 1 mm diameter fibers. They consist of a polystyrene (PS) core doped with fluorescent molecules, and PMMA cladding. They are characterized by an absorption band at 340 nm and an emission band in the blue spectrum, with a maximum emission at 432 nm. Neutron irradiations were performed at NUR research reactor in two positions: periphery of the reactor core position with a gamma ray dose rate of about 0.5KGy/h; and reactor core position with a gamma ray dose rate of 7 MGy/h. The samples are first placed in polyethylene bags and inserted in a well sealed container made of aluminum and then inserted into the irradiation position. The samples were irradiated at two different fast neutron (En>1 MeV) fluencies 1.5×10^{13} n.cm^2 and 4.6×10^{17} n.cm^{-2}. After irradiation the samples were characterized using X-ray diffraction, spectrophotometry UV-visible, photoluminescence and micro-hardness techniques.

Results: After irradiation, the samples become colored indicating point defect formation mainly radicals as well confirmed by a broadening of the absorption band; extended up to 500 nm compared to the unirradiated sample. While the emission band remains at the same position with a slight intensity improvement in the case of sample subjected to high fast neutron (4.6×10^{17} n.cm^{-2}) and gamma ray dose (28 MGy). In contrast, the band width exhibit a broadening towards high wavelengths. It increases from 80 nm before irradiation to 108 nm, an increase of about 26 %. This probably affect the detector resolution. Moreover, the XRD results reveal crystallinity

improvement after irradiation with a decrease in the domain size. It decreases from 16 Å to 12 Å.

Conclusion: Despite the high density of free radicals induced by irradiation, this did not influence the fluorescence and the crystalline structure; on the contrary, we observed a slight improvement in the intensity of the emission band and the crystallinity. This evidence the radiation tolerance of BCF12 scintillator, therefore its ability to operate in hostile environments such as nuclear reactor, accelerators and aerospace. Nevertheless, further studies are needed to explore the broadening of the emission band.

References

[1] Chanwoo Park, Kyu Bom Kim, Min Kyu Baek, In-soo Kang, Seongyeon Lee,Yoon Soo Chung, Heejun Chung, Yong Hyun Chung, Development of a muon detector based on a plastic scintillator and WLS fibers to be used for muon tomography system, Nuclear Engineering and Technology 55 (2023) 1009e1014, https://doi.org/10.1016/j.net.2022.11.016

[2] Atsushi Sato, Masanori Koshimizu, Yutaka Fujimoto, Keisuke Asai, Development of plastic scintillators doped with silole-based aggregation-induced emission phosphors for scintillation light yield improvement, Optical Materials, 136,(2023) 113493. https://doi.org/10.1016/j.optmat.2023.113493

[3] Wen Li, Yunyun Li, Martin Nikl, Matthieu Hamel, Hongshu Wu, et al.. Preparation and performance of plastic scintillators with copper iodide complex-loaded for radiation detection. Polymer, 2022, 249, pp.124832. DOI:10.1016/j.polymer.2022.124832.

[4] Yu. N. Kharzheev, Radiation Hardness of Scintillation Detectors Based on Organic Plastic Scintillators and Optical Fibers, Physics of Particles and Nuclei, 2019, Vol. 50, No. 1, pp. 42–
76. DOI: 10.1134/S1063779619010027.

[5] H. Jivan, J.E. Mdhluli, E. Sideras-Haddad, B. Mellado, R. Erasmus, M. Madhuku, Radiation damage effects on the optical properties of plastic scintillators, Nucl. Instr. And Meth. B 409, 15 October 2017, Pages 224-228. doi.org/10.1016/j.nimb.2017.05.061

Keywords: Plastic scintillators; Radiation damage; Neutron irradiation; Ion beam, Photoluminescence; X-ray diffraction.

T3-O1: Evaluation of patient received dose during an interventional cardiology examination using Monte Carlo simulation

K. Manai[1@], M. Bhar[2]

[1] *Faculty of Sciences of Tunis, Tunis El Manar University, Tunisia*
[2] *National Center of Nuclear Sciences and Technologies, Tunisia*
[@] *manaikais14@gmail.com*

Background/Purpose: Interventional cardiology performed under the control of an X- ray imaging tool is a widely used technique for the diagnosis and treatment of various cardiac pathologies. However, during these procedures, the patient and medical staff are likely to be exposed to significant doses. Among the reasons for these high doses is the long duration of these procedures, as well as the proximity of the medical staff to the patient who presents the center of scattered radiation.

Materials &Methods: The aim of this study is to assess the radiation exposure of the patient and the medical staff during interventional cardiology procedures. Realistic exposure scenarios were developed using the adult reference anthropomorphic phantoms adopted by the International Commission on Radiological Protection (ICRP110Male and ICRP110Female), and the radiation transport code Geant4 (version 10.3) [1]. The calculated equivalent and effective doses were normalised by the simulated Kerma-Area Product (KAP), resulting in two conversion coefficients HT/KAP and ET/KAP. To properly evaluate the risk of exposure, several dose-dependent parameters have been investigated, namely: radiological parameters (tube kilovoltage peak (kVp), type of projection, field size (FOV)), and operator positions. Four projections (AP, PA, LAO25° and RAO25°) were simulated for three X-ray energy spectra (80, 100 and 120 kVp) with four different values of FOV [2].

Results: The results showed that the conversion coefficients values increase with increasing tube voltage as well as the FOV size. The comparison of our results with the literature data showed good agreement allowing their use in the dosimetric characterization of interventional cardiology procedures [2].

Conclusion: In conclusion, the use of MC simulations using GEANT4 has been an important asset, to evaluate the patient received dose during an interventional cardiology examination

References:

[1]. S. Agostinelli, J. Allison, K. a. Amako, J. Apostolakis, H. Araujo, P. Arce, M. Asai, D. Axen, S. Banerjee, G. . Barrand, et al., Geant4a simulation toolkit, Nuclear instruments and methods in physics research section A: Accelerators, Spectrometers, Detectors and Associated Equipment, 506 (2003), pp. 250-303.
[2]. Bhar, M., Mora, S., Kadri, O., Zein, S., Manai, K., &Incerti, S. (2021). Monte Carlo study of patient and medical staff radiation exposures during interventional cardiology. Physica Medica, 82, 200-210.

Keywords: Interventional cardiology; human phantom; GEANT4

T3-O2: Investigate the effects of single X-ray doses (Low and high doses) on Haematological parameters of male Albino Rats

K. N. Abdulla@, S.P. Yaba, Asaad H. Ismail

[1] *Physics Department, Education College, Salahaddin University-Erbil, Erbil , IRAQ*
Corresponding author khadija.abdulla@su.edu.krd

Background/Purpose: X-rays can cause mutations in the DNA and, therefore, might lead to cancer later in life. For this reason, X-rays are classified as a carcinogen trusted by WHO. However, the benefits of X-ray technology far outweigh the potential negative consequences of using them Exposure of the human body to doses greater than 1 Gy at relatively high dose rates of 0.05 Gy/h or higher results in a range of clinical syndromes known as acute radiation syndromes (ARS). The study aimed to investigate the effects of single-dose exposure techniques using X- rays at low doses (35.44 7.5 µSv/hr) and high doses (323.66 23.7µSv/hr) on the haematological parameters have been investigated for male albino Rats.

Materials & Methods: A total of 10 groups (5 groups for low dose + 5 groups for high dose) were formed from the rats with the same biological and physiological characteristics, one of which was the control group (Group I) and the others were the experimental group (increasing time of irradiation from 10 min to 50 min for low and high irradiation dose), with those with similar body weights in the same group. Blood samples were taken from the heart directly anesthetized rats 48 h after irradiation. Complete blood cells (CBC), and erythrocyte sedimentation rate (ESR) were determined using an automated hematology analyzer

Results: The results showed that the rats' complete blood counts varied according to the time of irradiation and irradiation dose (high or low dose). Significant differences were observed between the groups in all hematologic parameters of RBCs, PLTs, Hb, WBCs, LYM, and GRAN ($p < 0.001$). Meanwhile, the irradiation of low and high doses, depending on the time of irradiation, does not affect relativity. The decrease in PLT parameters in rats exposed to high-dose rate radiation was 24.4% and 36.30% for low and high single irradiation doses, respectively.

Conclusion: The study practically evaluated that the in-vivo exposure of male rats to low and high exposure doses relatively has sufficient impacts on the haematological parameters. The time of exposure to the X-ray radiation dose is the most important factor in determining the biological risks of exposure to X-rays, whether the dose is high or low. The time of exposure had more effects on complete blood cells rather than the erythrocyte sedimentation rate

Keywords: CBC; radiation dose ; X-ray beam; ESR; Rats

T3-O3: Investigation of the Effect of Patient Body-Mass Index on Dose in CT Scan

H. Ünal[1,2@], I.H. Sarpün[1,3,4], T. Koca[1], B. Yılmazer[1]

[1] *Akdeniz University, Faculty of Medicine, Radiation Oncology, Antalya Turkiye*
[2] *Akdeniz University, Vocational School of Health Sciences, Radiaotherapy, Antalya Turkiye*
[3] *Akdeniz University, Physics Department, Antalya Turkiye*
[4] *Akdeniz University, Nuclear Research and Application Centre, Antalya Turkiye*
[@] *Corresponding author handeunal1985@gmail.com*

Background/Purpose: Computed Tomography (CT) is an imaging technique regularly used in Radiation Oncology clinics, and due to developing technology, its use in other departments is increasing despite the risk of low-dose radiation. It is difficult to precisely determine the specific stochastic risks caused by low-dose ionizing radiation. Therefore, in patients undergoing CT scans, it is sometimes necessary to estimate the radiation dose to which tissues are exposed to X-rays emitted from CT scanners.

Materials & Methods: In general terms, the most important quantity for estimating risk from diagnostic imaging procedures is the radiation dose absorbed by each organ, whether computed by classical methods or by computer codes. Various computer codes have been used to estimate patient organ doses. One of these codes is the National Cancer Institute dosimetry system (NCICT) developed by Lee et al. The NCICT code combines ICRP reference pediatric and adult voxel phantoms with Monte Carlo simulation of the reference CT scanner. The NCICT code has a graphical user interface (GUI) where users can easily enter scan parameters and calculate organ doses for CT patients.

Results: In this study, the dose received by some organs was calculated, using the NCICT code, by changing the mass (between 55 and 140 kg) of a male phantom whose height was kept constant at 180 cm. For this, the x-ray tube parameters were selected as 120 kV and 300 mAs. Thus, the changes in the body mass index (BMI) lung, kidney, liver and spinal cord doses were investigated.

Conclusion: It was determined that the doses of the selected organs and the effective dose decreased with increasing BMI.

Keywords: CT; NCICT; Dose calculation; Body mass index

T3-O4: Comparison of absorbed doses to kidneys calculated from three time points and two time points in neuroendocrine patients undergoing [177Lu]Lu- DOTATATE therapy using planar images

A. Khawar [1@], B. Khan [1], A. Ammar [2], N. Marwat [2]

[1] *Department of Medical Sciences, Pakistan Institute of Engineering and Applied Sciences, Islamabad, Pakistan*
[2] *Atomic Energy Cancer Hospital, Nuclear Medicine Oncology & Radiotherapy Institute (AECHNORI), Islamabad, Pakistan*
[@] *Corresponding author ambreen_khawar@hotmail.com; akhawar@pieas.edu.pk*

Background/Purpose: Evidence supports non validity of EBRT limit of 23 Gy (radiation absorbed dose) to kidneys for [177Lu]Lu-DOTATATE PRRT in neuroendocrine tumor (NET) patients, thus favoring exploration of feasible dosimetric methods for routine clinical use for personalized therapy. In this study the feasibility of two-time points (4;168& 24;168) h post injection (p.i)i. with standard three time points imaging (4; 24; 168) h p.i. dosimetric protocol using planar scintigraphy for kidney absorbed dose determination in NET patients. .

Materials & Methods: Seven inoperable NET patients (mean age: 46, M: F=4:3) underwent whole body planar imaging at 4, 24 and 168 h p.i., of [177Lu]Lu-DOTATATE (mean ± SD = 6.135 GBq) activity. Conjugate view method was used for activity quantification in kidneys. OLINDA/EXM 2.0 Beta version was used for calculation of absorbed dose (AD) to kidneys (Gy) using two time points i.e., AD4,168, AD24,168 and three time points i.e., AD4,24,168. Total absorbed dose and % age difference of kidney absorbed doses between AD4,168, AD24,168 and AD4,24,168 were compared. Pearson's correlation of AD4,168 and AD24,168 with AD4,24,168 was determined. Bland Altman plot was also generated to see bias of difference in means of these methods.

Results: AD4,168 were found higher than AD24,168 and AD4,24,168 with doses less than 10 Gy in most of patients. The absorbed doses varied due to individual patient pharmacokinetics, injected doses and kidney function. Both AD4,168, AD24,168 showed good correlation with AD4,24,168. Overestimation and underestimation of absorbed doses was seen with 4 and 24 h as initial time point respectively. Bland-Altman plots showed AD4,168 & AD24,168 to be within 95% limit of agreement. Use of 4 h and 24 h as initial time for imaging was shown to be better for PRRT patients with and without compromised renal function respectively. However using 24 h as initial data is better in context of radiation protection.

Conclusion: It is concluded simplified method with two time points can easily be employed in clinical routine.

References:

[1]. Sandström M, Garske-Romań U, Granberg D, et al. Individualized dosimetry of kidney and bone marrow in patients undergoing 177Lu-DOTA-octreotate treatment. J Nucl Med; 2013;54:33–41.

[2]. Hänscheid H, Lapa C, Buck AK, et al. Dose Mapping After Endoradiotherapy with 177Lu-DOTATATE/DOTATOC by a Single Measurement After 4 Days. J Nucl Med. Society of Nuclear Medicine; 2018;59:75–81.

[3]. Sandström M, Freedman N, Fröss-Baron K, et al. Kidney dosimetry in 777 patients during 177Lu-DOTATATE therapy: aspects on extrapolations and measurement time points. EJNMMI Phys. Springer; 2020;7

Keywords: **maximum 5 keywords; maximum 5 keywords; maximum 5 keywords;**

T3-O5: Toxicity and risk after using new modalities of radiotherapy in Algeria: Retrospective intercomparison study

A. Boughalia[1@], M. Fellah[2],Y. Chaouchi[2], N. Kebaily[2], A. Benamirouche[3], Z. El Ghribi[3], K. Benacer[3], S. Oukrif[4].

[1] *Atomic and Radiobiological department, Physics Section, Nuclear Research Centre of Algiers Algeria*
[2]*Physics Faculty, Houari Boumediene University Bab Ezzouar Algiers, Algeria*
[3]*Radiotherapy Oncology Department, Fatima El Azhar Centre Dely Ibrahim, Algiers, Algeria,*
[4]*Radiotherapy Oncology Department, Centre Pierre et Marie Curie, Algiers, Algeria*
[@]*Corresponding author: a.boughalia@crna.dz*

Background/Purpose: During the last decade, new advanced treatment modalities of radiotherapy have been introduced in different radiotherapy-oncology departments in Algeria. In this study we aim to assess these different types of treatments in terms of their toxicity and induced second cancers in the case of prostate cancer with high risk.

Materials &Methods: A cohort of 72 patients divided into three groups (GI, GII and GIII) using:VMAT,VMAT and HT& 3D-CRT where the median age:71,75 and 73 years old respectively. The 6 MV was planned using VARIAN HDX 2100C, VERSA HD linear accelerator, TOMOTHERAPY and ELEKTA Synergy. The prescribed dose was 76 Gy/2 Gy/fraction for GI and GII planned with VMAT and 71.3 Gy/2.3 Gy/fraction for GIII planned with HT and 3D-CRT.These treatments plans were assessed through their dose volume histogram (DVHs) in the case of rectum and bladder organ using the Lyman-Kutcher-Burman-model to calculate the toxicity (NTCP), and the corresponding Excess Absolute Risk (EAR) using different radiobiological models computed with the in-house software "COUPOLE"[1, 2,3].

Results: Lower toxicity was obtained for organs at risk when using HT treatment compared to VMAT and 3D-CRT where the results show that: The NTCP for rectum (rectal bleeding) %=9.5;7.1; 5.18 and 22.46 for GI, GII and GIII using HT and 3D-CRT.In the case of bladder NTCP (bladder contracture) %=0.05 for GI; 0.041 for GII; 0.0 and 1.67 for GIII. The corresponding risk EAR is more important for HT and VMAT treatment compared to 3D-CRT particularly in the case of bladder.The EAR(/10000PY) for rectum=0.07(GII); 1.71 and 1.60 (GIII);The EAR mean (/10000PY) for bladder=6.30(GI); 0.01 (GII) and 0.46 for HT and 3D- CRT(GIII).

Conclusion: Thanks to this study, we conclude that better protection of OARs with minor toxicity was obtained with HT but the risk is significant for the organs at risk (bladder) when using HT and VMAT compared to 3D-CRT.

References:

[1]. Kutcher GJ, Burman C. Calculation of complication probability factors for non-uniform normal tissue irradiation: the effective volume method. Int J Radiat Oncol Biol Phys., 1989. 16:1623-30.

[2]. Dasu A. Toma-DasuI.Models for the risk of secondary cancers from radiation therapy. Phys.Med 2017.

Keywords: NTCP, EAR, prostate cancer, OED, OARs

T3-O6: Monte Carlo simulation of a prototype of monitoring of positrons in biological matter: Application to Nuclear Medicine

M. Bhar[1], K. Manai[2], D. Ben Sellem[3]

[1]*National Center of Nuclear Sciences and Technologies (CNSTN), Tunisia*
[2]*Nuclear Physics and High Energy Unit, Faculty of Sciences of Tunis, Tunis El Manar University, Tunisia*
[3] *University of Tunis El Manar, Faculty of Medicine of Tunis, 1007, Tunisia.*
[@]*bhar.maroua@yahoo.com*

Background/Purpose: The use of, and interest in, Monte Carlo (MC) simulations in medical imaging is growing by leaps and bounds. Particularly, they involve a critical importance in Positron emission tomography (PET) imaging. By accurately modelling not only the interactions of particles in the detectors but also the whole PET system, these simulations contribute to significantly improve the quality and efficiency of PET images.

Materials &Methods: The present work focuses on the use of this method for the development of a numerical model of positron tracking in biological matter, applied to nuclear medicine, in particular for Positron Emission Tomography (PET) [1]. This model is based on the GEANT4 simulation tool [2]. Using the GEANT4 code, we have simulated positron interactions and optimized a PET detection system. This study is divided into two parts. The first studies the role of the Monte-Carlo method and its application in modeling the physical processes involved in the PET system [3]. The second evaluates the performance of this prototype.

Results: The results obtained, particularly in terms of energy resolution and temporal resolution, are in line with literature standards, confirming there liability of our approach. Taken together, the results confirm that the GEANT4 code is a realistic option for the design of medical imaging modalities, and in particular PET.

Conclusion: In conclusion, the use of MC simulations using GEANT4 has been an important asset, offering new perspectives for PET system modelling. Indeed, these simulations allow for fine-tuning of imaging performance while paving the way for past improvements.

References:

[1] Cindy Le Loirec. Simulation Monte Carlo de suivi de positrons dans la matière biologique: applications en imagerie médicale. PhD thesis, 2007.

[2] S. Agostinelli et al. Geant4: A simulation toolkit. Nucl. Instrum. Methods Phys. Res.A, 506(3):250–303, 2003.

[3] K. J.J.M.Van der Hoeven et al. Monte Carlo Simulation in pet: A review. Physics in Medicine and Biology, 54(17):R155–R176, 2009.

Keywords: Positron emission tomography (PET), MC simulation

T3-O7: Can be volumetric arc therapy alternative to brachytherapy in advanced cervical cancer radiotherapy?

Y. Bilek[1,2@], I.H. Sarpün[2,3], T. Koca[2]

[1] *Akdeniz University Health Services Vocational School Department of Radiotherapy*
[2] *Akdeniz University Medicine School Department of Radiation Oncology*
[3] *Akdeniz University Science Faculty Department of Physics*
[@] *Corresponding author yilmazbilek007@gmail.com*

Background/Purpose: The treatment method of choice for locally advanced cervical cancer, classified as IB2-IVA in the FIGO staging, has been external beam radiotherapy to the pelvis-cervix, uterus and parametrium and intracavitary brachytherapy (BRT) as an additional dose since 1999 [1]. Sometimes, the treatment team may be faced with patient refusal, a large cervical tumor with high lateral parametrial extension that is inaccessible for interstitial implants and/or medical indications that completely preclude BRT application. These challenging scenarios require an alternative plan to deliver the intended therapeutic dose without submitting to the dogma that BRT is therefore irreplaceable [2].

This study aims to design a volumetric modulated arc therapy (VMAT) plan with the same dose instead of brachytherapy applied as an additional dose in advanced stage cervical cancer radiotherapy and to investigate its applicability dosimetrically.

Materials & Methods: In the study, computerized tomography images and BRT plans of patients who received 45 Gy external radiotherapy at Akdeniz University Radiation Oncology Clinic and then received three-dimensional BRT treatment were used retrospectively. Using these cross-sectional images, external SBRT plans were created for each patient with the Elekta brand Monaco treatment planning system (TPS) using the VMAT technique. The created VMAT plans were compared dosimetrically with BRT plans. The plans were evaluated by comparing them in terms of dose coverage in the target volume and critical organ doses as well as treatment durations.

Results: The results obtained from the study shows that VMAT and brachytherapy plans are compatible.

Conclusion: As a result of the dosimetric data obtained from the study, it was concluded that VMAT treatment can be applied to advanced stage cervical cancer patients who cannot receive brachytherapy.

References:

[1]. Lisa et al. External beam boost for cancer of the cerviks uteri when intracavitary therapy cannot be performed: Int. J. Radiation Biol. Phys. 2008; Vol.71, No.3, pp. 772-778,.

[2]. Mahmoud et al. External beam techniques to boost cervical cancer when brachytherapy is not an option theories and applications. Annals of Translational Medicine. 2017;5(10), 207.

Keywords: VMAT; Brachytherapy; Servix CA; Radiotherapy.

T3-O8: First Dosimetric Study for Nasopharyngeal Cancer in Mauritania: Insights from Three Techniques: 3D-CRT, 3D-CRT + Electrons, and VMAT

Z. Y. Cheikh Sidiya [a,b,c@], A. Seyed [a], A. Tolba [a], C. Moussa[a], L. Ounalli [c,d],

[a] National Oncology Center, Nouakchott, Mauritania
[b] University of Tunis El Manar, Faculty
[c] Research Laboratory on Energy and Matter for Nuclear Science Development (LR16CNSTN02), Tunisia
[d] Tunisian Center for Nuclear Sciences and Technology, Technopark Sidi Thabet, Tunisia
[@] Corresponding author: zeinayaco@gmail.com

Background/Purpose: Nasopharyngeal carcinoma (NPC) is an aggressive malignancy requiring precise treatment, primarily through radiotherapy [1]. In Mauritania, no comprehensive dosimetric analysis had been conducted to optimize treatment techniques. This study is the first to compare three radiotherapy approaches for NPC treatment: three-dimensional conformal radiotherapy (3D-CRT), 3D-CRT combined with electrons (3D+E), and volumetric modulated arc therapy (VMAT).

Materials & Methods: The study was conducted on 67 patients treated at the National Oncology Center of Nouakchott. Dosimetric parameters such as dose coverage (D95), homogeneity index (HI), conformity index (CI), and doses to organs at risk (OAR) were analyzed using the Eclipse treatment planning system. Statistical comparisons between techniques were performed using the Wilcoxon test.

Results: The results indicate that the VMAT technique significantly improves dose coverage (D95) compared to 3D-CRT ($p = 0.04$) and 3D+E ($p = 0.01$). It also provides a better homogeneity index (HI) and conformity index (CI), while reducing doses to critical organs such as the spinal cord ($p= 0.001$), brainstem ($p = 0.005$), and parotid glands ($p < 0.002$). Additionally, VMAT minimizes high-dose exposure to healthy tissues (ISO30, ISO20, ISO10) compared to other techniques ($p < 0.05$).

Conclusion: This pioneering study highlights the significant advantages of the VMAT technique for NPC treatment in Mauritania. The findings support the adoption of this method to enhance clinical outcomes and reduce side effects [2]. Further studies are encouraged to refine local treatment protocols for NPC patients.

References:

[1] Fang W, Yang Y, Ma Y et al. Camrelizumab (SHR-1210) alone or in combination with gemcitabine plus cisplatin for nasopharyngeal carcinoma: results from two single-arm, phase 1 trials. Lancet Oncol. 2018 Oct;19(10):1338-1350. doi: 10.1016/S1470-2045(18)30495-9

[2] Ibrahim MS, Attalla EM, El Naggar M, Elshemey WM. Dosimetric comparison between three-dimensional conformal radiotherapy (3D-CRT) and intensity-modulated radiotherapy (IMRT) in the treatment of different stages of nasopharyngeal carcinoma. Journal of Radiotherapy in Practice. 2019;18(1):46-51. doi:10.1017/S1460396918000377

Keywords: Nasopharyngeal carcinoma, radiotherapy, dosimetry, 3D-CRT, VMAT

T3-O9: Impact of ionizing radiation and radiotherapy in cancer treatment

A. Mostefa-Kara@

[1] Univesité Paris Saclay
[2] Institut Gustave Roussy
@ Corresponding author ali.mostefa-kara@gustaveroussy.fr

Background/Purpose: Tumor-associated macrophages (TAMs) exhibit anti-inflammatory immunosuppressive properties that dictate prognosis and response to treatment in the majority of cancers. The functional reprogramming of these anti-inflammatory macrophages into pro-inflammatory macrophages has recently been proposed to improve the efficacy of anti-cancer treatments. A better understanding of the cellular and molecular mechanisms that regulate the biological functions of these macrophages is therefore necessary. Our team recently demonstrated the ability of ionizing radiation to trigger pro-inflammatory reprogramming of TAMs. [1]

Materials & Methods: The pro-inflammatory macrophage reprogramming program has been evaluated on different in vitro models (human and murine cell lines, on primary human and murine cultured cells) but also on in vivo models (human biopsies and mouse experiments). Different assay had been applied in order to evaluate the efficacy of radiation therapies on the macrophage reprogramming and its impact on tumor growth and survival time. In addition, different molecular actors have been identified as new actor in the process of macrophage reprogramming. [1-3]

Results: This process involves the activation of NADPH oxidase 2 (NOX2), the production of reactive oxygen species, the activation of ATM kinase as well as an increased expression of interferon regulatory factor 5 (IRF5), a transcription factor essential for the development of the pro-inflammatory phenotype of macrophages. In addition, our current work further characterized, on one hand this signaling pathway and revealed that following irradiation, the dynamic of macrophage's mitochondria is altered and leads to the accumulation of fragmented mitochondria in the cytoplasm of irradiated macrophages. On the other hand, we were able to characterized the activation of the proinflammatory phenotype after Gadolinium nanoparticles treatment alone or in combination with radiation [1]

Conclusion: This process induces a signaling pathway, which is similar to that triggered by viral infections, and increases the expression of IRF5. Overall, our team work contributes to a better understanding of the molecular mechanisms involved in the pro-inflammatory reprogramming of TAMs in response to ionizing radiation and makes it possible to identify new molecular targets whose therapeutic modulation could recondition the tumor microenvironment and increase the effectiveness of radiotherapy. [1]

References:

1. Wu Q, Allouch A, Martins I, Brenner C, Modjtahedi N, Deutsch E*, et al.* Modulating Both Tumor Cell Death and Innate Immunity Is Essential for Improving Radiation Therapy Effectiveness. Front Immunol 2017; 8: 613.
2. Biswas SK, Mantovani A. Macrophage plasticity and interaction with lymphocyte subsets: cancer as a paradigm. Nat Immunol 2010; 11: 889-896.
3. Mantovani A, Marchesi F, Malesci A, Laghi L, Allavena P. Tumour-associated macrophages as treatment targets in oncology. Nat Rev Clin Oncol 2017; 14: 399-416.

T4-O1: Numerical simulation of the IAEA benchmark regarding Nuclear Reactor Safety (NRS) accident scenarios

F. Ayad [1@], Y. Bouaichaoui [2]

[1] *Laboratory of Mechanical Engineering and Material Structures, University of Tissemsilt, Algeria*
[2] *Birine Nuclear Research Center/CRNB/COMENA/, BO180 Aïn Oussera, 17001 Djelfa, Algeria*
[@] *Corresponding author, E-mail address: fouad.ayad@univ-tissemsilt.dz*

Background/Purpose: The Computational Fluid Dynamics (CFD) code validation and verification activity, is frequently used for Nuclear Reactor Safety (NRS) relevant investigations. Typical application areas are studied: heterogeneous mixing and heat transfer in complex geometries, buoyancy-induced natural and mixed convection, etc., this work carried out at the Nuclear Research Center of Birine relevant of Atomic Energy Commission of Algeria as part of International Atomic Energy Agency (IAEA) Coordinated Research Project (CRP-I31034): Application of Computational Fluid Dynamics Codes for Nuclear Power Plant Design to assess the current capabilities of these codes and to contribute to technological progress in their verification and validation. With specific reference to (NRS) accident scenarios such as a Boron Dilution (BD) and Pressurized Thermal Shock (PTS).

Materials & Methods: Therefore, a set of Rossendorf Coolant Mixing (ROCOM) CFD- grade test data of mixing specifications was used to perform detailed calculations of the proposed benchmarks. The reference point is the injection of relatively cold core cooling water (ECC), which can induce buoyant stratification for PTS transient [1].

Results: The data obtained from the mixing experiment were compared with the results of Ansys-CFX calculations using Unsteady Reynolds-Averaged Navier–Stokes (URANS) for Shear Stress Transport (SST) k-ω turbulence model. Calculation results show a good qualitative and quantitative agreement with the experiment data using sensitivity and uncertainty measurement methods analysis for the error quantification and best estimate.

Conclusion: This work adds even more to the evaluation of CFD code capacities for in- vessel mixing simulation. comparing the tracer concentration space and time distribution in the downcomer and at the core inlet between the computational results and the experimental data. The creation of the perturbed zone in the lower plenum and downcomer was rationally inspected both qualitatively and quantitatively [2].

References:

[1]. Ayad, F., Baghdad, M., Bouaichaoui, Y., Höhne, T., 2023. Verification & validation of CFD predictions regarding pressurized thermal shock (PTS) situations in ROCOM installation: Comparison with IAEA benchmark. Nuclear Engineering and Design 413, 112498. https://doi.org/10.1016/J.NUCENGDES.2023.112498

[2]. IAEA-TECDOC-1908, Benchmarking of Computational Fluid Dynamics Codes for Reactor Vessel Design. (VIENNA, 2020). https://www-pub.iaea.org/MTCD/Publications/PDF/TE-1908_web.pdf. **Keywords:** Verification & Validation, ROCOM, mixing, ECC, PTS, boron dilution, uncertainty;

T4-O2: Analysis and simulation of passive systems in VVER reactors

E. Redondo-Valero[a], C. Queral[b@], K. Fernandez-Cosials[b], V. Sanchez-Espinoza[c]

[a]*NFQ Advisory Services S.L.*
[b]*Universidad Politécnica de Madrid (UPM)* [c]*Karlsruhe Institute of Technology (KIT)* [@]*Corresponding author*
cesar.queral@upm.es

Background/Purpose: A key function of safety systems is to remove core decay heat to maintain fuel integrity during an accident sequence. Conventional VVER reactor designs, such as the VVER-1000/V320, have safety systems that can remove residual heat in emergency situations, but these systems do not operate during station blackout conditions. To overcome this, some advanced VVER designs incorporate passive safety systems capable of maintaining decay heat removal even in the complete absence of AC power. This study focuses on analysing the performance of the air-cooled Passive Heat Removal System (PHRS) and Second Stage Hydro Accumulators (HA-2), two passive safety systems found in advanced designs such as the VVER-1000/V412, VVER-1200/V392M/V509/V523 and VVER-TOI [1].

Materials & Methods: In the present study, a model of the two passive safety systems of interest, the HA-2 and the air-cooled PHRS, have been implemented in a full plant model of a VVER-1000 reactor developed for the TRACE system code [2,3]. Subsequently, two accident sequences have been simulated, a Station Blackout (SBO) and an SBO along with a Loss of Coolant Accident (LOCA).

Results: The simulations show that the performance of the PHRS in an SBO scenario allows the core to be cooled for 24 hours. Furthermore, in the event of a LOCA following the SBO, the performance of the PHRS together with the HA-2 has been found to be able to replenish the reactor coolant system inventory and remove the decay heat for 24 hours as well.

Conclusion: This study shows that the combined performance of two passive safety systems incorporated in VVER reactors, the HA-2 and the air-cooled PHRS, allows not exceeding the core damage temperature in accident sequences under SBO conditions.

References:

[1]. Queral, C., Sanchez-Espinoza, V., Egelkraut, D., Fernandez-Cosials, K., Redondo-Valero, E,, Garcia-Morillo, A., 2021. Safety Systems of Gen-III/Gen-III+ VVER reactors. Nuclear España (october). http://www.revistanuclear.es/wp-content/uploads/2021/10/Art.seguridad-reactores.pdf

[2]. Redondo-Valero, E., Queral, C., Fernandez-Cosials, K., Sanchez-Espinoza, V. Safety margins improvement by means of the Passive Heat Removal System and the HA-2 in VVER-1000/V320 reactors. Progress in Nuclear Energy (preprint). http://dx.doi.org/10.2139/ssrn.4942879

[3]. Redondo-Valero, E., Queral, C., Fernandez-Cosials, K. Sanchez-Espinoza, V., 2023. Safety margins improvement by means of the passive second stage hydroaccumulators in a VVER-1000/v320 reactor. Nuclear Engineering and Design 414, 112644.
doi: https://doi.org/10.1016/j.nucengdes.2023.112644.

Keywords: advanced VVER; TRACE; Passive Safety Systems, PHRS, HA-2.

T4-O3: Numerical validation of fluid-to-fluid similarity theory for heat transfer with fluids at supercritical pressures

Y. Bouaichaoui[a@], F. Ayad[b]

[a] *Birine Nuclear Research Center/CRNB/COMENA/Algeria, BO180 Aïn Oussera, 17001 Djelfa, Algeria*
[b] *Laboratory of Mechanical Engineering and Material Structures, Tissemsilt University, B.P. 182, Algeria*
[@] *Corresponding author y.bouaichaoui@crnb.dz*

Background/Purpose: A summary is provided of the latest progress made in the creation of a fluid-to-fluid similarity theory for heat transfer with fluids at supercritical pressures using the Computational Fluid Dynamics (CFD) code validation activity, carried out at the Nuclear Research Center of Birine relevant of Atomic Energy Commission of Algeria as part of the International Atomic Energy Agency Coordinated Research Project (CRP) I31034 'Advancing Thermal-Hydraulic Models and predictive Tools for Design and operation of SCWR (Supercritical Water nuclear Reactors) Prototypes'. This activity was initiated at Experimental Thermohydraulics laboratory based on a study carried out to replace the primary fluid Freon 11 (CCl3F) through the fluid-to-fluid similarity analysis and CFD modeling of selected working fluid candidate to replace the R11: R123, R134a, R143a, Water and CO2[1,2]. The target is to provide a rationale for planning meaningful experiments with surrogate fluids and to suggest the best parameters of similarity to use and to propose heat transfer correlations.

Materials & Methods: For this purpose, heat transfer to fluids at supercritical pressure was modeled by Ansys-CFX CFDs[3] code for normal and buoyancy-affected conditions using different turbulence models for flow analysis.

Results: The results show that all turbulence models accurately predicted cases without heat transfer deterioration, but failed to accurately predict cases with heat transfer deterioration, although general trends were captured. Buoyancy phenomena occur inside a vertical flow, owing to the huge density changes along and across the channel, caused by the variation of the temperature, indicating that further improvements and modifications are needed for the turbulence models to better predict buoyancy deteriorated heat transfer.

Conclusion: In light of the evaluation of a significant body of information and understanding to support good prediction capacities for heat transfer with fluids at supercritical pressures, this work aims to contribute to a common reflection on the results obtained thus far.

References:

[1]. F. Ayad, Y. Bouaichaoui, H. Aboshighiba, Fluid-to-fluid similarity and CFD predictions of surrogate fluid as a replacement for R11 refrigerant used in a subcooled flow boiling analysis: validation against reference experimental data, Int J Heat Mass Transf 230 (2024). https://doi.org/10.1016/j.ijheatmasstransfer.2024.125772.

[2]. Y. Bouaichaoui, F. Ayad "CFD analysis of R123, R134a, R143a, R744 for replacement of CFC R11 used as refrigerant in thermal hydraulic test loop" 3rd International Conference on Radiations and Applications (ICRA-2022 Algiers, from 21 to 23 November 2022

[3]. Y. Bouaichaoui, B. Končar, Numerical and experimental investigation of convective flow boiling in vertical annulus using CFD code: Effect of mass flow rate and wall heat fluxes, Annals of Nuclear Energy 181 (2023). https://doi.org/10.1016/j.anucene.2022.109514.

Keywords: **Buoyancy, SCWR, CFD, Heat Transfer Deterioration;**

T4-O4: Development of a simulation platform and supervisory control for dynamic simulation of pressurized water reactor in load following mode of operation

M.F. Belazreg[1], B. Djaroum[2], H. Hasnaoui[1], M. Haddad[2], K. Halbaoui[2], A.C. Chergui[1], A. Berrahal[3], Y. Bouaichaoui[2]

[1]Department of Nuclear Safety, Nuclear Research Centre of Algiers
[2]Nuclear Research Centre of Birine [3]Nuclear Research Centre of Draria f.belazreg@crna.dz

Background/Purpose: This paper presents the new development platform using coupling program APROS, MATLAB and LabVIEW for modeling, simulation and control called "Co-Simulation". However, the Nodalization schemes is used to develop the nodal model of the reactor core, the steam generator, a non- equilibrium two-regions-three-volumes pressurizer model, were proposed based on the fundamental conservation of mass, energy and momentum. Then, these nonlinear models are controlled by supervisory systems were implemented in the MATLAB and APROS codes. The controllers are tested by two types of typical operational transients, namely the % step load change, the %/min ramp load change were simulated to study the dynamic behavior on the primary system of the VVER reactor. So, the adoption of coupling programming techniques and virtual machine, the Platform facilitates easy modification and runs, which easily allows the control system designer to test and compare various ideas efficiently.

Materials & Methods: The development of a "Co-Simulation" platform using coupling program APROS (neutronics and thermal-hydraulic), MATLAB (control parameters) and LabVIEW (display data) for modeling, simulation and control was carried out. The platform was designed using a code coupling approach that combines different APROS, MATLAB and LabVIEW programs. It allows to design a simulator for simulation purposes, to test controllers and safety analysis.

Results: In this paper, we focused our work on the development of new platform Software and aspect of the Multi-physics reactor modeling and simulation. The Co-simulation platform is composed by APROS thermal-hydraulic code, MATAB and LabVIEW HMI interface. The Exchange data is doing by TCP/IP protocol using machine virtualization and distributed component object model. Control approach has been applied from MATLAB to reactor core and pressurizer (APROS) to control reactor power over rods, pressure and level of the pressurizer.

Conclusion: In conclusion, this coupling provides a new ˝Co-Simulation Platform" to design and develops various approach controllers and safety analysis for the pressurizer water reactor VVER.

References:

[1]. M. S. El-Genk & al, 'Pressurizer dynamic model and emulated programmable logic controllers for nuclear power plants cybersecurity investigations ', Annals of Nuclear Energy, 2021.

[2]. Qingyang Wu & al, 'Analysis of critical pipe break sizes leading to reactor pressure vessel liquid level collapse and core uncovery with APROS', Progress in Nuclear Energy, 2021. [3]. Wang, and al. 'Multi-objective optimization of control parameters for a pressurized water reactor pressurizer using a genetic algorithm', Annals of Nuclear Energy 124, 9–20, 2019.

Keywords: VVER reactor, Supervisory control system, Advanced and intelligent controllers, APROS, MATLAB and Datalogging and Supervisory Control System LabVIEW, Co-simulation

T4-O5: Steady-State Qualification of the NuScale Small Modular Reactor Operation Using the RELAP5/SCDAPSIM3.4 System Code

A. HADJAM@, D. SAAD, A. L. Deghal-Cheridi , M. BOUAOUINA, A. DAHIA

Nuclear Research Center of Birine, B.P. 180 Ain Oussera,17200, Djelfa
@ Corresponding author a.hadjam@crnb.dz hadjam.ahmed@yahoo.fr

Background/Purpose: The NuScale Small Modular Reactor (SMR) represents a next-generation nuclear technology designed for enhanced safety, operational flexibility, and efficiency compared to traditional reactors. Utilizing a natural circulation cooling system and passive safety mechanisms, the NuScale SMR offers innovative solutions to nuclear energy challenges. This study aims to qualify the steady-state operational performance of the NuScale SMR using the RELAP5/SCDAPSIM3.4 system code, providing insights into its design reliability and operational stability under normal conditions.

Materials & Methods: The RELAP5/SCDAPSIM3.4 system code, known for its precision in simulating nuclear thermal-hydraulic behavior, was employed to model the NuScale reactor's core and primary coolant loop. A detailed model was developed, incorporating key features such as the integrated primary system, passive safety mechanisms, and modular design. Simulations focused on critical parameters, including temperature distributions, coolant flow rates, pressure levels, and heat transfer rates, under steady-state conditions. The results were compared to design specifications and operational safety limits.

Results: The simulation results demonstrate that the NuScale reactor maintains stable and safe operation within its design limits during steady-state conditions. Key thermal-hydraulic parameters were accurately predicted, validating the model's capability to replicate the reactor's operational characteristics. These results also highlight the effectiveness of the reactor's safety systems and its robustness in maintaining performance under nominal conditions.

Conclusion: This study validates the steady-state performance of the NuScale SMR and demonstrates the utility of the RELAP5/SCDAPSIM3.4 system code as an effective tool for reactor analysis. The findings support the NuScale SMR's design reliability and operational safety, offering valuable contributions to its licensing process and future deployment. Insights from this work further reinforce the potential of NuScale SMRs in advancing nuclear energy solutions globally.

References:

[1] Fridman, E., Y. Bilodid, and V. Valtavirta, Definition of the neutronics benchmark of the NuScale-like core. Nuclear Engineering and Technology, 2023.

[2] Kakaei, P., M. Zangian, and M. Abbasi, Multi-physics core analysis and verification of NuScale reactor with coupling PARCS/RELAP. Annals of Nuclear Energy, 2023. 193: p. 110021.

[3] Ingersoll, D., et al., NuScale small modular reactor for Co-generation of electricity and water. Desalination, 2014. 340: p. 84-93.

Keywords: NuScale; SMR; RELAP5/SCDAPSIM3.4; passive safety; natural circulation.

T4-O6: Impact assessment of electric grid resilience on nuclear power plant offsite power reliability considering HILP event

R. Benabid[1]

[1] *Electrical Engineering Department, CRNB*
r.benabid@crnb.dz

Background/Purpose: The Loss Of Offsite Power (LOOP) event can represent a major impact on nuclear safety where it can be caused by the High Impact Low Probability (HILP) events [1]. This paper presents an assessment method of the impact of electric grid resilience on the nuclear power plant (NPP) offsite power supply reliability in the presence of a HILP event.

Materials & Methods: A hybrid probabilistic/deterministic method is developed based on Monet Carlo method and electric grid time-domain simulation to assess the impact of high speed wind on electric grid resilience and therefore on an NPP offsite power reliability. The electric grid resilience is evaluated based on failure probability estimation of the grid transmission lines according to their fragility curves and wind speed. A LOOP event is considered occurred in case of voltage limits violation in the NPP connected bus compared to the nominal values [2-4].

Results: The proposed method is applied on IEEE 14-bus test system where the obtained results present the LOOP event probability, the set of failed transmission lines of each LOOP event. A LOOP event case is presented to show the voltage violation compared to its nominal values.

Conclusion: The impact of high speed wind on an NPP offsite power supply reliability was assessed in this paper using a hybrid probabilistic/deterministic method. This last is based on a combination of Monte Carlo method and electric grid time-domain simulation where the failure probability of transmission lines is calculated, at each sample, according to their fragility curves and the sampled wind speed Weibull distribution. The proposed method was applied on an interconnected IEEE 14-bus test system where it shows its efficiency and extension capability to consider more electric parameters and HILP events.

References:

[1]. Benabid, R., Henneaux, P. & Labeau, PE. Probabilistic assessment of switchyard-centered LOOP event frequency and duration in an NPP. Int J Syst Assur Eng Manag 15, 4105–4123 (2024). https://doi.org/10.1007/s13198-024-02416-6

[2]. Kamyab S, Nematollahi M, Henneaux P, Labeau P-E (2021a) Development of a hybrid method to assess grid-related LOOP scenarios for an NPP. Reliab Eng Syst Saf 206:1072–1098

[3]. Kamyab S, Nematollahi M, Henneaux P, Labeau P-E (2021b) Investigating the influence of the variation of the load characteristicon the occurrence frequency of grid-related loss of ofsite powerusing a probabilistic-deterministic methodology. Prog NuclEnergy 139:103870

[4]. International Atomic Energy Agency (2012) Electric grid reliability and interface with nuclear power plants, IAEA nuclear energy series. No. NG-T-3.8, IAEA, Vienna

Keywords: electric grid resilience; nuclear power plant; loss of offsite power; probabilistic modelling; fragility curve, high impact low probability event

T4-O7: Risk Reduction by means of Advanced Technology Fuels

C. Queral@, D. Canal[a], S. Courtin, J. Sanchez-Torrijos, E. Castro-Gonzalez,

[a]*Universidad Politécnica de Madrid (UPM)*
@*Corresponding author cesar.queral@upm.es*

Background/Purpose: At present, there is increasing interest in Accident Tolerant Fuels (ATFs) or Advanced Technology Fuels for light water reactors. These fuels have the potential to improve the nuclear safety and operational flexibility of commercial nuclear reactors. [1]. The ATFs incorporate advanced cladding materials and fuel compositions specifically designed to withstand higher temperatures, improve corrosion resistance and enhance fuel performance under both normal operating conditions and accident scenarios [2]. Among the various ATF designs, FeCrAl cladding is one of the most promising. Made from an iron- chromium-aluminium alloy, it offers exceptional resistance to oxidation and corrosion at high temperatures [3]. This makes it particularly useful in the event of accidents, where conventional zirconium-based cladding can oxidize rapidly and produce hydrogen. These reactions generate large amounts of heat and hydrogen, which can create a risk of explosion when mixed with oxygen [1].

Materials & Methods: To assess the safety aspect of ATFs, several analyses of typical accidental sequences in a LWR as the LOCA or the Station Blackout are performed using the TRACE system code. In particular the FeCrAl and Cr-coated claddings are used as the ATF fuel which will employ the oxidation correlations obtained during recent experiments. An assessment for a generic PWR Westinghouse. The main differences of using ATF will be exposed relative to regular fuel in terms of timings, temperatures and damage conditions along the accidental sequence. Besides, core damage frequency is quantified by means of a RiskSpectrum model for a generic PWR.

Results: The simulations show that the performance of the ATF in different accidental scenarios and the quantification with RiskSpectrum allows to obtain the risk reduction.

Conclusion: This study shows that the increase of available times during accidental sequences and the risk reduction (5%-25%) due to different ATF fuels.

References:

[1]. N. Doncel et al., "R&D in advanced technology fuels (ATFs) in Spain," Nuclear Engineering and Design, vol. 424, no. 113246, 2024, doi: https://doi.org/10.1016/j.nucengdes.2024.113246.

[2]. J. Zhang, P. Xu, M. Sevecek, K.-S. Sim, and A. Khaperskaia, "Contribution of IAEA coordinated research projects to light water reactors advanced technology fuel testing and simulation," Nuclear Engineering and Design, vol. 418, no. 112910, 2024.

[3]. J. Sanchez-Torrijos, "Assesment of safety issues in NuScale and Gen II PWR under accident conditions using TRACE. PhD Thesis, Universidad Politécnica de Madrid," 2024.

Keywords: LWR; TRACE; RiskSpectrum, ATF.

T5-O1: Chemical durability study of Rb doped nepheline syenite $RbAlSi_2O_6$ as a potential nuclear waste immobilization matrix

D. Moudir[a@], Y. Mouheb[a], N. Bensemma[b], F. Aouchiche[a], A. Amrane[c], A. Maachou[c]

[a] *Nuclear Research Centre of Algiers, 2. Bd frantz Fanon, BP: 399, AlgerRP,Algiers, Algeria*
[b]*Nuclear Research Centre of Birine (CRNB), BP 180, Ain Oussera, Djelfa* [c]*Nuclear Research Centre of Draria (CRNd), BP 43.Sebala. Draria Alger 16050*
[@] d.moudir@crna.dz

Background/Purpose: The leaching durability of the Rb doped nepheline syenite was carried out using the standard MCC-2 static leach test, simulating a radiological accident in a radioactive waste storage environment.

Materials & Methods: Material pellets are immersed in bi-distilled water, in flask closed in an oven at 90°C. The kinetic dissolution material was performed following: Si, and Al, elements dissolution in the leachates [1].The dissolution rate was monitored using plasma induction spectroscopy (ICP-OES). The concentrations of leachates, Ci (kg/cm³), for each element i, were determined using calibration curves from ICP-OES spectrometry, then the elemental mass loss, NLi (kg/m²) and the elemental leaching rate, RLi (kg/m².d) were calculated.

Results: There was a fast and intense increase in CSi until the 21st day, when it reached a maximum of 164.05 10^{-3}kg/m³, then decreased brutally until day 36.The C_{Si} reached 34.05 10^{-3}kg/m³ on the 42nd day. The evolution of CAl reached 4.915 10^{-3}kg/m³.However, NL_{Si} changed rapidly until the 21st day and then decreased to 4.7670 10^{-4}kg/m². Overall, Al mass losses are the lowest, reaching a maximum on the 7th day. At the end the values stabilise at lower values of around 1.4253 10^{-4} kg/m².

Conclusion: the dissolution rate of Al and Si is exponentially decreasing and stabilizes after the 3rdday; it is 1.5203.10^{-12} kg/m²d and 0.5335.10^{-4} kg/m2d respectively, which make our material a good candidate for the confinement of some RW elements.

References:

[1]. Strachan D. MGlass dissolution: testing and modeling for long-term behaviorJ. Nucl. Mater. 2001; 298: 69–77. doi:10.1016/S0920-5632(03)90969-8

Keywords: MCC2; nepheline syenite; radioactive waste; rubidium

T5-O2: Elemental Analysis of Medicinal Plants Using the k_o-INAA Method at NUR Research Reactor

L. Hamidatou[1@], S. Chahih[2], L. Benamar[2], A. Guesmia[1]

[1] *Nuclear Research Centre of Draria, PB43, Draria, 16050 Algiers, Algeria.*
[2] *Department of Physics, Faculty of Sciences, Saad Dahleb University, PB270. Blida 09022 Blida, Algeria*
[@]Corresponding author: l-hamidatou@crnd.dz

Background/Purpose: The exploration of medicinal plants for their nutritional and therapeutic potential is essential to advancing health and sustainability. This study aims to provide a detailed elemental analysis of three medicinal plants widely consumed in Algeria, renowned for their medicinal, culinary, and aromatic properties.

Materials & Methods: The k_o-Instrumental Neutron Activation Analysis (k_o-INAA) method was utilized to quantify 29 essential and trace elements in the selected plants. This method ensures high accuracy and reliability in assessing the elemental composition.

Results: The analysis revealed a rich presence of essential nutrients, particularly calcium, potassium, magnesium, and iron, which are crucial for human health. Zinc was also present in significant amounts, while toxic elements were detected at minimal concentrations, affirming the safety of these plants for consumption. Variability in elemental composition among the species was observed, attributed to their distinct ecological and geographical origins.

Conclusion: This study highlights the potential of Algerian medicinal plants as valuable dietary supplements and their contributions to sustainable food and health practices. The findings provide a robust scientific basis for the valorization of these plants in the food and pharmaceutical industries, emphasizing their role in promoting nutritional health and supporting environmentally sustainable approaches.

References:

[1] B. Nedjimi et al. Determination of some chemical elements in Rosmarinus tournefortii de Noé using instrumental neutron activation analysis, Journal of Applied Research on Medicinal and Aromatic Plants, Volume 2, Issue 1, 2015, Pages 34-37, https://doi.org/10.1016/j.jarmap.2014.12.001.

[2] S. Khaled et al. Elemental analysis of traditional medicinal seeds by instrumental neutron activation analysis. J Radioanal Nucl Chem 281, 87–90 (2009). https://doi.org/10.1007/s10967-009-0076-9.

Keywords: k_o-NAA, multi-elemental analysis, Medicinal plants, essential nutrients, trace elements.

T5-O3: Realization, control, and supervision of a laboratory-scale mini-pilot project to improve the removal and recuperation of radioactive pollutants by using new bioadsorbent.

I. Benettayeb[1], A. Benettayeb[1@], M. Hadj brahim[1], M. Belkacem[1], D. Moudir[2], B. haddou[1]

[1]*Université de Sciences et de la Technologie -Mohamed Boudiaf, USTO-MB, BP 1505 EL-M'NAOUAR, 31000 Oran, Algeria.*

[2]*Nuclear Research Centre of Algiers, 2. Bd Frantz Fanon, P.O.Box: 399, Alger-RP, Algiers,Algeria*

[@]Corresponding author ***asma.benettayeb@gmail.com***

Background/Purpose: In our work, we gained practical experience automating an industrial process with programmable logic controllers (PLCs). We identified and designed the necessary components, established their specifications, and optimized their placements using Siemens software (TIA Portal). We developed a mini-automated adsorption driver in dynamic mode to assist chemists in their research efficiently and created a guide focusing on the control aspects.

Materials & Methods: Adsorption is a spontaneous surface process where pollutant molecules adhere to a solid surface, forming layers. This ability to capture pollutants can occur in a partially reversible manner. Bio-adsorption specifically uses biological materials for pollutant fixation (Benettayeb et al., 2022). The effectiveness of adsorption for water purification is influenced by design efficiency and operating conditions. It can be performed in two modes: batch (discontinuous) or column (continuous) (Malbenia John et al., 2024). The main objectives of this study are the creation of new processes that can prove their effectiveness for the removal of radioactive metals from water by improved techniques to increase the efficiency of bioadsorbents X for the adsorption of pollutants Y. For this, We use for this creation, Automate programmable, column adsorption, pump, ect and for modeling we have use various software

Results: To carry out this realization, we went through several stages of modeling in different forms (specifications, grafcet, flowchart, etc.). During this work, we ordered, programmed, and supervised this process through well-known Siemens software (TIA Portal) which is software that can be used in the industry.

Conclusion: prototype ensures a high level of environmental protection and high-level treatment for nuclear waste. It is 100% automated with minimized and reduced human operator intervention this increases safety and can impact the economy because this prototype is widely used in laboratory scale and large industrial scale applications also we can use them for educational and/or research applications for different application in control and instrumentation in nuclear and also, environmental protection. We propose improvements in automation and chemical processes to enhance uranium removal and reduce chemists' workload.

References:

1. A Benettayeb et (2022). Some Well-Known Alginate and Chitosan Modifications Used in Adsorption : A Review. *Water Journal*, *14*(9), 1–26.
2. A Benettayeb et al (2024). Facile fabrication of new bioadsorbents from Moringa oleifera and alginate for efficient removal of uranium (VI). *Journal of Radioanalytical and Nuclear Chemistry*, *Vi*.

Keywords: metal elimination, industrial waste, Adsorption dynamique, Automatisation, Mini-pilote, Supervision,

T5-O4: Removal of silica from brackish water by electron beam-irradiation: membrane scaling prevention during water desalination by reverse osmosis process

F. Djouider

King Abdulaziz University, Nuclear Engineering Department, Jeddah, Saudi Arabia fdjouider@kau.edu.sa

Background/Purpose: Located in severe desert environment, many arid countries rely mainly on underground water as a water resource. However, silica concentration is high in this brackish water. This causes a recalcitrant deposit on the reverse osmosis (RO) semi- permeable membrane during desalination. This will reduce its lifetime and is a major limiting factor in water recovery rate. In this work we examined the efficacy of the electron beam- radiation induced removal of silica in water samples using zero valent metal iron as source of Fe^{3+} which serves as an adsorbent matrix for silica nanoparticles resulting in their co- precipitation and its removal by mechanical means.

Materials & Methods: In this work electron beam-irradiations of silica-containing water samples were performed using a continuous beam of electrons obtained from a 2.5 MeV van de Graaff linear accelerator. Irradiations were performed in 1.5 L tank reactors. Biochrom Libra S32 PC UV/visible double beam spectrophotometer was used to measure the residual silica concentration after each irradiation, following the silicomolybdate analytical standard protocol [1].

Results: At an initial pH of 2, equilibrium pH of 8.5 and for a dose rate of 2.7 Gy/min (Fe^0: 80 mg/L), residual silica concentration decreased with time at a faster rate for the first hour, then at a slower rate to reach a plateau after 3.5 hours. The optimum conditions for the removal of silica (up to 90%) were obtained with the following parameters: initial pH of 2, equilibrium pH of 8.5, dose rate of 2.7 Gy/min. Furthermore, the removal of silica reached a plateau at a concentration around 80 mg/L. The coagulation of ferric hydroxide by dissolved silicic acid proceeds via two different mechanisms depending on the equilibrium pH of the solution: charge neutralization or bridge formation [2].

Conclusion: This preliminary study shows that the ferric ions produced in the irradiated cell is effective in removing undesirable silica to prevent scaling of RO membrane in water desalination.

References:

[1]. Coradin T et al. The silicomolybdic acid spectrophotometric method and its application to silicate/biopolymer interaction studies. *Spectroscopy*. 2004;18:567–576. doi: 10.1155/2004/356207

[2]. Bremere I et al. 2000. Prevention of silica scale in membrane systems: removal of monomer and polymer silica. *Desalination*. 2000;132,89-100. doi: 10.1016/S0011-9164(00)00138-7

Keywords: Silica removal; Electron beam-irradiation; Absorbed dose effect; pH effect

T5-O5: Spatial assessment of natural soil radioactivity and its dosimetric impact on the population of Ghazaouet, Algeria

A. Hammadi[1@], Y. Bounouri[2], L.Boudjadi[2], D.Taieb errahmani[1], M.Boudria[1], M.Maache[1]

[1] *Centre de Recherche Nucléaire d'Alger (CRNA)*
[2] *Université A.Mira- Bejaia a-hammai@crna.dz*

Background/Purpose: Naturally occurring radionuclides such as Potassium-40, Uranium-238, and the Thorium-232 series contribute to natural radioactivity in geological formations and soils [1]. These radionuclides emit gamma radiation, which can have potential health implications. This study evaluates the specific activities of these radionuclides in soil and assesses the radiological risks associated with gamma radiation exposure in the Ghazaouet region of western Algeria.

Materials & Methods: Ten soil samples were collected from the Ghazaouet region using a standardized method over a 1 m² area. Subsamples (0–5 cm depth, ~200 g each) were combined into ~1 kg composite samples. After grinding and sieving, the samples were placed in 125 cc geometry containers and analysed via gamma-ray spectrometry using a high-purity germanium (HPGe) detector with an efficiency of 40%, over a 24-hour counting period.

Results: The average activity concentrations of Th-232, U-238, and K-40 across the study area were 22.56 Bq/kg, 18.12 Bq/kg, and 392.16 Bq/kg, respectively. These values are lower than the global averages of 30 Bq/kg, 35 Bq/kg, and 400 Bq/kg, respectively. The radium equivalent activity in Ghazaouet soils ranges from 37.78 to 139.92 Bq/kg, with an average of 80.57 Bq/kg, remaining well below the safety limit of 370 Bq/kg. The annual effective doses ranged from 0.092 to 0.370 mSv/year, with an average of 0.204 mSv/year, well below the 1 mSv/year limit recommended by UNSCEAR, ensuring no significant radiological risk to the public. The hazard indices Hin and Hex ranged from 0.136 to 0.439 and 0.120 to 0.378, respectively, all below the UNSCEAR-recommended threshold of 1, indicating no significant radiological hazard. The average excess lifetime cancer risk (ELCRT) was 0.779×10^{-3}, also below the UNSCEAR limit of 1.45×10^{-3}, further confirming a low radi- ological risk [3].

Conclusion: The findings confirm that the radiological hazards associated with soil in the Ghazaouet region fall well within internationally accepted safety limits, ensuring no significant health risks for the local population. Furthermore, the study provides valuable insights into environmental research and management, and establishes a strong foundation for addressing both current and emerging radiological challenges.

References:

[1] S.,Seow, P.M., Viswanathan, D., Dodge-Wan Jones, (2024). Distribution of natural radioactivity in different geological formations and their environmental risk assessment in Malaysia. Journal of Environmental Science and Pollution Research International, Volume 31, pages 43292–43308. https://doi.org/ 10.1007/s11356-024-33906-6.

[2] UNSCEAR. Sources and effects of ionizing radiation (2000). Annex B. Report to the general assembly, Exposures from natural radiation sources.

[3] R.D., Senthilkumar, and R., Narayanaswamy (2016). Assessment of radiological hazards in the industrial effluent disposed soil with statistical analyses. Journal of Radiation Research and Applied Sciences 9.4: pp 449-456. https://doi.org/10.1016/j.jrras.2016.07.002.

Keywords: Radium equivalent activity; gamma-ray spectrometry; annual effective dose; radiological hazards; excess lifetime cancer risk.

T5-O6: Dynamic study of Oklo cores, towards the influence on life

E.D. Durastanti Rabnga Mombo[1,2@], B. Gall[1], S.Y. Loemba Mouandza[2], T.B. Ekogo[2], S. Bentridi[3] And H. Hidaka [4]

[1] University of Strasbourg, CNRS, IPHC UMR 7178, Strasbourg F-67000, France
[2] University of Science and Technology of Masuku, Radioanalysis Laboratory, 943 Francville , Gabon
[3] LESI, Faculty of Science and Technology, Khemis Miliana University,44225, Algeria
[4] Department of Earth and Planetary Sciences, Nagoya University, Nagoya 464-8601, Japan
@ Corresponding author: dominique.durastanti@iphc.cnrs.fr

Background/ Purpose: It may be stated that the presence of natural nuclear reactors could have a significant impact on life in general on earth. But, despite the fact that they were discovered close to surface, the Oklo cores were approximately 2000 m underground when they were operated. They could therefore only affect the microbiota present in the rocks. Their discovery in 1972 in Gabon, offers a unique opportunity to study the interactions between the activity generated by their operation and the micro- organism in a geological environment. The inception and operation of such complex systems in a geological environment remains partially unexplained. In his study R. Naudet detailed quite a lot of observations [1] but could not give an exhaustive explanation. The work of S. Bentridi et al. in 2013 [2] could give for the first time an explanation of the inception and the start-up of these reactors. Our study aims to provide more answers to the various questions related to the Oklo phenomenon, in particular how did these reactors operate? Under what conditions did they evolve? What is the environmental impact induced by their operation?

Materials & Methods: Among all the Reaction Zones discovered, RZ9 will be the subject of our study. It is one of the smallest Oklo reactors whose characteristics are well known. We aim to use the realistic criticality conditions at the start-up of this core in order to model the temporal evolution of its operation through neutron simulation methods carried out by means of OpenMC, a Monte Carlo transport code, coupled with the Runge-Kutta 4 method to account for the temporal evolution, all implemented with Python. These simulations will make it possible to analyze the variations of several parameters such as the infinite multiplication factor k_∞, which gives information on the reactivity of the system, the neutron flux, the migrations of fission products and the evolution of the size of the reactor, in order to reconstruct the operating cycles of this particular reactor, which could extend to the others. Genetic dynamics approach will be developed to study the impact of radiation on surrounding microorganisms. By integrating biological models with neutron simulations, we will explore the effects of radiation on the evolution and adaptation of microbial species contained in the Oklo cores during reactor operation.

Results: This work is in progress; the different steps of the study will be presented as well as the present situation.

Conclusion: This work will be a contribution to the understanding of the functioning of natural nuclear reactors, but also to a better understanding of the interactions between natural nuclear systems and the micro biota, with potential implications in reactor physics, radiobiology, and management of radioactive environments.

References:

[1]. Naudet R., Oklo: Des réacteurs nucléaires fossiles – Etude physique (in French). France Eyolles, 1991.

[2]. Bentridi S-E, Gall B, Gauthier-Lafaye F, Seghour A and Medjadi D-E 2011 Inception and evolution of Oklo natural nuclear reactors Comptes Rendus Geoscience 343 738–48.

[3]. Bentridi S-E et al., The influence of some rare earth elements as neutron absorpers on the incetion pf oklo natiral nuclear reactors, https://doi.org/10.1093/rpd/ncad048.

Keywords: **Natural nuclear reactor, micro-organism, OpenMC, core dynamics, genetic dynamics**

T5-O7: New insights of the Oklo natural fission reactors elucidated from isotopic studies using state-of-the-art analytical techniques

H. Hidaka[1@], S. Kagami[2], S. Bentridi[3], B. Gall[4]

[1] *Nagoya University, Japan*
[2] *Tono Geoscience Center, Japan Atomic Energy Agency, Japan*
[3] *Khemis Miliana University, Algeria*
[4] *Université de Strasbourg, France*
[@] *Corresponding author* hidaka@eps.nagoya-u.ac.jp

Background/Purpose: It is known that 16 parts (called as reactor zones, hereafter "RZs") of the Oklo uranium deposit in the Republic of Gabon, central Africa, functioned as natural fission reactors around two billion years ago. Many elements of the Oklo RZs materials show variations in their isotopic compositions caused by a combination of nuclear fission, neutron captures, and radioactive decays. Isotopic data sets of several elements, particularly rare earth elements (REEs), of the Oklo RZs materials provide useful information on the determination of nuclear parameters during the RZs criticality, construction of the model for the reactor criticality by numerical simulation, evaluation of geochemical behaviours of fission products in geological media, and so on. Many of the isotopic data of the Oklo RZs materials were given more than a quarter of century ago [1,2]. However, if we can get more precise isotopic data of the RZ materials, we may get new insights of the Oklo phenomenon.

Materials & Methods: Two kinds of the Oklo reactor materials collected from RZs 13 and 16 were used in this study. Each sample was once dissolved by acid, and turned to the solution. Individual REEs and Hf of the acid solutions were chemically extracted for isotopic analyses of the individual elements by conventional resin chemistry. Then, the isotopic compositions of individual elements are now being determined by mass spectrometry.

Results: The isotopic compositions of REEs and Hf of the Oklo RZs materials have been planned to newly collect within 0.01 % of analytical precisions. In particular, Hf isotopic measurements of the Oklo materials have never been performed in any previous study, which may provide information on higher-energy neutrons rather than thermal neutrons.

Conclusion: Isotopic analyses of REE and Hf are still in progress. Most isotopic data have been collected within 0.01 % of analytical precisions which are expected to be sufficient to reconstruct the neutron energy spectra of the Oklo RZs.

References:

[1]. Holliger P. and Devillers C. Contribution à l'étude de la température dans les réacteurs fossiles d'Oklo par la mesure du rapport isotopique du lutétium. *Earth and Planetary Science Letters*. 1981;52:76-84. doi:10.1016/0012-821X(81)90209-0

[2]. Hidaka H. and Holliger P. Geochemical and neutronic characteristics of the natural fossil fission reactors at Oklo and Bangombé, Gabon. *Geochimica et Cosmochimica Acta*. 1998;62:89-108. doi:10.1016/S0016-7037(97)00319-0

Keywords: rare earth elements; isotope; neutron capture; natural fission reactor

POSTER SESSIONS

T1-P1: Assessment of thermal neutron capture cross section for the ^{197}Au (n, γ)^{198}Au reaction

F Meddad[1@], M Boussaid[2], N Belouadah[3], K Boukeffoussa[1] and T Seguini[4]

[1]*Division of Physics –Nuclear Research Center of Algiers (CRNA), 02 Frantz-Fanon Boulevard, P.O. Box 399, Algiers-RP, 16000, Algeria.*

[2]*University Ahmed Draia of Adrar, Algeria.*

[3]*SNIRM Laboratory, Faculty of Physics (USTHB), BP 32, 16111 Algiers, Algeria.*

[4]*Division of Physics and Nuclear Applications – Nuclear Research Center of Draria (CRND), Sebala Road, P.O. Box 43, Algiers, Draria 16050.*

[@] *Corresponding author f.meddad@crna.dz; Medd.fouzia@univ-adrar.edu.dz*

Background/Purpose: This study aims to evaluate the thermal neutron capture cross section for the ^{197}Au (n, γ) ^{198}Au reaction by analyzing both experimental data and existing library data. The goal is to predict the gold cross section at the thermal neutron energy for the NUR reactor. The approach combines theoretical data and available experimental data to interpolate and extrapolate the missing cross section values. Twenty-two data points were selected. After parameterization and proper treatment, the recommended value of the thermal neutron capture cross section for gold was determined to be 257.74 b at 0.003626 eV. Additionally, experimental measurements will be conducted at this reactor to measure the thermal neutron capture cross section using this predicted value as a reference reaction and to confirm their applicability in this specific reactor environment.

Materials & Methods: Data from numerous publications, both Exfor and data from the ENDF/B-VIII library, were reviewed and collected. These data come from various experimental setups designed to measure the thermal neutron capture cross section of gold. [1,2]

Results: We evaluated the standard cross section of the ^{197}Au (n,γ) ^{198}Au reaction at 3.626 meV using the experimental data reported by Dilg et al, Teutsch et al, Otuka et al and the data from the ENDF/B-VIII library, through a fitting procedure, as shown in Fig. 1. The obtained value was 257.74 b at 3.626 meV. This value is in agreement with most theoretical data, confirming the accuracy of the selected methods.

Conclusion: After a thorough analysis of the data, the recommended value for the gold capture cross section is presented. These results will be essential for future research and applications in nuclear physics, particularly in reactor design and neutron detection technologies. Furthermore, This will help refine the accuracy of neutron flux calculations, optimize the use of the NRF facilitie, and enhance simulation models for more advanced research in the field of nuclear physics.

References:

[1] W. Dilg, W. Mannhart, E. Steichele, P. Arnold, Precision neutron total cross section measurements on gold and cobalt in the 40 ?eV-5 meV range, Z. Fur Phys. 264 (1973) 427–444. https://doi.org/10.1007/BF01391712.

[2] D.E. Cullen, POINT2021: ENDF/B-VIII.0 Temperature Dependent Cross Section Library, IAEA Nuclear Data Section, 2021. https://doi.org/10.61092/iaea.v58f-apcv.

Keywords: Thermal neutron capture, gold, experimental methods, activation, transmission, neutron cross section.

T1-P2: Exploring the Weibel Instability: Self-Generated Magnetic Fields, Plasma Dynamics, and Energy Absorption through Inverse Bremsstrahlung

R. Naceur [@], A. Sid

[1] University of Batna 1
[2] Physics of radiation and its interactions with matter LRPRIM
[3] Department of Physics
[@] rebiha.naceur@univ-batna.dz

Background/Purpose: The Weibel instability is a physical phenomenon in plasma that arises from counter-streaming currents caused by the inhomogeneous motion of electrons, leading to the generation of self-induced magnetic fields.

Materials & Methods: The study examined Weibel instability in homogeneous plasma using a high-frequency laser to explore energy absorption via inverse bremsstrahlung. It employed the Fokker-Planck equation to model electron distribution and derived dispersion relations to analyze the interaction between self-generated magnetic fields and laser fields, focusing on unstable modes near the plasma's critical layer. The analysis was based on theoretical methods.

Results: Weibel instability generates strong magnetic fields (megagauss scale) from inhomogeneous electron motion and counter-streaming currents. These fields disrupt heat transport and plasma corona expansion, reducing energy transfer efficiency. Additionally, high growth rates of non-collisional modes (~10^{11} - 10^{12} s^{-1}) emerge near the plasma's critical layer, driven by laser interaction.

Conclusion: The Weibel instability, driven by counter-streaming currents from inhomogeneous electron motion, generates self-induced magnetic fields. It arises from non- uniform laser energy absorption, heat transport, and non-collisional processes in plasma. This instability impacts heat transfer and plasma dynamics, potentially stabilizing some modes under certain conditions. Understanding it requires theoretical, numerical, and experimental approaches, with applications in inertial confinement fusion research.

References:

[1]. A. Bendib, K. Bendib, and A. Sid Weibel instability due to inverse bremsstrahlung absorption Phys. Rev E 1997;55 7522: DOI: https://doi.org/10.1103/PhysRevE.55.7522

[2]. Slimen Belghit; Abdelaziz Sid Stabilization effect of Weibel modes in relativistic laser fusion plasma *Phys. Plasmas* 2016; 23: 87-96. https://doi.org/10.1063/1.4953106

DOI: https://doi.org/10.1063/1.4953106

[3]. Boultif Oussama, Ghezal Abdenasser and Abdelaziz Sid
Electron-ion inverse bremsstrahlung absorption in magnetized fusion plasma Europhysics Letters 2021;133: 55001. https://iopscience.iop.org/article/10.1209/0295-5075/133/55001

Keywords: the Weibel instability; Self-Induced Magnetic Fields Inverse Bremsstrahlung; Plasma Dynamics; Theoretical Modeling;

T1-P3: Semi empirical formula for (n,d) reaction cross section at 14-15 MeV

S. Nehaoua[1@], A. Ghezal[1] , F. Bouchelaghem[1], N. Benaidja[2]

[1]*Laboratory of materials and renewable energy, faculty of science, department of physics, University of Msila, University pole, Bordj Bou Arreridj, M'sila 28000, Algeria*

[2]*Common trunk, Faculty of technology, University of Msila, University pole, Bordj Bou Arreridj, M'sila 28000, Algeria*

[@] Corresponding author samra.nehaoua@univ-msila.dz

Background/Purpose: A semi empirical formula for (n,d) nuclear reaction cross section is proposed. The systematic was derived using analytical expressions for the calculation of the deuterium emission spectrum in (n,d) nuclear reactions. The pre-equilibrium exciton model and the evaporation model are used to describe the deuterium emission. The experimental data are used to adjust free parameters in systematic formula at 14-15 MeV. The systematics gives closer results to experimental data compared with formulas earlier studies.

Materials & Methods: The pre-equilibrium exciton model and the evaporation model are used to describe the deuterium emission; previous studies have ignored pre equilibrium mechanism.

Results: The proposed semi empirical systematic describe better (n,d) function excitation and gives least values of statistical parameters which proof the quality of our formula [1,2].

Conclusion: The systematics gives closer results to experimental data compared with formulas earlier studies. The proposed semi empirical systematic describe better (n,d) function excitation and gives least values of statistical parameters which proof the quality of our formula.

References:

[1]. Yiğit M (New semi-empirical formulae for (n,d) cross sections at 14–15 MeV). Applied Radiation and Isotopes. 2021; 176. doi: https://doi.org/10.1016/j.nucengdes.2014.09.018

[2]. Belgaid M. et Asghar M. Semi-empirical systematics of (n, p) reaction cross sections for 14.5 MeV neutrons. *Applied radiation and isotopes*, 1998, vol. 49, no 12, p. 1497-1503. doi:https://doi.org/10.1016/S0969-8043(98)00054-2

Keywords: semi-empirical **formula**; (n,d) reactionscross **section**; pre equilibrium model.

.

T1-P4: Evaluation of neutron capture cross-section at 25 keV for ^{165}Ho and ^{166m}Ho isotopes using Talys code

A. Dib[1@] and N. Belouadah1

[1] *SNIRM Laboratory, Faculty of Physics (USTHB), P.O. Box 32, El-Alia, Algeria*

[@] *Corresponding author* dib_amel@hotmail.com

Background/Purpose: Holmium-67 (Ho) caught the experts attention due to its medical properties. It is suitable for both diagnostic and treatment. It can be imaged thanks to its paramagnetic properties and by using single- photon emission computed tomography. Also, holmium is a good candidate for therapeutic treatments [1]. Since that the knowledge of cross sections of nuclear reactions induced by neutrons is required for such field, this study aims to calculate theoretically the neutron capture cross-section for the neutron-induced reactions 165Ho(n,γ)166Ho and 166mHo(n,γ)167Ho by using the Talys 1.96/2.0 nuclear code at 25 keV. The obtained values are 1.42 b and 2.60 b respectively. The Talys code is a nuclear reaction program which provides a complete and an accurate simulation of nuclear reactions. It combines various nuclear models in order to analyse basic nuclear reaction experiments or to generate nuclear data for applications [2].

Materials & Methods: The theoretical values obtained by the nuclear reaction porgram Talys 1.96/2.0 are compared with the experimental data extracted from the EXFOR database in order to test the validity of the Talys nuclear code and to seek agreement between the obtained and the experimental values.

Results and conclusion: Through the comparison of our calculations and the tabulated experimental values, a good agreement with the experimental data of EXFOR database is observed for the 165Ho (n,γ)166Ho reaction, however, there is no experimental available values for the 166mHo(n,γ)167Ho reaction. The difficulty of conducting experiments with radioactive targets is due to the complex decay and activation schemes. This is one of the reasons why the thermal neutron cross section are scarce in the literature for the 166mHo(n,γ)167Ho reaction, when compared with reactions with stable isotopes.

References:

[1]. Klaassen, N.J.M., Arntz, M.J., Arranja, A.G., Roosen, J., Nijsen, J.F.W., 2019. The various therapeutic applications of the medical isotope holmium-166: a narrative review. EJNMMI Radiophar, Chem, 4, 19

[2]. A.J. Koning, S. Hilaire, S. Goriely, TALYS: modeling of nuclear reactions, Eur. Phys. J. A 59, 131 (2023). https://doi.org/10.1140/epja/s10050-023-01034-3.

Keywords: cross-section; (n,γ) reaction; Talys code

T1-P5: Novel semi empirical systematic for (n,t) cross section at 14,6 MeV

A. Ghezal[1@], S. Nehaoua [1], Nouri Benaidja [2]

[1] *Laboratory of materials and renewable energy, faculty of science, department of physics, University of Msila, University pole, Bordj Bou Arreridj, M'sila 28000, Algeria.*

[2] *Common trunk, Faculty of technology, University of Msila, University pole, Bordj Bou Arreridj, M'sila 28000, Algeria.*
[@] *Corresponding author asma.ghezal@univ-msila.dz*

Background/Purpose: A theoretical semi-empirical formula is derived for calculating the (n, t) nuclear cross-section at 14.6 MeV neutron energy. This study aims to improve the prediction accuracy of cross-sections by incorporating Q-value dependence and asymmetry parameters, building on the pre-compound mechanism with the exciton model.

Materials & Methods: The proposed formula is derived using theoretical models that describe the pre-compound reaction mechanism. The Q dependence and asymmetry parameters were key inputs in refining the formula. Experimental data from the literature were utilized to validate and optimize the free parameters of the formula [1,2].

Results: The suggested formula provides a better fit to experimental data compared to previously established models. It accurately predicts the excitation function for energies greater than 15 MeV, showing consistency with observed trends and improving upon the limitations of earlier approaches.

Conclusion: The new formula enhances the accuracy of (n, t) reaction cross-section predictions at 14.6 MeV, offering a reliable tool for theoretical and applied nuclear physics. Future work will focus on extending the model to a broader energy range and validating it with additional experimental datasets.

References:

[1]. Qaim S. M., "Nuclear cross sections for (n, t) and related reactions." *Nuclear Physics A*. 1984;438:384.

[2]. Nehaoua S., "Semi-empirical systematic of (n, 3He) reaction cross section at 14.6 MeV." *Nuclear Instruments and Methods in Physics Research Section B*. 2020;484:71–74.

[3]. Nehaoua S., "Semi-empirical systematic of (n, 3He) reaction cross section at 14.6 MeV." *Nuclear Instruments and Methods in Physics Research Section B*. 2020;484:71–74.

Keywords: (n,t) cross section; tritium emission; semi-empirical systematic.

T1-P6: Excitation functions of (n, ^{3}He) and (n, t) reactions on ^{93}Nb

L. Yettou[1@], N. Belouadah [1], N. Amrani[2], N. Taibouni[1], F. Kadem[1], M. Belgaid[1]

[1] *University of Sciences and Technology Houari Boumediene, Faculty of Physics*
[2] *University Ferhat Abbas, Setif1*
[@] *Corresponding author lyettou@usthb.dz*

Background/Purpose: The (n, He-3) reaction in the energy range between 1 to 20 MeV is one of the weakest reactions. Through a very elaborate radio- chemical work [1] it was shown that its cross section is around a few microbarn where the (n, t) cross section is about
0.4 mb for 14.6 MeV and 1.08 mb for 19 MeV. The main purpose of this work is to investigate the sensitivity on the statistical model of the Hauser-Feshbach theory to describe the equilibrium emission from the compound nucleus and calculate the excitations functions of (n, He-3) and (n, t) reactions on 93Nb.

Materials & Methods: In this study, the calculations of (n, He-3) and (n, t) reactions on ^{93}Nb are used in the framework of equilibrium model by using the Talys code [2]. We used the statistical model which is an advanced implementation of the Hauser-Feshbach theory to describe the equilibrium emission from the compound nucleus. In Talys code [2], all optical model calculations are performed by ECIS-06 [3], which is used as a subroutine and the Fermi gas model has been used for the level density.

Results: The excitation functions of the (n, He3) and (n, t) reactions on 93Nb are described well by Hauser-Feshbach calculations and the investigation on optical model calculations with the Fermi gas model for the level density were important for our results.

Conclusion: In this work, we have analyzed the calculated of (n, He-3) and (n, t) reactions on 93Nb by using nuclear reaction model in Talys code [2]. Our results show that the calculations of the Hauser-Feshbach theory show the similar behavior with the experimental data of Exfor database.

References:

[1]. Qaim, S.M.,1974. A study of (n,He-3) reactions at 14.6 MeV on medium and heavy mass nuclei.J.Inorg.Nucl.Chem.36(2),239–244.

[2]. A.J. Koning, S. Hilaire, S. Goriely, TALYS: modeling of nuclear reactions, Eur. Phys. J. A 59, 131 (2023). https://doi.org/10.1140/epja/s10050-023-01034-3.

[3]. Raynal, J., 1994. Notes on ECIS94, CEA Saclay *Report No. CEA-N-2772*.

Keywords: (n, 3-He) and (n, t) reactions; Hauser- Feshbach theory; Talys code;

T1-P7: Nuclear Gamma-ray emission induced by protons on Aluminium

A. Belhout[1@], D. Moussa[1], N. Hebouche[1], D. Kerrai[1], Y. Rahma[2], W. Yahia-Cherif[2], S. Damache[2], S. Ouziane[1], A. Chafa[1], M. Debabi[1] and S. Ouichaoui[1]

[1] *Faculty of Physics, USTHB, B.P. 32 El alia, 16111 Bab Ezzouar, Algiers, Algeria*
[2] *Nuclear Technics Division, CRNA, 02 Bd. Frantz Fanon, B.P. 399 Alger-gare, Algiers, Algeria*
[@] *Corresponding author abelhout@usthb.dz*

Background/Purpose: This work is a contribution to the spectroscopic study of the nuclear lines emitted when matter is bombarded by protons. The main physical quantities evaluated in our study are the experimental and theoretical total cross sections of the reactions. The actual database consists of a scarce number of cross sections measured for incident energies not exceeding 66 MeV [1,2]. Whereas, data are required for energies extending up to ~ TeV. This data is important for applications such as fusion, accelerator- driven applications, nuclear astrophysics, nuclear medical applications and dosimetry.

Materials & Methods: The experiment was carried out at iThemba LABS (South Africa) in which proton beams accelerated to energies ranging from 30 to 200 MeV. The beam was directed to the target chamber to irradiate an aluminium target. The detection of γ rays was achieved by means of the AFRODITE array that consisted of 8 clover-detectors surrounded by BGO Compton-suppressor shields, giving us 256 spectra file to analyse.

Results: The analysis of the experimental spectra using the radware software allowed us to derive the angular distributions of eight γ-ray lines produced by the irradiation of the aluminium target. We obtained new cross sections data measured for the production of the γ-lines produced by the aluminium target irradiation via (p,xγ) reactions. We used the Talys calculation code to reproduce the cross-section measurements we had obtained experimentally, in order to determine a set of effective parameters used in nuclear reaction models. This will enable us to extrapolate to energies that have not been reached experimentally. The overall agreement between theory and experiment has been appreciably improved by using modified optical model potential (OMP), level deformation, and level density parameters. Hence, parameters relating to the nuclear structure are also deduced in this work.

Conclusion: Our data consistently extend the measured ^{27}Al(p,xγ) reaction cross sections to higher proton energies and then enriches the database. The confrontation of our data to their theoretical counterpart indicates that more reliable involved parameters must be used.

References:

[1]. W. Yahia-Cherif et al., Phys.Rev.C 102, 025802 (2020).
doi: 10.1103/PhysRevC.102.025802
[2]. Y. Rahma et al., Nucl. Phys. Nucl. Phys. A 1032, 122622 (2023).
doi: 10.1016/j.nuclphysa.2023.122622

Keywords: nuclear γ-rays, experiment cross sections, theoretical calculations.

T1-P8: Study of nucleon-^{nat}Ca reaction cross sections in the framework of the optical model potential. Comparison to experimental data and TALYS code predictions

W. Yahia Cherif[1,@], S. Damache[1], Y. Rahma[1],A. Belhout[2],D. Moussa[2], S. Ouichaoui[3]

[1] *CRNA, 02 Boulevard Frantz Fanon, B.P. 399 Alger-gare, Algiers, Algeria*
[2] *University of Sciences and Technology Houari Boumediene (USTHB), Laboratory of Nuclear Sciences and Radiation-Matter Interactions (SNIRM-DGRSDT), Faculty of Physics, P.O. Box 32, EL Alia, 16111 Bab Ezzouar, Algiers, Algeria*
[3] *Retired from University of Sciences and Technology Houari Boumediene (USTHB)*
[@] *Corresponding author w.yahiacherif@crna.dz*

Background/Purpose: Our aim is to determine through nucleon elastic/inelastic scattering and reaction cross section data the optical model potential (OMP) [1] parameters for nucleon-^{nat}Ca induced reactions. The improvement of the theoretical prediction for this reaction is of major interest in astrophysics as well as in medical physics (proton/neutron therapy).

Materials & Methods: We have optimized the optical model potential (OMP) parameters for protons and neutrons induced reaction on natCa, using a previously determined OMP for nucleon-40Ca [2], with the OPTMAN code [3] available on the RIPL-3 data library [4]. The potentials, geometrical and nuclear deformation parameters, previously extracted for 40Ca, were completed by determining the isospin contribution of the potentials via fitting angular distribution data for protons/neutrons elastic and inelastic scattering off 48Ca available in EXFOR data library [5]. We have, then, used our optimized OMP to calculate total and partial reaction cross sections for different outgoing channels using TALYS nuclear reaction code. Modifications to nuclear level density models used by default in TALYS was also performed to fine tune the results.

Results: Both calculations using TALYS built-in default parameters and our optimized OMP parameters were confronted to experimental data taken from the EXFOR library. Our calculations evidence betterment compared to the predictions of TALYS using default parameters.

Conclusion: We have extracted a new set of OMP and nuclear deformation parameters for both protons and neutrons interacting with calcium isotopes. Our OMP parameters and nuclear deformations improve the theoretical predictions compared to available OMPs in the literature for incident particle energies ranging between 0-200 MeV.

References:

[1]. Koning A.J. and Delaroche J.P.. Nuclear Physics A. 2003;713(3-4):231-310. DOI: https://doi.org/10.1016/S0375-9474(02)01321-0

[2]. W. Yahia Cherif, S. Damache, S. Ouichaoui, J. Kiener, E. A. Lawrie, *et al.*, Compound Nuclear Reactions and Related Topics (CNR*24), 8-12 July 2024, Vienna (Austria).

[3]. Soukhovitski E. S. et al., OPTMAN code v1. https://www-nds.iaea.org/RIPL-3/codes/OPTMAN/ [4]. Reference Input Parameter Library-3 (RIPL-3), https://www-nds.iaea.org/RIPL-3/

[5]. Experimental Nuclear Reaction Data (EXFOR), https://www-nds.iaea.org/exfor/exfor.htm

Keywords: nuclear reactions, cross sections, optical model potentials, OPTMAN, TALYS

T1-P9: Determination of cross sections for (*n*, *p*) reaction on Ge isotopes induced by 14 MeV neutrons

N. Belouadah[1@], L. Yettou[1], F. Kadem[1] N. Osmani[2], N. Taibouni[1] and M. Belgaid[1]

[1] *SNIRM Laboratory, Faculty of Physics (USTHB), P.O. Box 32, El-Alia, Algeria*
[2] *Neutron Activation Analysis Department, Nuclear Research Centre of Birine (CRNB), P.O. Box 180, Algeria*
@ Corresponding author: b_belouadah@yahoo.fr

Background/Purpose: Studies of excitation functions of neutron induced reactions around 14 MeV are of considerable importance for practical applications, such as in fusion reactor technology, integral calculation in the first wall, blanket, and shield of a conception fusion power reactor [1]. As an important semi-conducting material, the neutron induced reaction cross section of germanium around 14 MeV has been measured and determined by many laboratories. However, relatively large disagreement and uncertainty can be observed in these data [2]. The main purpose of this work is to determinate of the effective sections of the reactions (n,p) induced by fast neutrons of energy around 14 MeV for the ^{72}Ge, ^{74}Ge and ^{76}Ge isotopes.

Materials & Methods: : In this study, we have calculated the (n, p) reaction on germanium isotopes using the empirical formulas based on the Hauser-Feshbach statistical model, from which we deduce the formulas of the Weisskopf-Ewing evaporation model [3]. The theoretical values obtained by the nuclear reaction program SCAT-2 are compared with the experimental data extracted from the EXFOR database and Talys nuclear code.

Results: A systematic study of excitation functions based on the empirical formulas of compound nucleus formation isotopes was realized in this work. This analysis is to find a semi-empirical formula that allows rapid determination of the effective cross sections for the ^{72}Ge, ^{74}Ge and ^{76}Ge isotopes.

conclusion: In this work, We have performed a calculation of the cross sections of the formation of the compound nucleus by neutron and proton pathways based on the optical model. A parametric study of these cross sections will be carried out by performing an adjustment by the least squares method, of the reaction cross section as a function of the energy. This analysis consists of testing a new semi-permeable formula that allows rapid determination of cross-section reactions (n, p) induced by rapid neutrons of energy at about 20 MeV.

References:

[1] Changlin Lan et al. Measurement of cross sections for (*n*, 2*n*), (*n*, *p*) and (*n*, *α*) reactions on germanium isotopes induced by 14 MeV neutrons.Annals of Nuclear Energy , 2018.

[2] Experimental Nuclear Reaction Data. IAEA.NDS. https://www-nds.iaea.org/exfor/.2023

[3] Hauser.W and Feshbach.H, Phys. Rev. 87 . 366 (1952)

Keywords: (n, p) reactions; Hauser- Feshbach satistical; IAEA EXFOR nuclear experimental;

T1-P10: Radiological Risks measurements in Red Clay

N. Taïbouni [1 @], A. Amokrane[1], N. Belouadah[1], T. Azli[2], L. Yettou[1], 'O. Ben Azouz[1]

[1] *University of Sciences and Technology Houari Boumediene (USTHB), Algiers, Algeria.*
[2] *Nuclear Research Center of Draria (CRND), BP 43 Sebala, Draria 16050 Algiers, Algeria.*
[@] *taibouni_n@yahoo.fr*

Background/Purpose: Commonly used in industrial applications, the red clay may contain Radioactive Materials leading to potential radiological hazards. Several studies have been conducted on construction materials [1, 2], particularly on red brick [3] to assess their impact on human health and ensure their safe.
This study, conducted at the Nuclear Research Center of Draria (CRND), aims to determine the radiological risks associated with clay to compare it with red brick and raw earth. Radiological parameters were calculated to assess the impact of long-term exposure on the human body.

Materials & Methods: The assessment of natural radioactivity was conducted using a Ge(Hp) detector at the Fine Gamma spectrometry Laboratory of CRND.
The three samples of red clay, red brick and raw earth were collected then dried, ground, and homogenized before being hermetically sealed in airtight containers and stored for 24 days to reach secular equilibrium of ^{226}Ra with its short half-life descendants and ^{222}Rn before being analysed [4].
The energy of the emitted gamma rays enables the identification of the emitting radioisotope by measuring the intensity of the gamma radiation, which is proportional to the specific activity of the radioisotope in the sample. Radiological parameters are calculated based on the activities of radium ^{226}Ra, thorium ^{232}Th and potassium ^{40}K , they include the radium equivalent activity, external and internal radiation hazard indices, annual effective dose equivalent, alpha and gamma indices, effective dose rates to different organs and tissues, and the excess lifetime cancer risk [5].

Results: The analysis results revealed acceptable values close to the international standard values published by the European Commission [6]. The calculated values of external and internal hazard indices (H_{ex} and H_{in}) are below 1 unit as well, further confirming the safety of using these samples. All the AEDE (Annual Effective Dose Equivalent) values are well below the permissible limit of 1000 μSvy^{-1}. The effective dose rate to different organs and tissues values for the whole body and lungs, show that all values are within safe limits.
These analysis indicate that the samples have gamma and alpha indices lower than 1 unit. Potential external and internal radiation hazards are minimal and all the AEDE (Annual Effective Dose Equivalent) values are well below the permissible limit.

Conclusion: The analysis results revealed that the measured activity concentrations of radionuclides in the studied materials remain within the recommended safety limits established by international standards, such as those published by the European Commission. Furthermore, the calculated radiological hazard indices, including the radium equivalent activity, external and internal hazard indices, and annual effective dose, confirm that these materials pose no significant radiological risk to human health. Consequently, these findings suggest that red clay can be safely used in construction without restrictions related to radioactivity.
However, further studies, including long-term monitoring and leaching behavior analysis, could provide additional insights into potential variations in radiological properties over time and under different environmental conditions.

References:

[1]. Herrache N., Étude de la radioactivité naturelle dans certains matériaux de construction en Algérie, UBBA 2023.

[2]. Mineral Info - Le Portail Français Des Ressources Minerales Non Energetiques. Radioactivité naturelle des matériaux de construction : Recommandations pour l'application pratique des dispositions réglementaires – 2020

[3]. Doulat W., Radiation naturelle des matériaux de construction en briqueteries de Tafna et Tounane. UABBT, 2013.

[4]. L'Annunziata M. F., Handbook of Radioactivity Analysis, 2012; Third Edition, Elsevier, Amsterdam. [5].

Hemler R. G. Modern tools for precise γ-ray spectrometry with Ge detectors. Nucl. Instrum. Methods in Physc. Res. 2003; 505, 297 – 305.

[6]. AIEA International Atomic Energy Agency: Update of X Ray and Gamma Ray Decay Data Standards For Detector Calibration and Other Applications, Vol. 1, 2007; Vienna.

Keywords: Red clay, natural radioactivity, gamma spectrometry.

T1-P11: Nuclear ground state properties of superheavy nuclei

M. Ouhachi@, M.R. Oudih

Laboratoire de Physique théorique, Faculté de Physique, USTHB, BP 32 Bab-Ezzouar, Algérie
@ mouhachi@yahoo.com

Background/Purpose: A systematic study of superheavy nuclei in the range of N= 172 – 184 is carried out within the framework of the mean-field density functional, based on a zero range effective interaction. The ground-state properties, including binding energy, separation energy and nuclear radius, are estimated to provide evidence of magicity in these nuclei. A thorough examination of potential decay modes, employing various semi-empirical formulas, is also presented. The theoretical results obtained in this study show good agreement with related experiment results.

Materials & Methods: In this work we use the Hartree-Fock-Bogoliubov (HFB) self-consistent theory based on a zero-range effective interaction [1]. The nonlinear (HFB) equations were numerically solved, employing a harmonic oscillator basis with axial symmetry and comprising Nshell=16 major shells, in which the parameterization of the Skyrme interaction was considered: SLy4 [2].

Results: The binding energy of the superheavy nuclei in the range of N= 172 – 184, is calculated using the SLy4 Skyrme parametrization. For comparison, we use the available experimental values, the obtained results show good agreement with the available experimental data. From the difference in binding energy, we can calculate the separation energy of two neutrons, which is the energy required to separate two neutrons from a nucleus.

The alpha decay half-lives of the superheavy nuclei in the range of N= 172 – 184 are also studied using the unified fission model. The decay process is considered to be the result of a quantum tunnelling effect through a potential barrier, taken as the sum of the Coulomb potential, the centrifugal potential and the nuclear potential of the modified Woods-Saxon form. The alpha decay half-lives calculated with our model corroborate with the empirical and semi-empirical formulas. The calculated half-lives have subsequently been used as an indicator of possible region of increased stability that may correspond to shell closure.

Conclusion: In this work, the ground-state properties of the superheavy nuclei with N= 172 – 184, such as the binding energy and the two neutrons separation energy, have been calculated and compared to the available experimental data, the obtained results shows a good agreement with experimental values. The calculated half-lives have been used as an indicator of possible regions of increased stability that may correspond to shell closure.

References:

[1]. P. Ring, P. Shuk, The nuclear many-body, Springer Science & Business Media, (2004). [2]. Douchin, F., P. Haensel, and J. Meyer, Nucl. Phys. A, 665, 419 (2000).

Keywords: mean-field; effective interaction; superheavy nuclei; magic nuclei;

T1-P12: Occurrence of Bubble Structures in Z=8-20 Nuclei Using Skyrme-HF Plus BCS Approach

S. Berbache[@], A. Bouldjedri, A. Boubir

Department of Physics, LRPRIM Laboratory, Batna 1 University, Batna, Algeria
[@] Corresponding author:sihemberbacher@gmail.com

Background/Purpose: This study explores bubble nuclei, a class of atomic nuclei with depleted central nucleon density[1,2,3], using theoretical modeling for light nuclei (Z = 8 to 20). By analyzing nucleon density distributions, we identify promising bubble nucleus candidates and enhance understanding of exotic nuclear structures.

Materials & Methods: We employed the Skyrme-Hartree-Fock (HF) method combined with the BCS approximation to investigate bubble structures in light nuclei[4,5]. Our study covered isotopic chains including 12−26 O, 16−34 Ne, 20−40 Mg, 22−44 Si, 28−48 S, 30−54 Ar, and 36−60 Ca. To ensure a robust analysis, we used 18 different Skyrme interactions, including LNS, Sk3, KDE, NRAPR, Skz1, Skz2, Skz3, Skz4, Skm, Skm1, SLy6, SLy7, SLy8, SLy9, SLy10, KDE0, SKRA, and KDE0v1*. These interactions allowed us to assess the nuclear properties and conditions that favor the formation of bubble nuclei.

Results and conclusions: Our analysis identified promising bubble nucleus candidates with significant central nucleon depletion, influenced by nuclear forces and shell effects. Using diverse Skyrme interactions, we provided insights into nuclear structure variations, aiding future experimental detection of bubble nuclei.

References:

[1] C. Wong, ”Density isomer states in nuclei,” Phys. Lett. B, vol. 41, p. 451, 1972.
[2] J. Margueron, N. Van Giai, and G. Colò, ”The Equation of State in the Skyrme Model,” Nuclear Physics A, vol. 703, pp. 337–364, 2002.
[3] M. Grasso, L. Gaudefroy, E. Khan, J. Margueron, N. Van Giai, and I. Vidaña, ”Nuclear “bubble” structure in 34 Si,” Physical Review C, vol. 79, no. 3, p. 034318, 2009.
[4] Y. Wang, M. Liu, Z. Niu, and B. Sun, ”Bubble nuclei in the light mass region and their experimental observation,” Physics Letters B, vol. 819, p. 136463, 2021
[5] J. Skalski, S. Mizutori, and W. Nazarewicz, ”Bubble nuclei in the Hartree-Fock approach,” Nuclear Physics A, vol. 617, no. 3-4, pp. 282–296, 1994.

T1-P13: Quantum Machine Learning Application on the Determination of First Excited State Energy in Nuclei

S. Akkoyun[1],[@], C.M. Yeşilkanat[2]

[1] *Sivas Cumhuriyet University, Department of Physics, Sivas, Türkiye*
[2] *Artvin Çoruh University, Department of Mathematics and Science Education, Artvin, Türkiye*
[@] *Corresponding author sakkoyun@cumhuriyet.edu.tr*

Background/Purpose: In order to investigate various phenomena such as nuclear deformation in atomic nuclei, the shape of the nucleus and the lifetime of excited states, it is important to know the first 2^+ excited energy states in even-even atomic nuclei. These energy values can be determined by experimental methods as well as calculated by powerful theoretical models such as the nuclear shell model and the interacting boson model [1,2].

Materials & Methods: In recent years, it has been seen that the machine learning model, which is widely used in nuclear physics studies as an alternative approach, is also successful in this task. In the present study, the first 2^+ excited states of even-even nuclei were predicted by means of the quantum machine learning method, which is not yet widely used. The study was carried out by compiling existing experimental data in the literature and quantum machine learning approaches have been applied on the data.

Results: By using different quantum machine learning approaches as quantum random forest, quantum support vector machine, quantum neural network, we have predicted first excited states of the nuclei. We also compiled classical machine learning model results for the first excited state energies. Using rmse, mae and Pearson's correlation coefficient indicators, we calculated performances of the model results.

Conclusion: The obtained results were compared to the results obtained from classical machine learning models, the results obtained from theoretical models and experimental values.

References:

[1] M Goldhaber and A W Sunyar Phys. Rev. 83 906 (1951)
[2] P Stahelin and P Preiswerk Phys. Acta 24 623 (1951)

Keywords: Nucleus, Nuclear Structure, Excited State, Quantum Machine Learning

T1-P14: Exploring the Interplay of Dark Energy Models and Cosmic Radiation

A. Bensaid[@]

[1] *Mathematical Physics research team, Theoretical and Didactic Physics Laboratory, Faculty of Physics, USTHB*
[@] *Corresponding author abdelhakim.bensaid@usthb.edu.dz*

Background/Purpose: Radiation, including light from Type Ia supernovae and the cosmic microwave background (CMB), is critical in studying the accelerated expansion of the universe. This research explores the relationship between radiation and dark energy, investigating how various dark energy models, including quintessence and modified gravity theories, explain the observed cosmic acceleration.

Materials & Methods: The analysis focuses on radiation signatures from Type Ia supernovae (used as standard candles) and cosmic microwave background (CMB) data. The study utilizes a combination of theoretical models, such as quintessence and modified gravity theories, to interpret the impact of dark energy on the cosmic expansion rate, as inferred from radiation-based observations. We compare theoretical predictions with observational data from sources like the Planck satellite and previous studies on supernovae. Furthermore, we analyse the role of dark energy radiation in modifying the expansion rate.

Results: The results show that radiation from Type Ia supernovae provides strong evidence for the accelerated expansion of the universe. Analysis of the CMB data from the Planck satellite further confirms these findings and supports the existence of dark energy as a driving force. Moreover, different dark energy models produce varying signatures in radiation spectra, particularly in the way radiation interacts with the large-scale structure. For instance, modified gravity theories predict distinct radiation emission patterns, suggesting new ways that dark energy could influence radiation propagation across the universe. These differences could be observable in the upcoming generation of telescopes and satellite missions.

Conclusion: The interplay between radiation from supernovae, CMB, and theoretical dark energy models is pivotal in understanding cosmic acceleration. Our findings suggest that the role of radiation, as an observational tool, remains central in testing and refining dark energy models. Future radiation measurements, especially from next-generation CMB surveys and supernova observations, will provide further constraints on these models, potentially offering insights into new physics beyond the cosmological constant.

References:

[1]. Ade, P. A. R., et al. (Planck Collaboration), *Planck 2015 results. XIII. Cosmological parameters*, Astronomy & Astrophysics. 2016;A13:594. https://doi.org/10.1051/0004-6361/201525830

[2]. S. Perlmutter. Measurements of Omega and Lambda from Supernovae at High Redshifts. *Bulletin of the American Astronomical Society*. 1997;29:1351. https://doi.org/10.1086/307221

[3]. P. T. Silva and O. Bertolami. Accelerated Expansion from a Non-minimally Coupled Scalar Field. *Astrophysical Journal*. 2003;599:829.https://doi.org/10.48550/arXiv.astro-ph/0612382

Keywords: Dark Energy, Cosmic Radiation, CMB, Astrophysics;

T1-P15: Dipolar Bose Gases Under the GUP

A. Tahar Taiba[1@], A. Boudjemaa [2]

[1] *Department of Physics, Faculty of Sciences, University of Blida 1, SOUMAA, P.O. Box. 270, 09000, Blida, Algeria*
[2] *Department of Physics, Faculty of Exact Sciences and Informatics, Hassiba Benbouali University of Chlef, P.O. Box 78, 02000, Chlef, Algeria*
[@] *tahartaibaasma@etu.univ-blida.dz*

Background/Purpose: Quantum theory and general relativity are the fundamental pillars of our current understanding of physics[1]. However, unifying these theories into quantum gravity (QG) remains a significant challenge. QG theories suggest the existence of a minimum measurable length, leading to a modification of the Heisenberg Uncertainty Principle into a Generalized Uncertainty Principle (GUP). This study investigates the effects of QG on the ground-state properties of dilute homogeneous dipolar Bose gases.

Materials & Methods: Using the Hartree-Fock-Bogoliubov theory and the Generalized Uncertainty Principle incorporating both linear and quadratic terms in momentum, which implies a minimum measurable length parameterized with GUP parameters. We calculated quantum gravity corrections to the condensed fraction and superfluid fraction, The GUP parameters were determined from the observables of the condensed fraction and superfluid fraction for two types of dipolar atomic systems: ^{52}Cr and ^{168}Er.

Results: Our results show that the bounds on GUP parameters obtained from condensed fraction are $\alpha < 10^{22}$ and $\beta < 10^{44}$, which improve the bounds set by the model of an ideal Bose gas [2]. Similarly, the bounds derived from measuring the superfluid fraction are $\alpha < 10^{24}$ and $\beta < 10^{48}$, improving those obtained for weakly interacting Bose gases [3]. This demonstrate significant improvements in bounds on the GUP parameters. Therefore, the results reveal that the interplay between dipole-dipole interactions (DDIs) and quantum gravity corrections enhances the bounds on the GUP parameters.

Conclusion: This research represents a significant progress toward improving bounds on GUP parameters in dilute dipolar Bose gases. Our findings have the potential to be readily probed in current experimental setups, which may bring us closer to a deeper understanding of the reconciliation between quantum mechanics and gravity.

References:

[1]. Penrose R. On the gravitization of quantum mechanics 1: Quantum state reduction. Foundations of Physics. 2014;44:557–575.

doi:10.1007/s10701-013-9770-0

[2]. Das S et al.. Test of quantum gravity in statistical mechanics. Physical Review D. 2021;104:026014.

doi:10.1103/PhysRevD.104.026014

[3]. Boudjemâa A. Weakly interacting Bose gases with generalized uncertainty principle: Effects of quantum gravity. The European Physical Journal Plus. 2022;137:256 .

doi: 10.1140/epjp/s13360-022-02475-3

Keywords: Quantum Gravity; Dipolar Bose gases; Minimum length;

T1-P16: The KM3NeT Neutrino Telescope

A.B. Bouasla[a@], R. Attallah[b]

Laboratory of Radiation Physics (LPR), Badji Mokhtar University - Annaba
[@]Amani Besma Bouasla: amani-besma.bouasla@univ-annaba.dz

Background/Purpose: The Kilometer Cubed Neutrino Telescope (KM3NeT) [1] is a state-of-the-art underwater Cherenkov detector being constructed in the Mediterranean Sea to explore fundamental questions in astrophysics and particle physics. Comprising two detectors, KM3NeT offers unique capabilities for studying neutrinos across different energy scales.

Materials & Methods: ARCA (Astroparticle Research with Cosmics in the Abyss), situated near Sicily, is optimized for detecting cosmic neutrinos with energy above ~1 TeV from astrophysical sources like gamma-ray bursts, black holes, and supernovae, while ORCA (Oscillation Research with Cosmics in the Abyss), located off the coast of Toulon, is designed for the detection of neutrinos in the GeV energy range. Both detectors employ large-scale arrays of optical modules sensitive to the Cherenkov light produced by secondary particles from neutrino interactions.

Results: ARCA focuses on high-energy neutrinos from astrophysical sources, while ORCA is dedicated to determining neutrino oscillation parameters and investigating the neutrino mass ordering. These complementary capabilities allow KM3NeT to study neutrinos across different energy scales, enhancing our understanding of cosmic and particle physics phenomena.

Conclusion: In this presentation, we will provide an overview of the KM3NeT experiment, highlighting its scientific goals, unique detection capabilities, and contribution to the fields of astrophysics and particle physics.

References:

[1]. https://www.km3net.org

Keywords: KM3NeT; astroparticle physics; Neutrino Telescope;

T1-P17: The Effect of Simultaneous Variation in Zenith Angle and Geographical Latitude on the Earth's Upper Atmosphere

H. Marif [1@], D. Benmorsli[1], J. Lilensten[2]

[1] *University of science and Technology, USTHB, Alger*
[2] *Institut de Planétologie et d'Astrophysique de Grenoble IPAG, France*
[@] *Corresponding author hanmarif@gmail.com*

Background/Purpose: In the Earth's upper atmosphere (at altitudes above 80 km), photo-ionisation is the predominant process responsible for electron production during the day. The absorption of UV solar electromagnetic radiation triggers a series of reactions involving the ionisation, excitation and dissociation of neutral atmospheric constituents. These processes ultimately lead to the formation of the ionosphere.

Materials & Methods: The macroscopic parameters of the electrons are obtained by calculating the moments of different orders of the distribution function expressed as a function of the suprathermal flux solution of Boltzmann kinetic transport equation. The TRASSAOLO-MOMENT numerical code is used to obtain various results.

Results: The representations of the photoionization zones are plotted for a given declination, thus allowing the variation of ionisation in the upper atmosphere to be determined as a function of zenith angle, geographical latitude and local time. This enables the selection of the combination of parameters used to plot the variation of macroscopic parameters (essentially density, velocity and temperature) as a function of geographical latitude and solar zenith angle. The findings reveal that the variation of each parameter has minimal impact on the velocity and temperature densities of the suprathermal electrons. Conversely, the simultaneous variation of both parameters, in accordance with the distribution plotted above, shows a considerable variation in the densities, velocities and temperatures of the suprathermal electrons, which is an indicator of the variation in the state of the ionosphere and the neutral atmosphere.

Conclusion: The simultaneous variation in the zenith angle and the geographical latitude of the study point indicate fundamental changes in the solar irradiation collected at the top of the upper atmosphere, which has a decisive effect on the macroscopic parameters of the suprathermal electrons in the Earth's upper atmosphere. In future research, the hot to cold electron temperature and density ratios will be examined. These ratios, which are central to numerous studies of ionospheric plasmas, have not yet been calculated.

References:

[1]. Marif H and Liensten J. Suprathermal electron moments in the ionosphere. *Journal of Space Weather and Space Climate*. 10, 05 2020. doi:10.1051/swsc/2020021

[2]. Chapman S. The absorption and dissociative or ionizing effect of monocromatic radiation in an atmosphere on rotating earth. *Proceedings of the Physical Society*. 43 :483, 12 2002. doi:10.1088/0959-5309/43/1/305

Keywords: suprathermal electrons, ionosphere, UV radiation, photoionization.

T1-P18: The Differential and Integral Cross Sections of The Electron- Biomolecule (Uracil and Thymine)

S. Mokrani [a], H. Aouchiche[a], C. Champion[b]

[a]*Laboratoire de Mécanique, Structures et Énergétique, Université Mouloud Mammeri de Tizi-Ouzou, BP 17, 15000 Tizi-Ouzou, Algérie.*

[b]*Université de Bordeaux, CNRS, CEA, CELIA (Centre Lasers Intenses et Applications), UMR 5107, F-33405, Talence, France.*

[@]*Corresponding author mokranisaida@yahoo.fr*

Background/Purpose: This research work focuses on the study of the interaction of charged particles with the biomolecules composing deoxyribonucleic acid (DNA) and ribonucleic acids (RNA). More particularly, we were interested in the calculations of the differential and integral cross sections of elastic diffusion of electrons by uracil and thymine. Our main objective was to calculate the differential cross sections as a function of the scattering angle for different values of incident electronic energies as well as the integral electron cross sections for the two molecules mentioned above. This is of major interest in many fields linked in particular to radiobiology and medicine...

Materials & Methods: In this research, we elaborate the calculation of the differential and integral cross sections of the electron-biomolecule diffusion using the partial wave formalism using the independent atomic model [1]. To facilitate understanding, we took into account the interactions between the incident particle and the molecular target using an optical potential [2].It includes three fundamental concepts: static potential, exchange potential, and correlation-polarization potential.

Results: The differential cross sections of elastic electron scattering by uracil and thymine, were calculated for energies. Thus, we found that these cross sections strongly depend on the energy of the incident particles and the structure of the target. Indeed, all contributions, including interatomic, exchange, correlation-polarization and multiple scattering, are significant for low incident energies

Conclusion: The differential and integral cross sections of electron scattering by uracil and thymine, are calculated for different energies. These sections depend on the energy of the incident particles, the size and structure of the target. All contributions, including interatomic, exchange, correlation-polarization, are significant at low energies.

References:

[1]. Fuss M C et al.. (Differential and integral electron scattering cross sections from tetrahydrofuran (THF) over a wide energy range: 1–10000 eV):Eur. Phys. J. D 2014; 68:161-168 doi :10.1140/epjd/e2014-40820-5.

[2]. Jain A et al..(Total (elastic plus inelastic) cross sections for electron scattering from diatomic and polyatomicmolecules at 10—5000 eV: H2, Liz, HF, CH4, N2, CO, C2H2, HCN,Oz, HC1, H2S, PH3, SiH4, and Coz) Phys. Rev. A 1992; 45 :,202-218

doi:10.1103/PhysRevA.45.202

Keywords: **Electrons elastic scattering, Cross sections, ADN, ARN Interactions**

T1-P19: L_2-Subshell Coster-Kronig Transition Probabilities for Lanthanide

S. Meddah[1,2], A. Kahoul[1,2], S. Daoudi[1,2]

[1] *Department of Matter Sciences, Faculty of Sciences and Technology, Mohamed El Bachir El Ibrahimi University, Bordj-Bou-Arreridj 34030, Algeria.*

[2]*Laboratory of Materials Physics, Radiation and Nanostructures (LPMRN), Faculty of Sciences and Technology, Mohamed El Bachir El Ibrahimi University, Bordj-Bou-Arreridj 34030, Algeria.*

@ Corresponding author samia.meddah@univ-bba.dz

Background/Purpose: The theoretical, experimental and analytical methods for the calculation of Coster-Kronig transition of different elements are very important because of the large number of their applications. These transitions occur through non-radiative channels (i.e., without emitting photons). Based on the available experimental values of f_{23}, we suggest a set of new empirical values for the L_2-subshell Coster-Kronig transition probabilities, derived from the experimental values. Reasonable agreement has been obtained between our result and other works.

Materials & Methods: This research presents new parameters for calculating Coster-Kronig transition probabilities for lanthanide targets with atomic numbers ranging from 57≤Z≤71. We used the mathematical method of polynomial interpolation (least square method) to derive the empirical Coster-Kronig transition probabilities from the existing experimental data published during the period 1979 to 2003, The analytical function used for the interpolation is the following polynomial: $f_{23} = \sum_{i=0}^{2} a_i Z^i$.
with: $a_0 = 2.07123$,$a_1 = -0.05889$, and $a_2 = 4.4962 \times 10^{-4}$.

Results: The empirical L2-subshell Coster-Kronig transition probabilities were computed using least square method for elements 57≤Z≤71. Also provided were empirical, semi-empirical, and experimental values from Campbell [1], Krause [2], and Öz [3].
The obtained results generally show good agreement across all elements within the specified range. Notably, our calculations closely match those reported by Krause (1979), with relative percentage differences ranging from 0% to 9.21%. except for $_{57}$La (12.57%) and $_{71}$Lu (13.38%). Furthermore, the present data align well with those of Campbell (2003), with deviations between 0% and 9.14%, except for $_{71}$Lu (12.10%). The experimental values range from 0% to 9.14%, with findings closely matching Öz (2001) at 2.08% to 4.90%.

Conclusion: The results showed that the empirical method was important for precisely describing the spectral features of materials, and they were in strong accord with other research teams' conclusions. This agreement shows that the learnt method can improve the prediction accuracy, leading to a better understanding of the physical processes involved in heavy atom X-ray transitions.

References:

[1]. Campbell JL. Fluorescence yields and Coster–Kronig probabilities for the atomic L subshells. *Atomic Data and Nuclear Data Tables.* 2003;85:291–315. doi:10.1016/S0092-640X(03)00059-7.

[2]. Krause MO. Atomic radiative and radiationless yields for K and L shells. *Journal of Physical and Chemical Reference Data.* 1979;8:307–322. doi:10.1063/1.555595.

[3]. Öz E, Ekinci N, Özdemir Y, Ertuğrul M, Şahin Y, Erdoğan H. Measurement of atomic L shell Coster-Kronig yields (f12, f23, and f13) for some elements in the atomic number range 59 ≤ Z ≤ 90. *J. Phys. B: At. Mol. Opt. Phys.* 2001;34:631–638. doi:10.1088/0953-4075/34/4/311.

Keywords: X-ray; **Coster Kronig transition ; Empirical calculation.**

T1-P20: Relativistic Calculation of Radiative Vacancy Transfer Probabilities from K-shell to L2-subshell for Selected Elements

B. Berkani[1,2@], A. Kahoul[1,2], J. M. Sampaio[3,4]

[1]*Department of Matter Sciences, Faculty of Sciences and Technology, Mohamed El Bachir El Ibrahimi University, Bordj-Bou-Arreridj 34030, Algeria.*

[2]*Laboratory of Materials Physics, Radiation and Nanostructures (LPMRN), Faculty of Sciences and Technology, Mohamed El Bachir El Ibrahimi University, Bordj-Bou-Arreridj 34030, Algeria.*

[3]*LIP – Laboratório de Instrumentação e Física Experimental de Partículas, Av. Prof. Gama Pinto 2, 1649-003 Lisboa, Portugal.*

[4]*Faculdade de Ciências da Universidade de Lisboa, Campo Grande, C8, 1749-016 Lisboa, Portugal*

[@] *Corresponding author boualem.berkani@univ-bba.dz*

Background/Purpose: Understanding radiative vacancy transfer probabilities (RVTPs) is crucial for interpreting atomic de-excitation processes relevant to fields such as plasma and medical physics. This study focuses on calculating RVTPs from K to L2 for selected elements using a fully relativistic approach.

Materials & Methods: The multiconfiguration Dirac-Fock (MCDF) method, implemented via the MCDFGME code developed by Desclaux and Indelicato [1], was employed. This approach incorporates relativistic effects and electron correlations, ensuring precision and consistency.

Results: The calculated RVTPs show strong agreement with available theoretical [2,3] and empirical [4] data and offer significant insights into trends across the studied elements. Variations for elements with Z < 40 were observed compared to earlier results, likely due to differences in computational frameworks and the inclusion of advanced electron correlation models.

Conclusion: The MCDF-based calculations provide accurate RVTPs and underline the importance of relativistic methods for such studies. These results serve as a benchmark for further theoretical and experimental investigations in atomic physics.

References:

[1] J.P. Desclaux, A multiconfiguration relativistic DIRAC-FOCK program, Computer Physics Communications 9 (1975) 31–45. https://doi.org/10.1016/0010-4655(75)90054-5.

[2] B. Berkani, A. Kahoul, J.M. Sampaio, S. Daoudi, J.P. Marques, F. Parente, A. Hamidani, S. Croft, A. Favalli, Y. Kasri, A. Zidi, K. Amari, Relativistic and semi-theoretical calculations of K-shell to L-shell/subshell vacancy transfer probabilities, Spectrochimica Acta Part B: Atomic Spectroscopy 224 (2025) 107089. https://doi.org/10.1016/j.sab.2024.107089.

[3] P.V. Rao, M.H. Chen, B. Crasemann, Atomic Vacancy Distributions Produced by Inner-Shell Ionization, Phys. Rev. A 5 (1972) 997–1012. https://doi.org/10.1103/PhysRevA.5.997.

[4] B. Berkani, A. Kahoul, J.M. Sampaio, S. Daoudi, J.P. Marques, F. Parente, A. Hamidani, S. Croft, A. Favalli, Y. Kasri, A. Zidi, K. Amari, Vacancy transfer probability parameters: Database and a new empirical value for elements in the atomic number range 16 ≤ Z ≤ 92, Radiation Physics and Chemistry 225 (2024) 112106. https://doi.org/10.1016/j.radphyschem.2024.112106.

Keywords: Relativistic calculations; Vacancy transfer probabilities; Multi-configuration Dirac-Fock; Line width; MCDFGME.

T1-P21: Evaluation of Gamma-Rays Shielding Properties of PVC/Heavy Transition Metal Carbides Composites in Healthcare Applications

A. Hadjal[1], A. Saim[1], A.S.A. Dib[1], A. Tebboune[1] and N.Belkaid[1]

[1] *Laboratory of Analysis and Application of Radiation (LAAR), Faculty of Physics, University of Sciences and Technology of Oran Mohamed Boudiaf, (USTO-MB), BP 1505, El MNaouar, 31000, Oran, Algeria*

[@] *Corresponding author amina.hadjal@univ-usto.dz*

Background/Purpose: Gamma radiation is widely used in the medical field, particularly in radiotherapy and radiation imaging. However, its harmful effects on human health and the environment necessitate the use of effective shielding materials. Lead is commonly used for this purpose, but its toxicity and susceptibility to corrosion have led to the search for safer and more durable alternatives.

Materials & Methods: This study simulates the gamma radiation shielding properties of three composite materials made from 10 wt% of PVC, filled with heavy transition metal carbides (WC, TaC, and HfC), comparing their performance to lead. Radiation shielding parameters such as the mass attenuation coefficient (μ_m), linear attenuation coefficient (μ), half-value layer (HVL), mean free path (MFP), transmission factor (TF), and radiation protection efficiency (RPE) were evaluated using the Geant4 code over an energy range from (60 to 1332.5) keV.

Results: The mass attenuation results were compared with the XCOM database and showing good agreement. The study revealed that the three composite materials, particularly PVC-WC, provide comparable shielding to lead at energies below 120 keV,

Conclusion: These results suggest that PVC/Heavy transition metal carbides composites could be a viable substitute for lead as a shielding material in radiology diagnostic and nuclear medicine applications.

References:

[1] M. T. Alabsy and M. A. Elzaher, "Radiation shielding performance of metal oxides / EPDM rubber composites using Geant4 simulation and computational study," *Sci. Rep.*, no. 0123456789, pp. 1–14, 2023, doi: 10.1038/s41598-023-34615-9.

[2] B. Aygün, E. Şakar, T. Korkut, M. I. Sayyed, A. Karabulut, and M. H. M. Zaid, "Fabrication of Ni, Cr, W reinforced new high alloyed stainless steels for radiation shielding applications," *Results Phys.*, vol. 12, no. November 2018, pp. 1–6, 2019, doi: 10.1016/j.rinp.2018.11.038.

[3] F. Akman, M. R. Kaçal, M. I. Sayyed, and H. A. Karataş, "Study of gamma radiation attenuation properties of some selected ternary alloys," *J. Alloys Compd.*, vol. 782, pp. 315–322, Apr. 2019, doi: 10.1016/j.jallcom.2018.12.221.

Keywords: Gamma-rays, Radiation shielding, Composite materials, Heavy Transition metal carbides, Geant4;

T1-P22: Empirical calculation of jump ratios r_{L3} and jump factors J_{L3} for lanthanides

I. Hamied[1,2], A. Kahoul[1,2], S. Daoudi[1,2]

[1] *Department of Matter Sciences, Faculty of Sciences and Technology, Mohamed El Bachir El Ibrahimi University, Bordj-Bou-Arreridj 34030, Algeria.*

[2]*Laboratory of Materials Physics, Radiation and Nanostructures (LPMRN), Faculty of Sciences and Technology, Mohamed El Bachir El Ibrahimi University, Bordj-Bou-Arreridj 34030, Algeria.*

@ Corresponding author imane.hamied@univ-bba.dz

Background/Purpose: Determining the X-ray absorption jump factors and jump ratios is crucial for atomic, molecular, and radiation physics. These parameters are widely used in fields such as radiation dosimetry, shielding, atomic physics, and astrophysics. The theoretical, experimental, and analytical methods for calculating jump factors and ratios for various elements are significant due to their numerous applications. Based on available experimental values of r_{L3} and J_{L3}, we propose new empirical values for the L_3-subshell absorption jump factors and ratios. Our results align well with theoretical values, showing good agreement.

Materials & Methods: This study introduces novel parameters for determining L_3-subshell absorption jump factors and jump ratios for lanthanide elements with atomic numbers in the range $57 \leq Z \leq 71$. The empirical values of r_{L3} and J_{L3} were derived using the mathematical approach of linear interpolation, based on experimental data published between 2014 and 2016.

Results: Linear interpolation was employed to calculate the L3-subshell absorption jump factors and jump ratios for elements with atomic numbers ranging from 57 to 71. These calculated values were then compared with experimental and theoretical values reported by Akman [1], Gupta [2], and Kaçal [3]. The results obtained generally align with both experimental and theoretical values across the entire range of elements ($57 \leq Z \leq 71$). Specifically, the current values closely match those reported by Gupta [2], with a relative percentage difference ranging from 0% to 1.80%. Additionally, our data shows good agreement with the results of Kaçal [3], with matching percentages between 0% and 3%. For the data reported by Akman [1], the relative percentage difference ranges from 0% to 0.61%, except for the element Samarium ($_{62}$Sm), where the relative percentage difference is 8.21%.

Conclusion: Empirical methods accurately characterize atomic jump parameters, consistent with previous research. This validates the method's predictive power and enhances understanding of electronic transitions in heavy atoms.

References:

[1]. Akman, F., Kaçal, M. R., & Durak, R. (2016). The excitation probabilities of Kα, β and Lα1, 2 for some elements in 56≤ Z≤ 68 at 59.54 keV. Radiation Physics and Chemistry, 119, 29-36. http://dx.doi.org/10.1016/j.radphyschem.2015.09.015

[2]. Gupta, M. K., Singh, G., Dhaliwal, A. S., & Kahlon, K. S. (2014). Measurement of L3 subshell absorption edge parameters in the elements of lanthanide series (Z= 57–70). Radiation Physics and Chemistry, 100, 45-48. http://dx.doi.org/10.1016/j.radphyschem.2014.03.023

[3]. Kaçal, M. R. (2014). Measurement of L3 subshell absorption jump ratios and jump factors for high Z elements using EDXRF technique. Radiation Physics and Chemistry, 100, 80-84. http://dx.doi.org/10.1016/j.radphyschem.2014.03.026

Keywords: X-ray; **L_3-subshell absorption jump factors; L_3-subshell absorption Jump ratios; empirical calculation.**

T1-P23: Zirconium To Neodymium Empirical $2s_{1/2}$ Transition Fluorescence Yields

A. Bendjedi[1,@], A. Kahoul[2,3], S. Daoudi[2,3], Y. Kasri[4,5]

[1]*Department of Science,Messaoud Zeghar teacher Education college of Setif 19600, Algeria*
[2]*Department of Matter Science, Faculty of Sciences and Technology,Mohamed El Bachir El Ibrahimi University, Bordj-Bou-Arreridj 34030, Algeria.*
[3]*Laboratory of* Materials Physics, Radiation and Nanostructures *(LPMRN), Mohamed El Bachir El Ibrahimi University, Bordj-Bou-Arreridj 34030, Algeria*
[4]*Department of Physics, Faculty of Sciences, University of Mohamed Boudiaf, 28000 M'sila, Algeria*
[5]*Theoretical Physics Laboratory, Faculty of Exact Sciences, Bejaia University, 06000 Bejaia, Algeria*
@ Corresponding author a_bendjedi@yahoo.fr

Background/Purpose: L X-ray fluorescence cross sections and fluorescence yields are important for developing more reliable theoretical models describing the fundamental inner-shell processes. Experimental, theoretical and empirical data regarding the X-ray fluorescence (XRF) cross sections and the fluorescence yields are also important in many practical applications, like elemental analysis by the X-ray emission technique, basic studies of nucleair and atomic processes leading to the emission of X-rays and Auger electrons, and dosimetric computations for medical physics and irradiation processing. The experimental data ($\omega_{L1\text{-}exp}$) of the $2s_{1/2}$ Transition fluorescence yields were directly interpolated to deduce the empirical values.

Materials & Methods: In this paper we have performed the fittings using analytical function based on the available experimental data to derive the empirical L_1 sub-shell fluorescence yields for elements with 40≤Z≤60. These values of the experimental data have been interpolated by using the analytical function $\left(\omega_{L1\text{-}exp}/\left(1-\omega_{L1\text{-}exp}\right)\right)^{1/4}$ as function of Z to deduce the empirical fluorescence yield.

Results: New parameters were presented for the calculation of the L_1 subshell fluorescence yields for targets from $_{40}$Zr to $_{60}$Nd The experimental values $\omega_{L1\text{-}exp}$ were used to calculate the empirical L_1 subshell fluorescence yields. Taking into account the famous formula $\left(\omega/(1\text{-}\omega)\right)^{1/4}=\sum_n b_n Z^n$ the reduced *experimental values* $\left(\omega_{L1\text{-}exp}/\left(1-\omega_{L1\text{-}exp}\right)\right)^{1/4}$ is presented as function of Z and plotted with respect to atomic number Z. The analytical function used for the fitting is the following polynomial: $\left(\omega_{L1\text{-}exp}/\left(1-\omega_{L1\text{-}exp}\right)\right)^{1/4}=\sum_{n=0}^{3} b_n Z^n = f(Z)$

Conclusion: A new set of L1 subshell fluorescence yields were determined using simple methods for elements in the atomic region 40≤Z≤60. The deduced empirical fluorescence yields are in a relatively good agreement with those of other groups for the whole range of atomic numbers. In addition to the available experimental and theoretical average L-shell fluorescence yields, the present values can be added to the databases and made available for the scientific and technical community requiring updated atomic data.

Keywords: X-rays; Fundamental atomic parameters; L1 sub-shell fluorescence yield; empirical calculations.

T1-P24: Polar Field Reversal of Iota Horologii

A. Boulkaboul[1@], Y. Damerdji[1]

[1] *Centre de Recherche en Astronomie Astrophysique et Géophysique - Algeria*
[@] *Corresponding author* amina.boulkaboul@craag.edu.dz

Background/Purpose: Late-type stars exhibit magnetic activity cycles analogous to the Sun's 11-year cycle, driven by stellar dynamos that generate magnetic fields. A hallmark of these cycles is the periodic polarity reversal of the polar magnetic field, typically coinciding with the cycle maximum. This study focuses on the solar-like star Iota Horologii (HD17051) to investigate this characteristic.

Materials & Methods: Stellar magnetic fields induce weak polarization signals in individual spectral lines. To detect these, we employ the Least-Squares Deconvolution (LSD, Donati et al. 1997 [1]) method, which combines numerous spectral lines within a given wavelength range into a mean LSD profile using a line mask derived from the Vienna Atomic Line Database (VALD). From HARPS spectropolarimetric data, we estimate Stokes V and I profiles via LSD and derive the mean longitudinal magnetic field (B_l) from the first moment of Stokes V.

Stokes V profiles sampled across rotational phases are inverted to reconstruct the stellar magnetic field using Zeeman-Doppler Imaging (ZDI, Brown et al. 1991 [2]). The stellar surface is divided into discrete elements where the three components of the magnetic field are computed. Magnetic reconstructions over different epochs reveal polarity reversals of the polar fields, which indicate magnetic cycle phases. The interval between two consecutive reversals provides an estimate of the magnetic cycle period.

Results: For Iota Horologii, our analysis indicates B_l variations between ±4 G. We identify a polarity reversal between March and August 2016, followed by another in January 2018, suggesting a magnetic cycle period between 540 and 690 days. Periodic analysis of the S- index data supports this, revealing possible cycles periods of 5811.25±0.005 d and 673.44±0.02 d.

Conclusion: The secondary cycle period falls within the duration between polarity reversals, confirming that polarity reversals of magnetic fields can serve as reliable indicators of the magnetic cycle period.

References:

[1]. Donati, J-F., et al. "Spectropolarimetric observations of active stars." *Monthly Notices of the Royal Astronomical Society* 291.4 (1997): 658-682. doi:10.1093/mnras/291.4.658

[2]. Brown, S. F., et al. "Zeeman-Doppler imaging of solar-type and AP stars. IV-Maximum entropy reconstruction of 2D magnetic topologies." *Astronomy and Astrophysics (ISSN 0004-6361), vol. 250, no. 2, Oct. 1991, p. 463-474.* 250 (1991): 463-474.

Keywords: Stellar activity, magnetic field, spectropolarimetry, individual stars

T1-P25: Elastic and charge-transfer cross sections of He+/ He at lower energy

S. Lias[1@], F. Bouchelaghem[2], L. Aissaoui[3]

[1] *Laboratoire d'électronique Quantique, USTHB, Faculté de physique , El-Alia ,Alger, BP32*
[2] *Physics Department, Mohamed Boudiaf University, M'sila 28000, Algeria*
[3] *Université LahadjLakhdhar-Batna, Algeria*
[@] *slias@usthb.dz*

Background/Purpose: Elastic and charge-transfer cross sections for elastic collisions of ground-state He^+ ions (2S) with neutral He atoms are calculated over a range of reduced kinetic energies $10^{-12} \leq \varepsilon \leq 10^{-1}$. In this energy range, quantum effects become significant, necessitating the incorporation of symmetry effects into the calculations. These effects arise from the identical nature of the colliding atoms and the spin of their nuclei.

Materials & Methods: For this study, highly accurate interatomic potentials for the $He^+(^2S) + He(^1S)$ system, recently calculated by [1], were employed. These potentials facilitated the numerical integration of the radial wave equation, enabling the determination of phase shifts for each energy E and angular momentum These phase shifts were then used to compute elastic and charge-transfer cross sections relative to both gerade and ungerade states. This approach required explicit inclusion of symmetry effects due to the identity of the colliding atoms and the nuclear spin.

Results: Electron transfer between He^+ ions and neutral He atoms occurs during collisions without altering the particles' internal energy. Pronounced isotopic effects emerge at energies $E \leq 10^{-5}$, where both species display overlapping orbiting resonances. Computed charge-transfer cross sections at low energies align well with data from [2]. Below $E = 10^{-2}$, interference between gerade and ungerade potential-energy curves induces small oscillations. Additionally, the phase shift difference states varies sharply within the potential well region but becomes linear above $E=10^{-2}$[3], reflecting energy-dependent quantum interactions.

Conclusion: This study extends quantum collision theory to He^+–He interactions using *gerade/ungerade* potentials from the radial wave equation. Phase shifts enable precise cross-section calculations via thermophysical spectroscopy, revealing distinct quantum/semi- classical behaviors. Nuclear spin and symmetry critically shape cross-sections, particularly at ultracold temperatures ($T < 10^{-2}$ K).

References:

[1]. J. Gebala, M. Przybytek, M. Gronowski, and M. Tomza, PHYSICAL REVIEW A 108, 052821 (2023) doi:10.1103/PhysRevA.108.052821

[2]. A Chicheportiche, B Lepetit, M Benhenni, F X Gadea and M YousfiJ. Phys. B: At. Mol. Opt. Phys. 46, 065201(2013) doi:10.1088/0953-4075/46/6/065201

[3]. Barata J A S and Cond C A N, Elastic He+ on He collision cross-sections and Monte Carlo calculation of the transport coefficients of He+ ions in gaseous helium Nucl. Instrum. Methods Phys. Res. A 619 21–3(2010) doi:10.1016/j.nima.2009.10.070

Keywords: Quantum-mechanical cross sections; Elastic collisions ion-atom; Lower energy; Elastic cross sections; Charge-transfer cross sections

T1-P26: A Novel Orange-Emitting Phosphor: Praseodymium(III)-Doped Potassium Zinc Diphosphate for LED Applications

R. Belbal[1@], B. Kahouadji[2], L. Gacem[3]

[1]*National Higher School of Mathematics, Scientific and Technology Hub of Sidi Abdellah, P.O. Box 75, Algiers 16093, Algeria.*

[2]*Department of Technology, University of Bejaia, Bejaia, 06000, Algeria*

[3]*Faculty of Sciences, Ziane Achour University of Djelfa, BP 3117, Djelfa 17000, Algeria.*

[@] *Corresponding author rim.belbal@nhsm.edu.dz*

Background/Purpose: Recently, inorganic luminescent materials have shown significant potential for various applications, particularly in LED technology, as well as in displays, lasers and solid-state lighting [1-2].

Materials & Methods: In this work, we successfully synthesized a novel orange- emitting luminescent material using the solid state reaction method, its preparation is based on potassium zinc diphosphate ($K_2ZnP_2O_7$)[3] as the host crytal doped with praseodymium ions (Pr^{3+}) which serve as an efficient luminescent center. Pr^{3+} ions are particularly intriguing due to their energy levels containing multiple metastable states [4] and a rich emission spectrum extending from ultraviolet to infrared regions [5].

To study the characterization of the obtained phosphor and confirm its structure, X-ray diffraction (XRD) patterns were acquired using a Phillips X'Pert Pro diffractometer. Additionally, photoluminescence measurements were performed at room temperature using the RF-6000 spectrofluorophotometer. On the other hand, to determine the color of the prepared phosphor, we calculated the chromaticity coordinates.

Results: The XRD analysis confirmed that the synthesized sample possesses a stable tetragonal crystal structure, belonging to the space group *$P4_2/mnm$*. Otherwise, the luminescent mesearemens showed that the excitation wavelength of the $K_2ZnP_2O_7:Pr^{3+}$ phosphor is 440 nm corresponding to the $^3H_4 \rightarrow {}^3P_1$ transition, and the highest intensity in the emission spectra was observed at 658 nm, corresponding to the $^1D_2$ to $^3H_4$ transition. Furthermore, the chromaticity coordinates confirmed that $K_2ZnP_2O_7:Pr^{3+}$ emits orange light.

Conclusion: A novel orange-emitting phosphor, $K_2ZnP_2O_7:Pr^{3+}$, has been successfully synthesized. Characterization showed its potential for use in LED applications.

References:

[1]. J.L. Yuan, J. Wang, D.B. Xiong, J.T. Zhao, Y.B. Fu, G.B. Zhang,C.S. Shi, J. Lumin. 126 (2007) 717. https://doi.org/10.1016/j.jlumin.2006.11.001

[2]. S. Mahlik, A. Lazarowska, M. Grinberg, T. Liu, R. Liu, *Journal of Physical Chemistry C*, 117 (2013) 13181. 10.1021/jp402475n

[3]. Durif, A. Crystal Chemistry of Condensed Phosphates. Grenoble, France, 1995.

[4]. R. Shi, M.M. Qi, L.X. Ning, F.J. Pan, L. Zhou, W.J. Zhou, Y.C. Huang, H.B. Liang, J.Phys. Chem. C 119 (2015) 19326–19332. 10.1021/acs.jpcc.5b04803

[5]. G. Blasse, B. Grabmaier, Luminescence Materials, Springer-Verlag, Berlin, 1994. https://doi.org/10.1007/978-3-642-79017-1_1

Keywords: $K_2ZnP_2O_7:Pr^{3+}$; XRD; photoluminescence; excitation.

T1-P27: A Comparative Study of Analytical and Numerical Methods in Stark Effect Analysis for Lyman α Spectrum

A. Bekhouche[a@], I. Hannachi[a], R. Stamm[b]

[a] *University of Batna 1, PRIMALAB, Department of Physics, Batna, Algeria*
[b] *Aix-Marseille Univ. and CNRS, PIIM, 13397 Marseille, France*
[@]*Corresponding author name@ahlam.bekhouche@univ-batna.dz*

Background/Purpose: This study explores how the Stark effect modifies line profiles through detailed numerical integration of the Schrödinger equation. Our goal is to clarify the relationship between ion dynamics and quantum mechanical effects.

Materials & Methods: We calculate the electric field generated by numerous charged particles (ions) within a cubic volume, for over 1000 histories, using random conditions which help us understand plasma particle behavior. We compare analytical and numerical calculations for the Lyman-alpha case to highlight differences in accuracy. Subsequently, we numerically integrate the Schrödinger equation to investigate the quantum mechanical behavior influenced by the calculated electric fields to get the dipole autocorrelation function. The work of Stamm and Hannachi underscores the role of numerical simulations in exploring conditions beyond traditional impact approximations [1].

Results: Applying Fourier transformation to the dipole autocorrelation function, we derive the line profile, emphasizing spectral characteristics modified by Stark broadening. Our findings indicate significant differences in spectral characteristics between analytical and numerical methods, with the latter providing improved accuracy in predicting line profiles.

Conclusion: This research clarifies the relationship between ion dynamics and quantum mechanical effects, underscoring the need for precise modeling to understand line formation in plasma environments. The results have important implications for astrophysics and laboratory plasma.

References:

[1]. Stamm R et Al. Stark Broadening from Impact Theory to Simulations. Atoms. 2017;5(3):32.
Doi : https://www.doi.org/10.3390/ATOMS5030032

Keywords: **Stark broadening; Line profile; Lyman-alpha.**

T1-P28: Radiological Study of Long lived Natural Radionuclides: Population Exposure and Risque Assessment

S. Boukhalfa[1@], A.A. Benkhada[1], A.-K Fertas[2], R. Khelifi [1]

[1]*Laboratory of Theorical Physics and Interaction of Radiations with Matter, Department of Physic, Faculty of Sciences, University of Blida-1, Soumaa Street, BP 270, Blida, Algeria*

[2]*Geomaterial and Civil Engineering Laboratory, Faculty of Technology, University of Blida-1, Soumaa Street, BP 270, Blida, Algeria*

[@] *Corresponding author boukhalfasalma@gmail.com*

Background/Purpose: In the present study, a gamma spectrometry technique equipped with a 3"×3" NaI(Tl) scintillator detector was used to evaluate the long-lived natural radionuclides in soil samples associated with popular exposure and risque assessment. The deep concentration of the selected element was qualitatively measured at her single gamma-ray transition corresponding to 1.46MeV. The specific activity (in Bq/kg) shows mean values of 1527.21. The mean value of the absorbed dose at 1 metre from the ground state (in nGy/h) and the annual effective dose (in mSv/year) are 65.98 and 3.21 $\times 10^{-3}$ respectively. The results indicate an interesting difference between the specific activities in the selected sites and geological locations. The present results may contribute to enriched data of knowledge in Algeria.

Materials & Methods: in this study, we have employed a 7.6% energy resolution (at ^{137}Cs) tree-tree-inche iodide sodium (Tl) scintillator detector covered successively by 1cm and 5cm of copper and Lead shielding. The prepared samples in geometrical and civil engineering laboratory, were conserved polyethylene beakers until they attend secular equilibrium between ^{238}U and ^{232}Th. The spectrum acquisition was made via Gamma vision software, where the detection efficiency curves of the analysed samples were made via validated Monte Carlo Gean4.

Results: Considering the net area, from the spectrometric analysis, of the selected elements and their efficiency value; the concentration of the ^{40}K, ^{238}U, and ^{232}Th in the analysed samples are directly measured. The results indicate a high concentration of ^{40}K in the analysed soil, which may be due, even after the subtraction of the normalized background level, used of fertilizers (NPK formula).

Conclusion: the investigation of soil composition shows that the concentration of the long-lived radionuclides varies according to geometrical position. The absorbed dose at 1m is slightly higher than the word wide equivalent to 55nGy/h.

References:

[1]. UNSCEAR, Sources and Effects of Ionizing Radiation. Annex B Vol. 1 (2008)

[2]. Boukhalfa, S. (2021). DEVELOPMENT OF A GAMMA SPECTROMETRY DETECTION SYSTEM FOR RADIOACTIVITY EVALUATION IN DIFFERENT TYPES OF SAMPLES (Doctoral dissertation, UNIVERSITY OF BLIDA)

Keywords: Soil Analysis ; Environnement ; Radioprotection ; Radioelement ; gamma Spectrometry.

T1-P29: Energy spectra with the Klein-Gordon equation for the lithium dimer using the Faynman approach

A. Ghobrini[a,b@], H. Boukabcha[c], I. Ami[a,d]

[a:] *Department of Physics, Faculty of Sciences, M'hamed Bougara University of Boumerdes.*
[b:] *Laboratory of Coatings, Materials, and Environment (LRME), M'hamed Bougara Universty of Boumerdes (UMBB), Algeria*
[c:] *Laboratory of Energy and Intelligent Systems, University of Khemis Miliana, Khemis Miliana 44225, Algeria d: Laboratory of Theoretical Physics and didactic, Faculty of Physics, USTHB, BP 32 El allia Bab Ezzouar,Alger, Algeria.*
[@]*Corresponding author: a.ghobrini@univ-boumerdes.dz*

Background/Purpose: In this work, the relativistic and non-relativistic energy equations for the $a^3\sum_u^+$ state of $^7Li_2$ dimer of spinning and vibration are found.

Materials &Methods: The Greene-Aldrich approximation to the centrifugal term and the Feynman technique [1] with the enhanced deformed Pöschl-Teller oscillator [2] were used to solve the Klein-Gordon equation for the "l" state. Some of the numerical findings were displayed using Maple software.

Results: We assess the correctness of Feynman's technique by calculating the eigenvalues of the vibrational and rotational-vibrational energies of the $^7Li_2\left(a^3\sum_u^+\right)$ utilizing the experimental values of the bond length, equilibrium dissociation energy, and harmonic vibrational frequency constant as input data. We first compare our vibrational energy in the range of vibrational quantum numbers from 0 to 10 with RKR data [3], ab initio data, improved values of the Pöschl-Teller potential, and improved values of the Tietz potential using the supersymmetric invariant form approach in order to ascertain the relative deviations from the RKR experimental data [3]. When compared to the RKR data, the average absolute percentage deviations (AAPD) from the RKR data [3] for the lithium dimer are 0.3634%, significantly less than the 0.40357%, and 0.61279 percent values with the improved Pöschl-Teller potential and the improved Tietz potential, respectively, found in the literature. The values of En,ℓ were then acquired, and they were contrasted with the Deng-Fan potential values found in the literature Omar Mustafa's .

Conclusion: Finally, the findings predicted by the enhanced deformed Pöschl-Teller oscillator correspond well with the data available in the literature, suggesting that this potential is a perfect model to represent the rotational-vibrational energies for the lithium dimer.

References:

[1]. Ghobrini A et al. Energy spectra with the Dirac equation of the q-deformed generalized Pöschl-Teller potential via the Feynman approach for $^{39}K_2\left(a^3\Sigma_u^+\right)$. *Journal of Molecular Modeling. 2024;30: 340.* doi:https://doi.org/10.1007/s00894-024-06139-0

[2]. Eyube ES et al. Analytical prediction of enthalpy and Gibbs free energy of gaseous molecules. Chemical Thermodynamics and Thermal Analysis. 2022;6:100060. doi: https://doi.org/10.1016/j.ctta.2022.100060

[3]. Linton C et al. The high-lying vibrational levels and dissociation energy of the $a^3\sum_u^+$ state of $^7Li_2$. *Journal of molecular spectroscopy*. 1999; *196*:20-28. doi:https://doi.org/10.1006/jmsp.1999.7858.

Keywords: **Feynman method; Klein-Gordon equation; Rotation-vibrational energy; The improved deformed Pöschl-Teller oscillator; Lithium dimer**

T1-P30: Electron beam enlargement modelling in the environmental scanning electron microscope at the low gas temperature.

R. Belkorissat

Department of Computer Science. Ibn Khaldoun University Tiaret, Algeria.
Corresponding author belkhorissat_r@proton.me

Background/Purpose: Analyzing a sample using the environmental scanning electron (ESEM) microscopy is often confronted to a set of constraints due to the presence of gas during the passage of the primary electron beam. Indeed, the electrons beam gas atom scattering will deviate one fraction of the primary electrons beam from their initial axis direction and will forming a nearly cone shape around the initial electrons beam impact point with the sample surface. This cone shape is called the skirt of electrons, and the detected signal to noise ratio in the ESEM is more important if the electrons skirt radius is reduced. Many parameters affecting the change of the electron skirt radius are considered theoretically and experimentally. Among them, the electron beam energy (E), the working distance (WD), gas pressure (P) and gas type [1]. The effects of all these parameters were only studied under room ambient temperature. Recently, when the low temperature method (LTM) for water vapor gas is applied in ESEM analysis of biological samples with their native states, the gas temperature can be decreased from room temperature to (-20 °C) for gas pressure ranging from 10 Pa to 200 Pa. Therefore, this parameter effect on the electrons skirt radius must be elucidated for different gas pressure.

Materials & Methods: In this study, the effect of water vapor gas temperature on the electron skirt radius is calculated for two water vapor gas pressures (of 100 Pa and 10 Pa). This was done via a new calculation program based on Monte Carlo method [2] and by selecting the elastic or inelastic collision processes, when monitoring the electron trajectories for the considered ESEM conditions.

Results: The obtained results showed a decrease of the un-scattered electron-beam fraction when decreasing the gas temperature. On the other hand, this change is very low at 10 Pa gas pressure (The unscattered electrons beam fraction variation of 2% is obtained). This obtained results can be explained to the decrease of the electrons atoms scattering probability, resulted from the decrease of the water vapor molecules concentration when the gas temperature is increased).

Conclusion: The present improved Monte Carlo calculation of electron-gas interaction allowed us to obtain the minimum of beam skirt radius with change of un-scattered electron fraction at low scattering conditions. The obtained results showed that both the vapor gas pressure and temperature can affect the beam skirt radius.

References:

[1]. Danilatos G D, Fondations of environmental scanning electron microscope Advances in electronics and electron physics. 1988, 71 : 109-250.
[2] Joy D C, Monte Carlo Modeling for Electron Microscopy and Microanalysis, OUP: NY, 1995.

Keywords: ESEM; Monte Carlo simulation; electron-gas interaction; skirt

T1-P31: Eigensolutions of ro-vibrational bound states of the energy- dependent general molecular potential in the case of diatomic molecules

A. Haddouche[1,2], R. Yekken[1,*] and S. Boufas[1]

[1]*Laboratoire de physique théorique, Faculté de Physique, U.S.T.H.B, BP 32 El Alia, Bab Ezzouar 16111 Alger, Algéria.*

[2]*Département des classes préparatoires, Ecole Nationale Supérieure des Travaux Publics, BP 32 Rue Sidi Garidi, 16006, Kouba, Alger, Algeria.*

[@]*Corresponding author : ryekken@usthb.dz*

Background: This work investigates the analytical determination of the energy spectrum for ro-vibrational bound states using the energy-dependent general molecular potential (EDGMP). Energy-dependent potentials provide a framework for incorporating nonlinear effects [1,2,3]. The three-dimensional wave equation is solved for arbitrary angular momentum using the Pekeris approximation, which simplifies the centrifugal term. The Asymptotic Iteration Method (AIM) is then employed to derive analytical expressions for the energy spectrum and eigenfunctions. The method is applied to finite electronic states of various diatomic molecules, demonstrating its effectiveness in modeling molecular interactions.

Methods: The energy spectrum and wave functions of the EDGMP potential are obtained using the Asymptotic Iteration Method (AIM). This approach transforms the Schrödinger equation into a recursive form, while Pekeris approximation is used to handle the centrifugal term.

Results: The EDGMP potential successfully reproduces the RKR data of the N_2 molecule, outperforming the local GMP potential (γ=0). The ro-vibrational energy spectra for HCl, HF, and OH molecules were calculated using the EDGMP potential with three models: Deng-Fan, Improved Rosen-Morse, and Improved Tietz (γ=−0.1). The results show consistent trends, with Deng-Fan yielding the highest energies and Improved Tietz the lowest. This confirms the EDGMP potential's effectiveness in describing ro-vibrational states in diatomic molecules.

Conclusion: Few potentials have exact solutions of their spectra. Coulomb and harmonic oscillator potentials are typical examples. Using the EDGMP potential and the AIM method with the Pekeris approximation, we obtained analytical expressions for the molecular ro-vibrational spectrum and wave functions for any quantum state *nl*. Modeling the EDGMP molecular potential in terms of the spectroscopic parameters of diatomic molecules made it possible to generate various forms of well-known molecular potentials and successfully apply them to various real molecules.

References:

[1] R. Yekken, R.J. Lombard, J. Phys. A: Math. Theor.**43**, 125301 (2010)
[2] R. Yekken, M. Lassaut and R.J. Lombard, Few-Body Syst, vol.**54**, Nos.5-6 (2013)
[3] A. Haddouche, R. Yekken , R.J. Lombard, I. Ami, Eur. Phys. J. Plus, 137: 1066 (2022)

Keywords: Diatomic molecular analytic eigensolutions, energy dependent potential, general molecular potential, Schrödinger equation, asymptotic iteration method.

T1-P32: Study of Ro-Vibrational Energy Spectrum in the Case of the Energy-Dependent Kratzer Potential Applied to Diatomic Molecules

S. Boufas@, R. Yekken

Laboratory of Theoretical Physics and Didactics, Faculty of Physics, University of Science and Technology Houari Boumediene, USTHB

@ Corresponding author boufassamia@gmail.com

Background/Purpose: Diatomic molecules are physical systems made up of two atoms. They are characterized by their rotation and vibration movements due to oscillations near their equilibrium position.

Great interest has been paid to analytical solutions of such systems with potential physics describing the vibrational and rotational movements. Taking into account the weak relativistic effects, we can introduce an energy dependence in the potential expression [1,2]. In this work, our interest is focused on the analytical resolution of the three-dimensional Schrödinger wave equation governed by the energy dependent Kratzer potential. applied to diatomic molecular systems.

Materials & Methods: In order to calculate, analytically, the ro-vibrational energy spectrum of the bound states '*nl*', we used the asymptotic iteration method (AIM) [3]. However as the expression of the energy dependent Kratzer potential is a function of the spectroscopic parameters 'D_e' and '*a*' which represent, respectively, the spectroscopic dissociation energy and the range of the potential, we were led to determine these two molecular parameters. Applications to diatomic molecules I_2 and *LiH* were carried out followed by a parallel comparison with the numerical results.

Results: The results obtained for the energies of the vibrational states Ens and the energies of the ro-vibrational states E_{nl}, ($l \neq 0$) produced by (AIM) as a function of γ linked to the term of the energy dependence, are in excellent agreement with the numerical results. We have also plotted the energy-dependent Kratzer potential, in the state E_{2p} where $D_e = 10$, $r_e = 1$, taking γ = 0, γ = 0.1, γ = 0.3 and γ = 1. The corresponding curves clearly show that the shape of the Kratzer potential remains the same for the different values of γ except that the spectroscopic dissociation energy D_{nl} decreases as the constant γ increases. These same curves tend towards an identical limit whatever the value of γ, which reflects the same asymptotic behavior of the Kratzer potential depending on the energy

Conclusion: The calculations given by the AIM method reproduce the exact numerical results with a very high precision. These results prove the right choice and express the applicability of our calculation model to realistic cases.

References:

[1]. R. Yekken, R.J. Lombard, J. Phys. A: Math. Theor.**43**, 125301 (2010).

[2]. S. Boufas, R. Yekken, E. Hocine, I. Ami, Eur. Phys. J. Plus, 137: 951 (2022)

[3]. ORHAN Bayrak, I Boztosun, and HAKAN Ciftci. Inter. J. Quantum Chem. 107(3) :540–544,2007,

Keywords: Schrödinger wave equation, Energy-dependent potentials, Kratzer potential, asymptotic iteration method (AIM), Diatomic molecules;

T1-P33: ab-initio calculations of oscillator strengths for Ti II

F.Z. Boualili@, M. Nemouchi

Laboratoire d'Electronique Quantique, Faculté de Physique, USTHB, Alger.
@ Corresponding author naimaboualili24@gmail.com

Background/Purpose: Accurate atomic data for Ti II are essential for abundance analyses in astronomical objects. This work aims to provide accurate and extensive results of oscillator strengths. By comparing our results to existing experimental and semi-empirical data, we aim to assess the accuracy of our theoretical models.

Methods: Oscillator strengths were calculated using the multiconfiguration Hartree-Fock (MCHF) method combined with the Breit-Pauli (BP) approximation, implemented in the atomic structure package ATSP2k [1].

Results: We present oscillator strengths (length and velocity forms) for transitions between the 3d2 4p 4G0 9/2,7/2 and 3d2 4s 4F 7/2,5/2 states. These results are compared with previous calculations and measurements, including data from the NIST Atomic Spectra Database.
The analysis of our theoretical results begins with a comparison between the length and velocity forms. This comparison revealed a convergence between the two forms in our calculations, which then allowed us to proceed with comparisons to other studies.
Our results show good agreement with experimental data from NIST. Overall, the present theoretical oscillator strengths demonstrate better agreement with experiment than previous theoretical predictions.

Conclusion: We have performed a comparison of the computed oscillator strengths with experimental results. There is a significant improvement in the accuracy in the computed oscillator strengths of E1 transitions compared with previous theoretical works. These results can be further improved by including QED relativistic effects through the MCDHF (multiconfiguration Dirac-Hartree-Fock) method.

References:

[1]. Fischer C F et al.. An MCHF atomic-structure package for large-scale calculations. *Computer Physics Communications*. 2007;176:559-579. doi:10.1016/j.cpc.2007.01.006

[2]. Ruczkowski J et al. (Semi-empirical calculations of oscillator strengths and hyperfine constants for Ti II). *Journal of Quantitative Spectroscopy and Radiative Transfer*. 2014;149:168-183. doi:10.1016/j.jqsrt.2014.08.010

Keywords: Oscillator strength, Ti II, Breit- Pauli, MCHF.

T1-P34: Radiation-Matter Interaction and Instabilities for Inertial Confinement Fusion

H. Benmakrelouf[1@], K. Bendib-Kalache[1], A. Bendib[1]

[1] *Laboratoire d'Electronique Quantique, Faculté de Physique, University of Sciences and Technology- Houari Boumediène, El Alia BP 32, Bab Ezzouar 16111, Algiers, Algeria*

[@] *Corresponding author benmakrelouf.hind.sm8.g2@gmail.com*

Background/Purpose: The study of high-temperature plasmas has gained significant attention due to advancements in laser technology. Powerful laser pulses can now interact with solid targets, such as in inertial confinement fusion (ICF), producing plasmas with temperatures reaching up to 15 keV [1]. At such temperatures, the rest mass energy of electrons becomes comparable to their thermal energy. This work investigates the interaction between laser beams and plasma modes, focusing on parametric instabilities like the filamentation instability (FI), which is crucial for understanding energy absorption and laser- plasma coupling in ICF.

Materials & Methods: The filamentation instability (FI) is driven by laser energy absorption and the ponderomotive force, which alter the refractive index and amplify initial laser beam modulations [2]. The dispersion relation of the FI is derived from a hydrodynamic model coupled with Maxwell's equations, valid for arbitrary electron temperatures. An explicit analytical expression for the growth rate is deduced, depending on laser intensity and other parameters. The study is applied to laser-created plasmas with temperatures exceeding 10 keV [3].

Results: The analysis reveals that the optimum wavenumber for FI is located in the semicollisional range. Relativistic effects are shown to reduce the instability growth rate. Additionally, the ponderomotive force is found to be a more efficient driver of FI compared to thermal effects. These findings provide insights into the behavior of high-temperature plasmas and the role of FI in laser-plasma interactions.

Conclusion: This study highlights the importance of relativistic and ponderomotive effects in the filamentation instability within high-temperature plasmas. The results contribute to a better understanding of laser-plasma interactions in inertial confinement fusion, particularly in the context of energy absorption and instability growth. Future work will explore additional parametric instabilities and their implications for ICF applications.

References:

[1]. A. B. Langdon and D. E. Hinkel, Phys. Rev. Lett. 89, 015003-1 (2002).
[2]. A. Bendib, F. Bouzid, K. Bendib, and G. Matthieussent, Phys. Plasmas 6, 4008 (1999).
[3] . A. Bers, I. P. Shkarosfsky, and M. Shoucri, Phys. Plasmas 16, 022104 (2009).

Keywords: inertial confinement fusion; relativistic plasma; parametric instability; filamentation; fluid theory.

T1-P35: Stopping Power Calculation of Heavy Ions in A Compound Target Using the Readjusted Bohr Model

I. Hamache[1@], A. Guesmia[2], A. Belalia[3]

[1, 3]*LPTHIRM, Physics Department, Faculty of Sciences, Saad Dahlab Blida 1 University, BP 270, Route de Soumaa, Blida, Algeria.*

[2] *LNCSM, Department of Physics, Higher Normal School of Kouba -Echeikh Mohamed Elbachir Elibrahimi-, B.P N°92 16308 Vieux Kouba, Algeria.*

[2]*Materials Research Department, iThemba LABS, National Research Foundation, P.O. Box 722, Somerset West 7129, South Africa.*

[@] *Corresponding author* hamache_imane@univ-blida.dz

Background/Purpose: A large interest is attributed to energy loss of heavy charged ions in matter as it presents a significant importance to various applications of physics. This work presents a stopping power calculation for a compound target, polyethylene (PET), to a variety of elements using the readjusted Bohr model [1].

Materials & Methods: The stopping power of the following elements: C, H and O to Li, C, O, Ar, Ti and Cu was calculated by using the theoretical formula of the readjusted Bohr model [1]. Using the Bragg's additivity rule [2] the stopping power of PET to the cited elements was then deduced.

Results: The results of the stopping power were compared with the available experimental data and values generated by the simulation code "the stopping and range of ions in matter "(SRIM) [3]. The calculation reproduced well the overall behaviour of the stopping power curve, demonstrating good agreement in the low-energy range and high energies for most elements within discrepancies of 5-20%. The intermediate energy range, however, showed significant deviations, particularly for the heavier elements: Ar, Ti and Cu. In addition, Bragg's additivity formula provided satisfactory results for the most studied elements.

Conclusion: The RBM model provides good estimate for the stopping power of the compound target (PET). However, deviations remain around Bragg peak, where most theories fail to provide accurate predictions. The deviation may be due to the overlap term not included in our work [1], which will be a future aspect for further improvement of the model.

References:

[1]. Guesmia A, Msimanga M, Mtshali C, Pineda-Vargas C, & Nkosi M. Readjustment of the Bohr stopping force from energies of keV/n to a few tens of MeV/n ions in elemental targets. Physics Letters A. 2020; 384(31):126794.
doi: 10.1016/j.physleta.2020.126794

[2]. W. H. Bragg M.A. & R. Kleeman B.Sc.. On the α particles of radium, and their loss of range in passing through various atoms and molecules. Philosophical Magazine Series 6. 1905; (10)57: 318-340.
doi: 10.1080/14786440509463378

[3]. J.F. Ziegler, The stopping and range of ions in matter, http://www.srim.org/, version SRIM.

Keywords: Stopping power; Bragg's additivity rule; Polyethylene (PET);

T1-P36: Study of the Influence of Ion Charge-State Dependence on the Electronic Sputtering Yield Induced in Case of Mev I^{q+} Heavy Ions Incidents on Gold Thin Films

A. Boubir[1@], S. Mammeri[2], M. Saad[2], M. Salhi[3]

[1]*Department of Physics, LRPRIM Laboratory, Batna 1 University, Batna, Algeria*
[2]*Nuclear Research Center of Algiers, 02 Bd. Frantz Fanon, B.P. 399, Alger RP, Algiers, Algeria*
[3]*Nuclear Research Center of Birine, B.P. 180, Ain Oussera, Djelfa, Algeria.*
[@] *Corresponding author: abir.boubir@univ-batna.dz*

Background/Purpose: When a swift charged particle enters matter, it interacts with the target atoms, losing energy until it comes to rest. This energy loss occurs through two main processes: (i) electronic inelastic collisions, transferring energy to target electrons, and (ii) nuclear elastic collisions, transferring energy to atomic nuclei. These interactions cause irradiation effects, including atomic defects, phase transformations, and significant damage such as latent tracks and surface sputtering [1]. Investigating and controlling these effects is crucial and can be achieved using ion-beam analysis techniques or through theoretical modeling with computer simulation codes [2, 3].

Materials & Methods: In the present study, we examined the effect of ion charge-state, before equilibrium within the target material, on the induced sputtering yields. This was achieved using an extended three-dimensional inelastic thermal spike model, which incorporates radial distance, penetration depth, and irradiation time. We focused on 36, 55 and 210 MeV Iq+ heavy ions incident on a metallic gold target (100 nm thick) at different charge states (q= 7+, 8+,11+,15+,16+,21+and 29+). These used ions here, with their respective kinetic energies and charge states, were selected based on the availability of experimental data for energy losses and sputtering yields in metallic gold.

Results and conclusions: The evolution of the charge state before equilibrium within the target was determined using an analytical formulation based on penetration depth, combined with experimental and semi-empirical electron-loss cross-section data. These charge-state data were integrated into a 3D-iTS calculation program to generate numerical sputtering yields. The results were compared to experimental data on stopping power and sputtering yield [1].

References:

[1]. W. Assmann, in R. Behrisch, W.Eckstein (Eds.): Sputtering by particle bombardment: Experiments and Computer Calculations from Threshold to MeV Energies, Springer-Verlag Berlin Heidelberg, Top Appl Phys. 2007; 110: 401-450.

[2]. A. Boubir et al., Experimental study and thermal spike modeling of sputtering in SiO2 thin films under MeV Au^{q+} heavy ion irradiation. Surface & Interface Analysis. 2021; 53: 737-746. https://doi.org/10.1002/sia.6973

[3]. S. Mammeri et al., Sputtering and structural modifications induced in silicon dioxide (SiO_2) thin films under (10-40 MeV) Au^{q+} heavy ion irradiation. Surface & Interface Analysis. 2023; 55: 899-908. https://doi.org/10.1002/sia.7257

Keywords: Swift heavy ions; Sputtering yield; Ion charge-state; Inelastic thermal spike model and Irradiation effects.

T1-P37: Proton's Model for ^{4}He, ^{7}Li, ^{12}C, ^{16}O ions stopping power in Aluminum, Copper, Silver and Gold targets for the energy range 1 to 14 MeV/n

S. Foul[@], M. Chekirine, R. Khelifi[1]

[1] Department *of physics, Laboratory of Theoretical Physics and Radiation-Matter Interactions, University of Blida1, PB 270 Blida, Algeria.*

[@] *Corresponding author* Foul-Sihem@outlook.com

Background/Purpose: The measure of stopping power for swift ions is important for studies in several fields of fundamental and applied sciences such as radiation dosimetry, medical physics, ionic implantation and many others. The Modified Bethe-Bloch formula depends on several corrective terms; the most important of these is the shell correction especially for energies of a few MeV/n. The charge state of the incident ions also influences in this latter, particularly for heavy ions at intermediate speeds $2Z_1V_0 \geq V \geq V_0Z_1^{2/3}$.

Materials & Methods: In the present work, we have proposed an expression for the stopping power's calculation of charged particles which is deduced from the Modified Bethe- Bloch formula, our expression is based principally on accurate experimental data of protons' stopping power, without having to determine the shell correction and the mean ionization potential of the absorber film. We have calculated the stopping power of ^{4}He, ^{7}Li, ^{12}C and ^{16}O ions in Aluminum, Copper, Silver and Gold targets for the energy range [1,14] MeV/n.

Results: We notice that the maximum deviations of the present work are equal to 3% for helium and lithium ions, and mostly less than 5% for carbon and oxygen ions through all the targets compared to the Modified Bethe-Bloch formula and SRIM-2013[1], 2.9% for helium and lithium ions compared to ASTAR[2] and MSTAR[3], and mostly less than 5% for carbon and oxygen ions compared to MSTAR. We have found good results compared to the experimental data for helium and lithium ions the maximum discrepancy is 2.8%, the maximum differences for carbon and oxygen ions are mostly less than or equal to 5%.

Conclusion: Comparing our values with those calculated by the Modified Bethe-Bloch formula, obtained experimentally and generated by the calculation codes, we conclude that this expression has reproduced good results. Where we can clearly see its advantage that allows us to calculate the stopping power for ions of Z_1 superior than 1 without needing to calculate the shell correction and to insert the mean ionization potential.

References:

[1]. J. F. Ziegler, M. D. Ziegler J.P. Biersack, SRIM-2013 – the Stopping and Range of Ions in Matter, Version 2013.00, code. Available from: http://www.srim.org.

[2]. Berger, M.J., Coursey, J.S., Zucker, M.A., Chang, J., 2005. ESTAR, PSTAR and ASTAR: Computer Programs for Calculating Stopping-power and Range Tables for Electrons, Protons, and Helium Ions. Available from: http://physics.nist.gov/StarS.

[3]. Paul, H. and Schinner, A., program MSTAR, version 3.12 (2004). Available from: http://www.exphys.jku.at/stopping/.

Keywords: **Stopping power; SRIM-2013; ASTAR; MSTAR**

T1-P38: Quantum-mechanical analysis of transport coefficients for NO^+ in Helium gas

L. Aissaoui@, I. Ghodbane

[1] *Physics of Radiation and their Interaction with Matter Laboratory (PRIMALAB), Physics Department, University of Batna 1, Batna 05000, Algeria*

@ aissaouilamia@yahoo.fr

Background/Purpose: Helium is the most commonly utilized buffer gas in drift-tube experiments focused on measuring ion-neutral reaction rate coefficients. As a result, a precise understanding of energy potential surfaces (EPS) and transport cross-sections is essential for elucidating ion transport properties, including ion mobility and diffusion. This study aims to investigate the quantum-mechanical calculation of ion mobility for NO^+ ions in helium under low gas temperature conditions, employing the ab-initio potential energy surfaces of Viehland et al., [1].

Materials & Methods: The study employs the *Beyond Monchick–Mason Approximation* (BMM) [2] to calculate the effective potential, which is subsequently used to derive the quantum-mechanical diffusion cross-section through Viehland's PC.F95 program. Ion mobility and diffusion coefficients are then computed using Viehland's GC.F95 program, with calculations conducted for two distinct gas temperatures: 4.3 K and 300 K.

Results: The ion mobility of NO^+ ions in helium was calculated and compared against available experimental data, as well as against values derived using the effective cross- section method through the BMM approach. The computed results demonstrate that ion mobility values derived from the effective potential closely align with the experimental data, offering a superior match compared to those obtained via the effective cross-section approach.

Conclusion: Based on the outcomes of this study, we can underscore the reliability of using the BMM method for determining the effective potential over its application to the effective cross-section. This approach yields more accurate predictions for ion mobility, highlighting its potential for more precise modelling of ion transport in helium and other similar systems.

References:

1 Viehland L. A et al.. Transport coefficients for NO^+ ions in helium gas: a test of the NO^+-He interaction potential. *The Journal of Chemical Physics, 1996;211:1-15*. doi:10.1016/0301- 0104(96)00158-9

2 Monchick L et al.. Transport Properties of Polar Gases. *The Journal of Chemical Physics* 1961; 35: 1676–1697. doi:10.1063/1.1732130

Keywords: **EPS, diffusion cross-section, BMM, Ion mobility.**

T2-P1: Measurement of Scintillation Light Yield in Sol-Gel Synthesized Ce^{3+}-Doped Y_2SiO_5 Nanomaterials

B. Zahra[a@], H. Mekki[a]. L. Guerbous[b]. M. S.-E. Hamroun[c]. A. Bourenane[a]

[a]*Nuclear Research Center of Birine, B.P : 180 Ain Oussera , Djelfa, Algeria*
[b]*Nuclear Research Center of Algiers, 02, Bd Frantz Fanon, BP 399, Algiers, 16000, Algeria*
[c]*Centre de Recherche Scientifique et Technique en Analyses Physico-Chimiques, BP 384, Zone Industrielle, Bou-Ismail CP 42004, Tipaza, Algeria*
[@]Corresponding author b.zahra@crnb.dz

Background/Purpose: In this study, a sample detector was prepared using Y_2SiO_5: Ce^{3+} (YSO: Ce^{3+}) nanophosphor powder synthesized via the sol–gel method. The powder, with a Ce^{3+} concentration of 0.1%, was annealed at 1000°C in air atmosphere. The primary objective was to assess the scintillation light yield (SLY) of YSO: Ce^{3+} nanoscintillator under gamma-ray excitation, evaluating its potential for use in radiation detection applications.

Materials & Methods: Assessing the scintillator's SLY poses various complexities due to multiple factors [1] . Research has yielded differing findings for well-known crystals like NaI(Tl) and CsI(Tl), influenced by aspects such as the method of crystal growth and the approach employed to measure light output. In this research, 662 keV γ-rays from a ^{137}Cs source were used, with a bi-alkali GDB-4FF photomultiplier tube (PMT) serving as the photodetector. Additionally, a nuclear instrumentation setup was established to collect pulse height spectra. A NaI(Tl) single-crystal scintillator was used as a reference detector to estimate SLY through a comparative method [1].

Results: The YSO:Ce^{3+} nanoscintillator achieves a SLY of about 51% of the NaI:Tl reference, outperforming the Y_2SiO_5:Ce single-crystal films grown via liquid phase epitaxy, which only reach 31% [2]. Despite having a lower SLY than NaI:Tl, YSO:Ce^{3+} nanoscintillator offers benefits such as lower production costs, better scalability, material robustness, and flexibility in application design. However, its powder form presents challenges like opacity, leading to photons reabsorption that can diminish light yield.

Conclusion: The synthesized YSO: Ce^{3+} nanoscintillator demonstrates significant potential as a viable alternative to conventional scintillators in radiation detection applications. Future research will focus on optimizing the scintillation properties by varying the Ce^{3+} concentration within the YSO host matrix, aiming to enhance the performance of these nanoscintillators for advanced detection technologies.

References:

[1] M. Moszyński, M. Kapusta, M. Mayhugh, D. Wolski, S.O. Flyckt, Absolute light output of scintillators, IEEE Trans. Nucl. Sci. 44 (1997) 1052–1061. https://doi.org/10.1109/23.603803.

[2] K. Wantong, N. Yawai, W. Chewpraditkul, M. Kucera, M. Hanus, M. Nikl, Luminescence and scintillation properties of liquid phase epitaxy grown Y2SiO5:Ce single crystalline films, J. Cryst. Growth 468 (2017) 275–277. https://doi.org/10.1016/j.jcrysgro.2016.12.094.

Keywords: Y_2SiO_5: Ce^{3+}; scintillation light yield; sol-gel synthesis; radiation detection, nanoscintillator;

T2-P2: Characterization of SiC Thin Layers Elaborated by RF Magnetron Sputtering Technique for Radon sensing

N. Ait Kaci[1@], S. Kaci[2], H. Menari[2], K.H. Bentoumi[1], A. Nechaf[3], A. Lachemet[4]

[1] *Centre de Recherche Nucléaire d'Alger*
[2] *Centre de Recherche en Technologie des Semi-conducteurs pour l'Energétique*
[3] *Autorité Nationale de Sûreté et de Sécurité Nucléaires*
[4] *Université des Sciences et de la Technologie Houari Boumediene*
[@] n.aitkaci@crna.dz

Background/Purpose: Accurate detection of Radon-222 (Rn-222) concentrations is critical for indoor air quality assessment and occupant safety [1]. This study investigates silicon carbide (SiC) thin films, fabricated via sputtering magnetron, as sensitive and reliable Radon- 222 sensors.

Materials & Methods: The study explores SiC thin films fabricated using magnetron sputtering, highlighting their strong adhesion, uniformity, and controllable thickness [2]. SiC films were characterized using Four-Point Probe, UV-Vis Spectroscopy, SEM, XRD, XRF, and AES to assess, respectively, electrical, optical, morphological, and structural properties. Naturally occurring radioactive materials (NORM) from the petroleum industry, rich in radium- 226 (Ra-226) that produces radon-222 as a decay product, are used as a source of radon gas (Rn-222). The sensitivity of the thin film was evaluated by current-voltage (I-V) measurements on a Schottky contact diode structure (SiC/pSi(100)/Cu), before and after 43 and 71 days of NORM exposure. The exposure took place in a hermetically sealed container to ensure the secular equilibrium of Ra-226 and its progeny, including radon-222 (Rn-222), polonium-218 (Po-218), polonium-214 (Po-214), polonium-210 (Po-210) etc.

Results: Optimized sputtering parameters allowed for SiC thin films with a thickness of 1.1165 µm and a band gap of 1.8 eV [3]. SEM confirmed uniform deposition, while resistivity measurements indicated smooth current flow which indicate that the current could flow fluently. XRF and AES detected Si, C, and O elements, and XRD showed an amorphous structure. The I-V results demonstrated a Schottky metal-semiconductor contact with sensitivity variations in forward bias after Radon-222 exposure. The supposed detection mechanism is attributed to the diffusion of radon and the ionization of the SiC layer by alpha particles from the decay of radon and its progeny.

Conclusion: The results suggest that amorphous SiC thin films can be suitable as room-temperature radon-222 sensors due to their significant response changes upon radon exposure. Future developments could involve integrating the sensor into an electronic circuit to measure changes in electrical conductivity or measure the electrical current created by ionization, thus enabling accurate detection of radon concentration.

References:

[1] L.J.R. Nunes and all, Int J Environ Res Public Health, 19(7):3929 (2022), doi: 103390/ijerph19073929
[2] R. Saleh, L. Munisa, W. Beyer, Thin Solid Films, 11-2 (426), 117-123 (2003), doi:10.1016/S0040-6090(03)00003-8
[3] N. Ait Kaci, S. Kaci, K.H. Bentoumi and all, Acta Phys. Pol. A, 6 (145), 336 (2024), doi:10.12693/APhysPolA.145.336A

Keywords: SiC, Thin films, Schottky diode, Radon 222, Sensor;

T2-P3: Experimental stopping power data for alpha particles in Calcium Fluoride

N. Smati[1], D. Moussa[1@], S. Damache[2], W. Yahia Cherif[2], M. Saad[2]

[1] *Faculty of physics, USTHB BP 32 El Alia Bab Ezzouar 16111, Algiers*
[2] *Nuclear Research Center, CRNA 02 Bd Frantz Fanon, Algiers*
[@] *Corresponding author: djamelmoussa@gmail.com*

Background/Purpose: This work is a contribution to an experimental study of the stopping power of alpha particles in compound matter in the energy range of MeV/u. Stopping power of simple element have been subject of extensive experimental studies, those measured with compound matter are rarely considered, because of many difficulties involved in preparing, handling and characterizing those thin films. Moreover, the effects of ion irradiation can destroy their structures, which are often very fragile, thus compromising the reliability of the measurements. The aim of this study is to evaluate and compile these data into a complete database that can be used for fundamental research and various practical applications and to verify the validity of various new theoretical models in the field of ion- matter interaction.

Materials & Methods: The energy losses of ≈ (1 - 3) MeV alpha particles delivered by the CRNA's 3.75 MV Van de Graff accelerator are measured by the technique of transmitting secondary beam energy backscattered in a target composed of calcium fluoride deposited on a self-supporting aluminium target; this CaF2 target was manufactured using the vacuum evaporation technique well described in the previous group's work [1,2].

Results: The experimental stopping powers as a function of alpha particle energy which require a minute accelerator energy calibration, a good investigation of the characteristics of the targets (stoichiometry, impurity contents and thicknesses) by ion beam analysis techniques namely (Rutherford Backscattering Spectroscopy (RBS) and Nuclear Reaction Analysis (NRA). The experimental obtained results show in general good agreements with the generated ASTAR [4] values. Besides the calculated SRIM [3] code data are slightly lower than our new experimental results obtained in this present work but still remain in the error bars.

Conclusion: This work aims to complete the database by selecting compound material not available in the literature, studying the stopping power of composite materials experimentally enabling us to test the validity of Bragg and Kleeman's addition rule and also to deduce their atomic characteristic mainly the mean excitation and ionization potential.

References:

[1] S. Damache, D. Moussa and S. Ouichaoui, Nucl. Instr. and Meth. B 308 (2013) 46

[2] Ion beam analysis of CaF2 compounds Identification of some excited nuclear states in fluorine and Aluminum nuclei, 1st National Conference on Nuclear Techniques and their Applications, October 1st&2nd, 2024 Algiers.

[3] J.F. Ziegler. Helium - Stopping Powers and Ranges in All Elements, vol. 4 of The Stopping and Ranges of Ions in Matter. Pergamon Press, New York, 1977. 22, 86

[4] http://physics.nist.gov/physRefData/Star/Text/ASTAR.html.

Keywords: Stopping power; Thin films; Vacuum evaporation; Energy loss

T2-P4: Influence of Fpe and Resolution of Hpge Detector in Environmental Gamma Ray Measurements

M. Fares[1] *

[1] *Nuclear Detectors, Nuclear Instrumentation and Detection Department, Nuclear, Nuclear Instrumentation Study and Development Division, Nuclear Research Centre of Birine, P.O. Box, Ain Oussera 17200, Djelfa, Algeria.*
**Email: m.fares@crnb.dz*

Background/Purpose: In experimental research work, it is necessary to obtain quality control of the system used in a gamma spectrometry experiment. The HP-Ge semiconductor detector is often used in nuclear physics to measure the gamma ray activity of various samples, and it has many applications in the elemental analysis of neutron activation analysis, this is of utmost importance of distinguishing short half-life medical isotopes and radiological environment measurement. In each quantitative and qualitative analysis application [1], it is necessary to know the efficiency and accuracy of the detection of different gamma energies.

Materials & Methods: The equipment used consists of a coaxial HP-Ge detector with a resolution (FWHM) 1.8 keV to 1.33 MeV, the relative efficiency at 1.33 MeV for the ^{60}Co source is 20%; The efficiency and resolution of the HP-Ge detector was studied. Different photon energies of 356.01,511,661.60,1170, 1274.53 keV and 1330 keV were obtained from the radioactive sources (^{152}Eu, ^{137}Cs and ^{60}Co) used in this study.

Results: The FULL ENERGY PEAK EFFICIENCY (FPE) values for these gamma energies are 0.578, 0.281, 0.135, 0.115, 0.086 and 0.085% respectively with a combined relative standard uncertainty of less than 1%. The resolution values for the above different gamma ray energies are 0.69, 0.31, 0.18, 0.16 and 0.14% respectively, and we believe that these results are consistent with the reference results [2].

Conclusion: It was found that the efficiency of the detector decreases significantly with energy and that the accuracy of the detector is directly proportional to the energy of the gamma rays. We calibrated the noise spectrum in the laboratory and determined the radioactive elements present in it and the results were consistent with published research works.

References:

1. G.F. Knoll (2000) Radiation detection and measurements. *Third edition, John Wiley &Sons, Inc*, K,NewYork.
2. Nurgül Hafızo ˘glu, Efficiency and energy resolution of gamma spectrometry system with HPGe detector depending on variable source-to-detector distances, Eur. Phys. J. Plus (2024) 139:134 https://doi.org/10.1140/epjp/s13360-024-04903-y

Keywords: HP-Ge Detector, gamma-ray spectrometer, resolution, Full Energy Peak Efficiency;

T2-P5: Simulation and Modeling of Neutron Tomography Systems for Realistic Image Generation and Accurate 3D Reconstruction

A. Bourenane [@], O. Dendene, L. Boukerdja, R. Bouchama

[1] *Centre de Recherche Nucléaire de Birine, Algeria*
[@] *Corresponding author aissa.bourenane@crnb.dz*

Background/Purpose: Neutron tomography is a non-destructive imaging technique used to study the internal structures of materials. For the study of 3D reconstruction quality, it is essential to play on several experimental parameters. However, generating a significant number of real neutron images is prohibitively expensive due to the high operational costs of reactor usage [1]. This study aims to model a neutron tomography system using OpenMC[2] to produce realistic projection images and assess their suitability for 3D reconstruction, providing a cost-effective alternative to real reactor-based imaging.

Materials & Methods: The simulation model consists of a parallel neutron beam, a scintillator detector, and a cylindrical sample made of sedimentary rock spheres. Simulations were conducted with three different numbers of neutron histories (7 million, 70 million, and 700 million), and the computational time for each case ranged from 1 hour to 6 days on a 16-core Intel i7 workstation. These simulations generated synthetic projection images, which were analyzed for image quality and reconstruction potential.

Results: The results demonstrate a clear trade-off between the number of neutron histories and the quality of the generated images. Higher numbers of histories (700 million) produced images that closely resemble experimental results and enabled successful 3D reconstruction, while simulations with less numbers of histories yielded less accurate projections.

Conclusion: These synthetic images, which are computationally intensive to produce but cost-effective compared to reactor operation, provide a valuable alternative for developing neutron-imaging capabilities. Moreover, the use of such images to train artificial intelligence (AI) systems has become inevitable, given the increasing reliance on AI for image reconstruction, enhancement, and material analysis. This study not only demonstrates a framework for producing realistic and reconstructable neutron tomography images but also emphasizes the necessity of creating a comprehensive database of neutron images to support AI training. By addressing both computational and operational challenges, this work highlights the potential of simulation-driven methodologies in advancing neutron-imaging technologies.

References:

[1]. Kharfi, F., Denden, O., & Abdelkader, A. (2011). Implementation and characterisation of new neutron imaging system for dynamic processes investigation at the Es-Salam research reactor. Applied Radiation and Isotopes, 69(10), 1359-1364.

[2]. Romano, P. K., Horelik, N. E., Herman, B. R., Nelson, A. G., Forget, B., & Smith, K. (2015). OpenMC: A state-of-the-art Monte Carlo code for research and development. Annals of Nuclear Energy, 82, 90-97.

Keywords: **Neutron Tomography; OpenMC; Image Reconstruction; Monte Carlo Simulation; Synthetic Images**

T2-P6: Spectral and Chemical Characterization of Valued Pillared Clays

H. Cherifi-Naci[1@], H. Aksas[2]

[1] *Research Laboratory of Soft Technology, Valorization, physico-chemistry of Biological Materials and Biodiversity, L.T.D.V.P.M.B. Faculty of Sciences; Boumerdes university, Boumerces, 35000, Algeria*

[2] *Research Laboratory of Foot Technology,Faculty of Technology; Boumerdes University; Boumerces, 35000, Algeria.*

[@] Corresponding author:cherifi1ch@gmail.com

Background/Purpose: The purpose of our study is to determine the optimal activation conditions (Concentration: 7 M at temperature T = 90 ° C, Activation time = 4h, adsorbed H_2SO_4 = 1.45 meq / g of clay, CEC = 96 meq/100 g of clay) to achieve an adequate activated bentonite aimed to apply for pillaring operation. (Ag, Cu, Ti- oxides Pillared) Clays were synthesized from activated bentonite using $AgNO_3$, $CuCl_2$ and $TiCl_2$ solutions as pillaring agents. The pillared products were characterized by physic-chemical analysis (FTIR, SEM, XRD, XRF, CEC, specific surface area, Average pore diameter).The basal spacing for the (Ag, Cu, Ti-intercalated) bentonite and (Ag, Cu, Ti-pillared) bentonite are 40, 55 A° and 37 A°, respectively. The specific surface areas of (Ag, Cu, Ti-pillared) and natural bentonites are 410 and 65 m^2 g^{-1} respectively. With specific properties, the complexing Clay matrices are highly reactive nanomaterials and can be used in industrial wastewater treatment.

Materials & Methods: The chemical composition of the activated clay samples was analysed using X-Ray fluorescence spectrometry (Princeton Game Technology) [1].The structural modifications of the activated clay samples were identified by powder X-Ray diffraction pattern. The morphology of the modified clay materials was determined on a Philips L20 brand S.E.M from the XL 20 series, equipped with a PENTAX brand photographic camera.

Results: we notice by X-ray fluorescence: the decrease in the chemical composition of structural cations (Ca^{2+} and Na^{+}) of activated bentonites is due to washing several times with distilled water to remove sulfate ions. Under these conditions, activated bentonites do not undergo any very deep chemical modifications generally leading to the destruction of its crystal lattice which will be better confirmed by X-ray diffraction [1]. Analysis of physical properties of the raw and modified clay materials showing an improvement in the porosity of the modified materials compared with the raw material, which shows an increase in the interlamellar spaces and improving of the porous texture of the materials studied [2]. The (Ag, Cu, Ti-pillared) bentonite was studied by the scanning electron microscope has acquired a uniform and homogeneous structure at the 100 µm scale, which confirms the acid chemical treatment and pillaring operation of its particles which present an agglomeration of macro and microstructures is much more important.

Conclusion: The characterization results of this study show that the (Ag, Cu, Ti-intercalated) bentonite and (Ag, Cu, Ti-pillared) bentonite have high surface areas and porosity and can be obtained under certain optimal conditions of preparation. We managed to prepare pillared clays with basal spacing ranging from of 37 A° to 40.5 A° depending on the nature of the intercalated polycations complexes (mixed oxides).The textural analysis by the BET and DRX method of the (Ag, Cu, Ti-intercalated) and (Ag, Cu, Ti-pillared) bentonites allowed us to confirm the creation of a dense micro- porous network compared to the natural clay, caused by the acid activation and intercalation of large mixed metal pillars . The pillared clays are very reactive and high-performance adsorbents.

References:

[1] Pentrak M., Komadel P. and Madejova P., *Applied Clay Science*, 55, 100-107 (2012)
[2]Rao F., Song S. and Lopez-Valdivieso A., Nano Brief Reports and Reviews, 10, 1-9 (2015)

Keywords: Spectral, Characterization, Activation, Nanomaterial, (Ag, Cu, Ti)-mixed Oxides.

T2-P7: Comparative study of the Calcination-Reduction of Ammonium Uranyl Carbonate (AUC) and Ammonium Di-Uranate (ADU)

A. Amrane, A. Said, Y. Melhani, N. Aoudia, S. Ladjouzi, N. Ait Bouziad, A. Telmoune

Nuclear Research Centre of Draria
a-amrane@crnd.dz

Background/Purpose: The thermal decomposition of AUC and ADU plays a key role in the production of uranium oxides. Understanding the mechanisms and kinetics of these processes is therefore essential for determining the reaction mechanism involved in the decomposition of these materials [1]. This study focuses on the kinetics of the conversion process of AUC and ADU into uranium oxide (UO_2). It involves the production of U_3O_8 by calcining AUC and ADU under air, followed by reduction using hydrogen gas to obtain UO_2. The objective of this study is to analyze the kinetic mechanisms of converting into UO_2, in order to determine the influence of the product's origin and the thermal decomposition parameters on the final properties of UO_2.

Materials &Methods: The calcination was carried out under air in a muffle furnace at temperatures of 350°C, 650°C and 800°C. The resulting powders were then reduced to UO_2 in an ATD-TG analyzer (SATARAM TG96) under an Ar-10%H_2 flow at 3 l/h. Characterizations were performed on both the starting materials and the final powders (UO_3, U_3O_8, and UO_2), including the specific surface area by BET analysis (ASAP Micromeritics), particle size analysis using a laser granulometer (FRITSCH-NeXTNANO), and the O/U ratio determined by UV-Vis spectrophotometry [2].

Results: Calcination of AUC and ADU powders in air at 350°C and 500°C resulted in UO_3 powder with an O/U ratio of approximately 3 and a particle size ranging from 37 to 43 µm. In contrast, calcination at 800°C produced U_3O_8 with an O/U ratio of 2.66 and a particle size of 45 µm. The specific surface area of the resulting powders did not exceed 4 m^2/g. The UO_2 powders obtained by reducing the calcination products exhibit differences in specific surface area: those derived from AUC show 5 m^2/g, while those from ADU reach about 15 m^2/g.

Conclusion: The results showed that the properties of the produced powders depend on the calcination and reduction temperatures. It can be concluded that the UO_2 powders ex- AUC have more favorable properties for sintering than those ex-ADU, particularly in terms of specific surface area.

References:

[1]. Slycke J, Mittemeijer EJ, Somers MAJ (2015) Thermodynamics and kinetics of gas and gas–solid reactions. In: Mittemeijer EJ, Somers MAJ (eds) Thermochemical surface engineering of steels.

[2]. Sreenivasan NL, Srinivasan TG, Vasudeva Rao PR (1994) A spectrophotometric method for the determination of the oxygen to metal ratio in U3O8. Radioanal Nucl Chem Lett 188(6):463–470

[3]. ASTM 1267-11. Uranium by Iron II reduction in phosphoric acid followed by chromium VI

Keywords: Uranium oxide, Thermal analysis, Conversion, Kinetic parameter;

T2-P8: Influence of stoichiometry on uranium dioxide properties, comparison of methods for obtaining the O/U ratio

Y. Melhani[1@], N. Ait Bouziad[2], A. Amrane[3], Y. Hamoum[4], A. Said[5], S. Ladjouzi[6], A. Telmoune[7], N. Aoudia[8]

Nuclear Center Research of draria CRND

@ y-melhani@crnd.dz

Background/Purpose: The manufacture of nuclear fuel pellets relies on the quality of UO_2 powders, obtained by reduction of AUC (Ammonium Uranyl Carbonate) powders under hydrogen after calcination. The stoichiometric O/U (oxygen/uranium) ratio is a key parameter influencing sintering kinetics, fuel behavior and interaction with cladding materials. Prolonged exposure to air causes an increase in the O/U ratio, necessitating in-depth study of the properties of stored powders.

Objectives:

1. analyze the influence of storage time over 20 years on stoichiometry.
2. Compare three O/U ratio measurement methods: spectrophotometry, thermogravimetry and Davies Gray method.

Materials & Methods: Study of the physico-chemical properties of UO_2 powders from different batches and for different periods. Characterizations include:

- Thermogravimetry and the Davies Gray method for measuring uranium content.
- UV-visible for calculating the O/U ratio.
- Particle size measurement by laser granulometry.
- Measurement of specific surface area using the B.E.T. method.

The final step is to compare the results of the analytical methods in terms of precision, reproducibility, cost and environmental impact.

Results: Stored UO_2 powders show changes in specific surface area, particle size and O/U ratio, often out of specification after long periods.

- Powder stoichiometry evolves towards intermediate phases such as U_4O_9 or U_3O_7.

-Thermogravimetry provides the most accurate results for O/U ratio, while UV-visible spectrophotometry is fast and environmentally friendly.

Conclusion: UO_2 powders age naturally during storage, resulting in physico-chemical properties that do not comply with standards. Hydrogen reduction or the production of new UO_2 powders from AUC is necessary to restore the required specifications.

References:

[1]. Jean-Marc Delhaye. Thermohydrolyque des réacteurs, mai 2008.

[2]. F. Mernache. « The oxidation-reduction of UO_2: Implications for the recyclability of scrap and the reconditioning of UO powders ₂ ».
titration in the presence of vanadium (méthode Davies Gray).

Keywords: stoichiometry, powder, UO_2, O/U ratio, characterizations

T2-P9: Characterization of liquid radioactive waste by Gamma-ray spectrometry analysis

N. Bayou@, T. Azli,

Draria Nuclear Research Center, BP 43, 16003 Draria, Algiers, Algeria.
@Corresponding author n-bayou@crnd.dz

Background/Purpose:

Characterization of radioactive waste is important step for the radioactive waste management. It is necessary to determine the content of the radioactive waste, the type of radioisotope and its activity. In this work, liquid radioactive waste generated from the Nuclear Research Centre of Draria activities are characterized with using Gamma-ray spectrometry analysis.

Materials &Methods:

In this work, liquid radioactive waste generated from the Nuclear Research Centre of Draria activities are characterized with using Gamma-ray spectrometry analysis. The samples are collected and placed separately in polyethylene bottles of 450 cm^3 volume each. The bottles are completely sealed for more than 30 days to allow radioactive equilibrium to be reached. The measurement of elements activity is carried out using a detector hyper-pure germanium of 30% efficiency. The detector has a resolution of 1.9 keV at the ^{60}Co gamma-ray energy of 1332 keV. The gamma-ray spectrometer energy and efficiency calibration is performed using a ^{152}Eu source in a Marinelli beaker (multi-gamma volume source in a water-equivalent resin matrix). The samples are packaged in Marinelli-type containers, and the acquisition of gamma spectra duration is 86,400 s.

Results:

The results obtained of the gamma spectrometry analysis of the liquid radioactive waste show that the samples are uranyl effluents and the uranium activity and its progenies are determined.

Conclusion:

The gamma spectrometry analysis is nuclear technique recommended for the identification of the radioactive elements present in radioactive liquid waste. The determination of the activities of radioactive elements present in the radioactive liquid waste will be the first step for their management.

References:

[1] N.Bayou et al, C.R.Chimie. 20 (2017) 704–709

[2] J. D. Chen et al ,Journal of Radioanalytical and Nuclear Chemistry 123(2)(1988):695-

[3] P.Dyrcz et al, Applied Radiation and Isotopes 167 (2021) 109431

Keywords: Characterization, liquid radioactive waste, gamma spectrometry,

T2-P10: Enhancing the manufacturing process and corrosion resistance of MTR-type fuel plates through NaOH pickling optimization of the AlMgSi cladding alloy

F.Z.S. Mokhtar[1*] , M. Khalfa[1], A. Sahli[1], L. Mesai[1],Y.Larbah[2], B.Rahal[2],

[1] *Fuel Technology Division Nuclear Research Center of Draria,*
[2] *Electron Microscope and Material Science Department of Spectrometer Nuclear Technical Division, Nuclear Research Center of Algiers.*
[*]a-sahli@crnd.dz

Background/Purpose: In manufacturing nuclear fuel for MTR-type reactors, NaOH pickling is crucial for AlMgSi cladding alloy. This study focuses on optimizing the NaOH pickling process for AlMgSi alloys. The goal is to enhance the safety, performance, and lifespan of nuclear fuel.

Materials & Methods: The study comprised two phases. The first phase investigated the impact of pickling parameters roughness and its evolution during the fabrication of MTR fuel plates. Twenty-seven aluminum samples, processed through hot and cold rolling, were pickled at 70°C with a NaOH concentration of 50 g/L. The pickling solutions' saturation was monitored using colorimetric titration. Surface characterization included roughness measurement, optical microscopy, and analysis of mass and thickness loss. The second phase analyzed the oxidation behavior of Mg-Si alloys under typical MTR reactor conditions. Using SEM/EDX and XRD, the structure and composition of the oxide layers were examined. Samples underwent pickling at various immersion times (1–5 minutes and sequential combinations) in NaOH baths set at 100 g/L and 70°C.

Results: Sequential immersion resulted in more uniform roughness and improved homogeneity. SEM analysis showed a two-layer oxide structure: an inner dark gray layer (1.45 µm) and an outer light gray layer (3.45 µm). XRD identified boehmite (AlOOH) and bayerite (Al(OH)3) as the main phases. These findings highlight the effectiveness of sequential immersion in optimizing surface treatments and enhancing corrosion resistance. The stability and uniformity of the oxide layer suggest that the treated alloy can withstand the operating conditions of nuclear reactor.

Conclusion: This study emphasizes the role of optimized NaOH pickling in improving MTR nuclear fuel quality. Sequential immersion enhances surface uniformity and corrosion resistance, supporting safer and more durable cladding designs.

References:

[1] Guillotin, A. (2010). Study of surface roughness induced by plastic deformation of thin AA6016 aluminum alloy sheets. Page 18-19. (Unpublished master's thesis).

[2] Shahzad, M. (2011). Influence of roughness and anodizing treatments on the fatigue life of aeronautical aluminum alloys 2214 and 7050. University of Toulouse. Page 74. (Unpublished doctoral thesis).

[3] Lemaignan, C. (2003). Materials science for nuclear power. 3rd edition. EDP Sciences.

Keywords: **Pickling; AlMgSi alloys; Corrosion resistance; Nuclear fuel; MTR reactors**

T2-P11: Applications the Criteria of Luminescence in Rare Earth Doped Scintillator Materials (YPO4:Ce3+)

M. Taibeche[1], B. Kahouadji[2], L. Guerbous[1], N. baadji[3] and A. Bouhemadou[4]

[1]*Department of radiological and atomic physics, Physics Division/Nuclear Research Centre of Algiers, 02 Bd Frantz-Fanon, BP.399, Alger RP, Alger, Algeria,*
[2]*Department of Physics, Faculty of Exact Sciences, University of Bejaia, 06000, Bejaia, Algeria*
[3]*Faculty of Sciences, Med Boudiaf University -M'sila- BP 166 M'sila, 28000, Algeria.*
[4]*eLaboratory for Developing New Materials and their Characterizations, Department of Physics, Faculty of Science, University of Ferhat Abbas Setif 1, Setif,*
m.taibeche@crna.dz

Background/Purpose: A theoretical approach based on first-principles calculations is used to select candidate Ce activated scintillator materials. Our theoretical approach involves the calculation of the ground state band structure of the Ce-doped material as well as the calculation of the (Ce 3+) levels in fundamental state. From our theoretical studies of known scintillators and non-scintillators we have developed a set of criteria that are necessary characteristics of bright Ce activated scintillators. Applying these criteria to new compounds we were able to successfully predict that YPO4 doped Ce3+ would be a bright scintillator.

Materials & Methods: We have performed calculations using the Vienna Ab-initio Simulation Package (VASP) [1-3] based on the density functional theory, the initial atomic positions and symmetry information of the host crystal were taken from Bilbao crystallographic server [4]. The Y(4s4p5s4d), P($3s^2$ $3p^3$), O(2s2p) and cerium pseudopotential (5s,5p,6s,4f,5d) are treated as valence electrons in our calculations. The plane waves cut-off energy for the electronic wave functions was set to 550 eV. The Brillouin zone was sampled with a mesh of 4x4x4 centered at Gamma point. The total energy convergence criterion was set to 10−6 eV and the maximum component of force acting on any atom in the relaxed geometry was less than 0.01 eV/A.

Results: In this paper, we focused our work to verification the criteria of luminescence on YPO4 doped Ce^{3+}. In the goal to study the effect of one Ce^{3+} dopant ion in a host lattice (YPO4), we replace one atom of the host trivalent cations yttrium (Y^{3+}) with Ce^{3+}. For a very precise modeling of 4f electrons and their interactions, it is necessary to use DFT+ U, we found the Ueff correction for YPO4 doped cerium is give reasonable quantitative agreement between theory and experiment results for the energy levels of 4f electrons. Using the rotationally invariant method of Dudarev [5], we calculated the parameter Ueff for an onsite +U correction to treat the Ce 4f, electrons with a single parameter Ueff = U − J. The Ueff is tuned in such a way to localized 4f state in the band gap of the host for YPO4 nanomaterial, it is found that the value of Ueff to find the 4f -Cerium orbital in the band gap is equal 4.4 eV. We have in finally confirmed the criteria of luminescence in YPO4 doped Ce^{3+}.

1. The size of the host material bandgap, **2.** The energy difference between the VBM of the host and the Ce 4f level, **3.** The level of localization a host CB state or a Ce 5d character state.

Conclusion: The first principle calculations are performed to study YPO4:Ce^{3+} nanomaterial system using VASP code. It was been found that Ueff parameter must be 4.4 eV to make Ce^{3+}-f orbitals to be above the maximum of the valence at about 1.1 eV. The calculated band gap using hybrid functional (HSE06) was found to be 5.8 eV which with agreement with the experimental results. Furthermore, it was found that the calculated 5d orbitals are situated below the minimum of the conduction band.

References:

[1] G. Kresse and J. Hafner, Phys. Rev B. 47 (1993) 558.
[2] G. Kresse and J. Furthmuller, Phys. Rev B. 54 (1996) 11169.
[3] G. Kresse and J. Furthmuller, Comput. Mater.Sci. 6 (1996) 15.
[4] http://www.cryst.ehu.es/
[5] S. L. Dudarev, G. A. Botton, S. Y. Savrasov, C. J. Humphreys, and A. P. Sutton, Phys. Rev B. 57 (1998) 1505.

Keywords: **$YPO_4:Ce^{3+}$; Luminescence; 4f-5d transition; Ab-initio**

T2-P12: Effect of process control agent on the hyperfine properties of $Fe_{93.5}Si_{6.5}$ nanostructed powders.

M.E. Ayad [a@], M. Hemmous[a], A. Guittoum[a], T. Kacel[b], S. Kamariz[a], S. Maar[a].

[a] *Nuclear Research Centre of Algiers, 02 Bd Frantz Fanon, BP 399 Alger-Gare, Algiers, Algeria*
[b] *Research Center in Industrial Technologies (CRTI) P.O. Box 64, Cheraga 16014 Algiers, Algeria*
[@] *Corresponding author m.ayad@crna.dz*

Background/Purpose: FeSi nanostructed powders are widely used in many technological applications due to their many interesting properties [1, 2]. In this study, we investigate the effects of different process control agents (PCAs), including acetone, methanol, and ethanol, on the structural and hyperfine properties of $Fe_{93.5}Si_{6.5}$ synthesized through mechanical alloying.

Materials & Methods: The mechanical ball milling process was employed during the sample preparation, with a ball-to-powder weight ratio of 15:1. The milling was conducted at a speed of 500 rpm under an argon atmosphere for 72 hours in the presence of 5 wt.% of different PCAs. Mössbauer spectra were recorded in transmission geometry at room temperature using a ^{57}Co source in a rhodium matrix. The spectra were analysed using WinNormos for Igor Pro software. FTIR analysis was performed with a Thermo Nicolet NEXUS 670 spectrometer, utilizing OMNIC software for data acquisition and processing.

Results: The Mossbauer spectrum of the milled sample without process control agent shows a strong sextet, whereas in case of the acetone, ethanol and methanol a singlet appeared along with the sextet on the Mossbauer spectra. From FTIR analysis, the metal oxide bands characterizing the synthesized nanomaterial are located near 424.30 and 668.61 cm^{-1}, corresponding to Fe-O chemical bonds in the chemical structure.

Conclusion: Nanocrystalline $Fe_{93.5}Si_{6.5}$ were successfully elaborated by mechanical alloying using a three different process control agent (PCA). The Mossbauer spectra show the existence of paramagnetic and ferromagnetic phases which indicate the presence of different environments around the iron atom. The FTIR spectrum reveals characteristic bands for Fe-O, Si-O-Fe, Si-O-H, C-H_2, O-C-O, and O-H bonds, indicating its chemical structure and interactions.

References:

[1]. Cheng Z Y et al. Effect of Cu addition on microstructure, texture and magnetic properties of 6.5 wt% Si electrical steel. Journal of Magnetism and Magnetic Materials. 2021; 519 :167471. http://doi.org/10.1016/j.jmmm.2020.167471

[2]. Mihalache V et al. Thermal analysis and microstructure of oxide dispersion strengthened ferritic steels produced by ball milling with different amounts of process control agent. Journal of Thermal Analysis and Calorimetry. 2019; 138:2515–2528. http://doi.org/10.1007/s10973-019- 08593-y

Keywords: Mechanically alloying materials; process control agent; Mössbauer spectroscopy; FTIR spectrometry.

T2-P13: Effect of thickness on the physical properties of evaporated Fe/Si (100) thin film

S. Maar [a@], M. Hemmous [a], A. Guittoum [a], T. Kacel[b], M.E. Ayad [a], S. Kamariz [a].

[a] *Nuclear Research Centre of Algiers, 02 Bd Frantz Fanon, BP 399 Alger-Gare, Algiers, Algeria*
[b] *Research Center in Industrial Technologies (CRTI) P.O. Box 64, Cheraga 16014 Algiers, Algeria*
[@] *Corresponding author s.maar@crna.dz*

Background/Purpose: Fe/semiconductor systems have garnered considerable research interest because of their distinct physical properties, as well as their promising applications (MEMS, NEMS…) [1,2]. In this perspective, Thermal evaporation was used to elaborate Fe thin films onto Si substrates. The physical properties will be studied as a function of Fe thickness.

Materials & Methods: Fe thin films were deposited onto n-Si (100) substrates using thermal evaporation. RBS Spectroscopy was employed to examine the Fe/substrate interfaces and measure the Fe thickness. The RBS were conducted using 2 MeV He^+ ions from a 3.75 MeV van de Graaff accelerator. The physical properties were determined through AFM Microscopy, GIXRD X-ray diffraction and four-point probe, respectively. The hyperfine properties were determined by Conversion electron Mössbauer spectroscopy (CEMS).

Results: The RBS experiment shows well-separated peaks, indicating that there is no interdiffusion between the Fe and substrate interfaces. The Fe thicknesses, t, vary from 23 to 153 nm. The X-ray spectra show the presence of the pure Fe phase. The Fe films exhibit a <111> texture on all samples. As the thickness (t) increases, the lattice parameter a (Å) progressively increases. Similarly, the micro-distortion rate (⟨ε⟩ in %) follows the same trend. Additionally, the Fe grain sizes, D (nm), increase from 36 to 124 nm as the thickness increases. As the Fe thickness increases, small three-dimensional islands form and are distributed somewhat uniformly across the entire surface. Both square resistance and electrical resistivity are sensitive to film thickness. Specifically, electrical resistivity increase monotonically as the film thickness increases.

Conclusion: We studied the influence of thickness tt on the physical properties of evaporated Fe thin films. All Fe samples exhibited a predominant <111> texture. The Fe films experienced significant compressive stress, which decreased as the thickness increased. Additionally, the grain size DD was found to impact properties such as electrical resistivity ρ.

References:

[1]. Luo J K et al. Young's modulus of electroplated Ni thin film for MEMS applications. Materials Letters. 2004; 58: 2306. https://doi.org/10.1016/j.matlet.2004.02.044

[2]. Teh W H et al. Near-zero curvature fabrication of miniaturized micromechanical Ni switches using electron beam cross-linked PMMA. Journal of Micromechanics and Microengineering. 2003; 13: 591. https://DOI 10.1088/0960-1317/13/5/309

Keywords: **Fe films, Mössbauer spectroscopy, structure, electrical resistivity.**

T2-P14: Effect of ethanol concentration Structural and Hyperfine Properties of $(Ni_{60}Co_{40})_{85}Fe_{15}$ Nanoparticles

S. Kamariz [a@], M. Hemmous[a], A. Guittoum[a], T. Kacel[b], M.E. Ayad[a], S. Maar[a]

[a] *Nuclear Research Centre of Algiers, 02 Bd Frantz Fanon, BP 399 Alger-Gare, Algiers, Algeria*
[b] *Research Center in Industrial Technologies (CRTI) P.O. Box 64, Cheraga 16014 Algiers, Algeria*
[@] *Corresponding author s.kamariz@crna.dz*

Background/Purpose: The ternary compound $(Ni_{60}Co_{40})_{85}Fe_{15}$ composed of iron, cobalt, and nickel, was synthesized via the hydrothermal method. This study focuses on the impact of varying ethanol concentrations (0%, 25%, 50%, and 100%) on the structural, microstructural, and hyperfine properties of NiCoFe nanopowder.

Materials & Methods: The ternary compound $(Ni_{60}Co_{40})_{85}Fe_{15}$ was synthesized via the hydrothermal method with varying ethanol concentrations. Structural characterization was performed using X-ray diffraction, while Fourier Transform Infrared (FTIR) spectroscopy was employed to analyze the surface properties of the integrated Ni-Co-Fe nanocomposites. Atomic Force Microscopy (AFM) was utilized to study surface morphology. Additionally, Mössbauer spectra were recorded at room temperature in transmission geometry using a ^{57}Co source in a rhodium matrix to investigate the hyperfine properties.

Results: The X-ray diffraction revealed that all the sampels exhibited a FCC structure. The increasing of the ethanol concentration not result in a significant change in the lattice parameter. But, the grain sizes, D (nm), decrease from up to 12 nm. The FTIR spectroscopy enabling the detection of metallic ions present in these nanomaterials[1, 2]. AFM microscopy shows that the grain distributed somewhat uniformly across the entire surface. The Mössbauer spectra, confirm the XRD results and provide extra information not revealed by XRD, particularly regarding the formation of non-ferromagnetic phases.

Conclusion: In this study, (Ni60Co40)85Fe15 nanopowder was successfully synthesized via the hydrothermal method with varying ethanol concentrations. XRD analysis revealed that all (Ni60Co40)85Fe15 nanopowders crystallize in a face-centered cubic (FCC) structure. FTIR analysis confirmed the presence of vibrational bonds, including Ni-O, Fe-O, and Co-O, in all samples. Mössbauer spectra displayed a characteristic combination of a sextet (indicative of ferromagnetic behavior) and a doublet (indicative of paramagnetic behavior).

References:

[1] Augustin. J et al, Synthesis and characterisation of cobalt Ferrite magnitiqc nanoparticules coated with polyethylene glycol, Advanced NanoBio-materials Devives Research 2017;1(1):71.
[2] Hyewon C et al. Cube-shaped Triethylene Glycol-coeted Ni-Mn ferrite nanoparticules for use as T2 contrast Agents in magnitic resonance imaging, Journal of the Korean Physical Society, 2019;74(1):48-52. DOI:10.3938/jkps.74.48

Keywords : NiCoFe NPs, hydrothermal route, microstructure, hyperfine properties.

T2-P15: Validation of the k_o-NAA Method at the NUR Research Reactor for Multi-Elemental Analysis of Geological Samples

A. Guesmia[1,2@], L. Hamidatou[1], H. Slamene[3], M.E. Benamar[2]

[1]*Nuclear Research Centre of Draria, PB43, Draria, 16050 Algiers, Algeria..*
[2]*Energy and Materials Laboratory, University of Tamanghasset, 11001, Algeria.*
[3]*Nuclear Research Centre of Birine, PoBox 180, Ain Oussera, 17200, Djelfa, Algeria.*
[@]Corresponding author: a-guesmia@crnd.dz

Background/Purpose: This study aims to validate the implementation of the k_o-NAA method at the NUR Research Reactor for multi-elemental analysis of geological samples. The goal is to confirm the method's precision, accuracy, and reliability for analyzing trace and major elements in geological materials, supporting future applications in various fields, including environmental monitoring and resource analysis.

Materials & Methods: To assess the performance of the k_o-NAA method, neutron flux parameters, including the thermal-to-epithermal flux ratio (f) and the epithermal flux distribution shape factor (α), were determined using the bare triple-monitor method with 197Au, 96Zr, and 94Zr. Irradiations were performed in the central trap and thermal column of the reactor, optimizing both long-lived and short-lived radionuclide analyses through the pneumatic transfer system (PTS). The validation was conducted using certified geological reference materials: CRM GSD12 and SRM NIST 1646a (Estuarine Sediment). The data was analyzed statistically with relative bias analysis and Zeta-score (ζ-score) tests to assess the agreement with certified values [1, 2].

Results: The validation revealed strong agreement with certified values, with relative biases for most elements falling within a 10% margin. The Zeta-scores of the analysis predominantly ranged between ±2, indicating that the k_o-NAA method provides accurate and reliable results for multi-elemental analysis. These findings confirm the high precision and robustness of the method in the analysis of geological samples.

Conclusion: This study demonstrates the successful validation of the k_o-NAA method at the NUR Research Reactor for multi-elemental analysis of geological materials. The method proved to be highly accurate and reliable, making it a valuable tool for future research and practical applications in geological analysis and other related fields. Future directions will focus on expanding the range of analyzed elements and exploring its applications in environmental monitoring and resource management.

References:

[1] Hamidatou L. A. et al. k0-NAA quality assessment in an Algerian laboratory by analysis of SMELS and four IAEA reference materials using Es-Salam research reactor. NIMAV 682, 2012, PP 75-78. https://doi.org/10.1016/j.nima.2012.04.042.

[2] L. Alghem et al. The development and application of k0-standardization method of neutron activation analysis at Es-Salam research reactor, NIMA, V 556, N°1 (2006) 386-390. https://doi.org/10.1016/j.nima.2005.10.017.

Keywords: k_o-NAA, NUR Research Reactor, multi-elemental analysis, geological samples, neutron flux parameters.

T2-P16: Use of nuclear detection techniques for uranium prospecting and exploration: Example of the Tin Sériri ne sedimentary basin (South East of Algeria)

R. Chahdane@, S. A. Mokhtar, M. Amieur

Centre de RechercheNucléaire de Draria [2]Centre de RechercheNucléaire de Tamanrasset
@Correspondingauthorr-chahdane@crnd.dz

Background: The prospecting and exploration of uranium resources takes place in several phases [1] and involves the use of different techniques (satellite, airborne, ground and laboratory). In this work, we present the contribution of nuclear techniques used in the search for uranium resources in the Tin Sériri ne basin (South-East of Hoggar).

Materials & Methods: The aerogeophysical data survey at a scale of 1:200,000 [2], recorded above the Tin Sériri ne basin, constituted the basic tool for this study. The aerogamma-spectrometric measurements of this region were the subject of processing and interpretation work using Oasis Montaj software. In the field, ground gamma-spectrometric surveys were carried out (scales: 1/10,000 and 1/2000) by Sintrex GAD6 spectrometers. Mining works was undertaken as well as geochemical and mining sampling. The collected samples were studied by optical microscopy, SEM, XRD, XRF and neutron activation.

Results: Several uranium anomalies were detected, particularly in the center of the basin in the areas of Tamert-N-Iblis, Timouzeline and Tedjert. Ground gamma-spectrometric surveys led to the confirmation and delineation of three uranium anomalies in these areas. In terms of these anomalies, the mining work allowed the identification of three uranium mineralization showing hosted in the Lower Devonian sandstones. Laboratory studies carried out on samples from these showing indicate uranium contents varying between 0.005 and 1.139% and a uranium mineral paragenesis composed mainly of carnotite, autunite and torbernite. These minerals appear associated with clay minerals, altered potassium feldspars and organic matter. Analyzes carried out by neutron activation show an enrichment in certain LREEs at the Tedjert uranium showing.

Conclusion: All of these study results present the central part of the Tin Sériri ne sedimentary basin as a prospective region for the exploration of uranium resources and rare earths elements.

References:

[1]. P.M. Barretto, 1981. Recent developments in uranium exploration - Nuclear fuel cycle - IAEA BULLETIN, VOL. 23, No.2
[2]. AEROSERVICECORPORATION, 1975. Aero-magneto-spectrometric survey of Algeria, Final report, 3 volumes, Houston, Philadephia.

T2-P17: Validation of energy dispersive X-ray fluorescence (ED-XRF) Analysis results Through instrumental neutron activation analysis (INAA) as a High-Precision Method

A. Arabi[a@], S. Benarous[a], A. Azbouche[*], T. Azli[c], Z. Chekired[b], L. Boudraa[a], H. Silhadi[a].

[a] *Nulcear Research Center of Algiers, Algiers, Algeria,*
[b] *National Institute for Forest Research, Bainem, Algiers, Algeria,*
[c] *Nulcear Research Center of Draria, Algiers, Algeria,*
** Retired from Nulcear Research Center of Algiers, Algiers, Algeria,*

[@] *Corresponding author a.arabi@crna.dz*

Background/Purpose: Accurate elemental analysis is essential in various scientific fields. Among the widely used techniques, Energy Dispersive X-ray Fluorescence (ED-XRF) stands out for its rapid, cost- effective, and non-destructive capabilities. However, despite its efficiency, ED-XRF results may be affected by matrix effects, calibration limitations, and variations in detection sensitivity. To ensure the reliability of ED-XRF measurements for routine laboratory analyses, validation through Instrumental Neutron Activation Analysis (INAA) which is recognized as a high-precision and robust method is necessary. In this study, INAA will serves as reference method for validating ED-XRF technique.

Materials & Methods: Three soil samples were prepared and analysed with INAA and ED-XRF. The data obtained from both techniques were analysed to assess their correlation and agreement. Statistical tools such as correlation coefficients, bias analysis, and relative error calculations were applied to evaluate the precision and accuracy of ED-XRF in comparison to INAA. The study focused on commonly detected soil elements, including heavy metals and rare earth elements, to determine the effectiveness of ED-XRF in environmental analysis.

Results: A comparison between instrumental neutron activation analysis (INAA) and energy-dispersive X-ray fluorescence (EDXRF) in soil sample analysis reveals no significant difference in the concentration values obtained by both techniques. This finding indicates that EDXRF can serve as a reliable alternative for measuring elements typically analysed using long-lived INAA.

Conclusion: Since both techniques produce comparable concentration values for heavy metals and rare earth elements, EDXRF appears to be a practical alternative to INAA, particularly for routine soil analyses requiring rapid, non-destructive, and cost-effective measurements. However, INAA remains superior for detecting ultra-trace levels of some rare elements or actinides due to its higher sensitivity.

References:

[1] ISO 13528: 2015, Statistical Methods for Use in Proficiency Testing by Interlaboratory Comparisons, issued by ISO-Geneva (CH), International Organisation for Standardisation, 2015

[2] I. Silachyov, Interrelation of EDXRF and comparator INAA to analyze REE mineral Journal of Radioanalytical and Nuclear Chemistry · April 2024 DOI: 10.1007/s10967-024-09473-y.

T2-P18: Blue method for calculating errors of the strong coupling constant at LHC

L. Kellouche

Laboratoire de Physique Théorique Oran
@ Corresponding author aelkaderkalouche@gmail.com

Background/Purpose: The study of uncertainties has an important role in physical measurements.
In this work, we convert the asymmetrical errors of different measurements made by the ATLAS detector of the strong coupling constant in proton-proton collision interactions into symmetrical errors using the method cited in ref.[1], then extract from these measurements different measurements of the strong coupling constant αs , and calculate the mean value of this constant, plus the error committed in measuring this mean value, at a center of mass energy equal to 7TeV, 8TeV and 13TeV.

Materials & Methods: To obtain the average value of the strong coupling constant αs from nominal values extracted and the error made when calculating this average value ,we must take into account their correlations using The Best Linear Unbiased Estimate ref. [2] .

Results: Together with the results of table, these give a best estimate,the BLUE code gives us the final result of the strong coupling constant, after calculating the covariance matrix.
αs=0.116±0.0005806(stat)±0.0008976(syst)±0.000067(Ebeam)±0.00266(PDF)±0.001546(scale)(Scale)±0.001256(Mt) = 0.116 ± 0.0006(stat) ± 0.0034(sys) = 0.116 ± 0.0035(tot)

Conclusion: We applied the Best Linear Unbiased Estimate (BLUE) method through the program for calculating the mean values of and the error made in the calculation of this average value by extracting from a table of three different values for the ATLAS experiments which are ATLAS 7 Tev, ATLAS 8 Tev and ATLAS 13 Tev, where we get the result with symmetric errors: αs = 0.116 ± 0.0006(stat) ± 0.0034(syst) = 0.116 ± 0.0035(total) which is in good agreement with the most recent world average value 0.117+0.0034−0.0036 [3]

References:

[1].Asymmetric Uncertainties:Sources, Treatment and Potential Dangers.D‟Agostini, G. Universit„a “La Sapienza” and INFN, Roma, Italia : s.n., 2004. arXiv:physics/0403086
[2].Max-Planck-Institut f¨ ur Physik (Werner-Heisenberg-Institut) F¨ ohringer Ring 6, D-80805 M¨ unchen, Germany, http://www.mpp.mpg.de/˜nisius, Richard.Nisius@mpp.mpg.de
[3].Determination of the strong coupling constant . Thomas Klijnsma, Siegfried Bethke, Gunther Dissertori, Gavin P. Salam. Eur. Phys. J. C (2017) 77:778 https://doi.org/10.1140/epjc/s10052-017- 5340-5

Keywords: **ATLAS, CMS,parton distribution function (PDF), correlationmatrix, covariancematrix.**

T2-P19: Monte Carlo calculation of Self-shielding factor for instrumental Neutron Activation Analysis: Determination of lanthanide concentration in Algeria phosphates

S.E. Addali [b@], A. Azbouche [a], R. Khelifi [b], S. Benarous [a].

[a] *Nuclear ResearchCenter ofAlgiers, 2 Bd Frantz Fanon, Algiers, Algeria.*

[b] *Laboratory of Theoretical Physics and Radiation-Matter Interactions, University of Blida 1, PB 270 Blida, Algeria.*

[@] *Corresponding author: sabahelhoudaaddali@gmail.com*

Background/Purpose: The presence of rare earth elements in the phosphate matrix leads to the self-shielding of thermal and epithermal neutrons by the matrix during irradiation in a nuclear reactor. This work aims to estimate the neutron fraction absorbed by the matrix to improve the detection limit of neutron activation analysis.

Materials & Methods: The irradiation of phosphate samples in the nuclear research reactor (CRND) under a thermal flux of $2.36*10^{13}$ neutrons cm^{-2} s^{-1} and an epithermal flux of $8.7*10^{11}$ neutrons cm^{-2} s^{-1} is affected by the local perturbation of neutron fluxes produced mainly by the samples, especially when many absorbers are present in the sample. The sample size during the experimental neutron activation study may not be small enough, the self- shielding effects should be taken into account.

A methodology for the analysis was developed based on Monte Carlo simulation to estimate thermal and epithermal neutron self-absorption factors.

Results: The results obtained in this work constitute an important rule for improving the detection limit of neutron activation analysis of rare earths in phosphate samples. The values of the thermal and epithermal self-absorption coefficients are respectively: 0.976 and 0.999.

Conclusion: The evaluation of the correction factors of the self-absorption of thermal and epithermal neutrons by Monte Carlo simulation leads to improving the detection limits and allows the determination of the concentration of rare earth elements in phosphate with good precision.

References:

[1]. Azbouche, A., Moulla, A. S., & Belgaid, M. (2022). Rare-earth elements distribution in Algerian soil samples using neutron activation analysis: Monte Carlo analytical method approach. International Journal of Environmental Analytical Chemistry, 102(12), 2792-2804.

[2]. Trkov, A., Žerovnik, G., Snoj, L., & Ravnik, M. (2009). On the self-shielding factors in neutron activation analysis. Nuclear Instruments and Methods in Physics Research Section A: Accelerators, Spectrometers, Detectors and Associated Equipment, 610(2), 553-565.

[3]. Goncalves, I. F., Martinho, E., & Salgado, J. (2002). Monte Carlo calculation of epithermal neutron resonance self-shielding factors in foils of different materials. *Applied Radiation and Isotopes*, *56*(6), 945-951.

T2-P20: Monte Carlo Simulation of End-Window X-ray Tubes with Rhodium Targets: Insights into Energy and Thickness Optimization for ED-XRF

M.I. Khadir[1@], A. Azbouche[2], A. Bouldjedri [1]

[1] *Department of Physics, LRPRIM Laboratory,University Of Batna 1 , Batna, Algeria.*
[2] *Nuclear Division Techniques, Nuclear Research Center of Algiers, Algiers, Algeria.*
[@] *Corresponding author: islam.islam.khadir6@gmail.com*

Background/Purpose: End-window X-ray tubes, despite their growing application in energy-dispersive X-ray fluorescence (ED-XRF), remain less studied than side-window designs. This work focuses on using Monte Carlo simulations to investigate the effect of Rhodium (Rh) target thickness and beam energy on X-ray spectra. The goal is to optimize these parameters to enhance spectral quality and improve the efficiency of ED-XRF analysis, especially for environmental applications.

Materials & Methods: Monte Carlo simulations were performed using the Penelope code to model the behaviour of an end-window X-ray tube with a Rh target. Target thicknesses ranging from 5 µm to 50 µm and beam energies from 30 kV to 50 kV were simulated. The peak-to-background (P/B) ratio for the Rh Kα line was used as a metric to assess spectral quality under varying conditions. Spectral results were analysed using PyMca to extract characteristic peak intensities and evaluate background contributions. [1,2].

Results: The P/B ratio for the Rh Kα line exhibited a consistent increase with both target thickness and beam energy. At higher beam energies (40 kV and 50 kV), thicker targets (30– 50 µm) produced significantly higher X-ray yields, compensating for the increased Bremsstrahlung background. Conversely, thinner targets (5–15 µm) demonstrated reduced background levels at lower beam energies, leading to better peak clarity and higher P/B ratios in these configurations. The Rh L line was excluded from P/B analysis due to its dominance in thin targets and its absence in spectra for thicker targets. These findings indicate a trade-off between spectral clarity and X-ray yield, with thicker targets favouring high-energy applications and thinner targets excelling at low-energy analysis.
The study also highlights that optimizing the target thickness is critical for achieving the desired analytical performance, especially in applications requiring precise quantification of trace elements.

Conclusion: This work provides insights into the optimization of Rhodium target configurations in end-window X-ray tubes, emphasizing the balance between target thickness and beam energy to enhance spectral quality for ED-XRF applications. These findings can guide the design of sources tailored for environmental and analytical studies.

References:

[1]. Salvat, F., Fernández-Varea, J. M., & Sempau, J. (2019). *PENELOPE-2018: A Code System for Monte Carlo Simulation of Electron and Photon Transport*. OECD Publishing.

[2]. James E. Penner-Hahn Handbook of X-ray Spectrometry, 2nd ed Journal of the American Chemical Society **2002** 124 (42), 12627-12627 DOI: 10.1021/ja015389k

Keywords: Monte Carlo simulation; End-window X-ray tubes; ED-XRF optimization

T2-P21: Innovative Machine Learning Approaches to Neutron Spectra Unfolding

R. Boufenar @, M. Fares

Birine nuclear research center BP 180 Ain Oussera/Djelfa
@ Corresponding author: r.boufenar@crnb.dz

Background/Purpose: Neutron spectrometry is inherently challenging due to its ill- posed nature, where spectral information cannot be directly extracted from measurements. Traditional unfolding methods, including Monte Carlo simulations, iterative approaches, Bayesian theory, and the maximum entropy principle, have several drawbacks, leading to an increasing interest in alternative approaches [1]. In light of these challenges, innovative approaches based on Machine Learning, have emerged as a promising alternative to traditional calculations and conventional techniques [2].

Materials & Methods: To address these challenges, a machine learning model was developed and trained using database containing two hundred and ten Bonner Sphere Spectrometer count rates from the IAEA neutron spectra compendium [3]. Data were split into 80% training and 20% testing subsets, ensuring representation of various spectra types (continuous, monomodal, and multimodal). Data from the test subset are not included in the training process; they were used solely to evaluate the model's generalization capabilities.

Results: The Machine Learning model demonstrated notable stability against perturbations and adaptability to diverse spectra types. The calculated neutron spectra closely matched the reference shapes and energy peaks, confirming the model's accuracy and generalizability compared to traditional method.

Conclusion: In this work, a machine learning-based model was designed and implemented to effectively unfold neutron source spectra from Bonner Sphere Spectrometer (BSS) count rates. The simulation results reveal that the calculated spectra align very closely with the benchmarks found in the literature, demonstrating a high degree of accuracy.

References:

[1]. Bin Liu et al, (Study on iterative regularization method and application to neutron spectrum unfolding of multi-sphere spectrometer measurement), *Nuclear Instruments and Methods in Physics Research Section A*. 2021; 992.

doi:10.1016/j.nima.2021.165027

[2].Chenglong Cao et al, (A two-step neutron spectrum unfolding method for fission reactors based on artificial neural network), *Annals of Nuclear Energy*, 2020; 139.

doi: 10.1016/j.anucene.2019.107219

[3].Compendium of neutron spectra and detector responses for radiation protection purposes, *International Atomic Energy Agency (IAEA), Technical reports series* No. 403, 2001.

Keywords: machine learning; neutron spectrometry; unfolding;

T2-P22: Silicon Irradiation with High-Energy Proton Beam

D. Kerrai[1@], A. Belhout [2] , D. Moussa[2] , S. Ouichaoui[2] , W. Yahya-Cherif[3] , Y. Rahma[3] , S. Damache[3] , M. Debabi[2], S. Ouziane[2]

[1 2] *Laboratory of Nuclear Sciences and Radiation-Matter Interactions (SNIRM-DGRSDT), University of Sciences and Technology Houari Boumediene (USTHB), Beb ezzouar, Algiers , algeria*
[3] *CRNA, 02 Boulevard Frantz Fanon, B.P. 399 Alger-gare, Algiers, Algeria*
[@] dkerrai@usthb.dz

Background/Purpose: This study was carried out at iThemba LABS (Cape Town, South Africa), where a high-energy proton beam was used to irradiate a **silicon (Si)** target. The purpose of this experiment was to extend the existing database of cross-section data for nuclear γ-ray production, specifically focusing on higher proton energies ranging from 125 to 200 MeV. This investigation aimed to address discrepancies between experimental data and theoretical predictions by comparing the results with previous studies.

Materials & Methods: A high-energy proton beam was accelerated using the separate- sector cyclotron at iThemba LABS [1]. The proton beam irradiated a **silicon (Si)** target, and the resulting γ rays were detected using the AFRODITE array, consisting of eight Compton- suppressed clover detectors of the EUROGAM phase II type. These detectors were arranged in a fixed geometry at 90°, 135°, and 168° relative to the beam direction. Data were collected for several proton energies, and cross-section data were determined for the production of nuclear γ-lines. [2].

Results: The preliminary results of the experiment provide cross-section data for nuclear γ-line production in a silicon target, extending the existing database to higher proton energies (125–200 MeV). Dozens of cross sections were measured for different γ-ray transitions at four proton energies.

For example, the measured cross sections (in barn) are:

- 350.7 keV: **σ** = 3.51 ± 0.16 b (125 MeV), 6.06 ± 0.38 b (150 MeV), 3.8 ± 0.18 b (175 MeV), 4.64 ± 0.29 b (200 MeV).
- 416.8 keV: **σ** = 7.39 ± 0.35 b (125 MeV), 10.32 ± 0.75 b (150 MeV), 5.90 ± 0.47 b (175MeV), 8.10 ± 0.46 b (200 MeV).
- 780.8 keV: **σ** = 4.14 ± 0.17 b (125 MeV), 6.67 ± 0.41 b (150 MeV), 3.68 ± 0.18 b (175MeV), 4.59 ± 0.23 b (200 MeV).

A comparison with previous experimental data (γ emission induced by protons and α particles) and theoretical predictions revealed significant discrepancies. The default input parameters in theoretical models failed to accurately reproduce the experimental findings, emphasizing the need for improved parameter selection.

Conclusion: The results of this study demonstrate the necessity of refining theoretical models to ensure more accurate predictions. The discrepancies observed suggest that the default parameters used in many theoretical calculations are inadequate for representing the data accurately. Future research should focus on selecting more reliable input parameters to enhance the agreement between theory and experiment. These findings contribute to the growing database of experimental data for proton-induced γ-ray emission and have important implications for the refinement of nuclear models.

References:

[1]. iThemba LABS, www.iThembaLabs.ac.za
[2]. W. Yahia-Cherif et al., Phys.Rev.C 102, 025802 (2020).doi: 10.1103/PhysRevC.102.025802

Keywords: nuclear γ-rays, experiment cross sections, theoretical calculations.

T2-P23: Thermal neutron cross section measurement for the $^{164}Dy(n,\gamma)^{165}Dy$ reaction

A. Taibi[1@], T. Azli[2]

[1] *Nuclear Research Center of Algiers (CRNA).*
[2] *Nuclear Research Center of Draria(CRND).*
[@] *Corresponding author a.taibi@crna.dz*

Background/Purpose: The precise determination of thermal neutron cross section ($\sigma\sigma_0$) for Dysprosium 164 (^{164}Dy) is of great importance for nuclear reactors field, for theoretical studies concerning the interaction of neutron with matter, and for neutron data evaluation [1-3]. In this work, the thermal neutron cross section of the ^{164}Dy (n,γ) ^{165}Dy reaction was measured by the activation technique, using two reference materials: Indium (In) and gold (Au) foils.

Materials & Methods: An irradiation facility composed mainly of an Am-Be neutron source with an activity of 37 GBq (1 Ci). The source is put at the mid-height level of a Perspex tube of about 40 mm inner diameter and 1.3 mm thickness. The tube is immersed in a cylindrical tank made of polyethylene. The tank has a diameter of about 44 cm, 40 cm height, and with a 5 mm thickness. Two disc foils (indium and gold) were irradiated at different distances with and without cadmium filter for 6 h and 3 day, respectively, to estimate the maximum thermal neutron flux position. An MCNP5 (Monte-Carlo N-particle) code was also used to simulate the irradiation setup, and to calculate the thermal neutron flux. The Dy_2O_3 prepared sample was irradiated with and without cadmium foil for 10 h. The induced activities were then measured using gamma ray spectrometry; The HP (Ge) detector has a relative efficiency of 40 ٪, and energy resolution (FWHM) of 1.8 keV for 1.33 MeV γ-energy of ^{60}Co.

Results: The results measured at 0.0253 eV for the ^{164}Dy (n,γ) ^{165}Dy reaction are 2694±180 b relative to the reference value of 162.3±0.7 b for the ^{115}In (n, γ) ^{116m}In reaction, and 2767±127 b relative to the reference value of 98.3±0.3 b for the ^{197}Au (n, γ) ^{198}Au reaction.

Conclusion: The discrepancies between the present results and most of the previous values reported in the literature is acceptable. It is between 0.22 and 3.78 ٪ for the thermal neutron cross-section for the ^{164}Dy (n,γ) ^{165}Dy reaction using indium (In) foil, and between 0.98 and 6.42 ٪ using gold (Au) foil.

References:

[1]. C. Hyun-j et al., Measurement of thermal neutron cross-sections and resonance integrals for ^{164}Dy (n, γ) ^{165}Dy and ^{180}Hf (n, γ) ^{181}Hf reactions, Nucl. Instr. and Meth.A (2001); 462: 442-450. doi: 10.1016/S0168-9002(01)00158-9

[2]. M. Karadag, H. Yücel; Thermal neutron cross-section and resonance integral for ^{164}Dy (n, γ) ^{165}Dy reaction , Nucl. Instr. and Meth.A (2005); 550: 626-636. doi: 10.1016/j.nima.2005.04.091

[3]. N. Belouadah et al., Experimental cross section of the 164Dy (n, γ) 165Dy reaction at the neutron energy of 0.0372 eV using Neutron Diffraction Facility, Radiochim.acta (2022). doi:10.1515/ract-2022-0052

Keywords: ^{164}Dy (n, γ) ^{165}Dy thermal cross section; activation method; ^{241}Am-Be neutron source; Indium (In) and gold (Au) monitors.

T2-P24: Geant4 application software in labVIEW requiring no C++ coding

A.C. Chergui@, Lakhdar Guerbous, Mohamed Fouzi Belazreg

[1] *Division of Physics, Department of Nuclear Safety Nuclear Research Centre of Algiers, Algeria*
@a.chergui@crna.dz

Background/Purpose: Geant4 is a powerful and free software toolkit used to accurately simulate the passage of particles through matter. However, due to its relatively complex software system, which requires a fair amount of knowledge of C++, most users avoid it. In this work, we present an alternative (but non-exhaustive) software interface application that allows the user to easily build his own simulation project via a graphical programming environment. Where, this application converts it into an equivalent C++ script, which it can then compile and execute by Geant4. The interface application was designed under the LabVIEW platform, it contains libraries in the form of pre-designed blocks that allow the user to insert data and/or select the type of variables, functions and attributes…; However, this LabVIEW blocks use a MySQL database to include the data related to the detectors such as efficiency and optical features, and on the other hand, to store and retrieve historical measurements and plot the spectra extracted from the execution of the program on Geant4. There are several pre-designed blocks for each specific function, connecting them together in the right way allows building a detector from specific materials and geometric shapes, and embedding it in electromagnetic fields, as well as configures the display of detector geometry, tracks and events. This application also provides block for writing and reading graphs and data in several formats: Root, hdf5 format and CSV. As a start to the design of this interface application, emphasis was placed on the requirements for simulating scintillator detectors. In conclusion, this software allows experimenters, especially novices, to simulate their models without the need for prior knowledge of C++.

Materials & Methods: The development of Geant4 software toolkit was carried out using the LabVIEW environment applications and MySQL database. The program includes a set of toolbox in the form of blocks, each of which has a specific function. For example, to create a geometric model, a block is provided containing several the geometric shapes, their dimensions, physical and optical properties and their positioning coordinates...The user only has to choose the shape and fill in the data or select the constituent materials previously included in the MySQL database. The same thing applies to specifying the radioactive source, its properties, coordinates, and the data to be extracted. The blocks are linked in the bloc diagram section in LabVIEW, which ultimately collects the information and forms it into files that are then executed in the Geant4.

Results: In this paper, we focused our work on the development software toolkit and aspect of modelling scintillation detectors on Geant4. The simulator correctly connects the different blocks VI and then the labVIEW application collects the data and converts the whole into a program that is finally executed via Geant4. Finally, the program can be executed on Geant4 installed on Linux or Windows, and extract all the data and graphics that we want to get.

Conclusion: We have focused our study in the development of Geant4 software toolkit using the LabVIEW environment applications and MySQL database. Its main tasks are to create simulations in an easy way through ready-made blocks designed in labVIEW and convert them into a program that can be executed by Geant4. In the future, this toolkit can be used to model a whole chain of detectors available in our laboratories. Thus, all the user has to do is modify the samples to be modelled and measured.

Keywords: Geant4; scintillation detector; LabVIEW; MySQL; Object Oriented Programming in C++.

T2-P25: Neutron Activation Analysis at the CRND NAA Facility Using the NUR Reactor for Trace Element Profiling of Whole Blood in Breast Cancer Research

Z. Bouhila-Khodja@, A. Hadri, D. Boukhadra, S. Benbouzid, A. Chettah, Y. Amrane and R. Nouri.

Nuclear Research Centre of Draria (CRND), Algiers, Algeria
@Corresponding author e-mail: Z-Bouhila@CRND.dz

Background/Purpose: Neutron Activation Analysis (NAA) is a powerful nuclear technique widely used for quantifying trace elements in biological samples [1]. This research aims to establish a trace element profile in whole blood samples from breast cancer patients, comparing it to healthy individuals, and to explore potential links between trace element concentrations and cancer development. This could provide insights into more accurate diagnostics and a deeper understanding of cancer pathogenesis.

Materials & Methods: The NAA laboratory at CRND participates in proficiency tests with IAEA, significantly refining the NAA techniques used. In this study, whole blood samples were irradiated in the NUR reactor for four hours to analyze both medium- and long-lived elements. Two measurement campaigns were conducted to acquire gamma spectra for these elements using a high-purity germanium detector. The data were processed using Microsoft Excel, supported by an in-house developed application that automates the calculation of trace element concentrations. This tool ensures accuracy by reducing manual errors and providing efficient analysis based on gamma spectra inputs. The reliability of the results was confirmed by referencing the IAEA-A13 standard material used in the NAA process.

Results: Our findings show elevated sodium (Na) levels in breast cancer patients, suggesting a potential marker for cancer, while other trace elements like zinc (Zn) and selenium (Se) did not display significant differences between the two groups. The advanced statistical analysis of these results could further refine these observations, potentially uncovering deeper correlations and enhancing our understanding of the role trace elements play in cancer development.

Conclusions: This study highlights the importance of NAA in cancer research and emphasizes the role of computational innovations in advancing biomedical investigations. The insights gained from this work could contribute to more refined diagnostic tools and a better understanding of cancer's underlying mechanisms. Moreover, the potential for targeted cancer therapies based on trace element profiles opens up new avenues for personalized medicine in cancer. treatment [2; 3].

References:

[1]. Smith, R., & Kaplan, S. (2022). "Trace Element Analysis in Blood Samples Using NAA". *Analytical Chemistry Reviews*, 44(5), pp. 320-335.

[2]. Tabbassum, S., Nie, L. H. (2020). "In Vivo Neutron Activation Assembly Design for Quantification of Trace Elements Using MCNP". *Physiological Measurement*, ePub ahead of print. doi: 10.1088/1361-6579/abc322

[3]. Byrne, P., Coyne, M., Nie, L. H. (2020). "Improved MCNP Simulation Considering Neutron Angular Distribution and Its Experimental Verification". *International Journal of Atomic and Nuclear Physics*, Vol. 5, Article 023. doi: 10.35840/2631-5017

Keywords: **Neutron Activation Analysis (NAA), NUR Reactor, Trace Elements, Cancer Research, Diagnostic Tools.**

T2-P26: Synthesis and Spectral Properties of Li^+ Co-Doped $(Gd_xY_{1-x})_2O_3$: Eu^{3+} Nanopowders

F. Riahi[1,3@], L. Guerbous[2], [1] N. Bensemma [1], C. Djebbari [3]

[1]*Nuclear Research Centre of Birine, Djelfa- Algeria*
[2]*Nuclear Research Centre of Algiers , Algiers Algeria;*
[3]*Faculty of sciences, August, 20th; 1955 University of Skikda, Algeria;*
[@] *Corresponding author f.riahi@crnb.dz*

Background/Purpose: Yttrium–gadolinium–europium oxide is an important material with many applications in various fields. It is a well-known luminescent material widely used for red light emission in modern optoelectronic devices [1]. It is also used in the production of ceramic scintillators for computed tomography (CT) medical imaging [2]. The Gd in the matrix has a high X-ray absorption coefficient, and this property allows for tuning the X-ray attenuation length by adjusting the Gd_2O_3 concentration [3]. In this work, we investigated the $(Gd_{0.95-x}Y_x)_2O_3$ doped with Eu^{3+} and co-doped with Li^+ ions used in the production of powder scintillators.

Materials & Methods: The nanopowders of $(Gd_{0.95-x}Y_x\ Eu_{0.05}Li_{0.05})_2O_3$ (x = 0, 0.475, 0.95), were prepared using the sol-gel method. First, stoichiometric amounts of high-purity gadolinium nitrate, yttrium nitrate, europium nitrate, and lithium nitrate, corresponding to the different compositions, were dissolved in concentrated nitric acid and deionized water to make their respective nitrate solutions. These three solutions were then mixed under magnetic stirring to obtain a transparent liquid. Next, polyethylene glycol was added. The pH of the solution was adjusted by adding ammonium. The resulting solution was dried at 120°C to obtain the powders. Finally, the powders were heated in a muffle furnace at 600°C for 2 h to obtain white phosphor powders. The crystallinity and optical properties were studied using X-ray diffraction (XRD) and photoluminescence techniques.

Results: We obtained particles with excellent structural ordering in the cubic bixbyite-type structure for all mixed oxide compositions. Luminescence emission measurements revealed characteristic transitions of the trivalent europium ion incorporated into the insulating host. The decay time values for the ^5D_o–$^7F_2$ transitions of the trivalent europium ion were measured to gather information on the different kinetic processes occurring at this emitting level

Conclusion: The nanopowders of $(Gd_{0.95-x}Y_xEu_{0.05}Li_{0.05})_2O_3$ have been successfully synthesized by a Sol-Gel method. XRD results revealed the cubic structure of samples and it confirmed that no change in the crystal structure was observed with the incorporation of alkali metal ions. The co- doped phosphors exhibited enhanced red light emission at 612 nm under U.V. excitation at 250 nm.

References:

[1] P. Majewski et al, Phase Diagram Studies in the Systems La2O3-SrO-Ga2O3 and La2O3-MgO- Ga2O3 at 1400 °C in Air, Int. J. Inorg. Mater., Vol 3 (No. 8), 2001, p 1343–1344. doi: 10.1016/S1466-6049(01)00158-1

[2] G. Blasse, Reviews: scintillator materials, Chem. Mater. 6 (1994) 1465–1475, doi:10.1021/cm00045a002.

[3] S.Singh et al, Synthesis and optical properties of Gd2(12x)O3: 2xEu3+nanophosphors via tartaric assisted sol–gel route, J Sol-Gel Sci Technol, doi: 10.1007/s10971-014-3566-3

Keywords: **Sol–gel; Nanophosphor; photoluminescence**;

T2-P27: Radiological Characterization in Drinking Water Samples from Bordj-Bouarreridj Region, East Algeria

H. Kebir[@],

[a]*Faculty of Sciences and Technology, University of Mohamed El Bachir El Ibrahimi of Bordj Bou Arreridj, Algeria. Birine Nuclear Research Center Ain Oussera.Bp 180, Djelfa-Algeria (CRNB). Laboratory of Materials Physics, Radiation and Nanostructures, Physics Department, Faculty of Sciences, Mohamed El-Bachir El Ibrahimi Bordj-Bouarrerid University, 34000 BBA, Algeria*

[@] *Corresponding author hadda.kebir@univ-bba.dz*

Background/Purpose: Three drinking water samples were collected from the Bordj-Bouarreridj region in eastern Algeria: Chenia-source (artesian well), Zemala-source, and Ksir El Ghoul-source in Ain Taghrout. The total cancer mortality and cancer morbidity risk associated with the ingestion of ^{238}U, ^{232}Th and ^{40}K for the three sources of drinking water for different age groups, the mass concentrations and the total annual dose for 1–5 y, for 6– 10 y, for 11–15 y and for adults of age > 15 y were calculated.

Materials & Methods: 1.5 L of drinking water per sample were collected. Is decanted an amount of about 600 ml in a 1 L beaker and subjected to evaporation. The samples were stored for at least 21 days to ensure a secular equilibrium before measurement by gamma spectrometry. Using gamma spectrometry based on HPGe detector (efficiencies 36%) [1]. The efficiency calibration is done using two calibration sources provided by a Marinelli type and in gel form: ^{133}Ba and ^{152}Eu. The regions of interest and peak areas were automatically selected and calculated with GENIE 2000.

Results: The total cancer mortality and cancer morbidity risk associated with the ingestion of ^{238}U, ^{232}Th and ^{40}K for the three sources of drinking water for different age groups ranged from 0.55×10^{-5} and 1.24×10^{-5} with mean value of 0.84×10^{-5} and 35.36×10^{-5} to 40.53×10^{-5} with mean value of 37.27×10^{-5} respectively [2, 3].

Conclusion: According to the acceptable level of 10^{-3} for the radiological risk, the cancer risks at the 10^{-5} and 10^{-4} are low. Comparing uranium concentrations in the three samples obtained in this study with the recommended safe limit of 15 µg/L, 20 µg/L and 30 µg/L, it was noted that the Zemala-Bordj El Ghedir spring mineral water sample had a value 63.56 µg/L exceeded the limits, for this reason we suggest that the investigated spring mineral water of Zemala-Bordj El Ghedir region is not acceptable as a drinking water.

References:

[1]. Canberra, 2013. Model 747 and 747E Lead Shield, Canberra Industries, Inc.

[2]. Calin MR, Ion AC, Radulescu I (2014) Evaluation of quality parameters and of natural radionuclides concentrations in natural mineral water in Romania. J Radioanal Nucl Chem 303:305-313. https://doi.org/10.1007/s10967-014-3401-x

[3]. WHO (2003) World Health Organization Guidelines for drinking water quality, 2nd edn. Total dissolved solids in Drinking-water, Geneva, 1996.

Keywords: spectroscopy gamma; cancer mortality; cancer morbidity; public health; drinking water;

T2-P28: Study by DFT of Structural, Elastic, Thermal and Optoelectronic Properties of Single Perovskites for Detection and Scintillator

K Hamiche@ Y. Yamina, A. Zitouni

Faculty of Sciences and Technology
University of Mostaghanem
korichi.hamiche.etu@univ-mosta.dz

Perovskites have shown important properties for various technological applications since their discovery in 1839, which is why they have attracted the interest of researchers and scientists. In this study, using the DFT by FP-LAPW method implemented in the wien2k code, we focus on the structural, elastic, thermal and optoelectronic properties of single perovskites CsPbX3(x=Br, I), which motivates the use of these perovskites for detecting light in the UV range, especially for surveillance and security applications due to their structural and elastic stability, their gap ranging from 1.1 to 1.7 eV and an acceptable ZT figure of merit and their good absorption in a part of the visible and in a wide UV range, which also make them prime candidates to serve as scintillators in detection devices.

Keyword: DFT, wien2k, elstic, thermal, optoelectronic, perovskites, detection.

T3-P1: Study on dosimetric characteristics of β-irradiated YAG:Ce

R. Berreksi[a@], D.E. Kdib[a], S.A.A. Sahbi[a], A. Boukerika[a], Y. Larbah[a], S. Saadi[a]

[a] *Nuclear Research Center of Algiers*
[@] *Corresponding author r.berreksi@crna.dz*

Background/Purpose: Ce-activated Yttrium Aluminum Garnet ($Y_{2.97}Al_5O_{12}:Ce_{0.03}$, commonly referred to as YAG:Ce^{3+}) is widely utilized across various fields due to its outstanding properties, including high chemical stability, excellent optical properties , and resistance to thermal creep at high temperatures. In recent years, YAG:Ce^{3+} has been extensively explored for its potential applications in radiation dosimetry, particularly in thermoluminescence dosimetry (TLD) for personnel, medical, and environmental monitoring. However, the thermoluminescence (TL) efficiency of YAG:Ce is notably affected by factors such as the type of radiation (β, X, and γ rays), the concentration of Ce^{3+} ions, and the applied dose range. This study focuses on investigating the dosimetric properties of β-irradiated YAG:Ce synthesized using the sol-gel method. Key aspects such as the TL glow curve, repeatability, fading behaviour, and dose-response were analyzed and discussed.

Materials & Methods: YAG:Ce^{3+}nanopowder was synthesized using the sol-gel method and calcined at 1100°C for 4h. Phase identification of the YAG:Ce^{3+} sample was carried out using a PANalytical X'Pert Pro (Philips) diffractometer with Cu Kα radiation (λ = 1.5425 Å), operating at 40 kV and 30 mA, and scanning over a 2θ range of 10° to 90°. The photoluminescence spectra of the YAG:Ce sample was recorded at room temperature using a PerkinElmer LS-50 B spectrometer. TL glow curves of YAG: Ce^{3+} irradiated with β-rays were recorded using the automated RISØ TL/OSL Reader Model DA-20.

Results: XRD analysis confirmed the presence of a pure garnet phase, consistent with the standard diffraction data for YAG (JCPDS card 01-079-189). The emission spectra revealed a broad band spanning 500–700 nm, attributed to Ce^{3+} transitions from the 5d excited state to the 4f ground states (5d → 4f). The TL glow curves of the YAG:Ce sample were dominated by a peak centered at 150°C. The dose response of YAG:Ce exhibited two distinct regions, the first from 10-100 Gy with a perfect linearity, and a second from 100 to 500 Gy with a clear supralinear behaviour. In addition, the study of fading was carried and showed a lost of TL signal about ~93% after 16 h and a clear stability for the rest values, as well as the repeatability of TL measures were performed and demonstrated a reusability of this material for evaluation of dose.

Conclusion: YAG:Ce^{3+} sample was successfully synthesized via a sol-gel method. XRD analysis indicated that prepared sample were crystallized in a pure cubic garnet phase. PL spectraexhibited a yellow emission band centered about 520 nm, attributed to 5 d → 4f transitions of Ce3+ ions. This study highlights the promising dosimetric characteristics of YAG:Ce^{3+}, indicating its potential suitability for thermoluminescence (TL) dosimetry.

References:

[1]. S. Saadi et al.: Investigation of structural, photo and thermoluminescence properties of YAGG:Ce nanogarnet for medical dosimetry application. *Radiation Physics and Chemistry.* 2024;221: 111776. doi: doi.org/10.1016/j.radphyschem.2024.111776 *

Keywords: **Dosimetry; YAG:Ce3+; thermoluminescence; dose-response;**

T3-P2: Effect of heating rate on *β*-irradiated Cerium doped $Y_{2.97}Al_4Ga_1O_{12}:Ce_{0.03}$ thermoluminescence glow dosimetric peak and its kinetic parameters

S.A.A. Sahbi[@], D.E. Kdib, R. Berreksi, A. Boukerika, Y. Larbah, S. Saadi

Nuclear Research Centre of Algiers
[@]Corresponding author s.sahbi@crna.dz

Background/Purpose: Cerium doped Yttrium Aluminium Gallium Garnet ($Y_{2.97}Al_4Ga_1O_{12}:Ce_{0.03}$) commonly referred to as YAG1G:Ce^{3+} nanophosphors have demonstrated a potential suitability for application thermoluminescence dosimetry [1]. it is well known that the variation in linear heating rate (HR) can affect the kinetic parameters, and the other TL characterises. Consequently, the variation of HR during TL readouts can affect the evaluation of radiation doses. Furthermore, investigating of TL glow curves and its kinetic parameters dependence on HR is crucial to the best evaluation of radiation doses and the thermoluminescence properties of the TL material. This work aims to study the behaviour of the main TL dosimetric peak of β-irradiated YAG1G:Ce^{3+} for different HR and the variation of its trap parameters using Initial Rise (IR) and peak shape (PS) methods.

Materials & Methods: In this study, the sample of YAG1G:Ce^{3+} weight was about ~5 mg on a powder form of nanoparticles and was exposed to a dose of ~33.5 Gy from a $^{90}Sr/^{90}Y$ source with a dose rate of ~67 mGy/s. The TL measurements were performed using automatic RisØ TL/OSL reader Model DA-20 with five (05) different linear HR of 1 K/s,2 K/s, 3 K/s, 5 K/s, and 10 K/s in the temperature range of 300-573.15 K in a nitrogen atmosphere. The determination of kinetic parameters principally activation energy and frequency factors for each value of HR was performed using Initial rise (IR) and peak shape (PS) methods.

Results: The obtained TL glow curves of YAG1G:Ce^{3+} have a single strong peak with temperatures at maximum intensities T_M shifting to higher values and maximum TL intensity I_M decreasing with the increasing of HR for TL measurements. These results are predicted by theory and showed the common normal behaviour as the most used TL materials. The kinetic parameters of the main dosimetric peak for each HR value were calculated by IR and PS methods, compared to each other and with other works for the same type of materials.

Conclusion: It has been successfully demonstrated that, the effect of heating rate on YAG1G:Ce^{3+} TL glow curve for different values of HR was in agreement with the common studied materials and no anomalous behaviour was observed. In addition, the obtained values of the trap parameters by IR and PS methods were very close to each other, and in accordance with those obtained in different studies for similar type of materials.

References:

[1]. S. Saadi et al.: Investigation of structural, photo and thermoluminescence properties of YAGG:Ce nanogarnet for medical dosimetry application. *Radiation Physics and Chemistry.* 2024;221: 111776. doi: doi.org/10.1016/j.radphyschem.2024.111776

Keywords: **Dosimetry; Thermoluminescence; TL Kinetic parameters; HR effect**;

T3-P3: Performance testing of the DXTRAD Ring TL Detector used for Extremity Dosimetry Monitoring.

A. Meziane@, S. Nateche, M. Aït-Ziane

Centre de Recherehce Nucleaire d'Alger, 02, Bd Frantz Fanon B.P. 399 Alger-R.P., Algeria
@Corresponding author a.meziane@crna.dz

Background/Purpose: Monitoring of workers constitutes an important part of any radiological protection programme. In some medical applications of radiation, there is a high risk of locally high exposures because of direct handling of radiation sources specially beta- emitters and working close to radiation fields. Extremity dosimetry ensures the optimization of occupational exposure, compliance with regulatory limits, and prevention of deterministic skin effects in these applications, where the fingers are often in contact or very close to the radiation beam or radiopharmaceuticals [1-2]. The DXTRAD ring dosimeter based on ^{7}LiF: Mg, Ti detector, manufactured by THERMO, is commonly employed for extremity monitoring. This study aims to characterize the performance of this ring dosimeter according to ISO-12794 standards, focusing on operational reliability metrics such as homogeneity, reproducibility, linearity, and detection threshold.

Materials & Methods: The characterization of the DXTRAD dosimeters was carried out using a Harshaw 6600 Plus TLD reader and reference radiation sources (^{137}Cs, ^{60}Co, and X-rays) in terms of Hp(0.07), under controlled reference conditions at the Secondary Dosimetry Standards Laboratory (SSDL). The performance evaluation focused on key operational parameters as homogeneity, reproducibility, linearity, and detection threshold following the guidelines of ISO-12794(2000) [3].

Results: The performance test were carried out for a group of 15 irradiated dosimeters. The obtained homogeneity and reproducibility variation coefficients were 6% and 5% respectively. It assures us the homogeneity and the reproducibility of the batch being studied. According to ISO-12794 guidelines, the batch is considered homogeneous up to a maximum value of 15%, and the value obtained for reproducibility do not exceed 10% difference between readings [3].

The response linearity has been carried out, the variation response was found between 0.8 and 1.08 for doses ranging from 1 to 100 mSv. The obtained detection threshold was equal to 60 µSv. These results demonstrate that DXTRAD dosimeters comply with ISO-12794 standards [3], confirming their operational reliability for extremity dosimetry.

Conclusion: The DXTRAD ring dosimeters exhibit high reliability and precision for extremity dosimetry monitoring, meeting regulatory requirements. This characterization validates their suitability for precise occupational exposure monitoring. Future research could focus on enhancing sensitivity and evaluating performance under varying environmental conditions.

References:

[1]. Vanhavere, F. et al. An overview on extremity dosimetry in medical applications, Radiation Protection Dosimetry (2008), Vol. 129, No. 1–3, pp. 350–355

[2]. Muthia'tul Maula E. et al. Characteristic testing (performance) of CaSO4: Dy thermoluminescent ring dosimeter according to the ISO 12794:2000, (2021) J. Phys.: Conf. Ser. 1796 (2021) 012061

[3]. ISO 12794 Individual thermoluminescence dosemeters for extremities and eyes, (2000), ISO, Geneva.

Keywords: Extremity dosimetry, TL detector, DXTRAD ring dosimeter, ISO-12794,

T3-P4: Assessment of increased radiation exposure from ^{18}FDG PET/CT in children

D. Ben-Sellem[a@], N. Ben-Rejeb[b]

[a]*Université de Tunis El Manar, Faculté de Médecine de Tunis, Laboratoire de recherche en Biophysique et Technologies Médicales ISTMT, Institut Salah Azaiez : Service de Médecine Nucléaire, 1006, Tunis, Tunisia*
[b]*Université de Tunis El Manar, Laboratoire de recherche en Biophysique et Technologies Médicales, Institut Supérieur des Technologies Médicales de Tunis, 1006, Tunis, Tunisia*
[@]*Corresponding author bensellemdorra@gmail.com*

Background/Purpose: Cancer cells are characterised by a low rate of energy from glycolysis. In order to sustain a higher glycolytic flux, these cells increase their glucose uptake. This augmentation has been exploited clinically for cancer diagnosis and monitoring through the use of 18 Fluoro-2-deoxy-D-glucose (^{18}FDG), which is a radiolabelled glucose analogue used in positron emission tomography (PET) imaging [1]. PET imaging provides information on molecular and metabolic alterations. However, it lacks anatomical landmarks and has poor spatial resolution [2]. These issues have been overcome by adding a computed tomography (CT) scanner to the same machine. Nevertheless, this hybrid PET/CT imaging exposes patients to double irradiation: PET radiopharmaceutical and CT rays. The aim of this study was to estimate and compare the contributions of ^{18}FDG-PET and CT to the effective dose of this hybrid imaging, in oncologic paediatric patients.

Materials & Methods: This study included 37 oncologic paediatric patients, aged between 4 and 17 years, divided into three groups according to their age. The total effective dose of PET/CT is the sum of the effective doses of ^{18}FDG and CT. The percentage contribution of the additional radiation from the scanner is given by the following equation: $\%E_{CT} = (E_{CT}/E_{Total}) \times 100$

Results: The included population was composed of 37 children (21 boys and 16 girls). The effective dose due to ^{18}FDG was 4.3 mSv. It ranged from 3 to 7 mSv. The mean effective dose from CT scans was 7 mSv, varying from 3 to 17 mSv. The mean total effective dose was 11.5 mSv and ranged from 6 to 23 mSv. The mean contribution of CT to the total effective dose for PET/CT was 61%. It was in the range 42% to 77%.

Conclusion: Despite the great importance of hybrid imaging, the percentage contribution of CT remains very high. It is therefore essential to optimise the dose of the PET/CT protocol in order to keep the dose as low as reasonably achievable (ALARA).

References:

[1]. Weiler-Sagie M et al.. ^{18}F-FDG activity in lymphoma readdresses: a study of 766 patients. *Journal of Nuclear Medecine*. 2010;51(1):25-30.

[2]. Parghane RV et al.. PET/Computed tomography and PET/MR imaging basic principles, methodology, and imaging protocol for musculoskeletal application . *PET Clinics.* 2018;13:459- 476.

Keywords: ^{18}FDG; PET/CT; Effective dose; paediatric.

T3-P5: Contribution of computed tomography to the total effective dose of ^{99m}Tc-MIBI hybrid parathyroid imaging

D. Ben-Sellem[a@], N. Ben-Rejeb[b]

[a]*Université de Tunis El Manar, Faculté de Médecine de Tunis, Laboratoire de recherche en Biophysique et Technologies Médicales ISTMT, Institut Salah Azaiez : Service de Médecine Nucléaire, 1006, Tunis, Tunisia*
[b]*Université de Tunis El Manar, Laboratoire de recherche en Biophysique et Technologies Médicales, Institut Supérieur des Technologies Médicales de Tunis, 1006, Tunis, Tunisia*
[@]*Corresponding author bensellemdorra@gmail.com*

Background/Purpose: Primary hyperparathyroidism is a frequent endocrine pathology [1]. Currently, as with all hybrid imaging, metastable technetium 99-labelled Methoxy- IsoButyl-Isonitrile (^{99m}Tc-MIBI) Single Photon Emission Computed Tomography/Computed Tomography (SPECT/CT) is recommended as part of the preoperative topographic assessment to guide minimally invasive surgery [2]. However, the introduction of a CT scan, even at a low dose, increases the total radiation dose delivered to the patient. The aim was to assess the additional effective dose delivered by CT to ^{99m}Tc-MIBI parathyroid scintigraphy.

Materials & Methods: This prospective study included 100 adults with primary hyperparathyroidism undergoing ^{99m}Tc-MIBI SPECT/CT. The total effective dose of SPECT/CT is the sum of the effective doses of ^{99m}Tc-MIBI and CT. The percentage contribution of the additional radiation from the scanner is given by the following equation:
$\%E_{CT} = (E_{CT}/E_{Total}) \times 100$

Results: The mean age was 55.6 years with extremes ranging from 21 to 82 years. The effective doses received from ^{99m}Tc and ^{99m}Tc-MIBI were 1.44 mSv and 8.33 mSv respectively. The effective dose from scintigraphy was 9.77 mSv. The effective dose induced by CT was 1.77 mSv. It varied from 0.9 to 3.1 mSv. The total effective dose from the hybrid examination was 11.54 mSv on average and ranged from 10.66 to 12.88 mSv. The contribution of the additional radiation induced by the CT scan varied from 8.3 to 24.1%, with an average of 15%.

Conclusion: This dose is not negligible. However, when the benefits of hybrid imaging are considered, the additional irradiation is still justified.

References:

[1]. Pappachan JM et al.. Primary hyperparathroidism : findings from the retrospective evaluation of cases over a 6-year period from a regional UK centre. Endocrine. 2018; 62:174-81.

[2]. Scerrino G et al. The intraoperative use of the mini-gamma camera (MGC) in the surgical treatment of primary hyperparathyroidism Technical reports and immediate results from the initial experience. Annali italiani di chirurgia. 2015;86(3), 212-218.

Keywords: hyperparathyroidism; SPECT/CT; ^{99m}Tc-MIBI; effective dose.

T3-P6: Assessment of Inhaled Dose of Natural Uranium in a Nuclear Research Laboratory: A Workplace Monitoring Approach

M. Mebarka

Nuclear Research Center of Draria
Corresponding author m-mebarka@crnd.dz

Background/Purpose: The objective of this study is to evaluate the effectiveness of workplace environmental monitoring, particularly regarding atmospheric contamination by radioactive substances, to better understand both internal and external radiation exposure to workers. Since 1990, the dose limitation system proposed by the International Commission on Radiological Protection (ICRP), detailed in Publication ICRP 60 [1] and later updated in ICRP 103 of 2007 [2], specifically aims to reduce such exposures. Environmental monitoring relies on passive dosimetry, which allows for measuring and evaluating doses received from inhalation of radioactive materials suspended in air, with a delay.

Materials & Methods: Air sampling is performed using an adjustable flow-rate air sampling pump, with a flow range between 0.1 and 6 m^3/h and sampling durations ranging from 1 to 6 hours during twelve (12) months sampling period, using 0.8 µm pore size and 48 mm diameter cellulose nitrate filters. This specific filter is capable to trap radioactive particles suspended in the air including alpha emitters. The duration of sampling is adjusted depending on the workplace requirements and the expected level of contamination.

The methodology for assessing the inhaled dose primarily relies on two measurement techniques. The first technique involves analyzing the filter using a gamma-ray spectrometer with an HPGe detector (from Canberra) and gamma Vision software, version 6.08 (from EG&G ORTEC). The resolution is 1.90 keV on the 1332.5 keV line of ^{60}Co with efficiency of ~30%. The second technique involves using a surface contamination detector for the determination of the total activity of the filter, expressed in Becquerels (Bq).

Results: The total activity measured in Becquerels (Bq) for natural uranium is used to assess the inhaled dose, calculated using the following formula: $Einh = Ci \times BR \times Ei \times Te$

The results show that inhaled doses range from 0.922 pSv/h to 1.14 nSv/h, which do not exceed the annual limit for workers exposed to ionizing radiation, which is 20 mSv for workers in environments with ionizing radiation.

Conclusion: This work highlights the fundamental importance of effective environmental monitoring in nuclear research laboratories, particularly for minimizing the internal exposure of workers to alpha emitters. The evaluation of inhaled dose, at the core of this study, strengthens the proactive approach to ensuring compliance with exposure limits set by radioprotection organizations. This not only guarantees worker safety but also ensures compliance with radioprotection standards.

However, further research should be conducted on the effects of other types of radionuclides in similar environments, to expand knowledge on exposure management in various contexts.

References:

[1]. ICRP, 1991. 1990 Recommendations of the International Commission on Radiological Protection. ICRP Publication 60. Ann. ICRP 21 (1-3).

[2]. ICRP, 2007. The 2007 Recommendations of the International Commission on Radiological Protection. ICRP Publication 103. Ann. ICRP 37 (2-4).

Keywords : Workplace Environmental Monitoring, International Commission on Radiological

T3-P7: Radon exhalation rates of some building materials using can technique method

M. Bakalem[1, @], L. Chabouni[1], R. Chahdane[2], M. Mezaguer - Lekouaghet[1], M. Aït-Ziane[1], Z. Lounis-Mokrani[1]

[1]Nuclear Research Center of Algiers (CRNA)
[2]Nuclear Research Center of Draria (CRND) @ Email: m.bakalem@crna.dz

Background/Purpose: Radon-222 is a naturally occurring radioactive gas resulting from the decay of uranium-238 found in rocks and soils. This gas can accumulate in buildings, particularly through construction materials, posing a health risk due to its potential to damage the lungs and increase the risk of cancer through inhalation. To assess the radon exhalation rate, samples of various building materials, such as sand, cement, and brick, were collected from different regions of the country.

Materials & Methods: Building material samples were prepared and analyzed using the "can technique" method [1]. A passive method, which consist of the use of LR-115 Solid-State Nuclear Track Detector (SSNTD). The technique involves placing the sample in a sealed container with an SSNTD detector attached to the lid.

Results: Radon exhalation rate (in terms of mass (E_M) and surface area (E_A)) in building materials samples ranged from 0.07 ± 0.01 to 1.98 ± 0.53 $mBq \cdot kg^{-1} \cdot h^{-1}$ and from 4.11 ± 0.76 to 130.5 ± 37.43 $mBq \cdot m^{-2} \cdot h^{-1}$ respectively. The lowest value of radon exhalation rate was in a sample of brick and the highest value of radon exhalation rate was in a sample of crushed sand 0/3. The wide variation can be attributed to varying porosity and degree of firing in the kiln of analyzed samples.

Conclusion: Radon exhalation rates from the most common building materials collected from some provinces of Algeria have been determined using Solid state nuclear track detectors (SSNTD LR-115). The determined rates were well below the world average value of 57600 $mBq \cdot m^{-2} \cdot h^{-1}$ [2], hence, these materials contribute very little to the radon concentration in a dwelling, and it may be used for construction purposes, as they do not pose any health hazards.

References:

[1]. Abu-Jarad, F., J.H. Fremlin and R. Bull, 1980. A study of radon emitted from building materials using plastic alpha-track detectors. Phys. Med. Biol., 25: 683-694. PMID: 7454758.

doi: 10.1088/0031-9155/25/4/007

[2]. UNSCEAR 2000: United Nations Scientific Committee on the Effects of Atomic Radiation Report to the General Assembly, Vol. 1: ANNEX B exposures from natural radiation sources: New York, United Nations, 2000.

Keywords: Radon exhalation rate, Building material, Can technique, LR-115.

T3-P8: Optimization of cytogenetic parameters for use in biological dosimetry

M. Mezaguer[@], N. Bennoui, A. Biout, L. Aberkane, K. Aouragh, S. Souilah and S. Allali.

Algiers Nuclear Research Centre, 02BdFrantz Fanon, P.O.Box 399Alger-RP,16000, Algiers, Algeria.
[@] Corresponding author *m.mezaguer@crna.dz*

Background/Purpose: Ionizing radiation damages cell molecules, including the DNA molecule [1], leading to their destabilization and cellular modifications [2]. Despite DNA repair mechanisms, this damages can persist and cause stable and unstable chromosomal aberrations [3]. The number of these aberrations is proportional to the dose received [4]. Therefore, this characteristic is used in dosimetry in case of accidental exposure, by counting unstable aberrations on lymphocytes in culture at the metaphase stage using cytogenetic techniques. In this work, we have managed to optimize the protocol of the cytogenitic technique to highlight chromosomal aberrations following irradiation at 2, 4 and 6 Gy. The culture medium, the colcemid concentration, the duration of the hypotonic shock, and the denaturation technique have been optimized.

Materials & Methods: The peripheral bloods from a healthy donor have been collected in tubes. A portion was irradiated at 2, 4 and 6 Gy in a CRNA irradiation facility (^{60}Co) and another tube was used as a control. After irradiation, all the tubes were sent to the cell culture laboratory for a 72 hour culture with Phytohematoglutinin. Two hours before the end of the culture, the colcemid has been added in culture medium. After 72 of culture, a hypotonic shock was applied followed by a series of fixation steps, and the cells have been deposit on slides. The Metaphases were observed for chromosomal aberrations used Leica 5500DM microscopy.

Results: The results showed that the better culture was obtained with the RPMI 1640 culture medium, a concentration of 75 µl of colcemid and the time of 40 min of hypotonic shock. The application of denaturation step before staining, allowed a good visualization of the chromosomal strands and a better observation. The observation of the samples irradiated at different doses 2, 4 and 6 Gy compared to the controls showed on the one hand, a decrease in the cell number proportionally to the dose, on the other hand, the presence of some dicentric aberrations and fragments which are the signatures of ionizing radiation.

Conclusion: The comparison between the metaphases on the slides irradiated at 2, 4 and 6 Gy compared to the controls shows the appearance of di-centric, rings and fragments.

References:

[1] Laurier, D. *et al.,* (2023). Chapitre 31. *Rayonnements ionisants. In Environnement et santé publique* (p. 829-849). Presses de l'EHESP.

[2] Mondal, T. *et al.,* (2019). 18FFDG-induced DNA damage, chromosomal aberrations, and toxicity in V79 lung fibroblast cells. *Mutation Research/Genetic Toxicology and Environmental Mutagenesis*, 847, 503105.

[3] Roy. (2006). La dosimétrie biologique par les aberrations chromosomiques radio-induites.

[4] IAEA. (2001). Cytogenetic analysis for radiation dose assessment. *Technical Report Series International Atomic Energy agency.*

Keywords: Biology dosimetry. Instable aberrations. Cytogenetic. Gamma irradiation.

T3-P9: Optimization of the optical performance of an air-core Ag-PTFE dosimeter for brachytherapy

N. Boughaba[a@], B. Bouzid[a], N. Yahlali[b]

[a]*SNIRM Laboratory, USTHB, Bab-Ezzouar, BP 32 El-Alia, 1611, Algiers, Algeria,*
[b]*Instituto de Física Corpuscular (IFIC), Centro Mixto Universitat de València (UV) – CSIC*
[@]*Corresponding author: nboughaba@usthb.dz*

Background/Purpose: Brachytherapy (BT) is an internal radiotherapy technique in which sealed radioactive sources are directly placed near or inside a tumour [1]. *In-vivo* dosimetry for high-dose rate (HDR) brachytherapy is required for the control of the source dwell positions and the optimal delivery of the prescribed dose to the tumour. Scintillation dosimeters using plastic scintillating fibres have raised lots of interest due to their notable dosimetric properties. However, their main drawback in HDR BT is the presence of Cerenkov photons produced by electrons with velocities exceeding the speed of light in the plastic medium. Several techniques have been implemented to minimize this optical noise, among them the air-core light guide method, which consists in the suppression of Cerenkov radiation at its source by replacing the optical fibre light-guide by an air-core fibre. The current air-core dosimeter based on a silica light-guide [1] has a limited clinical use, despite of its proven accuracy, due to its high light loss and its mechanical rigidity, which limits its application for in-vivo BT requiring flexible applicators [1].

Materials & Methods: A new flexible scintillation dosimeter with an Ag-PTFE air-core light-guide, read out by a silicon photomultiplier, was built and characterized [2]. This dosimeter was compared to a standard prototype with a solid-core light guide using GATE simulations in a prostate BT scenario. The effect of silver coating of the scintillating fibre on the light collection efficiency of the Ag-PTFE air-core dosimeter was studied.

Results: Simulations of the optically optimized Ag-PTFE air-core dosimeter in a prostate brachytherapy scenario show that its collection efficiency is improved beyond 15% by silver coating of the scintillating fibre, resulting in a substantial increase in the dose signal.

Conclusion: The simulation studies of the Ag-PTFE dosimeter with a silver-coated scintillating fibre, show a substantial increase of the dosimeter light collection efficiency due to the additional coating, which allows the recovery of part of the stray light from the fibre light-guide interface. A procedure for building an optimized Cerenkov-free dosimeter for HDR BT is outlined.

References:

1. *Veronese, I., Andersen, C.E., Li, E., Madden, L., Santos, A.M., 2024. Radioluminescence-based fibre optic dosimeters in radiotherapy: a review. Radiat. Meas. 107125.http://dx.doi.org/10.1016/j.radmeas.2024.107125.*

2. *Nor El Houda Boughaba, Boualem Bouzid, Nadia Yahlali, Assessment of Cerenkov optical noise in a brachytherapy scintillating fibre dosimeter with an air-core Ag-PTFE light guide,Radiation Measurements,Volume 181,2025, 107348. ISSN 1350-4487, https://doi.org/10.1016/j.radmeas.2024.107348.*

Keywords: Brachytherapy, Cerenkov, Scintillating fibre, Air-core fibre, Dosimetry, GATE.

T3-P10: Radiation protection consideration in clinical facility design for accelerator-based Boron Neutron Capture Therapy

L. Zaidi[a@], M. Belgaid[a], S. Taskaev[b]

[a] *University of Science and Technology Houari Boumediene, Faculty of Physics, SNIRM Laboratory, BP 32 El Alia 16111, Bab Ezzouar 16111, Algeria*

[b] *Budker Institute of Nuclear Physics, Siberian Branch, Russian Academy of Sciences, pr. Akademika Lavrentieva 11, Novosibirsk 630090, Russia*

[@]*Corresponding author liliazaidi16@gmail.com*

Background/Purpose: The design and construction of a safe radiotherapy system based on the Boron Neutron Capture Therapy (BNCT) technique require more stringent radiation protection measures compared to conventional techniques. This is due to the nature of the treatment beam, which consists primarily of neutrons with a significantly long mean free path. Based on the calculations, different wall compositions and thicknesses were tested, and the equivalent dose distributions in air were estimated. Radiation protection calculations were performed using the MCNP code based on the Monte Carlo method [1].

Materials & Methods: We considered the accelerator and therapeutic beam generated by an optimized device developed at the Budker Institute of Nuclear Physics in Novosibirsk, designed for deep tumor treatment using BNCT [2][3].The attenuation of high-energy neutrons and methods for reducing activation are the primary concerns related to shielding materials.In general, three key aspects are expected from a neutron shielding material:
(i) High attenuation rate, (ii) Efficient thermal neutron capture, and (iii) Secondary gamma-ray attenuation generated by neutron interactions with shielding nuclei.

Results: The results showed that the dose rate outside the proposed treatment room can be reduced to less than 0.5 µSv/h using a multilayer shielding approach. Lead and iron provide the best attenuation of gamma ray, while barite concrete offers a good balance between efficiency and cost.Recommended multilayer shielding: Borated concrete (100 cm) and Barium-enriched concrete around the BSA and Lithium-doped polyethylene (10 cm). Ensures compliance with radiation protection limits (< 0.5 µSv/h)

Conclusion: Based on the obtained results, it can be concluded that a multilayer shielding system is ideal for improving radiation protection performance. This shielding design is proposed in accordance with the characteristics of neutrons and gamma rays produced by the studied accelerator, allowing each layer to optimally fulfill its function in radiation protection.

References:

[1]. X-5 Monte CarloTeam, 2003. MCNP — A General Monte Carlo N-Particle Transport Code, Version 5, LA-UR-03-1987.
[2]. Taskaev, S., 2015. Accelerator-based epithermal neutron source. Phys. Part. Nucl. 46,956–990. http://dx.doi.org/10.1134/S1063779615060064.[3]. Zaidi, L., Kashaeva, E., Lezhnin, S., Malyshkin, G., Samarin, S., T, S., Taskaev, S., Frolov, S., 2017. Neutron-beam-shaping assembly for boron neutron-capture therapy. Phys. At. Nucl. 80, 60–
66. http://dx.doi.org/10.1134/S106377881701015X.

Keywords: Accelerator-based BNCT; Dosimetry; Radiation protection.

T3-P11: Calculations of absorbed dose in voxelized phantom using Monte Carlo simulation

S. Merai @, F. Benrachi, N. Laouet

Laboratoire de Physique Mathématique et de Physique Subatomique, Department of physics, Constantine-1 Frères Mentouri University, Algeria
@ Corresponding author sondes.merai@doc.umc.edu.dz

Background/Purpose: The Mice are frequently used in radiopharmaceutical development due to their well-characterized biology (The anatomy, physiology and genetics of mice), which allows scientists to understand any type of changes in mice and translate them to human processes. With the increasing use of radiopharmaceuticals in nuclear medicine for both diagnostic and therapy, it becomes very important to achieve a higher level of accuracy in internal dosimetry on small animal studies as well. To obtain appropriate preclinical absorbed dose response−effect relationships, the absorbed dose must be determined as accurately as possible.

Currently, the reference method to estimate dose calculations is the use of Monte Carlo radiation transport codes in computational phantoms, and several program packages are available to treat problems in radiation protection and radiotherapy dosimetry.

Materials & Methods: In this work, GATE/Geant4 code (version 9.3) [1] have been used to derive dosimetric parameters for a voxelized mouse phantom [2]. Different radiation sources (^{131}I and ^{64}Ga) are used to compute the absorbed dose [3]. The activity was assumed uniformly distributed in the organs, and simulation was performed for different organ sources: kidney, liver and thyroid. Furthermore, dosimetric parameters were calculated for different target regions in the body (kidney, liver, lung and heart).

Results: The results of absorbed dose showed a strong correlation with radiation energy and organ mass, with additional influence from the relative positions of the source and target organs for both beta and gamma emissions. Additionally, good agreement was observed between the simulation results and published data. For the ^{131}I source, self-irradiation absorbed dose values for the kidney were 5.34 x 10^{-2} in the simulation and 5.53 x 10^{-2} (mGy/MBq.s) in the published data [4].

Conclusion: The results confirm the consistent of MC simulation in estimating dosimetric parameters for different emission types.

References:

[1]. Open GATE collaboration. https://opengate.readthedocs.io/en/latest/introduction.html.
[2]. Dogdas, B., Stout, Chatziioannou D. A. F. and Leahy R. M., Digimouse: a 3D whole body mouse atlas from CT and cryosection data, Phys. Med. Biol. 52, 577. 2007
[3]. Laazouzi, K., Cavedini, N. G., Belhaj, O. E., Hadouachi, M., Boukhal, H., Jeckel, C. M. M., ... & Salas- Ramirez, M. Development and validation of a comprehensive S-value database for small animal internal dosimetry in nuclear medicine using the DM_Bra mouse phantom. *Radiation Measurements*, *178*, 107277. 2024
[4]. Mohammadi, A. Kinase, S. Electron absorbed fractions and S values in a voxel-based mouse phantom. Radioisotopes 60 (12), 505–512. 2011

Keywords: ***Absorbed dose, GATE/Geant4, Dosimetry, Digimouse.***

T3-P12: Validation of bladder preparation in prostate cancer radiotherapy

A. Mamache*[1], A. Merzoug[1], A. Sidi Moussa[2]

[1]*Physics department, University of Saad Dahlab Blida, Algeria*
[2] *Sidi Abdellah Oncology Center, Algiers, Algeria*
**for.abdellah.mamache@gmail.com*

Background/Purpose: Prostate radiotherapy relies heavily on consistent patient preparation to ensure accurate treatment delivery. This study evaluates the effectiveness of preparation protocols by analysing variations in bladder volume and evaluating impact of poor preparations among patients undergoing tomotherapy[1].

Materials & Methods: Ten patients underwent dose-volume analyses over multiple fractions, generating over 200 bladder contours using MVCT scans and treatment planning systems. Dose-volume histograms (DVHs) were constructed to compare planning, poor, and optimal preparations, with regression analyses exploring the relationship between bladder volume and mean dose.

Results: Poor preparations led to significant dose-volume variations, with an average bladder volume reduction of 53.5% compared to preparations that were done before CT Simulation. Optimal preparations had an increase in bladder volume by 30.39%, improving dose consistency. An exponential regression model (R^2 = 77.33%) confirmed a strong correlation between bladder volume and mean dose[2], showing a reducing bladder dose with an increasing bladder volume. Summation doses revealed that re-preparations effectively reduced deviations for patients exceeding dose constraints.

Conclusion: Effective bladder preparation is crucial for maintaining dose constraints and optimizing radiotherapy accuracy. Larger planning bladder volumes allow for greater tolerance to preparation variability, improving treatment outcomes. Further research can expand on these findings in broader clinical settings.

References:

[1] T. R. Mackie *et al.*, 'Tomotherapy: A new concept for the delivery of dynamic conformal radiotherapy', *Medical Physics*, vol. 20, no. 6, pp. 1709–1719, 1993, doi: 10.1118/1.596958.

[2] S. Huang *et al.*, 'Validation of bowel and bladder preparation by rectum and bladder variation in prostate radiotherapy based on cone beam CTs', *Journal of Radiation Research and Applied Sciences*, vol. 16, no. 1, p. 100513, Mar. 2023, doi: 10.1016/j.jrras.2022.100513.

Keywords: Prostate radiotherapy, Bladder preparation, Planned Adaptive, DVH;

T3-P13: Controlling proton therapy with a variable external magnetic field: an approach with nanoparticles

A. Boukorra, A.A.S. Dib, F. Rahal

Mohamed Boudiaf University of Science and Technology of Oran
[1]asma.boukorra@univ-usto.dz

Background/Purpose: The techniques of therapy developed currently and know a big progress in medical research. Among these techniques, the proton therapy. It is an advanced technology which allows to issue a high dose in tumor, while sparing at the healthy tissue neighboring, due to the ballistic properties of protons. The proton therapy took fast an increasing place in the armory of techniques used in cancer research.

Materials & Methods: In the present job, a simulation Monte Carlo based on the code GEANT4 of a proton therapy was established. This simulation is in presence of an external magnetic field.

Results: Our job is aimed first, at controlling the proton therapy with a variable, external magnetic field. Then to study the effects of the different nanoparticles such as Platinum, Gold, Silver and Graphen, in enhancing the dose in the tumor by irradiation of a protonic beam.

Conclusion: Our results show that the magnetic field influences of some millimeters. Indeed, active method Pencil Beam can be considered to be a control of very good precision.

References:

[1]. G. Boissonnat. Chambres d'ionisation en Protonthérapie et Hadronthérapie. Physique Médicale [physics.med-ph]. Université Caen Normandie, 2015.

[2]. Valentin Calugaru. Efficacité biologique relative (EBR) des faisceaux de protons utilisés en radiothérapie. Ingénierie biomédicale. Université Paris Sud - Paris XI, 2011.

Keywords: Proton therapy ; Magnetic Field ; Nanoparticles;Monte Carlo GEANT4

T3-P14: Saturation yield in medical cyclotron performance evaluation

Kh. Bensadallah, A. Taibi, S. Rahabi. A. Falleh, A. Amimour

Nuclear Medicine Department, CHU BAB EL OUED, Algiers

KH.BENSADALLAH kheir_eddine34@yahoo.com

Background/Purpose: BAB EL OUED CHU produces fluorine-labelled radio-pharmaceutical drugs. The latter is obtained in situ using a medical cyclotron which requires several additional systems for its operation. Throughout its use, the medical cyclotron is subject to unannounced (corrective and curative maintenance) and scheduled (preventative maintenance) interventions. The objective of our work is to study the relevance of the "saturation yield" parameter as an indicator of success or failure of an intervention and as a parameter of reduction or increase in the performance of the cyclotron. To do this, saturation yields were calculated for all production, listed according to the type of maintenance carried out and analyzed over a period of two years.

Materials &Methods: A GE MINItrace Qilin medical cyclotron was used. It operates at a fixed energy of 9.6 MeV and a maximum beam intensity of 50 µA. The Target used is lithium fluoride enriched in oxygen 18 in the form of water. To calculate the cyclotron saturation yield we use the following data: Isotope halflife (min), Beam current (µA), Irradiation time (min), Activity(mCi), ActivityCORR (mCi), Activity EOB (mCi) , Activity SAT (mCi) , SAT YIELD (mCi/µA). [1]

Results: We have three series of cyclotron saturation yield calculations relating to three different periods, namely: P1: for this period that we carried out (65 production and pre- irradiation) with a high current intensity knowing that this period corresponded to the first production (1st year of cyclotron start), the Average saturation yield is 93.74 and Standard deviation 3.74; P2: for this period that we carried out (192 productions and pre-irradiation, proton target, preventive maintenance) and with a reduced current intensity compared to period 1 the Average saturation yield is 90.05 and Standard deviation 6.06; P3: for this period that we carried out (25 production, proton target) with an average current intensity, the Average saturation yield is 90.37 and Standard deviation 2.66. [2]

The best saturation yield is observed for period P1 (average saturation yiled 93.74 with a standard deviation of 3.47) compared to the other two periods (P2 / P3) because there were no recurring breakdowns of the cyclotron and this is mainly due to the correct application of the optimal parameters (current intensity). [3]

Conclusion: For better saturation yield, we recommend regular preventive maintenance and periodic monitoring to ensure correct and lasting operation of the cyclotron.

References:

[1]. MINItrace Qilin Service Manual – Maintenance. Available at: https://www.scribd.com/document/510295725/2233000-100-Rev-18-MINItrace-Service_x0002_Manual-Maintenance

[2]. IAEA (Ed.), 2012. Cyclotron produced radionuclides: guidance on facility design and production of FDG, IAEA radioisotopes and radiopharmaceuticals series. https://www.iaea.org/publications

[3]. Yaofei, W., Kang, X., 2020. The Maintenance and Common Troubleshooting of GE MINItrace Qilin Medical Cyclotron. Zhongguo Yiliao Qixie Zazhi 44,374 -376 https://jglobal.jst.go.jp/en/detail?JGLOBAL_ID=202002232258349105

Keywords: saturation yield, proton target, pre-irradiation, Cyclotron

T3-P15 : Sensitivity Analysis of Neutron and Photon Equivalent Doses in Organs During Prostate radiotherapy Using Monte Carlo Simulation

A. Alem-Bezoubiri [1@], F. Bezoubiri [2], M. Speiser [3], H. Donya [4]

[1] *Radiological and Atomic Physics Department, Division of Physics, Algiers Nuclear Research Center (CRNA), Algiers, Algeria*

[2]*Atomic Energy Commission (COMENA), Algiers, Algeria*

[3]*Englewood Hospital and Medical Center, Englewood, NJ, USA*

[4]*Department of Physics, Faculty of Science, King Abdulaziz University, Jeddah, Saudi Arabia Corresponding author : Asma Alem-Bezoubiria. Email: a.alem@crna.dz*

Background/Purpose: This study investigates the sensitivity of neutron and photon equivalent doses in patient organs during 3D conformal radiotherapy (3D-CRT) for prostate cancer. A detailed Monte Carlo simulation was conducted to evaluate the contributions of key LINAC components to secondary radiation exposure.

Materials & Methods: A Monte Carlo model of the Varian 2100C LINAC head was developed, integrating a hybrid XCAT phantom to replicate patient anatomy. Key LINAC components and treatment room shielding were modelled. The MCNP code was used to simulate neutron and photon transport. A sensitivity analysis was performed by systematically excluding individual LINAC components to assess their influence.

Results: The analysis revealed that different LINAC components contribute variably to secondary radiation. The primary collimator and multi-leaf collimators were major sources of neutron and photon production, while treatment room shielding significantly influenced neutron dose distribution on both in-field and out-of-field organ doses.

Conclusion: This study provides a detailed evaluation of LINAC components' contributions to secondary radiation during 3D-CRT for prostate cancer. The findings can guide the optimization of LINAC design and treatment planning to reduce secondary radiation risks and improve patient safety.

References:

[1]. Alem-Bezoubiri, Asma, et al. "Monte Carlo study of organ doses and related risk for cancer in Algeria from scattered neutrons in prostate treatment involving 3D-CRT." *Applied Radiation and Isotopes* 180 (2022): 110065.doi: 10.1016/j.apradiso.2021.110065

[2]. Alem-Bezoubiri, Asma, et al. "Monte Carlo study of organ doses and related secondary cancer risk estimations for patients undergoing prostate radiotherapy: Algerian population-based study." *Applied Radiation and Isotopes* 216 (2025): 111595.doi: 10.1016/j.apradiso.2024.111595

Keywords: linac modeling, hybrid Phantom, secondary radiation, patient radiation protection.

T3-P16: Radioprotective and Radiosensitizer Properties of Silymarin/Silibinin in Response to Ionizing Radiation

F. Arghidash

Department of Medical Biotechnology and Nanotechnology, Faculty of Medicine, Mashhad University of Medical Sciences, Mashhad, Iran
Shabnamarghidash7666@gmail.com

Background/Purpose: The main complications of radiotherapy include toxicity to normal cells and radioresistance. To address these issues, it is beneficial to combine medicinal plants with conventional treatments. Silymarin and its active ingredient, silibinin, have been used in traditional medicine for a long time. The purpose of this review is to investigate the radioprotective and radiosensitizing effects of silymarin/silibinin in cancer.

Materials & Methods: The present study was conducted based on the results of two recent systematic reviews in 2023 and 2024 [1, 2].

Results: During cancer radiotherapy, healthy cells may be damaged by oxidative stress, apoptosis, inflammation, and other processes. The combination of silymarin/silibinin and irradiation decreased the toxicities caused by ionizing radiation because of their antioxidant, anti-apoptotic, and anti-inflammatory properties. On the other hand, silymarin/silibinin sensitizes cancer cells to ionizing radiation and significantly enhances treatment. The synergy between them increases the activation of free radical generation, DNA damage, and apoptosis, preventing angiogenesis and metastasis. However, the radioprotective and radiosensitizer effects of this bioactive ingredient may be important in treating cancer and radiotherapy for different types of cancer; it is necessary to carry out more extensive studies in this field.

Conclusion: The studies conducted thus far have differed in radiation dose, silymarin/silibinin dose, incubation duration, and dosing schedule. As a result, the impact of silymarin/silibinin differs among different cancer cell types.

References:

1. Latacela, G.A., et al., The radioprotective potentials of silymarin/silibinin against radiotherapy- induced toxicities: A systematic review of clinical and experimental studies. Current Medicinal Chemistry, 2023. **30**(33): p. 3775-3797.
2. Gupta, J., et al., The Radiosensitizing Potentials of Silymarin/Silibinin in Cancer: A Systematic Review. Current Medicinal Chemistry, 2024. **31**(42): p. 6992-7014.

Keywords: **Silymarin; Silibinin; Cancer; Radioprotective; Radiosensitizer**

T3-P17: Assessment of a new technetium radiopharmaceutical (^{99m}Tc-NPMIDA) intended for diagnosis in nuclear medicine

S. Achour, R. Khelili, A. Kiared, R. Nouri

Draria Nuclear Research Center, B.P.43, 16003, Sebala- El Achour-Draria, Algiers, Algeria
**Corresponding author: S-ACHOUR@crnd.dz*

Background/Purpose: Technetium-99m is the most widely used radioisotope in nuclear medicine diagnostics. Radiopharmaceutical products labeled with Technetium are constantly evolving, and presented to nuclear medicine departments under the name of radiopharmaceutical drugs.
The present work aims to assess a new Technetium radiopharmaceutical, which was prepared and studied using a commercial powder molecule N-(Phosphonometyl)-Iminodiacetic acid (NPMIDA), and then radiolabeled with 99mTc. Quality control and the pharmacokinetic evaluation of the (99mTc-NPMIDA) radioligand were carried out.

Materials &Methods: The pharmaceutical molecule NPMIDA was analyzed by infrared spectroscopy (IR) using (Perkin Elmer FTIR Spectrometer SpectrumTwo), Ultra violet spectroscopy (UV-visible) using (T 90 +UV/VIS Spectrometer PG Instruments Ltd) and the melting point was identified using a Wangner and Munz Heizbark System Kofler type WME instrument, indicating temperature values < 260°C. The solutions in the kit were prepared and adjusted to a pH between 6 and 7 using a pH meter from HANNA instrument 211model, and then stored in the refrigerator at 8°C. The labeling of the NPMIDA kit was conducted with 99mTc eluted from the (99Mo/99 mTc) generator in the form of sodium perdechnetate (99m TcO4--Na+); reduced using the Sn2+ ion as a reducing agent in the form of stannous chloride dihydrate (SnCl2.2H2O). Quality control of the prepared technetium radioligand (99mTc-NPMIDA) was performed by measuring its radiochemical purity (RCP) using an ISOMED 1010 dose calibrator. The biodistribution of the radiomarked complex was carried out using the Perkin Elmer type 2470 gamma counter.

Results: The labeling of the precursor N (Phosphonomethyl) iminodiacetic acid with 99mTc was successfully carried out. The radiochemical purity of the produced radiopharmaceutical drug is estimated at a percentage of 95.74%. The biodistribution study shows that the prepared radioligand (99mTc-NPMIDA) was bound to the organs: bladder, muscle and bone according to the detected activity measured in percentage of 28.19, 24.5 and 16.58% respectively. These results show that the complex was able to bind to the bone as a target organ; according to the phosphorylated and acetic functional groups in the structure of the NPMIDA molecule.

Conclusions: In this work, a new technetium radiopharmaceutical was evaluated and produced with high radiochemical purity, by a ligand exchange reaction between N-(phosphonomethyl) iminodiacetic acid, NPMIDA and pertechnetate ions. Biodistribution of this product in mice was successfully achieved on bone as a target organ. Although the fixation rate is low, these results remain encouraging, which leads us to continue our research.

Keywords: **Radiopharmaceutical, Technetium-99m, Diagnosis, Technetium kit, PRC, Biodistribution, NPMIDA.**

T3-P18: Preparation, characterisation and calibration of two fundamental reagents for the immunoradiometric (IRMA-125I) TSH assay.

N. Hamdi[@], D. Asselah, R. Nouri, S.A. Megatli

[1] *Department of Nuclear Applications, Nuclear Research Center of Draria, B.P.43 Sebala-Draria; Algeria.*
[@] *Corresponding author: n-hamdi@crnd.dz*

Background/Purpose: Thyroid-stimulating hormone (TSH) is a glycoprotein hormone of pituitary origin whose primary function is the synthesis and release of thyroid hormones. The slightest disruption of this hormone could indicate a thyroid disorder. Therefore, the measurement of its levels represents the initial step in biological diagnosis [1].As part of the application of radioisotopes in medicine and biology, we plan to develop a radioimmunometric assay (IRMA) kit for human TSH to aid in the diagnosis of thyroid disorders. This project involves preparing key reagents for TSH IRMA assays and developing an in-house IRMA system. Specifically, it includes the preparation of standards, which must be calibrated prior to use in the IRMA kit, as well as the production of a monoclonal antibody (MAb) tracer labeled with **^{125}I** and purified to obtain a highly pure tracer.

Materials &Methods: Anti-TSH monoclonal antibodies (Mab) and pure TSH were procured from a commercial source. Radioiodination of anti TSH-Mab (detection) with ^{125}I was carried out according to the method of Greenwood & Hunter [2] using chloramine-T. The labelled MAb was purified by gel chromatography over a column.Estimates were made of the tracer's radioisotope yield, radiochemical purity (RCP) and immunoreactivity.TSH standards in a range of 0 to50 mIU/mL were prepared in fetal bovine serum and calibrated with the help of a commercial kit.

Results: The quality control parameters of the TSH tracer were found to be very satisfactory. The radiochemical purity of Na^{125}I shows high purity (99.46%) of the radioiodine and suitability for preparation of the tracer TSH-MAb. High labelling yields of ~97% was achieved. The adopted procedure allows to obtain tracer solutions with free 125 Iodide content lower than 1%.The specific activity was of the order of 48.5 µCi/µg.It was demonstrated that the in-house tracer MAb exhibited good immunoreactivity and low non- specific binding.This finding indicates that the radiolabelling parameters are suitable and do not induce degradation of the anti-TSH MAb molecule. R^2 and slope values for the commercial and in-house standards are found to be extremely close indicating that both provide nearly identical linearity and sensitivity. The differences are minimal and are unlikely to affect the overall reliability of the assay.

Conclusion: An anti-TSH MAb from a commercial source can be readily radioiodinated to obtain a tracer. In-house standards can be used as an alternative to commercial standards, provided that other parameters (e.g. reproducibility, detection limits) are also validated.

References:

[1]. J-L.Wemeau. Les maladies de la thyroïde, Elsevier Masson, Issy –les-Moulineaux, 2010

[2]. Greenwood,F.C.,W.M.Hunter ,and J.S.Glover. The preparation of^{131}I-labelled human growth hormone of high specific radioactivity. *Biochem J.*1963, 89(1);114-123. doi: 10.1042/bj0890114

Keywords: Immunoradiometric assay, radioiodination,^{125}I-TSH-Mab,In house standards, comparaison test.

T3-P19: Hippocampal Preservation: A Major Challenge for Physicists in Pediatric Brain Tumor Radiotherapy.

R. Amimour[a@], L. Naoun[b], B. Bacha[c]

[a] houari boumediene university of science and technology
[b]clcc annaba radiotherapy service
[c]clcc annaba radiotherapy service
[@]Corresponding author roumaissaamimour01@gmail.com

Background/Purpose: In children, hippocampal irradiation during brain tumor radiotherapy can lead to severe neurocognitive deficits. Therefore, preserving this structure is crucial. This study evaluates and compares hippocampal preservation achieved with *IMRT* and *VMAT* techniques, using a mix of coplanar and non-coplanar beams, to optimize pediatric treatment plans.

Materials & Methods: Fifteen pediatric patients with brain tumors were included. For each patient, adequate delineation of the hippocampus using *MRI* images was performed; two treatment plans were generated: *IMRT* and *VMAT* (using treatment planning system Monaco), both using a mix of coplanar and non-coplanar beams. The doses received by the hippocampus, organs at risk, and target volumes were analyzed and compared. Hippocampus was defined both as a single and as pair organ. Constraints analysed were [1, 2]:

$$D_{max} < 16 \text{ Gy}, \quad D_{40\%} < 7.3 \text{ Gy}.$$

Results: VMAT plans demonstrated significantly superior hippocampal preservation compared to IMRT plans, with a notable reduction in mean dose and maximum dose to this organ. The use of a mix of coplanar and non-coplanar beams contributed to an overall reduction in hippocampal dose, while maintaining better optimization in both techniques.

Conclusion: *VMAT,* using a mix of coplanar and non-coplanar beams, represents an effective planning strategy to minimize hippocampal dose in pediatric radiotherapy. Medical physicists play a key role in optimizing these techniques to reduce the risk of long-term neurocognitive deficits. Prospective clinical studies are needed to confirm these results and evaluate the impact on patients quality of life.

References:

[1]. A. Lapriea, L. Padovanic, V. Bernier, S. Supiote, A. Huchetg, A. Ducassoua, L. Claudeh: Radiotherapy for paediatric cancers https://doi.org/10.1016/j.canrad.2016.07.021

[2]. C. Di Carlo , M. Trignani , L. Caravatta , A. Vinciguerra , A. Augurio , F. Perrotti , M. Di Tommaso, M. Nuzzo , S. Giancaterino , M.D. Falco , D. Genovesi: Hippocampal sparing in stereotactic radiotherapy for brain metastases∗ Department of Radiation Oncology, "G. D'Annunzio" University of Chieti, SS. Annunziata Hospital, Via Dei Vestini, 66100 Chieti, Italy. https://doi.org/10.1016/j.canrad.2017.08.113

Keywords: Hippocampus, IMRT, VMAT, Coplanar and Non-Coplanar Beams, Brain Tumors

T3-P20: Heavy Metal Contamination in Herbal Medicines: Determination by ICP-OES

Z. Lamari[a@]H. Negache[b], M. Arabi[c],R. Cheriguene[b], L. Guerda[b], A. Ouafek[b]

[a]*NUR Reactor Division/Reactor Technical Management Department ; Nuclear Research Center of Draria BP n°43, Sébala, Draria, Algiers, Algeria*

[b]*Radiobiology and Ionising Radiation DosimetryDivision ; Department of Radiobiology and Life Sciences; Nuclear Research Center of Algiers. 2 Bd Frantz-Fanon BP-399 Algiers-Gare, Algéria.*

[c]*Nuclear Techniques Application Development Division,Nuclear Research Center of Algiers.*

[@]*Corresponding author z.lamari@crnd.dz*

Background/Purpose: Under the National Cancer Plan 2015-2019, projectP4/DRD/CRNA/2022/4, we investigated a mixture of *Saussurea lappa* root and *Rosmarinus officinalis*.L leaves. While medicinal herbs are widely recognized for their therapeutic properties by organizations like the FAO and WHO, it is important to consider that the preparation methods, environmental factors, and contamination risks can significantly impact their safety and effectiveness. To advance our research on the radio- protective effects of *Saussurea lappa* and *Rosmarinus officinalis.*L, we focused on assessing contaminants such as cadmium (Cd) and lead (Pb), along with other potentially toxic elements like copper (Cu), iron (Fe), cobalt (Co), and selenium (Se) using Inductively Coupled Plasma Optical Emission Spectrometry (ICP-OES) analysis to ensure a comprehensive health risk evaluation.

Materials &Methods: A 2-gram sample of plant powder was placed in a 250 mL Erlenmeyer flask, to which 28 mL of concentrated HNO_3 was added and thoroughly mixed. The mixture was then heated between 50 and 150°C for 2 hours, after which 4 mL of concentrated H_2O_2 was added dropwise. After cooling, the solution was filtered using Whatman No. 41 filter paper and syringe filter (0.45 µm) then, diluted with demineralized water in a 50 mL volumetric flask. The digested samples were subsequently analyzed by ICP- OES, measuring the emission of characteristic wavelengths to determine the concentration of each element in the samples.

Results: The concentrations of Cu and Fe were 4.72 and 3.84 ppm and 11.51 and 5.04 ppm in *Saussurea lappa* roots and *Rosmarinus officinalis* leaves, respectively. Pb, Cd and Se were not detected in either herb, while Co was only detected in rosemary at 0.1 ppm. The ICP-OES method was validated for each element (linearity, R^2, LoD, LoQ). The measured exposure levels were below the regulatory limits set by FAO/WHO and the European Pharmacopoeia.

Conclusion: Our analysis shows that the herbs studied are free from these contaminants, ensuring their safety for use.

References:

[1] Luo, L., Wang, B., Jiang, J., Huang, Q., Yu, Z., Li, H., et al. (2020). Heavy metal contaminations in herbal medicines: determination. Comprehensive risk assessments. Front. Pharmacol. 11, 595335. doi:10.3389/fphar.2020.595335

Keywords: **medicinal herbs, Heavy metals, ICP-OES, radio protective Effect.**

T3-P21: Radiation protection in radiotherapy: current status and challenges

H. Graine [1@], B. Makoudi[2], M. Alliti [2] M. Sadaoui [2]

[1] *Division Sûreté Nucléaire et Radioprotection DSNR/CRNB/COMENA*
[2] *Département Radioprotection Opérationelle, (DSNR/CRNB/COMENA)*

[@] *Corresponding author h.graine@crnb.dz*

Background/Purpose: Radiotherapy is a key method in the treatment of many cancers, using ionizing radiation to target and destroy cancer cells. However, the use of this radiation poses risks to patients, medical staff, and the environment, making radiation protection crucial. For this purpose the radiation protection is essential in medicine to minimise the risks associated with medical procedures using radiation. Medical examinations using ionizing radiation present health risks. Radiation protection in medicine requires a multidisciplinary approach to minimize risks and optimize benefits. Training, awareness and application of fundamental principles are essential to protect patients and medical personnel.

Materials & Methods: This article presents in first part the fundamental principles and recommended practices to protect patients and medical personnel. And the description of the protection measures to ensure effective protection during radiotherapy treatments, Monitoring of doses (dosimeters, detectors). The last part is the role of medical personnel and training

Results:

- Medical personnel must be regularly trained in good radiation protection practices.
- A rigorous risk assessment must be carried out before each treatment.
- Radiation doses should be optimised to minimize secondary effects
- Radiation protection standards must be respected und updated regularly.

Conclusion: Radiation protection is an essential element of radiotherapy, ensuring the safety of patients and medical staff. Technological progress and international recommendations have made it possible to improve radiation protection practices. However, it is crucial to continue efforts to minimize the risks associated with ionizing radiation.
Continuing research in the field of radiation protection will enable the development of safer and more effective technologies. The adoption of new methods, will provide improved therapeutic possibilities while reducing risks.

References:

[1] IAEA Safety Standards Radiation «Protection and Safety in Medical Uses of Ionizing Radiation». Specific Safety Guide No. SSG-46

[2] «National Networks for Radiotherapy Dosimetry Audits» IAEA HUMAN HEALTH REPORTS No. 18

[3] PAG Manual: Protective Action Guides and Planning Guidance for Radiological Incidents, EPA-400/R-17/001 | January 2017

Keywords: Radiation protection; Radiation monitoring; Safety protocols; Justification.

T3-P22: Investigating γH2AX as biomarker of DNA damage in blood samples and cell lines following exposure to γ rays.

S. Gais[a@], A. Biout[a], F. Yakoubi[a], Y. Boubekeur[a], S. Allali[a], K. Aouragh[a], B. Mansouri[a], M. Souidi[b], F. Fazouane[c.], A. Djefal[d]

[a] *Nuclear Research Center of Algiers, 02 Bd F. PO Box-399 Algiers-RP, 16000, Algeria.*
[b] Autorité de Sûreté Nucléaire et de Radioprotection (ASNR), France.
[C] *Faculté des Sciences Biologiques, Université M'hamed Bougara, Boumerdès, Algeria.*
[d]*Retired from Nuclear Research Center of Algiers @Corresponding author s.gais@crna.dz*

Background/Purpose: Radiotherapy is the most commonly used treatment after surgery against cancer. Individual response to ionizing radiation is essential data for effective radiotherapy treatment against the tumor while preserving healthy tissues.

Many studies have been conducted to propose predictive tests of radiosensitivity, based on the cellular response to radiation *in vitro*, including DNA damage. One of the earliest responses following irradiation is the phosphorylation of thousands of histone H2AX variant molecules at the sites of DNA double-strand breaks (DSBs) to form γH2AX. This could serve as a predictive biomarker for radiation-induced damage and radiosensitivity.

The objective of this work is the development of a γH2AX test and its application *in vitro* and *in vivo*.

Materials & Methods: The study was conducted on two cellular models: peripheral blood mononuclear cells (PBMCs) from healthy volunteers and human epidermoid laryngeal carcinoma cells (HEp-2) exposed to different doses of gamma radiation (1 to 6 Gy) from a Cobalt 60 source. After immunostaining, the foci are visualized after irradiation by fluorescence microscopy at 30 minutes, 2 hours, 5 hours, and 24 hours [1, 2].

Results: A significant increase in γH2AX levels was detected across all γ-ray doses 30 minutes post-irradiation. The percentages of foci observed were as follows: 32.5%, 43.3%, 60%, 71%, 71.5%, and 100% for PBMC cells at doses of 1, 2, 3, 4, 5, and 6 Gy, respectively,
and 33.61%, 52.53%, 61%, 64%, 72.6%, and 80.92% for the HEp-2 cell line under the same conditions. A peak γH2AX response occurred within 30 minutes post-irradiation, followed by a decline in foci numbers after 24 hours. The formation and disappearance rates of γH2AX induced by ionizing radiation were dose-dependent.

Conclusion: The quantification of γ-H2AX foci by fluorescence microscopy is a sensitive, reliable, and practical method for measuring radiation-induced DNA damage.γH2AX constitutes a potential biomarker for the prediction of individual radiosensitivity for clinical studies in external or internal radiotherapy.

References:

[1]. Popp H.D., Brendel S., Hofmann W.K., Fabarius A., 2017. Immunofluorescence Microscopy of γH2AX and 53BP1 for Analyzing the Formation and Repair of DNA Double-strand Breaks. [1]. *J Vis Exp*. 3;(129):56617. doi: 10.3791/56617.

[2]. Valente D., Gentileschi M.P., Guerrisi A., Bruzzaniti V., Morrone A., Soddu S., Verdina A., 2022. Factors to Consider for the Correct Use of γH2AX in the Evaluation of DNA Double- Strand Breaks Damage Caused by Ionizing Radiation. *Cancers*. 15;14(24):6204. doi: 10.3390/cancers14246204.

Keywords: **γH2AX, DNA double-strand breaks, Fluorescence microscopy.**

T3-P23: Radiation Safety in Nuclear Medicine: Addressing Gender- Specific Challenges for Female Workers and Patients at Medical Facilities

L. Ong'ayo

Kenyatta University Teaching Research and Referral Hospital
@ Corresponding author lonah.moraa@kutrrh.go.ke

Background/Purpose: Radiation safety in nuclear medicine is crucial, particularly for female workers and patients who face unique risks due to biological and occupational factors. This study explores gender-specific radiation safety challenges at Kenyatta University Teaching, Referral & Research Hospital (KUTRRH), emphasizing radiation sensitivity, reproductive health concerns, and the necessity for gender-inclusive safety protocols. The objective is to ensure the protection and well-being of women in nuclear medicine.

Materials & Methods: A comprehensive review of current radiation safety protocols at KUTRRH was conducted, alongside an analysis of international guidelines from the International Atomic Energy Agency (IAEA) and the World Health Organization (WHO). Occupational exposure data were assessed, and strategies for minimizing radiation risks, including personal protective equipment (PPE) use, flexible work policies, and patient education initiatives, were also examined [1,2].

Results: Findings indicate that radiation exposure poses significant risks to female reproductive health. For women of childbearing age, exposure to ionizing radiation can affect fertility and increase the risk of birth defects in future pregnancies. Pregnant women require special considerations, as radiation can harm the developing fetus. Over 55% of nuclear medicine staff at KUTRRH are women, requiring tailored policies, including flexible work schedules and counseling programs. Effective patient communication strategies, including educational materials and radiation warning signage, were also found to be essential in minimizing risks for female patients.

Conclusion: Gender-inclusive radiation safety measures are critical in nuclear medicine. Institutions must implement policies addressing the unique risks faced by female workers and patients, ensuring a safer working environment through continuous monitoring, education, and regulatory compliance. International collaboration is essential to develop standardized guidelines that reflect best practices in gender-specific radiation safety.

References:

[1]. IAEA Safety Standards Series No. GSR Part 3. Radiation Protection and Safety of Radiation Sources: International Basic Safety Standards. Published: 2014

[2]. World Health Organization (WHO), Radiation Safety in Medical Applications, WHO, Geneva, Switzerland (2020).

Keywords: Radiation safety; nuclear medicine; gender-specific risks; occupational exposure; reproductive health.

T3-P24: Radiological Justification Criteria of Pediatric Computed Tomography in Kenya

L. Ong'ayo

Kenyatta University Teaching Research and Referral Hospital
@ Corresponding author lonah.moraa@kutrrh.go.ke

Background/Purpose: Computed Tomography (CT) has been acknowledged as the most widely used imaging modality in both adults and children. However, CT contributes to a high radiation dose posing relatively high risks of stochastic effects to patients. Stochastic risks are of special concern in pediatric imaging since children are more vulnerable to effects of ionizing radiation than adults. Justification of pediatric CT examinations is of paramount importance. The main objective of this study was to evaluate the current radiological justification for pediatric CT in Kenya and propose strategies to enhance justification. The specific objectives were to investigate the current radiological justification process for pediatric CT in Kenya and evaluate Kenyan referring medical practitioners' knowledge and attitude regarding pediatric Computed Tomography (CT) referral guidelines.

Materials & Methods: Questionnaires were designed to assess the understanding of Kenyan referring medical practitioners regarding radiation risks to pediatrics and usefulness of referral guidelines. International guidelines of ICRP and IAEA, and individual publications on pediatric CT justification applicable to the country were reviewed. The foundation of the review mainly focused on the 3 A's: awareness, appropriateness, and audits as remedies to serious problems with justification. Analysis of the survey data consisted of descriptive procedures and bivariate comparisons [1,2].

Results: This study has pioneered in evaluating the current radiological justification for pediatric CT in Kenya, identifying guidelines on pediatric CT justification applicable to Kenyan hospitals and carrying out a survey to assess the level of awareness of Kenyan referrers. The review findings generally indicated that the current radiological justification process is inadequate and thus, requires overhaul. In addition, survey results indicated referrers had low awareness regarding pediatric CT referral guidelines and possible radiation risks from medical exposures.

Conclusion: Therefore, the 3A's (Awareness, Appropriateness and Audit) highlighted by IAEA are important solution to facilitate and enhance justification in the country. In addition, different levels of training for all referring medical practitioners in matters concerning justification should be conducted to improve their awareness.

References:

[1]. International Commission on Radiological Protection. The 2007 recommendations of the International Commission on Radiological Protection. ICRP Publication 103. Oxford: Elsevier, 2007.

[2]. IAEA Safety Standards Series No. GSR Part 3. Radiation Protection and Safety of Radiation Sources: International Basic Safety Standards. Published: 2014

Keywords: Computed Tomography; Justification; Pediatrics; Stochastic;

T3-P25: Radiation Doses and Size-Specific Dose Estimate from Pediatric Head CT Examinations

A. Merad [1@], S E. Marouk[2], N. Toutaoui[3], F. Meddad[1], R. Ait Challal[4]

[1] *Algiers Nuclear Research Center*
[2] *USTHB*
[3]Atomic Energy Commission
[4] Bab-El-Oued University Hospitals
[@] *Corresponding author* a.merad@crna.dz

Background/Purpose: Current CT dose descriptors, volume CT dose index (CTDI$_{vvvvvv}$) and dose length product (DLP) are based on a standard size homogeneous phantom only. Hence, these parameters fail to reflect the dose variation due to variable body sizes of the patient.
To resolve this issue, the American Association of Physicists in Medicine (AAPM) introduced a new dose indicator, Size-Specific Dose Estimate (SSDE), taking into account both X-ray output and patient size [1].
The objective of this study is to examine pediatric CT practices within the Medical Imaging Department of Bab-El-Oued University Hospital. This investigation aims to determine the frequency of pediatric CT examinations, evaluate and compare radiation doses for various CT procedures, and propose typical paediatric CT dos based on the Size-Specific Dose Estimate (SSDE).

Materials & Methods: A total of 1016 paediatric (0–15 years) CT examinations of head region performed during six months in university hospital of bab-El-Oued were included. The patients were categorised into four age groups of 0–1), 1–5, 5–10 and 10–15 years Dose indices (CTDI$_{Vol}$ and PDL) and examination parameters (kV, mAs, lateral (LAT) and anteroposterior (AP) dimensions were collected. The anteroposterior diameter (D$_{AAP}$), lateral diameter (D$_{LAT}$), a combination of AP and LAT diameters (D$_{AAAA\ +LLAALL}$), and effective diameter (D*ee*ff) methods were introduced for SSDE calculations. The median of doses distributions was given as typical dose.

Results: The number of pediatric patients represents 9% Typical dose based on CTDI$_{Vol}$ is 40.63 mGy for all age categories,
Typical doses ranges (depending on the dimension used for its calculation) based on SSDE are 37.62–48.77 mGy for 0-1y; 33,95-47,08 mGyr for 1-5y ; 32,53-46,41 mGy for 5-10 y and 31,65-45,9641 mGy for10-15 y ac on the dimension used for its calculation. .
The (SSDE) increases as the patient's age decreases.
- The SSDE calculated according to ***AP*** dimension underestimates CTDI$_{Vol}$.
- The SSDE calculated according to **LAT** dimension is higher than CTDI$_{Vol}$. By 20% for patients aged 0 to 1 year 13% for patients aged 10 to 15 years.
- The SSDE calculated with (AP+LAT) and (AP*LAT) dimension measurements are similar to each other. They are greater than CTDIVol by 11% for new-borns (0-1 year).

Conclusion: The Size-Specific Dose Estimate (SSDE) varies with age (patient body size) and this variation from CTDIvol is different depending on the dimension used for its calculation.

References:

[1]. Boone, J. M., Strauss, K. J., Cody, D. D., McCollough, C. H., McNitt-Gray, M. F., & Toth, T. L. (2011). Size-Specific Dose Estimates In Pediatric and Adult Body CT Examinations: Report No. 204. American Association of Physicists in Medicine,

T3-P26: In vitro cytotoxic activity and radioprotective effect of formulation on monkey kidney epithelial cells (Vero line)

H. Negache[a], A. Ouafek[a] R. Cheriguene[a@], L. Guerda[a], Z. Lamari[b]

[a]*Department of Radiobiology and Life Sciences; Radiobiology and Ionising Radiation Dosimetry Division; Algiers Nuclear Research Center,2, Bd Frantz-Fanon BP-399 Alger-RP, 16000, Algiers, Algeria.*
[b]*Reactor, /Nuclear Research Center of Draria, Bp 43, Sebala Draria 16000, Algeria*
[@]*r.cheriguene@crna.dz*

Background/Purpose: Radiation is an important component of therapy for a wide range of malignant conditions. However, it triggers DNA damage and cell death in normal cells and results in adverse side-effects [1]**.** *Rosemarinus officinalis*.L and *saussurea lappa*, which contain phenolic compounds, are known to be antioxidant plants capable of scavenging free radicals in the biological environment; the formulation derived from the crude extracts of these two plants is therefore expected to have a radioprotective effect to protect patients undergoing radiotherapy. The aim of the present study was to evaluate the cytotoxic effect and radioprotective potential of three formulations (F1, F2, and F3) as natural compounds against radiation-induced changes in Vero cell proliferation.

Materials & Methods: In this experimental study, the toxicity of the formulations were assessed by the 3-(4, 5-dimethylthiazolyl-2)-2, 5-diphenyltetrazolium bromide (MTT) assay.Vero cells were treated with formulations (F1, F2, F3), 1 h before exposure to gamma rays in the exponential phase using a radioactive source of Cobalt 60 at dose 2 Gy and survival enhancement factors of cells were analyzed by MTT [2].

Results: The results showed variability in viability rates according to the different formulations used and the incubation time. After 24h formulations did not exhibit cytotoxic activity against Vero cell line, with viability rates of 108.69%, 95.08% and 94.51% respectively. After 48 hours, the three formulations exerted a toxic effect, reducing the viability rate to 50.13%; 43.69% and 44.50% respectively. Irradiation of cells in the presence of formulations caused a significant increase in cell survival compared with the control, in particular for formulation F2 with survival rates of 115.07% and 103.97% compared with F1 (91.79% - 82.10%) and F3 (101.33% - 78.72%) after 24 h and 48 h of incubation.

Conclusion: Our preliminary results suggest that the Formulation F2 as a natural and non-toxic compound could show favorable radioprotective effects in such a way that significantly increases the survival rate of Vero cells. This emphasizes the need to continue these studies in the near future, exploring different radiation doses and employing other cell lines. In the long run, we aim to implement this approach in preclinical in vivo models.

References:

[1] P. Uma Devi and Paban K Agrawala: Normal Tissue Protectors Against Radiation Injury. Defence Science Journal, Vol. 61, No. 2, March 2011, pp. 105-112

[2] Mosmann, T. (1983). Rapid colorimetric assay for cellular growth and survival: Application to proliferation and cytotoxicity assays. J. Immun. Methods., 65:55–63

Keywords: radiation therapy, toxicity, radioprotector, medicinal plants, cancer

T3-P27: Radiological control tests on the efficiency of the manual Tc- 99m production cell

A. Benbetka@, I. Benzian, R. Abaidia

Centre de Recherche Nucléaire de Draria
@ a-benbetka@crnd.dz

Background/Purpose: The laboratories producing Tc-99m, used in medical imaging, from MoO3 irradiated as powder, present potential risks of radioactive contamination. In order to ensure the radiological safety of personnel, premises and environment, it is imperative to check the tightness of production cells to prevent any dispersion of contaminants.

Materials &Methods: The leak-tightness assessment of a manual production cell included the monitoring of radiological exposure levels, surface contamination tests conducted at various strategic points within the cell, as well as air sampling carried out after the rupture of a 5 g target of irradiated MoO3 powder introduced into the cell. Finally, spectrometric analysis of the filters was performed to identify potential contamination by Mo-99 and Tc-99m.

Results: The external exposure levels measured were below the regulatory limits and the scan tests did not reveal any contamination. Air sampling was conducted after the quartz ampoule containing the irradiated MoO3 powder was broken and before phase separation. In the case of contamination, we should expect a spectrum indicating the presence of Mo-99, Tc-99m, and any impurities in the powder.
In a gamma spectrum, the peak at 140 keV (characteristic of Tc-99m and Mo-99) with an activity of 4.6 Bq was observed, but the absence of other peaks associated with Mo-99 can be explained by low Mo-99 activity, or by the absence of a calibration or control spectrum, which prevents background interference from being subtracted.

Conclusion: To validate the results obtained and confirm the compliance of this cell, it is recommended to: Repeat the assessment of air contamination using two filters and Perform spectrometric analyses on both samples under identical conditions. Finaly, ensure that the filter specifications are available to allow accurate calculation of the volumetric activity.

References:

[1]. Huguesi B., Practical radiation protection for industry and research, ISBN 978-86883-951- 0 2009.

Keywords: Safety,cell,contamination,TC-99m,Mo-99.

T3-P28: Crude leaves Rosemary Extract from Algeria: Radioprotection Conferred to DNA of Vero Cells

H. Negache[a@], Z.Lamari[b], R.Cheriguene[a], L. Guerda[a], M.Ousmaall[c]

[a]*Radiobiology and Ionising Radiation Dosimetry Division ; Department of Radiobiology and Life Sciences; Nuclear Research Center of Algiers. 2 Bd Frantz-Fanon BP-399 Algiers-Gare, Algéria.*

[b]*NUR Reactor Division/Reactor Technical Management Department ; Nuclear Research Center of Draria BP n°43, Sébala, Draria, Algiers, Algeria*

[c]*Department of nature and life sciences, University of Algiers, Benyoucef Benkhedda, Algeria.*

[@] *Corresponding author h.negache@crna.dz*

Background/Purpose: Radiotherapy is the most common modality of cancer treatment; however, this clinical therapeutic option is limited because normal cells are also unavoidable targets of gamma radiation. This makes the protection of normal healthy tissues challenging. Rosemary plant, with phenolic compounds, is known as an antioxidant herb and able to scavenge free radical agents in the biological environment [1].The purpose of the present study is to evaluate the radioprotective effect of crude rosemary extract (CRE) as natural compound against radiation induced DNA double-strand breaks damage (DSBs) on Vero cells.

Materials & Methods: cytotoxicity of CRE was assessed by 3-(4,5-dimethylthiazolyl-2)- 2,5-diphenyltetrazolium bromide (MTT). Vero cells were pretreated with CRE, 1-hour before exposure to ɣ-ray (2Gy) using radioactive source of Cobalt 60 and survival enhancement of cells was analyzed by MTT. The non-toxic concentration of 1mg/ml of CRE was chosen to assess its activity on the induction of apoptosis by the biomarkers annexin and propidium iodide (PI), analysed by flow cytometry. The immunofluorescence technique was used to detect DNA damage, by observing γ-H2AX bound to double-strand breaks (DSBs) [2].

Results: cytotoxic activity of CRE was dose-dependent, with an IC50 of 13.42 mg/ml. Relative cell viability, remained statistically constant ($p > 0,05$) revealing the inocuity of the CRE during 24 and 48 h of incubation. Maximum protection against radiation-induced damage was observed at 1 mg/ml of CRE, showing 92% relative cell survival. CRE significantly reduced the frequency of γ-foci. An important reduction in apoptosis to 6.4% under the influence of CRE, compared to 81.1% in the negative control.

Conclusion: These positive results observed in all the tests carried out indicate that CRE could offer a promising therapeutic prospect as a radioprotectant, and underline the importance of continuing these studies in the short term, varying the radiation dose and using other cell lines. In the longer term, we plan to apply this strategy in preclinical in vivo models.

References:

[1]. Parisa Zhaeintan , Abolfazl Nickfarjam , Ali Shams ,Sepideh Abdollahi-Dehkordi , Nima Hamzian: Radioprotective Effect of Rosmarinus officinalis L (Rosemary) Essential Oil on Apoptosis, Necrosis and Mitotic Death of Human Peripheral Lymphocytes (PBMCs). J Biomed Phys Eng 2022; 12(3).

[2]. Alazhar Colombowala , Aruna K: Phosphorylated H2AX: Prospective Role in DNA Damage Responses and a Credible Tool for Translational Cancer Research. J Appl Biotechnol Rep. 2022 March;9(1):464-476. doi 10.30491/JABR.2021.255221.1307.

Keywords: radioprotector, Rosemary extract, radiothérapie, γH2AX, apoptosis

T3-P29: Assessment of Leakage Radiation and Radiobiological Impacts in Gamma Knife Radiosurgery: Dosimetric and Biological Analysis

B.N. Mohammeda[1@], A.H. Ismail[2], E.M. Tahir[3];

[1] *Physics Department, Science College, Salahaddin University-Erbil, 44002, Erbil, IRAQ* [2]*Physics Department, Education College, Salahaddin University-Erbil, 44001, Erbil, IRAQ* [3]*Erbil Polytechnic University, 44001, Erbil, IRAQ*
[@]*Corresponding authors* bazhdar.sh.mouammed@su.edu.krd

Background/Purpose: Gamma Knife RadioSurgery (GKRS) is a stereotactic device that delivers high-dose cobalt-60 radiation to treat brain lesions. The radiation dose is determined by the type, size, and depth of the lesion. While the treatment is highly targeted, some radiation scatter, potentially affecting surrounding brain tissue or nearby organs. The purpose of this study is to measure the leakage radiation produced in the collimators of the Gamma Knife (GKRS) during radiosurgery and to calculate the effective dose impact on various radiosensitive organs. Additionally, the radiobiological impact on patients' biochemical parameters is investigated for both short-term and long-term treatment exposure.

Materials & Methods: Scatter radiation was measured using dosimeters placed at various body regions. Blood samples were collected from 30 patients, divided into two groups: one receiving a low dose and the other a high dose. Samples were taken at three time points: before treatment, after treatment, and approximately three weeks post-treatment. The changes in parameters were analyzed using one-way ANOVA to evaluate significant differences across the time intervals for each group.

Results: The highest scatter radiation levels were recorded at the face and neck, exceeding other regions, with effective dose calculations showing high exposure in these areas. Long- term exposure 58.2 min at 80 Gy led to significantly greater blood changes ($p \leq 0.05$) compared to short-term exposure 19.4 min at 20 Gy. Significant differences were observed at blood sampling stages, indicating both immediate and delayed impacts of GKRS.

Conclusion: These findings highlight distinct blood parameter changes among patients receiving different radiation doses, emphasizing the complex biological responses to high- dose gamma radiation. The study reinforces the importance of adhering to ICRP safety recommendations to minimize potential secondary damage, particularly when using high doses for treatment.

Keywords: Gamma knife radiosurgery; Radiation dose; Patient Safety; Leakage radiation; Radiobiological impacts

T3-P30: Identification the Rabbits species via bone mass attenuation coefficient and Element trace concentration using XRF technique

R.D. Haider[1@], A.H. Ismail [2], Z.A. Hussein [3]

[1] *Department of Physics, Faculty of Science and Health, Koya University, Koya KOY45, Kurdistan Region - F.R. Iraq*
[2] *Physics Department, Education College, Salahaddin University-Erbil, Erbil, 44001, IRAQ*
[3] *Department of Physics, Faculty of Science and Health, Koya University, Koya KOY45, Kurdistan Region - F.R. Iraq*
[@] *Corresponding author rozhan.haider@su.edu.krd*

Background/Purpose: The animal species has been identified biologically through chromosome analysis. Here in this research, the Rabbit species were identified by radiological approach through two techniques: the mass attenuation coefficient (μm) of X-rays from rabbit bones, and measuring the element concentration in the bone samples of six species of rabbits using X-ray diffraction technology (XRF).

Materials & Methods: The rabbits (Six different species of rabbits) were kept in identical housing with the same ecological, healthy, and housing circumstances. The bone samples of the rabbits were dried and powdered. The mass densities of all the pressed samples were in the range of 0.842–0.239 g/cm3. The samples were exposed to 35KeV and 1mA of the X-ray source, and the X-ray fluorescence spectrometers (XRF) technique was used to detect and measure the element contents (ppm) in the bone samples.

Results: The mass attenuation coefficient (μm) of the rabbit's species bone was variable with the rabbit's species. This work is employed in XRF analysis to estimate the attenuation properties of the rabbit's bones and identify element contents. It was seen that the highest number of elements (18) was in the rabbits of English Angora, New Zealand, and Bourgogne. Followed by rabbits of English Spot (17) elements, Holland lop, and Netherland Dwarf had the lowest number of elements (16), respectively. Light elements could be found in all six rabbits' species from high to low concentration (Ca, P, Mg, S, K, Al, Cl) other elements differed among species. Elements of Ca, P, and Mg were found in the highest proportions. , so that four elements (As, Y, Mn, Ga) were present in three species of bone; however the heavy metals (Ta and Zr) are found. The heavy metal Sb could not be present in Holland lops rabbit's bones.

Conclusion: The study practically provided that can identify the rabbit species via evaluation mass absorption coefficient of X-rays for the bone samples of the different rabbit species, and via evaluation of the concentration of certain elements in the bone samples using the X-ray diffraction technique (XRF). This method is considered a new model for determining the rabbit's species instead of the biological method

References:

[1]. Angelone M et al.. Measurement of mass attenuation coefficients for four mixtures using X-rays from 13 keV up to 40 keV. Radiation Physics and Chemistry. 2001;61:547-548. doi:10.1016/S0969-806X(01)00328-0
[2]. Akar A et al.. Transfer R. Measurement of attenuation coefficients for bone, muscle, fat and water at 140, 364 and 662 keV γ-ray energies. Journal of Quantitative Spectroscopy and Radiative Transfer. 2006;102:203-211. doi:10.1016/j.jqsrt.2006.02.007

Keywords: mass attenuation coefficient; x-ray fluorescence analysis; bones; species

T3-P31: Stratification of Risk of Thyroid Cancer: A Machine Learning Model to Identify High-Risk Cases and Analyze the Link with Recurrence

F. Bouchelaghem [1@], B. Bouchelaghem [2], S. Neheoua [3] , A. Ghezal[4]

[1,3,4] *Physics Department, Science Faculty, Mohamed Boudiaf University, Msila, 28000, Algeria*
Team*: Multiscale simulation and materials modeling, Materials and renewable energy laboratory.*

[2]*Freelance consultant in software development and machine learning, Paris, France*
[@] *Corresponding author* fouzia.bouchelaghem@univ-msila.dz

Background/Purpose: Thyroid cancer, particularly in its recurrent forms, requires precise risk stratification for optimal patient management. This study focuses on applying several machine learning models to assess the risk of thyroid cancer across three categories: low, intermediate, and high.

Materials & Methods: The models tested include **logistic regression**, **decision tree**, **K-Nearest Neighbors (KNN)**, and **Random Forest**.

Results:

Model	Accuracy	Precision	Recall	F1-Score	High-Risk Prediction
Logistic Regression	92%	0.93	0.92	0.92	Excellent
Random Forest	91%	0.91	0.90	0.91	Very Good
Decision Tree	90%	0.89	0.85	0.87	Good
K-Nearest Neighbors (KNN)	86%	0.85	0.80	0.82	Fair

Conclusion : The results of this study demonstrate the effectiveness of machine learning models in predicting thyroid cancer risk, with a particular focus on high-risk patients who are more likely to experience recurrence. While the models tested varied in performance, they provide powerful tools for risk stratification. Integrating recurrence as an additional predictive factor could enable more personalized care, guiding early and targeted interventions for the most vulnerable patients.

References :

[1] Haugen, B. R., et al. (2016). 2015 American Thyroid Association Management Guidelines for Adult Patients with Thyroid Nodules and Differentiated Thyroid Cancer: The American Thyroid Association Guidelines Task Force on Thyroid Nodules and Differentiated Thyroid Cancer. Thyroid, 26(1), 1-133

[2] https://www.kaggle.com/kaggle/input/prdiction-du-risque-desmaladies-thyrodiennes/Thyroid_Diff.csv

Keywords: Cancer risk; Logistic regression; Machine learning in health.

T3-P32: Reducing Ring Artifact Noise in CT Imaging for Medical Diagnosis Using the Denoising Convolutional Neural Network (DnCNN)

F. Mokeddem

University Ibn Khaldun of Tiaret, Faculty of Material Sciences Physics department
fatima.mokeddem@univ-tiaret.dz

Background/Purpose: Ring artifacts are a common and critical issue in medical CT imaging, caused primarily by detector inconsistencies or miscalibrations. These artifacts can severely degrade the diagnostic quality of images and hinder accurate interpretation. This study focuses on reducing ring artifact noise using the Deep Learning-Based Denoising Convolutional Neural Network (DnCNN) model. The purpose of this research is to evaluate the efficiency of DnCNN in artifact removal while preserving image quality, thereby enhancing the reliability of CT imaging for medical diagnosis.

Materials & Methods: The proposed methodology utilized a publicly available dataset of simulated and real CT images affected by ring artifacts. Preprocessing included normalization and artifact simulation for consistent input to the DnCNN model. The DnCNN model, designed for Gaussian noise removal, was fine-tuned to detect and suppress ring artifacts specifically. The implementation framework was employed for training, testing, and deploying the model. Performance metrics, including Peak Signal-to-Noise Ratio (PSNR) and Structural Similarity Index Measure (SSIM), were employed to assess denoising efficiency. Comparative analysis was performed against traditional denoising methods such as median filtering and Fourier-based ring artifact correction[1,2].

Results: The results demonstrated a significant improvement in image quality with the DnCNN model. On average, the PSNR improved by 12 dB, and the SSIM increased by 0.25 compared to the original artifact-laden images. The DnCNN model outperformed traditional methods, particularly in preserving fine details and minimizing edge distortion. Visual inspection confirmed the reduction of ring artifacts with minimal loss of diagnostic information. Additionally, the proposed framework facilitated seamless implementation, providing an efficient pipeline for model training and evaluation.

Conclusion: The DnCNN model proved to be an effective solution for reducing ring artifact noise in medical CT imaging. This approach not only improved quantitative image quality metrics but also enhanced the visual interpretability of images, crucial for accurate medical diagnosis. The findings underscore the potential of deep learning-based techniques in addressing common imaging artifacts. Future research will explore real-time deployment and the integration of additional artifact correction features to further augment CT image quality.

References:

[1]. Zhang K et al. Beyond a Gaussian denoiser: Residual learning of deep CNN for image denoising. IEEE Transactions on Image Processing. 2017;26(7):3142-3155.
doi:10.1109/TIP.2017.2662206
[2]. Abadi M et al. TensorFlow: Large-scale machine learning on heterogeneous systems. arXiv preprint arXiv:1603.04467. 2016.

Keywords: ring artifacts; medical CT imaging; deep learning; DnCNN; denoising

T3-P33: Monte Carlo simulation of Shielding Prototype for Am-Be neutron source.

A. Sehili [a@], M. Sadoudi[a], T. Segueni [b]

[a] *Division de SuretéNucléaire et Radioprotection, Centre de Recherche Nucléaire de Draria CRND*
[b] *Division de Physique et Applications Nucléaire, Centre de Recherche Nucléaire de Draria CRND*
[@] *Corresponding author a-sehili@crnd.dz*

Background/Purpose: Neutron sources are widely used in many fields of research and Industry. Am-Be is considered as an important and most famous neutron source, provides adequate neutron intensity [1]. The Am-Be neutron is a sealed source with an activity of 4.6 Ci, this type of source is a neutron emitter encapsulated in a compact and portable self-shield. In order to ensure the safe use of this source and to effectively protect personnel from neutron exposure, it is necessary to characterize it and design adequate shielding to minimize dose rates in the vicinity. After characterization of the source, the neutron spectrum thus determined will be used to calculate the ambient dose rate around.

Materials & Methods: In this work, a Monte-Carlo shielding model of the 241Am-Be neutron source is developed with MCNP5 code. The simulated Am-Be source is in a cylindrical shape with a radius of 1.26 cm and a length of 5.05 cm. The energy spectrum and neutron emission yield used in simulation is ISO 8529-1:2021 [1,2], three (03) channels one vertical and two horizontals, with 4 cm diameter were added to the model to allow irradiating large volume samples for NAA, neutron dosimetry and also for detectors Testing with a proper neutron flux.
The shielding materials and thickness (polyethylene, steel...etc.) required were selected based on experimental measurement setup using Boron 3- Fluor Neutron detector to ensure safety.

Results: The evaluation of the neutron flux and dose rates of the 241Am-Be neutron source is carried out using a Monte Carlo method. Equivalent dose rate of 5 µSv/h for 30 cm thicknesses of Polyethylene is obtained by simulation and confirmed by comparison with experimental measurements.
For neutron flux in the canal, the maximum thermal/fast neutrons flux ratio equal to 3.94 was obtained at 10.5 cm with maximum flux of 1.57E+04 n.cm-1.s-1

Conclusion: This work was carried out to study the feasibility of shielding the Am-Be neutron source using Monte Carlo simulation. The values obtained are very satisfactory for optimal shielding, the dose rates calculated by the Monte Carlo method are in good agreement with experimental measurements, thus ensure its safety.
Monte Carlo simulation proves to be a very useful tool to study the shielding of neutron sources with different configurations and the evaluation of neutron fluxes from various sources.

References:

[1] M.N. Nasrabadi *et al.*Neutron shielding design for ^{241}Am–Be neutron source considering different sites to achieve maximum thermal and fast neutron flux using MCNPX code. Ann. Nucl. Energy(2013).
[2] Thomas, D., Bedogni, R., Méndez, R., Thompson, A., &Zimbal, A. (2018). Revision Of Iso 8529 Reference neutron radiations. Radiation Protection Dosimetry, 180(1–4), 21–24.

Keywords: Am-Be Source, Shielding, Monte Carlo Simulation, MCNP5, Dose rate.

T3-P34: AI-Driven Evaluation of VMAT Plan Complexity: Assessing Key Parameters and Predictive Correlations

S. Malki [*1,2], L. Naoun[3], S. E. Chouaba[1,2], D.E.C. Belkhiat [1,2], B. Bacha[3]

[1]*Department of physics, Faculty of sciences, University Ferhat Abbas Sétif1, Sétif, Algeria*
[2]*Dosing Analysis and Characterisation with High Resolution Laboratory (DAC- HR), Sétif, Algeria*
[3] *CLCC ANNABA, Ibn Rochd University Hospital Center, Annaba, Algeria*
**Corresponding author e-mail: malkisouadfadwa@gmail.com*

Background/Purpose: Volumetric Modulated Arc Therapy (VMAT) is an advanced radiation therapy technique that delivers precise radiation doses to tumors while minimizing exposure to healthy tissues. During VMAT, a machine rotates around the patient, continuously adjusting the shape and intensity of radiation beams. Artificial Intelligence (AI), particularly machine learning, can analyze complex VMAT plans, optimize treatment delivery, and predict potential side effects. This can help simplify treatment planning, improve treatment accuracy, and ultimately enhance patient outcomes.
This study investigates the possibility of AI in evaluating the complexity and deliverability of VMAT plans. It will focus on analyzing the VMAT plans based on critical parameters such as arc segment count, dose modulation patterns, and doses to organs at risk (OAR). Further, performance of various models of AI-driven systems in plan evaluation will be compared with conventional methods to assess the efficacy of AI in this domain.

Materials & Methods: This study employed the Monaco treatment planning system from Elekta, using both Monte Carlo and collapsed cone algorithms for dose calculations. VMAT plans were generated for Elekta Versa HD, Infinity 1, and Infinity 2 accelerators. Dosimetric measurements were acquired using an EPID phantom and subsequently analyzed with Dosi-Soft for gamma index evaluations. Plan complexity was assessed through the computation of complexity indices, including PMU, MAD, MFA, MD, and C/A. Machine learning models, including Support Vector Machine and Random Forest, will be employed to analyze these parameters.

Results: C/A and MD exhibited positive correlations (C/A: Pearson 0.36, Spearman 0.55; MD: Pearson 0.44, Spearman 0.32), while PMU showed a weak negative correlation (Pearson -0.33, Spearman -0.17). MAD and MFA displayed negligible correlations.

Conclusions: C/A and MD may be the most influential factors among those examined, while the influence of PMU, MAD, and MFA appears considerably less pronounced. . Machine learning can enhance analysis by identifying complex patterns. Further AI model application is warranted to understand the underlying mechanisms driving these correlations and to explore the potential predictive power of these variables.

Keywords : VMAT; AI; COMPLEXITY; MACHINE LEARNING; EPID.

T3-P35: Uncertainties Estimation for Dose Rate of Treatment Beams in External Radiotherapy: Deterministic vs. Monte Carlo Approach

Z. Sakhri-Brahimi [1], A.Merad [1@], N. Toutaoui-Kkelassi[2], H. Benmahdjoub[3], O.A. Meghnous [3], A. Khelifi [4], K.E. Laterech [4], F. Meddad[1]

Algiers Nuclear Research Center [2]*Atomic Energy Commission* [3]*USTHB*
[4] *EMP*
[@] *Corresponding author* a.merad@crna.dz

Background/Purpose: In medical physics, measurement results are essential for verifying compliance with standards and evaluating therapeutic risks. Considering measurement uncertainties, which reflect the degree of doubt about a value due to unknown true values, is vital to ensuring reliability. Standards mandate the evaluation and reporting of uncertainties, particularly for the dose rate and delivered dose.

In radiotherapy, uncertainties arise from various factors, including measurement errors, calculation inaccuracies, positioning errors, and patient variability. Key sources of uncertainty include measuring devices (e.g., calibration, repeatability, stability, resolution), correction factors (e.g., K_{TP}, K_{ion}, $z_{réf}$, $A_{réf}$, SSD), and transitions from reference to treatment conditions (e.g., PDD, OAR, FOC, W_f, F_{DSA}).

The primary objective of this work is to estimate the expanded uncertainty associated with the treatment dose rate using two complementary approaches based on statistical tools: the deterministic method (LPUM) and the Monte Carlo method (MCM).

Materials & Methods: The LPUM analytically combines random and systematic uncertainties using the law of uncertainty propagation. Conversely, the MCM employs random sampling to propagate probability density functions (PDFs), enabling precise and flexible uncertainty estimation. Guidelines from the JCGM and IAEA provided the theoretical framework for this work. Simulations utilized a modified version of the RANECU subroutine (RAND function implemented in FORTRAN), renowned for its quality and reliability, ensuring optimal precision in generating unique random numbers per draw.

Results: Uncertainties associated with the reference and treatment dose rates were calculated and simulated. Validation was performed by comparing the expanded uncertainties obtained through the MCM and LPUM approaches. The differences, quantified by the minimum distance (d_{min}) and the maximum distance (d_{max}), were within the numerical tolerance (ξ) derived from the previously defined expanded absolute standard uncertainty.

Conclusion: The Monte Carlo method represents a significant advancement in uncertainty evaluation. This approach provides a robust and efficient alternative, overcoming the limitations of traditional analytical methods, particularly in contexts involving non-linear and complex parameter interactions.

This work serves as an initial iteration that will benefit from further development and refinement as research progresses and new data become available. It also highlights the importance of raising awareness about uncertainty management, which is often overlooked across various disciplines.

T3-P36: Study of the Feasibility of Calibration of Ionization Chamber in Machine Specific Reference at the SSDL

S. Hayoune[a@], T. Medjadj[a]

[a]*Nuclear Research Center of Algiers (CRNA)*
[@]*Corresponding author: s.hayoune@crna.dz*

Background/Purpose: Conventional radiotherapy dosimetry relies on the codes of practice (COPs), such as TRS 398 [1] and AAPM's TG-51 [2]. With the increasing use of small fields, a new COP, TRS 483 [3], was introduced, incorporating the machine-specific reference (msr) field. This study evaluates the feasibility of calibrating an ionization chamber in Algeria's Secondary Standards Dosimetry Laboratory (SSDL) for the msr field, in accordance with TRS 483.

Materials & Methods: This study was conducted at the Algerian SSDL using the ^{60}Co calibration unit (Eldorado78) and two ionization chambers, TW30013 (0.6cc) and CC13 (0.13cc). The calibration was performed in a water phantom for various field sizes, employing the substitution method.

Results: This study presents a procedure for calibrating an ionization chamber in the msr field of a ^{60}Co photon beam, following the guidelines of TRS 483. The results demonstrate good agreement between the calibration coefficients obtained under reference conditions and those obtained in the msr fields. The maximum difference observed for the TW30013 was 0.83% for the 10 x 6 cm² field size.

Conclusion: This study demonstrates that calibration for the msr fields can be performed in Algeria's SSDL using the ^{60}Co photon beam. The results show that this approach is feasible and consistent.

References:

[1]. Andreo et Al (2000). Absorbed dose determination in external beam radiotherapy: An International Code of Practice for dosimetry based on standards of absorbed dose to water, IAEA Technical Reports Series no. 398, International Atomic Energy Agency, Vienna.
[2]. Almond, Peter R., et al. "AAPM's TG-51 protocol for clinical reference dosimetry of high-energy photon and electron beams." Medical physics 26.9 (1999): 1847-1870.
[3]. IAEA, AAPM. "Dosimetry of small fields used in external beam radiotherapy." International Atomic Energy Agency Technical Report Series 483 (2017).

Keywords: Ionization chamber; msr field; calibration; TRS 483

T4-P1: Neutronic and Thermal-Hydraulic Study of the Steady State Research Reactor

O. Mokhtari[1@], L. Radji[2]

[1] *Division de la Sûreté Nucléaire et de la Radioprotection, Centre de Recherche Nucléaire de Draria (CRND)*
[2] *Division Réacteur NUR, Centre de Recherche Nucléaire de Draria (CRND)*
[@] *Corresponding author O-MOKHTARI @crnd.dz*

Background/Purpose: Adherence to safety standards and limitations throughout a nuclear reactor's useful life is crucial for preventing incidents and accidents that could have detrimental effects on workers, general public, and environment. Calculation of the Power Peaking Factors (PPFs) in nuclear reactors allows the location of the hottest channel in the reactor core and thus the determination of the maximum temperature of the fuel cladding which constitutes an important safety limit.

Materials & Methods: In this work a model for the NUR research reactor (IV-N) core configuration during steady state operation was developed for neutronic and thermohydraulic analysis by using OpenMC [1]and PARET [2]codes.
The power density distribution and other neutronics parameters calculated by the OpenMC model were injected into the PARET model, to obtain the fuel; cladding and coolant temperatures in each axial node. In the MC calculations, the estimation of the axial power density distribution and PPFs was performed by calculating the fission energy depositionby dividing the hottest fuel plate axially into twenty segments. In OpenMC, filters (EnergyFilter) and scores (fission score) are used to define tallies.
In the thermal-hydraulic model, the core was modelled by two parallel regions. The first region represents the hottest channel and the second one the remainder part of the core named the average channel. In axial direction, the two regions were subdivided in twenty sections.

Results: In this work, the values of the radial and axial power peaking factors obtained are: 1.40 and 1.31 respectively. The temperature profiles within the hottest and the average channels were determined.The clad and coolant Maximum temperatures attain, respectively, 55.09 ◦C and 46.54 for the hot channel, 51.02 °C and 45.04 °C for the average channel.

Conclusion: According to the calculations predictions at normal operation of the NUR reactor start-up configuration, temperature limit (90°C) of the clad in the hottest channel is not exceeded. The results are in good agreement with those obtained using deterministic code (WIMS and CITATION) [3] for calculating power peaking factors and temperatures.

References:

[1]. Romano P K et al.. OpenMC: A state-of-the-art Monte Carlo code for research and development. *Annal of Nuclear Energy 82, 90–97*. 2015. https://doi.org/10.1016/j.anucene.2014.07.048.

[2]. Obenchain CF.. PARET: A program for the analysis of reactor transients, *Idaho National Engineering Laboratory*, Report IDO-17282. (1969).

[3]. Mokeddem M Y et al .. Analyse comparative de transitoires des configurations actuelle et anterieure de NUR *(Rapport interne)*. Centre de Recherche Nucléaire de Draria (CRND), Division Réacteur Nucléaire.(DRN). Alger.2005

Keywords: Safety limits; OpenMC; PARET; clad temperature; Peaking Factor

T4-P2: Contribution to the Cooling of a Nuclear Reactor after Shutdown

A. Bouam@, A. Dadda Khorsi, A.L. Deghal Cheridi, K. Messilem, Sd. Rahmani Bouzina, A. Dahia, H. Taguemount & L. Bouam

Nuclear Research Centre of Birine
@Corresponding author a.bouam@crnb.dz

Background/Purpose: The radioactivity of isotopes (actinides and fission products) is a relatively small source of energy compared to the fission energy released during reactor operation. However, after the reactor is shut down, this residual energy does not immediately disappear like the fission energy, but gradually decreases as a function of the cooling time. This residual energy is characterized by a thermal power called *residual power*. Cooling a nuclear reactor after shutdown is an essential step to ensuring the safety of nuclear facilities and to minimize risks associated with residual heat. This involves:

- Efficiently dissipating residual heat to prevent excessive temperature increases in the core,
- preserving the integrity of the nuclear fuel and internal structures,
- Preventing the formation of steam or flammable gases that could compromise safety.

Although the controlled fission reaction is interrupted, the nuclear fuel continues to generate heat due to the radioactive decay of the fission products. This study aims to develop a computer program capable of predicting the number of cooling cycles required and the duration of each activation of the primary circuit pump after a nuclear reactor shutdown.

Materials & Methods: A computational model was developed using a Fortran compiler, incorporating empirical correlations from the literature [1-3]. Furthermore, benchmark nuclear research reactor experimental data were utilized to assess and validate the model's accuracy through comparison.

Results: The results obtained are comparable to those observed by the operators, particularly regarding the increase in core temperature and the activation delay of the cooling circuit pump.

Conclusion: Cooling a nuclear reactor after shutdown is a critical aspect of nuclear safety. Through visual monitoring by reactor operators or the use of advanced technologies, the risks associated with residual heat can be minimized, ensuring the protection of the reactor, operators, the public, and the environment.

References:

[1]. S. Glasstone & A. Sesonske, "Nuclear reactor engineering", ISBN: 0-442-02725-7; 1967.

[2]. K. Way, E. P. Wigner: "Radiation from Fission Products", Technical Information Division, United States Atomic Energy Commission, Oak Ridge, Tennessee, 1946. K. Way, E. P. Wigner: "The Rate of Decay of Fission Products", in: Physical Review 73 (1948), 1318–1330.

[3]. J. Sierchuła, 2019, "Analysis of passive residual heat removal system in AP1000 nuclear power plan", IOP Conf. Series: Earth and Environmental Science, doi:10.1088/1755-1315/214/1/012095.

Keywords: **Nuclear Reactor; Residual Heat; Cooling; Computational Model.**

T4-P3: Simulation and Analysis of SPERT reactivity insertion transients using the PARET computer code

M. Bouaouina[a@], A Hadjam[a], D Saad[a]

Nuclear engineering Division, Nuclear Research Center of Birine, Djelfa, Algeria
[@]Corresponding author m.bouaouina@crnb.dz

Background/Purpose: The primary objective of this work is to validate the PARET code by comparing its results to experimental tests conducted on the SPERT III-E core. Specifically, the ongoing study aims to demonstrate the capabilities of the PARET code through the reproduction of fifteen experimental tests. This paper presents the preliminary results obtained by the PARET code. Comparisons are made between the calculated and experimental results, focusing on power profiles for multiple tests showing good agreement, where the inserted reactivity ranged from 0.77 $ to 1.21 $ [1].

Materials & Methods: PARET, developed at the Idaho National Laboratory, is a computational tool designed to analyse reactivity insertion events in research and test reactors cooled by light or heavy water, with fuel configurations comprising plates or pins. This tool has validated by several experimental tests, especially from the SPERT experiments [2, 3].

Results: This paper presents the preliminary results obtained by the PARET code. A series of comparisons have been conducted between the calculated and experimental power profiles for several tests, with reactivity insertions ranging from 0.77 $ to 1.21 $. These comparisons aim to evaluate the code's accuracy and reliability in reproduction of experimental conditions.

Conclusion: This study highlights the capabilities of the PARET code through the analysis of fifteen reactivity insertion tests conducted on the SPERT III-E core. The results demonstrate that computer code provides acceptable prediction of dynamic behaviour during reactivity insertion events, reinforcing its applicability to performing safety analyses.

References:

[1]. R. K Mckardell Et Al, « Reactivity Accident Test Results And Analysis For The SPERT III E CORE, Small Oxide Fueled, PWR, IDO 1782, March 1969.

[2]. M. Bouaouina Et Al, « Les Expériences SPERT I & SPERT III Et La Préparation Des Fichiers De Données Pour Les Configurations SPERT-I 12/25 Et SPERT III-E 12/68 Core », Juin 2024.

[3]. D. Ferraro And All, « Serpent/Subchanflow Pin By Pin Coupled Transient Calculations For The SPERT-IIIE HOT FULL POWER TESTS», July 2020, Annals Of Nuclear Energy.

Keywords:PARET; SPERT TESTS; VALIDATION, SPERT III-E CORE

T4-P4: Importance Measures in Probabilistic Safety Assessment of a Nuclear Research Reactor

M. Boufenar[1@], M. Azzoune[1]

[1]*Centre de Recherche Nucléaire de Draria, CRND*
[@]*Corresponding author m-boufenar@crnd.dz*

Background/Purpose: In risk-informed decision-making, identifying weaknesses in nuclear reactor safety systems and implementing mitigation measures are fundamental to safety assessments. These assessments rely, among other factors, on importance measures, which rank system components based on their contribution to overall risk [1]. By systematically detecting vulnerabilities and applying targeted interventions, these measures help maintain high safety standards and strengthen the resilience of reactor systems against potential failures.

Materials & Methods: This study involves a comparison between the traditional Fussell-Vesely (FV) and Risk Achievement Worth (RAW) methodologies with Birnbaum's approach, for assessing the importance of system components within a Probabilistic Safety Assessment (PSA) framework. The traditional approach, while widely used, can be complex when understanding system changes, as the dependencies between measures can be challenging to interpret [2]. In contrast, the Birnbaum's method is highlighted for its simplicity and clarity, offering absolute changes in reliability that provide a more intuitive and straightforward assessment of system modifications.

Results: To validate this methodology, this work presents a case study on the primary cooling system of the NUR nuclear research reactor. The objective is to assess the impact of redundancy addition on system reliability and identify the most effective method for ranking system components based on their contribution to overall risk. The results show that introducing a redundant pump affects the values of the importance measures, highlighting key differences in how the importance measures capture system changes.

Conclusion: By focusing on absolute measure, Birnbaum's importance measure effectively addresses the limitations of FV and RAW, offering a more robust and independent metric, particularly in capturing real changes in system reliability and supporting risk-informed decision-making with greater precision and clarity.

References:

[1] . J. Cheng, J. Liu, S. Chen, Y. Li, J. Wang, F. Wang, 'A new method for safety classification of SSCs by reflecting nuclear reactor operating history into importance measures', *Nuclear Engineering and Technology*, 54 (2022) pp. 1336-1342, https://doi.org/10.1016/j.net.2021.09.039.

Mohammed BOUFENAR

[2]. Y. Dutuit, A. Rauzy, 'On the extension of Importance Measures to complex components', *Reliability Engineering and System Safety* 142 (2015) pp. 161-168, https://doi.org/10.1016/j.ress.2015.04.016.

Keywords: Importance Measure; Risk Achievement Worth; Fussell-Vesely; Birnbaum.

T4-P5: Importance Factors Analysis of the Reactor Protection System (RPS) for the Nuclear Safety of the MTR Research Reactor

D. Kemikem[a@], S. Mellal[b]

[a@] *Technical Management Department, CRND, Algiers, Algeria*

[b] *Maintenance Department, CRND, Algiers, Algeria*

[@] D-KEMIKEM@crnd.dz

Background/Purpose: In this paper, reliability analysis of RPS is investigated using the minimum cut set (MCS) and importance analysis (IA). This can lead to the calculation of system failure probability and identification of critical failure modes. The proposed method is applied to the RPS-NUR research reactor.

Materials & Methods: In this work, the reliability modeling was performed using the dependency diagram method (DD), minimum path method, and important factors such as Birnbaum importance and Fussell-Vesely importance. For this purpose, the DD of RPS was developed using Isograph Reliability Workbench 15.0 software, the path method was based on the knowledge of the minimum path between input and output, and the importance analysis was programmed using Matlab software.

Results: the dependency diagram method is useful to model the complex systems with sufficient detail to be able to detect the effects of the different designs and components interactions. The obtained results show clearly that the probability of failure of RPS-NUR in both failure modes (manual and automatic) are in accordance with the design probability of failure. The most important failure of the system is the RPS failure due to human error, the failure of detection channels, failures of SCRAM unit and loss of offsite power.

Conclusion: This paper presents the reliability assessment of RPS-NUR using DD, MCS and importance factor methods. DD is proposed to quantify the probability of system failure. MCS is derived using the minimum path method, which can be used for quantitative and qualitative reliability assessment. In order to improve the reliability of the system, we also identify the components that should be modified or replaced with higher quality components based on the importance measures. This model can be developed further by considering the effects of ageing components using the operation data of NUR reactor.

References:

[1]. Ajit Kumar Verma, Srividya Ajit and Durga Rao Karanki, "*Reliability and Safety Engineering*", Springer-Verlag London Limited 2010
doi: 10.1007/978-1-84996-232-2

[2]. P. Kalpesh. Amrutkar, Kirtee K. Kamalja. 'An Overview of Various Importance Measures of Reliability *System' International Journal of Mathematical, Engineering and Management Sciences* Vol. 2, No. 3, 150–171, ISSN: 2455-7749, 2017.
doi: 10.33889/IJMEMS.2017.2.3-014

[3]. Jinlei Qin, Yuguang Niu and Zheng Li, "Reliability Modeling and structure importance analysis of electric power station distribution control system". *Information technology journal* 13(16): 2593-2601; ISSN 1812-5638.
doi: 10.3923/itj. 2014.2593.2601. 2014

Keywords: NUR reactor, reliability assessment, dependency diagram method, minimal paths method, Importance analysis.

T4-P6: SB-LOCA Accident Simulation in a Research Reactor: A Thermal-Hydraulic Analysis

A.L. Deghal Cheridi@, A. Hadjam, A. Dadda, A. Dahia, A. Bouam

Nuclear Research Centre of Birine
@ Corresponding author a-l.deghal@crnb.dz

Background/Purpose: Modeling and simulation play a crucial role in ensuring the safe operation of nuclear reactors, predicting plant behavior under accidental conditions, and improving our understanding of thermal-hydraulic phenomena. The effectiveness of numerical simulation tools is driven by advancements in computational methods, programming techniques, and high-performance computing resources [1, 2].

Today, state-of-the-art simulation codes enable accurate predictions of the thermal- hydraulic response of nuclear reactors, both under normal operating conditions and during accident scenarios. Among these, the Small Break Loss-of-Coolant Accident (SB-LOCA) represents a critical safety concern in research reactors. This type of accident, which can result from equipment failure, pipeline rupture, or valve malfunction, poses significant risks, including loss of core integrity, environmental contamination, and the spread of fission products.

Materials & Methods: This study focuses on simulating a SB-LOCA in the cooling circuit of a research reactor using the RELAP5 code. The scenario under investigation involves a rupture in the main inlet pipe of the reactor core, leading to a partial coolant loss. The simulation aims to analyze key safety parameters and system response under accident conditions. The boundary conditions and initial system states have been defined based on reactor operational data to ensure a realistic and accurate representation of the transient behavior.

Results: The findings reveal the time-dependent evolution of the reactor's key thermal-hydraulic parameters during the SB-LOCA accident scenario. The results demonstrate the importance of effective accident management in preserving reactor integrity. The study evaluates operator actions taken during the event, including their classification and impact on mitigating the transient conditions. Additionally, the simulation assesses whether safety systems, such as the Emergency Core Cooling System (ECCS), responded effectively to maintain core cooling.

Conclusion: This study aimed to analyze the thermal-hydraulic behavior of a research reactor during a SB-LOCA and evaluate its impact on reactor safety. The analysis of simulation results indicates that:

- The accident significantly affects the reactor's operating conditions,
- The Emergency cooling system responds effectively, ensuring that fuel and cladding temperatures remain within acceptable safety limits,
- The reactor's safety mechanisms successfully mitigate the consequences of the transient, preserving core integrity and preventing any risk of severe degradation.

References:

[1]. Omar, H., Ghzi, N., Alhabit, F., Hainoun, A., 2010. Thermal hydraulic analysis of Syrian MNSR research reactor using Relap5/Mod3.2 code. Ann. Nucl. Energy 37, 572–581.

[2]. Deghal Cheridi , A.L; et al., Flow blockage accident analysis in a multi purposes research reactor using Relap5 system code, Progress in Nuclear Energy, 168 (2024) 105019.

Keywords: Research reactor, Safety analysis, Modeling and simulation, RELAP5/Mod3.2, SB-LOCA Accident.

T4-P7: Security of computer and communications systems in NPPs of generation III and III+

Y. Kaloune[1@], D. Boukhadra[2], A. Bouhzila[3]

[1] *Draria Nuclear Research Center, Algiers, Algeria*
[2] *Draria Nuclear Research Center, Algiers, Algeria*
[3] *Birine Nuclear Research Center, Ain Oussera, Algeria*
[@] *y-kaloune@crnd.dz.*

Background/Purpose: The increasing digitization of nuclear power plants has changed the type of communications systems by using network technologies in NPP I&C systems compared with traditional design. However, this growth has transformed the cyber-attacks into a serious threat. The Stuxnet case in 2010 evoked enormous about the computer security for the digital I&C systems of NPPs, and applying security measures to the systems, has become more important nowadays for nuclear safety [1].

Materials & Methods: Our work concerns the security of computer and communication systems in NPPs of generation III and III+ [2]. We have presented the different approaches that are used for each model of NPPs. Then, we have presented the computer security measures that are applied throughout the lifecycle of computer systems, the particularity of our approach lies in the network segmentation method and also on the level of security implemented. Finally, we have presented a unified method that determines the most secure measures to be implemented when upgrading computer and communication systems in nuclear power plants.

Results: The obtained results represent a useful and practical approach to the implementation of computers, communication systems and network technologies in nuclear power plants, taking into account computer security and maintaining this concept in the context of continuous technological advancement.

Conclusion: In conclusion, the integration of appropriate computer security measures into communications systems is more crucial for nuclear safety.

References:

[1]. Do-Yeon Kim,«Cyber security issues imposed on nuclear power plants», Sunchon National University, Annals of Nuclear Energy- Volume 65, March 2014, Pages 141-143, Republic of Korea.

[2]. «Cyber security programs for nuclear facilities» u.s. nuclear regulatory commission, janury 2010, appendix c to rg 5.71, page c-34 ,usa.

Keywords: Stuxnet , cybersecurity, I&C systems, Safety.

T4-P8: Multipoint kinetics modeling of a pressurized water reactor core and analysis of its behavior to reactivity insertions

B. Djaroum[a@], B. Mohammedi[a], K. Halbaoui[a], M.F. Belazreg[b], S. Laouar[a], S. Mechraoui[a] S. Medguedem[a], and A. Khelil[a]

[a]*Nuclear Research Center of Birine (CRNB), BP 180, Ain-oussera, Djelfa*
[b]*Nuclear Research Centre of Algiers (CRNA), BP 399, Algiers, Algeria*
[@] *Corresponding author b.djaroum@crnb.dz*

Background/Purpose: Modeling of nuclear reactor cores is imperative for understanding their behavior under operating conditions. While point kinetic models are appropriate for small reactors, they fall short in capturing the complex dynamics of large reactors, particularly regarding xenon effects and power distribution. To address these limitations, multi-point kinetic models, which consider temporal and spatial variations in neutron flux, have emerged as the prevailing model for studying axial power distribution and xenon oscillations suppression in pressurized water nuclear reactors during load-following operation [1]. This study aims to develop a multi-point kinetic model, to analyze its responses to reactivity insertions, and quantify the axial offset of core power.

Materials & Methods: This study employs the MATLAB/SIMULINK programming environment and the nodal dynamics approach to model the core of a pressurized water nuclear reactor. The core is subdivided into axial nodes, which are treated as mini-reactors. The neutron and thermohydraulic parameters for each axial node are determined by their respective integrated average values over the volume. Furthermore, each node incorporates reactivity contributions from control rods, coolant feedback, Doppler effects, and xenon poisoning. The coupling of nodes is facilitated via neutron scattering, which is described by nodal kinetic equations derived from the energy group diffusion equation. The multipoint model is developed with four nodes and three delayed neutron groups [2, 3].

Results: Reactivity variations in the pressurized water reactor core at nominal power, controlled by a PID, reveal negative reactivity in nodes 1 and 3, indicating subcriticality and higher burnups compared to nodes 2 and 4 where criticality was achieved and maintained. Furthermore, an external reactivity insertion of 0.7 β caused a power excursion, with reactivity changes between nodes and a power Axial Offset (AO) of – 3 %. A subsequent reactivity insertion of 0.2 β and 0.7 β in the upper and lower halves of the reactor core, respectively, increased the Axial Offset (AO = - 3.5 %).

Conclusion: The multi-point kinetic model developed in this study incorporates and quantifies the axial offset (AO) to improve axial power distribution control. In addition to analyzing reactivity variations in the four core nodes, the measured and analyzed AO will serve as an initial condition for future simulation experiments to design advanced algorithms for this pressurized water reactor model.

References:

[1]. Gang Li, Xueqian Wang, Bin Liang, XiuLi, Bo Zhang, Yu Zou, 2016. Modeling and control of nuclear reactor cores for electricity generation: A review of advanced technologies. Renewable and Sustainable Energy Reviews 60(2016)116–128. DOI: 10.1016/j.rser.2016.01.116

[2]. G.R. Ansarifar, H.R. Akhavan, 2015. Sliding mode control design for a PWR nuclear reactor using sliding mode observer during load following operation. Annals of Nuclear Energy, Volume 75, January 2015, Pages 611-619. https://doi.org/10.1016/j.anucene.2014.09.019

[3]. M. Zaidabadi nejad, G.R. Ansarifar, 2017. Adaptive robust control for axial offset in the P.W.R nuclear reactors based on the multipoint reactor model during load-following operation. Annals of Nuclear Energy, Volume 103, 2017, Pages 251-264. DOI.org/10.1016/j.anucene.2017.01.025

Keywords: Modeling, MATLAB/SIMULINK, core nodes, reactivity insertion and Axial Offset.

T4-P9: Assessment of Safety Margins for Positive Reactivity Insertions: A Case Study of the NUR Research Reactor

M. Azzoune[a@], M. Boufenar[a] , D. Lababsa[a]

[a]*Nuclear Reserach Center of Draria*
[@]*Corresponding author m-azzoune@crnd.dz*

Background/Purpose: Maintaining fuel integrity is paramount for the safe operation of research reactors. This study establishes the maximum allowable positive reactivity insertion in the NUR research reactor core that would result in reaching the aluminium alloy fuel cladding's softening [1] temperature. This limit is crucial for defining safe operating parameters and ensuring adequate margins to fuel damage.

Materials & Methods: A computational model was developed using the RELAP5 thermal-hydraulic system code [2] to simulate reactor behavior under protected reactivity insertion conditions. The model incorporates detailed representations of the reactor protection systems, including cooling systems [3] and reactor trip functions at standard setpoints. To establish a conservative upper bound for safety analysis, reactivity feedback mechanisms were deliberately excluded from the simulation.

Results: This analysis determined that a positive reactivity insertion of 2.58$ would cause the fuel cladding temperature to reach its softening point of 200°C. This threshold is a critical safety parameter for maintaining fuel integrity.

Conclusion: This study establishes a conservative positive reactivity insertion limit of 2.58$ for the NUR research reactor. This conservative limit, derived by excluding the mitigating effects of temperature feedback, provides a robust basis for safe reactor operation. Future work will investigate the impact of temperature feedback to determine actual safety margins.

References:

[1]. Biplov Kumar Roy et al..Plastic deformation of AA6061-T6 at elevated temperatures: Experiments and modeling. International Journal of Mechanical Sciences, Volume 216, 15 February 2022, 106943.
doi:10.1016/j.ijmecsci.2021.106943

[2]. Idaho National Engineering Laboratory. RELAP5/MOD3 code manual, code structure, system models, and solution methods, Vol. I. Idaho Falls: INEL; 1999. (NUREG/CR-5535)

[3]. Mohammed Azzoune et al.. Analysis of a loss-of-flow accident resulting from the primary pump shaft break transient of the NUR research reactor. Journal of Nuclear Science and Technology Volume 56, 2019-Issue 1 .
doi:10.1018/00223131.2018.1532845

Keywords: Reactivity-initiated accidents; safety limit; fuel integrity; RELAP5

T4-P10: Handling of Prolonged Power Outages in a Nuclear Center: Risks, Security, and Solutions

D. Boukhadra@, Z. Bouhila, M. Mebarka, K. Remil

Nuclear Research Center of Draria
@ Corresponding author d-boukhadra@crnd.dz

Background/Purpose: The Draria Nuclear Research Center (CRND) hosts critical nuclear facilities essential for advancing research in various scientific fields. To ensure the safe and reliable operation of these facilities, maintaining an uninterrupted power supply is paramount, particularly for critical systems such as nuclear material cooling and containment. Prolonged power outages (whether due to technical failures, sabotage, or natural disasters) pose significant risks to safety, security, and the environment. Robust security measures, including backup generators and infrastructure protection, are in place to mitigate these risks. This study aims to assess the risks associated with power outages and evaluate the effectiveness of the security measures implemented.

Materials & Methods: This study adopts a comprehensive approach that integrates a real-world case analysis with simulations of potential outage scenarios. It is grounded in a case study conducted at CRND, utilizing internal reports on site safety and security, as well as international standards set by the International Atomic Energy Agency (IAEA) [1,2]. The analysis examined the functionality of electrical systems, backup generators, and radiation monitoring devices during critical power outages.

Results: The investigation at CRND demonstrated that the implemented security measures effectively counter prolonged power outages. Backup generators provided a stable power supply, ensuring the uninterrupted operation of essential cooling and containment systems. Infrastructure protection and radiation monitoring systems adhered to IAEA standards, enhancing the facility's ability to handle critical scenarios. No incidents were recorded during the case study or simulations, confirming the reliability of existing measures. However, recommendations were proposed to further enhance system autonomy and redundancy. These include upgrading electrical components and introducing advanced monitoring systems to preemptively address potential vulnerabilities.

Conclusion: The findings underscore the resilience of the security measures at CRND in mitigating risks associated with prolonged power outages. The combination of backup power systems and radiation monitoring ensures robust protection of the facilities. While no failures were observed, the proposed improvements will further strengthen the safety and security of CRND's operations, ensuring its preparedness for future challenges.

References:

[1]. IAEA (International Atomic Energy Agency) – "Nuclear Power Reactors : Safeguards and Security," IAEA Safety Standards.

[2]. L. M. Garrison et al. (2019), "Environmental Impacts of Nuclear Power and the Role of Advanced Safety Systems," Journal of Nuclear Energy.

Keywords: Nuclear safety; Security measures; Risk assessment; prolonged power outages.

T4-P11: Advancements and Ongoing Challenges in Small Modular Reactors (SMR)

N. Amrani[a,B @], A. Tokuhiro[c]

[a]*Physics Department, Faculty of Sciences, Setif-1 University, Ferhat ABBAS, Setif, Algeria*
[b]*Dosing, Analysis and Characterization in High-Resolution Laboratory, Setif-1 University, Ferhat ABBAS, Setif, Algeria*
[c]*Faculty of Engineering and Applied Sciences, Ontario Tech University, 2000 Simcoe Street North, Oshawa, Ontario L1G 0C5 Canada*
[@]*Corresponding author naima.maiza@univ-setif.dz*

Background/Purpose: Small Modular Reactors (SMRs), particularly water-cooled and Advanced Modular Reactors (AMRs), have gained attention for their potential to provide flexible and low-carbon energy solutions. They are suitable for diverse applications, including remote regions and industrial settings. Despite this potential, several deployment barriers remain, particularly in regulation, economics, and waste management. This study critically analyzes these challenges by examining specific SMR designs and their implications, with a particular focus on distinguishing water-cooled SMRs from AMRs.

Materials & Methods: A comprehensive assessment of SMR deployment is conducted using policy analysis, case studies, and technical reviews. The study considers existing international reports from organizations such as the IAEA, OECD, and national regulatory bodies (e.g., UK, Canada). The challenges addressed include licensing complexity, economic competitiveness compared to alternative energy sources, and waste management strategies unique to SMRs and AMRs. Additionally, we investigate the role of regulatory harmonization and stakeholder engagement in facilitating SMR deployment [1, 2].

Results: The analysis confirms that while SMRs offer advantages in terms of flexibility and safety, their initial capital costs, when compared to gas power plants or other renewables, present an economic challenge. The study also identifies specific factors contributing to regulatory complexity, including the need for new licensing frameworks tailored to smaller reactor designs. Additionally, waste management challenges differ depending on reactor type, with AMRs potentially requiring new disposal and reprocessing strategies. These findings underscore the need for targeted regulatory adaptations and international collaboration to streamline SMR deployment.

Conclusion: SMRs, including both water-cooled and AMRs, hold great promise for sustainable energy production. However, their successful integration depends on addressing economic viability, regulatory frameworks, and waste management through clear policy directives and international cooperation. By refining licensing strategies and financial models, the potential of SMRs can be fully harnessed for a cleaner and more resilient energy future.

References:

[1]. Hussein, E.M. Emerging small modular nuclear power reactors: A critical review. Phys. Open 2020, 5, 100038, https://doi.org/10.1016/j.physo.2020.100038

[2]. Hussein, E.M. Emerging small modular nuclear power reactors: A critical review. Phys. Open 2020, 5, 100038, https://doi.org/10.1016/j.physo.2020.100038

Keywords: Small Modular Reactors (SMRs); Advanced Modular Reactors (AMRs); Regulation; Waste Management; Energy Policy

T4-P12: Comprehensive Neutronic Analysis of the Advanced Small Modular Reactor CAREM-25: Validation of OpenMC model

K. Ziche[1@], A. Guessoum[1], R. Abed[1], N. Amrani[1]

[1] *Faculty of Sciences, University of Farhat Abbas Satif1, Algeria.*
[@] *Corresponding author karimazh93@gmail.com*

Background/Purpose: The CAREM-25 is an advanced PWR-like SMR designed with hexagonal geometry to generate an electrical power of 25 Mwe. The CAREM-25 core is made from 61 fuel assemblies (FAs). With 127 emplacements, each FA could contain 108 fuel rods, 18 guide tubes for Adjustment Control Rods (ACRs) and Safety Control Rods (SCRs) and one instrumentation tube. Only the central FA is loaded with 1.8% enriched UO2 fuel, where the remain 60 FAs include 3.1% enriched one. Besides that, Burnable Poisoned Rods (BPRs) made from a mixture of natural UO2 and Gd2O3 could be included in some configurations of FAs for a better use of reactivity excess [1]. The aim of the present work is to model and simulate the CAREM-25 fresh core by using an open-source calculation code, OpenMC [2] to validate it on the basis of already existing model with MCNP code [1].

Materials & Methods: In the present study, we use a Monte-Carlo based open-source code for criticality and neutron transport calculations, namely OpenMC [2]. The validation process was performed at various levels of the model. Simulations with OpenMC were conducted under the same conditions of the MCNP5 model (Cycles, neutrons, $SS(\alpha\alpha, \beta\beta)$ and the same nuclear data library (endf/B7.0) [1].

Results: As indicated in the opposite table, the initial findings of the criticality calculations at various levels of the model (pincell, fuel assembly and whole core) show a good accuracy when compared to the MCNP5 simulations. In the same direction, tallied scores of neutron flux spectrum, flux distribution, fission rate and power distributions indicate a global coherence and similarities.

	MCNP5/X	OpenMC (0.15)
Pincells		
	$kk_{\infty} \pm \sigma\sigma$	$kk_{\infty} \pm \sigma\sigma$
UO2 (1.8%)	1.21508 ± 0.00038	1.21389 ± 0.00069
UO2 (3.1%)	1.37640 ± 0.00039	1.37475 ± 0.00062
Fuel assemblies		
FA18BP00	1.14151 ± 0.00031	1.14274 ± 0.00056
FA31BP00	1.32161 ± 0.00041	1.31934 ± 0.00061
FA31BP06	1.12334 ± 0.00044	1.12253 ± 0.00063
FA31BP12	0.95819 ± 0.00048	0.95667 ± 0.00062
Reactor Core		
	$kk_{eeeeee} \pm \sigma\sigma$	$kk_{eeeeee} \pm \sigma\sigma$
50%ACR 10%SCR	1.00027 ± 0.00035	1.00035 ± 0.00008

Conclusion: The present study is based on the Monte-Carlo modelling and simulation of the LWR-like SMR CAREM-25, by using open- source code, OpenMC. The obtained preliminary results were very satisfactory and the final model could be validated to launch a new series of simulations in the aim to prospect new possible configurations for the same reactor.

References:

1. *S. Zare Ganjaroodi and A. Pazirandeh, Neutronic study of CAREM-25 advanced small modular reactor using Monte carlo simulation, (2020), ATW Vol. 65, Issue 8/9 August/September*
2. *Marco Antonio C. Lima, Edson Henrice, Daniel A.P. Palma, Amir Zacarias Mesquita, Critical configuration of a SMR based on CAREM 25 using the SERPENT code, Nuclear Engineering and Design, Volume 423, 2024, 113192, https://doi.org/10.1016/j.nucengdes.2024.113192.*

Keywords: CAREM-25; SMR, OpenMC, PWR, Integrated System, Python.

T4-P13: Comparative Study of a Loss of Flow Accident (LOFA) Analysis in the IAEA 2MW Reactor Benchmark Using Two Calculation Codes

Y. Bensemane [a], O. Tihala[a], K. Sidi-Ali[b@],

[a]*Ecole Nationale Polytechnique, El Harrach, Algiers, Algeria*
[b]*Nuclear Research Centre of Draria, Seballa, Draria-Algiers, Algeria*
[@]*Corresponding author k-sidiali@crnd.dz*

Background/Purpose: The loss of flow accident (LOFA) in the nuclear reactor core occurs following various events such as the failure of a pump or a valve, the obstruction of a channel or flow redistribution. This can lead to poor cooling of the reactor core and boiling of the coolant and then an increased fuel cladding rupture risk [1]. In this work, one proposes to study the case of a LOFA in a nuclear research reactor. Two calculation codes will be used and a comparative study of the results obtained will be conducted.

Materials & Methods: An equation set-up is established using the transient state conservation equations coupled with a turbulence model. The meshing of the numerical domain of the hot channel is carried out and its independence from the obtained results is verified [2]. The code FLUENT and the code COMSOL-Multiphysics are used for the analysis of a 20% LOFA.

Results: A 10-second loss of flow transient is performed. The temperature evolutions of the coolant, the fuel cladding and the fuel meat core temperatures are obtained. It is noted that the code FLUENT gives a sinusoidal evolution of the cladding temperature profile while the COMSOL-Multiphysics code gives a linear evolution and a large difference between the two codes results appears along the reactor core channel. On the other hand, the maximum coolant temperature at the channel outlet is almost the same for both codes. The transient analysis shows that the coolant reaches higher temperatures with the code FLUENT than with the code COMSOL-Multiphysics.

Conclusion: The two codes FLUENT and COMSOL-Multiphysics give similar results for the coolant at its exit from the channel. The code FLUENT gives a correct evolution of the temperature of the cladding along the channel, thanks to the use of a UDF available in this code. It is also noted that the code COMSOL-Multiphysics treats the power evolution in the fuel as being uniform while the code FLUENT treats it as being sinusoidal, hence the differences in profiles.

References:

[4]. Qing et al., 2009, Development of a thermal–hydraulic analysis code for research reactors with plate fuels, Annals of Nuclear Energy 36 (2009) 433–447, doi:10.1016/j.anucene.2008.11.038

[5]. N. Akhal et al.,2023, Loss Of Flow Accident (LOFA) with protection in NUR nuclear reactor; three dimensional analysis of a Fast LOFA and a Slow LOFA, Progress in Nuclear Energy 162 (2023) 104779. doi: 10.1016/j.pnucene.2023.104779

Keywords: Nuclear reactor; LOFA; Fluent; Comsol; transient;

T5-P1: Applications and Importance of Radiochemical Separation Techniques in Biology, Geology, and Environmental Science

M. Messaoudi[@], A. Brahimi, A. Ouanezar, A. Malki, R. Lamouri, F. Arbaoui, S.A. Amzert and F. Rebhi

Reactor Chemistry Department, Nuclear Research Centre of Birine, P.O. Box 180, Djelfa, Algeria,
[@]Corresponding author m.messaoudi@crnb.dz

Background/Purpose: Radiochemical separation is a highly sensitive analytical technique used to isolate and identify radioactive isotopes in various scientific fields. Its primary purpose is to enhance the accuracy of isotope analysis by efficiently isolating specific radionuclides. This study highlights the significance of radiochemical separation in biology, geology, and environmental science, exploring its applications and *importance* [1].

Materials & Methods: Radiochemical separation utilizes well-established methods, including precipitation, solvent extraction, ion exchange, and chromatography, to isolate radioactive isotopes from complex mixtures. In biology, isotopes such as ^{14}C (carbon-14) and ^{131}I (iodine-131) serve as tracers in metabolic studies and medical imaging. In geology, radiometric dating methods like uranium- lead and potassium-argon dating rely on the isolation of specific isotopes to determine the age of rocks and fossils. Environmental applications focus on contamination monitoring, using radiochemical separation to isolate radionuclides such as ^{137}Cs (cesium-137) and ^{90}Sr (strontium-90) from soil, water, and air samples. Sample preparation involves chemical separation followed by precise measurement using gamma spectrometry and liquid scintillation counting

Results: Radiochemical separation has significantly improved analytical precision across multiple scientific disciplines. In biology, it plays a critical role in the production of radiopharmaceuticals used in imaging techniques such as positron emission tomography (PET) and single-photon emission computed tomography (SPECT), enhancing the diagnosis and treatment of diseases like cancer. Additionally, radiotracers facilitate in-depth studies of metabolic pathways and drug distribution. In geology, this technique is fundamental to radiometric dating, enabling scientists to reconstruct Earth's geological history, including volcanic activity and fossil records. In environmental science, radiochemical separation supports nuclear accident response efforts by tracking radioactive pollutants, ensuring environmental and public health safety.

Conclusion: With increasing global challenges in climate change, resource management, and public health, the demand for precise analytical methods continues to grow. Radiochemical separation remains a cornerstone in nuclear science, with ongoing advancements in automation, microfluidic separation, and enhanced spectroscopic techniques improving its efficiency and applications. Future research should focus on refining separation methodologies to further enhance sensitivity, reduce processing time, and improve environmental monitoring capabilities.sustainability.

References:

[1]. Kolupaev, D. N., & Apalkov, G. A. (2023). Development and Tasks of Radiochemical Technologies: History and Modern Challenges. *Radiochemistry*, *65*(2), 132-140. https://doi.org/10.1134/S1066362223020017

Keywords: Radiochemical separation, Environmental science, Contamination monitoring, Analytical techniques.

T5-P2: Radiological Impact Assessment of a Hypothetical Accident at the G.A. Siwabessy Research Reactor: Human and Environmental Exposure Using HotSpot and ERICA codes.

S. Roby[@], F.Z. Dehimi, A. Maâchou,

[1]*Centre de Recherche Nucléaire d'Alger*
[@]*Corresponding author s.roby@crna.dz*

Background/Purpose: This study assesses the impact of atmospheric radioactive releases following a hypothetical accident scenario at the G.A. Siwabessy Research Reactor [1] in Indonesia.
Materials & Methods: Three case studies were conducted under different meteorological conditions, considering variations in wind speed, atmospheric stability, and dispersion patterns. The total effective dose (TED) to humans was calculated using HotSpot, while the ERICA tool was applied to estimate dose rates for non-human biota. Four reference organisms, representative of the local ecosystem and not included in the ERICA database, were generated for the radiological impact assessment.
Results: HotSpot modelling indicated that the maximum total effective dose (TED) for the first 7 days of exposure was 2.0 mSv, which is well below the IAEA safety threshold of 100 mSv [2]. This value was observed 200 m from the release source under atmospheric stability condition A in case study 3. The thyroid dose for the same case was 20 mSv, remaining under the IAEA limit of 50 mSv. In contrast, ERICA analysis revealed that the dose rates to non-human biota were significantly higher. The highest values, ranging from 66.73 to 360.39 µGy/h, were recorded 400 m from the source in case study 3. These levels exceeded the IAEA screening limit of 10 µGy/h [3] for all reference organisms, indicating potential ecological risks.
Conclusion: While radiological exposure to humans remained below IAEA safety thresholds, non-human biota experienced dose rates exceeding environmental protection limits. These findings emphasize the necessity of integrating human and ecological risk assessments in nuclear safety studies. Future research should explore long-term ecological consequences and mitigation strategies for radiological contamination.

References:

[1]. A. Yuniarto, M. C. Hikmat, The Study of Atmospheric Dispersion Model on Accident Scenario of Research Reactor G. A. Siwabessy using HotSpot Codes as A Nuclear Emergency Decision Support System, Jurnal Teknologi Reaktor Nuklir, Tri Dasa Mega Vol. 21 No. 1, (2019), pp. 1-8.
doi: 10.17146/tdm.2019.21.1.5092
[2]. World Health Organization. (2015). Preparedness and Response for a Nuclear or Radiological Emergency. General Safety Requirements.
[3]. International Atomic Energy Agency, 2001, Generic models for use in assessing the impact of discharges of radioactive Substances to the environment. In: Safety Reports Series No. 19. IAEA, Vienna.

Keywords: Atmospheric dispersion, radiological impact, non-human biota, HotSpot modeling, ERICA code.

T5-P3: Comparative study of Iodine-131 released during a nuclear accident

A. Dadda Khorsi[1@], A. Bouam[1], A. Dahia[1], A. L. Cheridi Deghal[1], A. Kentouche[1], B. Bouali[2]

[1]Nuclear Research Centre of Birine, P.O. Box 180, Ain-Oussera 17200, Djelfa, Algeria [2]Process [2]Engineering Laboratory, AmmarTelidji University, Laghouat, 03000, Algeria [@]

Corresponding author: a.dadda@crnb.dz

Background/Purpose: Iodine-131 poses the greatest environmental contamination during a short-term nuclear accident. Because it is concentrated primarily in the thyroid gland, when it is released into the air and through ingestion or inhalation, it affects the thyroid gland of exposed populations. Hypothyroidism may result from complete or partial destruction of thyroid cells due to the radioactivity carried by absorbed iodine molecules.
At high doses, radiation can cause cell mutations and thyroid cancer, especially in children under five years of age and those exposed to pollution during pregnancy. Natural (non- radioactive) iodine pills are required in this case in order to iodine-saturate the thyroid.

Materials & Methods: This work aims to determine the total quantity of Iodine-131 released into the atmosphere using the Origen-JR code [1] and the HOTSPOT code [2] in order to assess the radiological effects on the environment and people in the initial stages following the accidents in Fukushima and research reactors. The Total Equivalent Dose (TED) and the Committed Effective Dose Equivalent (CEDE) values for thyroid are estimated and analyzed.

Results: The simulation results showed that the TED of the research reactor is about 0.06 Sv at a distance of 0.56 km from the source and the CEDE for thyroid is 48 mSv of equivalent dose to thyroid. In contrast, the TED was higher, about 2.7 Sv at 0.71 km from the source of the Fukushima reactor and the CEDE for thyroid is higher than 50 mSv of equivalent dose to thyroid. At these distances, the absence of inhabitants ensured that the population was not exposed to I-131 at the time of the accident for both reactors.

Conclusion: In the Fukushima accident, the TED and CEDE exceeds the IAEA standards annual regulatory limits [3]. Therefore, in case of iodine dispersion, the population needs Iodine prophylaxis and immediate evacuation. In contrast, in the case of the research reactor, the population does not need Iodine prophylaxis, but must be subject to sheltering.

References:

[1] Koyama, Kinji, Naoki, Yamano, shun-ich, Miyasaka, 1979. ORIGEN-JR: A Computer Code for Calculating Radiation Sources and Analyzing Nuclide Transmutations. Japan Atomic Energy Research Institute JAERI-M-8229.

[2] Steven, G., 2020. Homann and fernandealuzzi, HotSpot health physics codes, version 3.1.2. In: National Atmospheric Release Advisory Center. Lawrence Livermore National Laboratory, Livermore, CA 94550, USA.

[3] IAEA, Case Study On Assessment Of Radiological Environmental Impact From Potential Exposure, IAEA-TECDOC-1914. VIENNA 2020.

Keywords: **Fukushima reactor**; **Research reactor**; **Nuclear accident**; **Iodine-131 released; Radiological impact**; **Thyroid gland.**

T5-P4: Identifying the National NORM Inventory a First Step to Prevent its Spreading

F. Zidouni [1@] and M. Bogusław [2]

[1]*LMFTA Laboratory, Faculty of Physics, University of Sciences and Technology Houari Boumediene- USTHB, Algiers, Algeria*

[2]*Silesian Centre for Environmental Radioactivity, Central Mining Institute (GIG), Poland*

[@] *Corresponding author zidounifaiza@yahoo.fr*

Abstract: NORM (Naturally Occurring Radioactive Materials) refers to materials with high concentrations of natural radionuclides like ^{238}U, ^{232}Th and ^{40}K, which may emit radiation exceeding natural background levels. Originally confined within the earth, these materials can be released into the natural or human work environment through industrial activities like mining, drilling, and oil production, where various physical and chemical processes are employed. These processes result to increased NORM concentrations in products, by products, residues, waste, and liquid effluents. Moreover, in many practical scenarios, radionuclides accumulate in specific compartments of technological processes, leading to considerable radiological risks. Comprehensive radiological assessments are crucial for effective remediation, implementing radioprotection measures, and ensuring the safety of public health and the environment.

At the governmental level, before implementing protective measures, it is essential to conduct a national inventory of all active or dismantled industries potentially associated with enhanced natural radioactive materials. This study suggests a four-tier system for the inventory of technologically enhanced natural radioactive materials (TENORMs). The system encompasses the inventory of natural resources, ongoing mining industries, mineral processing industries, and the application and disposal of products. Subsequently, lifecycle analysis (LCA) methods are proposed to capture environmental impacts.

Inventory System using four tiers system of identification

1. Inventory of natural resources
2. Ongoing mining industry (including other underground workplaces)
3. Mineral processing industry
4. Product application and disposal

Application of LCA methods

LCA is a methodical tool used to assess the environmental impacts of a product, process, or human activity throughout its lifecycle, from raw material extraction and production to usage and waste disposal.

Conclusion: This communication urges environmental researchers and authorities to closely examine radiological pollution within the industrial sector. Algeria has several industries that generate massive amounts of NORM. The largest generator is the oil sector due to the large-scale exploitation of fossil fuels on which the Algerian economy is based. When there is no NORM management policy, the quantities generated become increasingly important. Therefore, it becomes necessary to find a treatment solution to guarantee the safety of workers in the concerned sectors and the cleanliness of our environment.

References:

[1]. Bogusław Michalik, ''How to build the national-level NORM inventory? An example developed from scratch'' NORM IX - The 9th International Symposium on NORM, September 23– 27, 2019 Denver, Colorado.

bmichalik@gig.eu

[2]. Naturally Occurring Radioactive Material (NORM VIII). Proceedings of an International Symposium Held in Rio de Janeiro, Brazil, 18-21 October 2016 Proceedings Series - International Atomic Energy Agency

Keywords: Technologically Enhanced Natural Radioactive Materials (TENORM), radionuclides, four-tier system, LCA.

T5-P5: Vitrification of a solid residue from the purification of an effluent

Y. Mouheb[1@], D. Moudir[1], N. H. Kamel[2], F. Aouchiche[1], A. Maachou[1]

[1] Nuclear Research Centre of Algiers
[2] *Retired from Nuclear Research Centre of Algiers*
2. Bd Frantz Fanon, B.P:399, AlgerRP, Algiers, Algeria
y.mouheb@crna.dz

Background/Purpose: The confinement of radioelements as toxic waste in aluminosilicate glass ensures environmental safety. Aluminosilicate glass is a highly resistant matrix capable of incorporating multiple elements into its chemical structure [1]. This study aims to investigate the vitrification of sulfonated polystyrene (PSS) residue as a second confinement barrier in glass. The objective is to assess the effectiveness of PSS incorporation and its potential for permanent isolation.

Materials & Methods: The aluminosilicate glass was synthesized using a mixture of different oxides, including [Na_2O, Al_2O_3, SiO_2, Y_2O, MoO_3 …]. The PSS content was varied at 2% and 6%. The glass mixture was melted in a furnace at T=1450°C for 1h30, with a heating rate of 5°C/min. The resulting glass pellets were characterized using X-ray diffraction to determine crystallinity, Fourier-transform infrared spectroscopy to identify chemical bonding, and density measurements to assess structural properties.

Results: XRD analysis confirmed that the synthesized glass matrices are amorphous, with no detectable crystalline phases. FTIR analysis identified characteristic bonds, including Al-O at 640-692 cm^{-1}, Si-O-M (M = Si, Al, Na) at 950-1100 cm^{-1} and SiO_4 vibration in the 1000-1200 cm^{-1} range. The measured density of 2.39 g/cm^3 aligns with reported values for aluminosilicate glasses, supporting the successful incorporation of PSS.

Conclusion: "The successful synthesis of aluminosilicate glass with PSS incorporation confirms its amorphous nature, as verified by XRD. FTIR analysis identified key structural bonds, including Si–O, Al–O, and Si–O–M linkages. These findings support the feasibility of PSS vitrification as a secondary confinement barrier for radioelement waste. Further studies will assess the long-term stability and leaching behaviour of the confined material.

References:

[1]. Gin S et al. Insights into the mechanisms controlling the residual corrosion rate of borosilicate glasses. *Npj Materials Degradation*.2020;*4*:41.

Keywords: aluminosilicate glass, PSS, confinement, radioelement

T5-P6: Operational safety assessment for disposal zone in near- surface repository site

S. Zare Ganjaroodi[1], M. Fani[1], A.M. Farsani[2], N. Amrani[@3]

[1] *Energy and Physics Department, Amirkabir University of Technology, 424 Hafez Ave., Tehran, Iran*
[2] *Iran Radioactive Waste Company (IRWA), Atomic Energy Organization of Iran (AEOI), Postcode: 1439955931, Tehran - Iran*
[3] *Department, Faculty of Sciences, Ferhat ABBAS University, 19000, Setif, Algeria*
[@] *Corresponding author: naima2073@yahoo.fr*

Background/Purpose: According to IAEA reports, around 95% of existing Radioactive Waste (RW) has Very Low Level (VLLW) or Low-Level (LLW) radioactivity, while about 4% is intermediate Level Waste (ILW) and less than 1% is High-Level Waste (HLW) [1]. The main aim of present paper is to discuss the safety assessment of Iranian RW repository site in the operational phase for disposal zone in conservative terms using monte carlo codes.

Materials & Methods: Anarak RW disposal, a near-surface trench-type repository, is the most suitable site for the VLLW and LLW disposal which is selected according to the national and international requirements and fundamentals during eight years' site selection phase. In this study, both normal operation and accident scenarios for solid and solidified RW barrels and overpacks [2] in disposal zone are modelled to calculate the dose reached to employees and environment by the MCNPX and SuperMC codes which are general-purpose, continuous- energy, generalized-geometry, time-dependent monte carlo radiation transport tools for nuclear and radiation physics simulation.

Results: The maximum surface dose is associated with solidified waste containing concentrated salt, which reaches approximately 15 mSv/h for 600 barrels per year. In contrast, the surface dose from solidified waste containing sludge is around 0.305 mSv/h for 15 barrels per year. Moreover, In the event of collecting the leaked waste during the accident scenario, workers within 20 cm of the RW will be exposed to 1.55 mSv/year after 30 minutes of exposure. On the other hand, the use of concrete overpacks for final disposal significantly reduces the dose received by the workers.

Conclusion: The radiation dose to employees and the environment during both normal operation and accident scenarios remains below the acceptable limits set by the IAEA. Additionally, given that the repository site is 25 km from the city center, there is no risk to the public during the accident scenarios. Hence, The Anarak site has been meticulously designed with a strong emphasis on safety, fully adhering to national and international standards and regulations.

References:

[1]. IAEA Tecdoc, Classification of Radioactive Waste, General Safety Guide (No. GSG-1), 2009, *IAEA* (Vienna), https://www-pub.iaea.org/MTCD/Publications/PDF/Pub1419_web.pdf.

[2]. IAEA Project, Safety Assessment Methodologies for Near Surface Disposal Facilities (Results of a co-ordinated research project), 2004, *IAEA (Vienna)*, https://www-pub.iaea.org/mtcd/publications/pdf/isam/iaea-isam-vol1_web.pdf.

[3]. IAEA Tecdoc, Disposal of radioactive waste, specific safety requirements No. SSR-5, 2011, *IAEA (Vienna)*, https://www-pub.iaea.org/MTCD/Publications/PDF/Pub1449_web.pdf.

Keywords: **Radioactive Waste, Safety Assessment, Operation, Near-surface, Dose.**

T5-P7: Modelling the Dispersion of Respirable and non-Respirable Radioactive Release.

A. Gheziel [a@], A. Ghadbane [a], A. Loubar [a]

[a] *Nuclear Research Center of Birine (CRNB)/COMENA*
[@] *Corresponding author a.gheziel@crnb.dz*

Background/Purpose: The atmospheric dispersion of radioactive substances, whether respirable (ϕ < 10 µm) or non-respirable (ϕ > 10 µm), is a major issue in nuclear safety and environmental and health risk management. This issue is particularly crucial in the context of industrial accidents, controlled releases or incidents involving radionuclides. A thorough understanding of dispersion mechanisms is essential to limit population exposure and minimize environmental impacts. The main objective of this study is to develop and refine atmospheric dispersion models by integrating the physicochemical properties of the source terms, as well as meteorological and topographical conditions.

Materials & Methods: This study focuses on the numerical modeling of the cobalt-60 atmospheric dispersion, a radionuclide commonly used in industrial and medical applications, during a hypothetical release in a radiological accident. The HotSpot code is used to assess the respirable fraction influence on the spatial distribution of radioactive contamination, as well as the potential radiological impacts on the population and the environment. The simulations are performed under specific and well-defined meteorological conditions. A series of numerical simulations are performed by varying the respirable fraction (RF) from 0 to 1. The radioactive activity considered in all simulations is set at 3.72×10^{12} Bq.

Results: This approach highlights a significant difference in the dispersion behaviour of respirable and non-respirable particles. Due to their small size, respirable particles can be transported over long distances by air currents, increasing their potential for large-scale contamination and their dispersion in areas far from the source. In addition, this method allows to quantify the risks associated with the inhalation of radioactive particles and to assess the potential radiological consequences on public health and the environment.

Conclusion: The results highlight the importance of considering particle size in the management of radiological accidents, particularly due to the ability of respirable particles to disperse over long distances. These conclusions contribute to the optimization of prevention and response strategies, thus strengthening the protection of populations and the environment against radiological risks.

References:

[1]. Bathula Sreekanth et al. "Modeling the evolution of aerosol particles from a radiological dispersal device."Journal of Aerosol Science, Vol.181, Sept.2024. https://doi.org/10.1016/j.jaerosci.2024.106433

[2]. James L. Regens et al. "Estimating Total Effective Dose Equivalents from Terrorist Use of Radiological Dispersion Devices." Human and Ecological Risk Assessment: An International Journal, Vol. 13, 2007. https://doi.org/10.1080/10807030701506165.

[3]. Steven G. Homann. HotSpot Health Physics Codes Version 3.1.2 User's Guide. Lawrence Livermore National Laboratory, Feb. 11, 2020. LLNL-SM-636474.

Keywords: **Respirable and non-Respirable particles; Atmospheric dispersion; HotSpot modelling code; Cobalt-60; Radiological impact.**

T5-P8: Gamma Radiation Pretreatment for Enhanced Cellulose Extraction from Date Palm Waste

S. Benamer-Oudih@, A. Nacer khodja[1], D. Tahtat[1], S. Djenadi[2], Y. Benrezkellah[2]

[1] *Algiers Center for Nuclear Research, BP-399 Algiers, Algeria*
[2] *National Polytechnic Schools, Algiers, Algeria*
@ *Corresponding author s.oudih@crna.dz*

Background/Purpose: Date palm waste, abundant in lignocellulose, presents a sustainable and promising source of cellulosic material for various applications. This study explores an innovative approach to cellulose extraction from date palm fibers and leaves (*Phoenix dactylifera L.*) by introducing gamma radiation into the separation process.

Materials & Methods: Date palm waste, including leaves and fibers, was harvested from local agricultural fields in palm groves located in the province of Adrar. The effects of gamma radiation on the biomass's chemical composition specifically lignin [1], cellulose, and alpha cellulose [2], as well as the quality of the extracted cellulose, were thoroughly examined. Characterization techniques including FTIR, XRD, DTA-TGA, and SEM were employed to assess the material.

Results: The findings demonstrate that gamma irradiation enhances the biomass's degradability, resulting in a notable increase in alpha cellulose content following delignification. Fourier Transform Infrared spectroscopy confirmed the complete elimination of lignins and hemicelluloses by the disappearance of the corresponding functional groups, in addition to an abundance of cellulosic groups, showing a high degree of similarity to commercial cellulose especially that isolated from fibers treated with gamma rays.
Differential thermal analysis (DTA) and thermogravimetric analysis (TGA) showed that the cellulose extracted from fibers and leaves pre-treated with gamma radiation was of higher purity, reflecting its stable crystalline structure. X-ray diffraction analysis showed that the application of irradiation, particularly to the fibers, led to the elimination of amorphous zones, resulting in an increase in the crystallinity index to 69.5%.

Conclusion: Physico-chemical analyses confirm that gamma radiation improves the quality of the extracted cellulose, indicating its potential as an effective pretreatment method. This approach could produce cellulose of competitive quality and cost compared to cellulose derived from other biomass sources.

References:

[1]. Shaikh H et al. Isolation and Characterization of Alpha and Nanocrystalline Cellulose from Date Palm (Phoenix dactylifera L.) Trunk Mesh. *Polymers*. 2021;13, 1893. doi:10.3390/polym13111893

[2]. Al-Awa Z et al. Effect of leaf powdering technique on the Characteristics of Date Palm-Derived Cellulose. *ACS Omega.* 2023;8, 18930−18939. doi:10.1021/acsomega.3c01222

Keywords: Date palm waste; valorization; cellulose; gamma radiation.

T5-P9: Rare Earth Elements Distribution in Clays: A Study via k_o-Instrumental Neutron Activation Analysis

L. Hamidatou[1@], A.K. Aklouf[2]

[1] *Nuclear Research Centre of Draria, PB43, Draria, 16050 Algiers, Algeria.*
[2] *Department of Physics, Faculty of Sciences, USTHB, BP32 Bab Ezzouar, 16111-Algiers, Algeria.*

[@]Corresponding author: l-hamidatou@crnd.dz

Background/Purpose: Rare earth elements (REEs) are indispensable in advanced technologies and industrial applications, driving the need for detailed characterization of their natural sources. This study investigates the distribution and concentration of REEs in Algerian clay samples using the k_o-Instrumental Neutron Activation Analysis (k_o-INAA) method. The aim is to provide precise evaluations of both light and heavy REEs while exploring the geological factors influencing their variability.

Materials & Methods: Eight clay samples (ARG01 to ARG08) collected from distinct geological formations in Algeria were analyzed to quantify REE concentrations in mg/kg. The k_o-INAA method was chosen for its high precision and ability to accurately profile elemental concentrations. Variability in REE distribution was correlated with the geological characteristics of the sampling sites to elucidate the influence of environmental and mineralogical factors.

Results: Substantial variability in REE distribution was observed among the samples. Light REEs such as cerium (Ce: 1.05–82.01 mg/kg), lanthanum (La: 0.758–38.75 mg/kg), and neodymium (Nd: 0.302– 32.63 mg/kg) were found in higher concentrations compared to heavy REEs. Among the heavy REEs, notable levels of ytterbium (Yb: 0.29–3.27 mg/kg), terbium (Tb: 0.14–0.725 mg/kg), and gadolinium (Gd: 1.505–49.42 mg/kg) were detected in specific samples. Samples ARG02 and ARG04 exhibited significant enrichment in REE concentrations, strongly influenced by their geological origins.

Conclusion: This study demonstrates the potential of Algerian clays as strategic resources for high-value industrial and technological applications. The comprehensive REE profiles provide critical insights into the distribution of these elements, laying the groundwork for sustainable exploitation and economic development. By leveraging Algeria's natural resources, this research supports advancements in materials science, environmental technologies, and industrial innovation.

References:

[1] L. Hamidatou et al. Determination of rare earth elements in Algerian bentonites using k_0-NAA method. Radiochimica Acta, vol. 112, no. 1, 2024, pp. 45-52. https: // doi.org/10.1515/ract2023-0210.

[2] Hamidatou, L et al. Determination of chemical elements in two Algerian bentonites by k_0-NAA and WDXRF techniques. J Radioanal Nucl Chem 332, 573–580 (2023). https://doi.org/10.1007/s10967-023-08787-7.

Keywords: Rare earth elements, Algerian clays, k_o-INAA, elemental analysis, resource valorization, light REEs, heavy REEs, sustainable development.

T5-P10: Comparative study of the retention kinetics of total phenolic compounds from olive oil mill discharges by adsorption, conventional and under microwave irradiation, on natural soils

M. Arabi-Hocine[1], B. Mansouri[1@], A. Elias[2]

[1] *Nuclear Research Center of Algiers, Algeria*
[2] *Faculty of Sciences, Mouloud MAMMERI University of Tizi-Ouzou, Algeria*
[@] *Corresponding author b.mansouri@crna.dz*

Background/Purpose: Olive oil wastewater is an effluent rich in non-biodegradable pollutants that affect the ecosystem. This work focuses on the application of three different natural soils to remove total phenolic compounds (TPC) from olive oil crushing water by adsorption in two modes: conventional and under microwave irradiation. The effect of contact time was studied. Kinetic modeling was performed using reaction and diffusion based models. The results indicate that the pseudo-second-order model is favorable in both modes, and microwave irradiation accelerates the adsorption of TPC.

Materials & Methods: The adsorbate was collected according to the ISO 5667-3 standard in a dark jerrycan. Different characterizations were carried out on these materials: the TPC content, pH, and electrical conductivity were measured for the olive oil discharge, and on the other hand, the pH, specific surface, morphology by SEM, functional groups, and pHpzc were determined for natural soils. Microwave irradiation was carried out in a modified domestic microwave oven. Adsorption was carried out in batch for both modes. The residual quantity of TPC was measured according to the Box method [2].

Results: The results showed that the liquid discharge studied is representative of olive effluents (acid pH). The soils differ from each other by the color, which is most likely related to their compositions; also, the morphology shows that two of the adsorbents have a porous surface, unlike the third, which appears with a rough image. The adsorption kinetics is described by the pseudo-second-order reaction model. The rate of the kinetics of elimination of TPC is variable in both adsorption modes. It is found that under conventional conditions, the retention is maximum (36.693%) by soil N_1, unlike the conditions under microwave irradiation where the retention of TPC reached 33.151% by soil R'.

Conclusion: Although the results of the kinetic study for all the pollutants show that the retention of TPC is very rapid under microwave irradiation conditions, the retention rate is better under conventional conditions.

References:

[1]. NI ISO 5667-3. Qualité de l'eau- Echantillonnage. Partie 03: Conservation et manipulation des échantillons d'eau. 2012.

[2]. Box JD. Investigation of the Folin–Ciocalteu phenol reagent for the determination of polyphenolic substances in natural waters. *Water Research*. 1983; 17:511-525.

Keywords: Adsorption; total phenolic compounds; natural soils; kinetics.

2

T5-P11: Investigation of Nuclear Radiation Shielding Properties of BaO, V_2O_5, and TeO_2-Based Glasses

A. Alomari[1@], O. Bawazeer[2], S. Al-Qahtani[2], A. Ismail[3], T. Alnaemi[4], I. Alshaikhi[4], A-W. Ajlouni[5]

[1]*Physics Department, Al-Qunfudah University college, Umm Al-Qura University, Makkah, Saudi Arabia.*

[2]*Physics Department, College of Science, Umm Al-Qura University, Makkah, Saudi Arabia*

[3]*Physics Department, Education College, Salahaddin University-Erbil, 44001, Erbil, IRAQ*

[4]*Radiology Department, Al-Qunfudah General Hospital, Ministry of Health, Saudi Arabia* [5]*Scientific Consultant, Anfas Arabia Group, Riyadh, Saudi Arabia*

[@] *Corresponding author ahomari@uqu.edu.sa*

Background/Purpose: Although ionizing radiation is crucial for various aspects of modern life, it poses risks when interacting with biological tissues; hence, appropriate shielding is required. Lead is the conventional shielding material; however, its toxicity, its opacity, and its heavy weight highlight the need for better alternatives. Glasses have been introduced as an alternative material due to a number of advantages including their low melting point, low cost, simplicity of preparation, high thermal stability, and transparency [1].

Materials & Methods: This study examined the radiation shielding characteristics of various tellurite glass structures with compositions of $xV_2O_5 - (35\text{-}x)\ BaO - 65TeO_2$, where $5 < x < 30$ mol%. These samples were synthesized using the conventional melt-quenching method. Phy-X software [2] and XCOM program [3] were employed to study the fundamental shielding parameters, including MAC, LAC, HVL, TVL, MFP, Z_{eff}, N_{eff}, EBF and EABF. The computations were conducted over wide photon energy ranges (0.015–15 MeV).

Results: The methods (Phy-X and Xcom) provided similar results, with a 6.73% average standard deviation, confirming the data's accuracy. The shielding efficiency of the investigated samples followed the order: S1 > S2 > S3 > S4 > S5 > S6. For example, the maximum LAC was achieved for S1, with values ranging between 0.18 cm^{-1} and 231.94 cm^{-1}, while the minimum LAC was recorded for S6, varying between 0.14 cm^{-1} and 158.80 cm^{-1}.

Conclusion: The obtained results indicate that the investigated tellurite glasses, particularly those containing higher BaO concentration, are effective, environmentally friendly, transparent, and safe radiation shielding materials, making them valuable for radiation-related applications.

References:

[1]. Alomari, A. H. (2024). Elucidating the multiple contributions of increasing MoO3 concentration on phosphate glasses for radiation safety applications. Radiation Physics and Chemistry, 218, 111593.

[2]. Şakar, E., Özpolat, Ö. F., Alım, B., Sayyed, M. I., & Kurudirek, M. (2020). Phy-X/PSD: development of a user friendly online software for calculation of parameters relevant to radiation shielding and dosimetry. Radiation Physics and Chemistry, 166, 108496.

[3]. Berger, M. J., & Hubbell, J. H. (1987). XCOM: Photon cross sections on a personal computer (No. NBSIR-87- 3597). National Bureau of Standards, Washington, DC (USA). Center for Radiation Research.

Keywords: Tellurite glasses; radiation shielding; BaO; Phy-X; Xcom

T5-P12: Kinetic study of the effect of gamma irradiation dose on the adsorption of Rovamycin by a composite material

M. Arabi-Hocine[1], K. Remil[2@], C. Bouarnouna[3], I. Ghebraoui[3], M. Bouarnouna[3], B. Mansouri[1]

[1] *Nuclear Research Center of Algiers*
[2] *Nuclear Research Center of Draria*
[3] *Faculté des Sciences et Technologie- Université de Blida 1, Algérie*
[@] *Corresponding author k-remil@crnd.dz*

Background/Purpose: The present study focuses on the effect of the gamma irradiation dose on the adsorption kinetics of rovamycin by composite materials. The retention of this antibiotic is closely related to this parameter. The adsorbent beads equilibrate with the macrolitic solution after 270 minutes, and the maximum adsorption capacity is 20 mg/g. In addition, the adsorption obeys the pseudo-first-order kinetics for the bioadsorbent prepared based on orange peel powder (OPP) irradiated at 4 kGy and the intra-particle model for those prepared based on OPP irradiated at 1, 2, and 3 kGy.

Materials & Methods: The composite adsorbent prepared in the form of beads is based on sodium alginate (Na-A) and OPP [1]. The latter was previously irradiated before the design of the adsorbent at different doses at 15 Gy/min. The gamma radiation is emitted by a sealed source of Co-60. The adsorption of the macrolide named rovamycin (3 M.I.U., SAIDAL, Algeria) was carried out in batch mode. The molecular weight of Na-A was determined by Ubbelohde viscometer according to the Mark-Houwink equation [2].

Results: Activation of OPP by gamma irradiation increased the elimination rate of rovamycin, and the result of the adsorption kinetics study test of adsorbate confirmed it. The highest adsorption rate initially reached 61.36 %. After optimization of the parameters (hydration rate and amount exposed to gamma ray), this rate increased to 67.17 %.

Conclusion: This study showed that the use of a new bio-adsorbent prepared from less expensive agro-food waste (orange peels) irradiated as materials and a polymer (sodium alginate) can be a good alternative for the treatment of water loaded with pharmaceutical pollutants. It is therefore suggested to continue the adsorption process by varying the other remaining parameters, namely pH, concentration, mass quantity, etc.

References:

[1]. Remil K. Et al.. Development of new composite adsorbents (agro-food waste/sodium alginate) raw and treated with gamma ionizing radiation for solid-liquid separation: study test of adsorption kinetics of spiramycin. *Proceeding of the Second International Congress on Energy and Industrial Processes Engineering ICEIPE'24*. 2024, 595-596.

[2]. Ramsackal KN et al.. Determination of intrinsic viscosities and Mark-Houwink-Sakurada constants for sodium alginates. *Caribbean Science and Innovation Meeting.* 2019; Le Gosier, France. (hal- 02899128).

Keywords: Natural soils; adsorption; kinetics; isotherm; modelling.

T5-P13: Adsorption of Sr^{2+} Ions from Aqueous Solution: Optimization Study

A. Brahimi[1@], N. Boucherit[2], M.L. Yahiaoui[3], M. Messaoudi[1], A. Bouaichaoui[2], A. Ouanezar[1], A. Malki[1], F. Rebhi[1], N. Kaci[1] and R. Lamouri[1]

[1] *Nuclear Research Center of Birine (CRNB), COMENA, BP180 Ain Oussera , Djelfa, Algeria.*
[2] *Department Sciences of material, Faculty of Sciences, University of Medea, BP (26000) Algeria.*
[3] *Department of Physics, University of Jijel, Algeria.*
[@] *Corresponding author Abdelkarim.brahimi@crnb.dz*

Background/Purpose: For a technological application in the field of water treatment, mathematical optimization study is carried out by exploiting the results obtained in the laboratory.

Materials & Methods: The influence of physico-chemical parameters such as: (initial concentration of Sr^{2+}, Agitation speed, temperature, pH of the solution, amount of adsorbent), on the removal of Sr^{2+} ions from aqueous solution is conducted in batch mode [1]. The results obtained in the parametric study are used to carry out statistical modelling [2]

Results: The parametric study allowed to establish an experimental database, multiple regression is used with second degree polynomial terms, and with interaction terms to predict the response according to the parameters as well as the precision of the model. The independent parameters selected are: the amount of the adsorbent (X_1, g/l), the initial concentration of Sr^{2+} (X_2, mg/l) and the temperature of the solution (X_3, K). The adsorption capacity of Sr^{2+} (q_e, mg/g) is retained as the response. the model formula is:

$$q_e = a_0 + a_1 X_1 + a_2 X_2 + a_3 X_3 + a_{11} X_1^2 + a_{22} X_2^2 + a_{33} X_3^2 + a_{12} X_1 X_2 + a_{13} X_1 X_3 + a_{23} X_2 X_3.$$

the value of the coefficient of determination R^2 is greater than 0.99. Optimal regions (maximum adsorption capacity values) are obtained in the contour map.

Conclusion: A perfect linearity is obtained by comparing the predicted values of the model with the values obtained through experiments, the value of R^2 indicates that the model is efficient. The contour map indicates that the maximum values of the adsorption capacities are obtained at low amount of adsorbent and at high concentrations of Sr^{+2}. The optimization study allowed us to minimize the number of experiments, achieve maximum capacities and save time, which opens up perspectives on the application on a technological scale in the field of water treatment.

References:

[1].Brahimi A, Mellah A,Hanini, S.(Adsorption of strontium (II) ions from aqueous solution onto bottom ash of expired drug incineration). Journal of Radioanalytical and Nuclear Chemistry (2021), 330,929-940. https://doi.org/10.1007/s10967-021-08054-7.

[2]. Brahimi A et al. (Optimization of adsorption capacity: Application of mathematical modeling). ICMSE'2024, The 3rd edition of the international conference on materials science and engineering and their impact on the environment, Université djilali liabés Sidi Bel Abbés Algeria (2024).

Keywords: Adsorption; Optimisation ; ions Sr^{2+}; Mathematical model.

T5-P14: Assessment of the Radioactivity Level of Algerian Phosphate Wastewater

S. Soltani [1@], T. Azli [2], F. Zidouni [3]

[1] *Physical Chemistry of Surfaces and Interfaces Research Laboratory of Skikda (LRPCSI), August 20th; 1955 University, 26 El Hadaiek, Skikda, Algeria*

[2] *Nuclear Research Centre of Draria CRND, / COMENA. Algiers, Algeria*

[3] *LMFTA Laboratory, Faculty of Physics, University of Sciences and Technology Houari Boumediene- USTHB, Algiers, Algeria*

[@] *Corresponding author* s.soltani@univ-skikda.dz

Abstract: The study aimed at evaluating the level of gamma radioactivity in wastewater around the Djebel-Onk/TEBESSA phosphate deposit due to phosphate ore extraction activities in the Bir El Ater region. To achieve this, two sites were selected for liquid sampling, including two samples. The analysis method using hyper-pure gamma spectrometry GeHp allowed the identification and quantification of radioelements from the natural series of 235U, 232Th, and 40K. The activity of the two radioelements, 214Pb and 214Bi, was exploited to determine the volumetric activity of 226Ra.

Materials & Methods: Two samples (wastewater and industrial water) were collected and placed in a plastic Marinelli beaker of 450 cm^3 volume using paraffin tape and stored for 24 days to achieve secular equilibrium between 226Ra and its short-lived descendants, as well as 222Rn, before being analysed by gamma spectrometry. The activity concentrations of 226Ra, 232Th, 235U, and 40K in water samples were determined using gamma-ray spectrometry. The efficiency calibration is theoretically carried out by the MCNPX code [1].

Results The activity of the radionuclides is calculated using the values of emission probability and efficiency for each gamma ray. For the 232Th, the activity was calculated as 372.38 ± 111.47 mBq/L and 221.66 ± 81.09 mBq/L for the industrial and wastewater, respectively. The activity of 235U was calculated to be 200.50 ± 41.6 mBq/L and 136.14 ± 30.52 mBq/L for the industrial and wastewater, respectively. Finally, the 226Ra concentration in the water was estimated using the activities of 214Pb and 214Bi to be 248.92 ± 47.63 mBq/L and 194.08 ± 33.98 mBq/L for industrial water and wastewater, respectively.

Conclusion: These values obtained in this work are considered to be very important for human public health and the environment. We also need to address the chemical pollution caused by the treatment of phosphate with heavy metals [2]. To assess the combined radiation and chemical pollution in an area, a more comprehensive study is required. Efforts should be made to find suitable solutions to safeguard public health and the environment.

References:

[1]. Azli T et al.. Performance revaluation of a N-type coaxial HPGe detector with front edges crystal using MCNPX, Applied Radiation and Isotopes 97 (2015) 106–112.

[2]. Ahmad N et al.. Health implications of natural radioactivity in spring water used for drinking in Harnai, Balochistan. International Journal of Environmental Analytical Chemistry. 2019;101(9):1302- 1309.

Keywords: NORM; Radioactivity; Phosphate; Gamma Spectroscopy; Wastewater

T5-P15: Design and development of Supervisory environment GMSAS for radiological early warning Monitoring system for National Network detection

M.F. Belazreg[1@], A. Hammadi[2], M. Maache[2], M. Boudria[2], D. Taieb-Errahmani[2], A.C. Chergui[3] A. Yaiche[4] and A. Messaadi4

[1]*Department of Nuclear Safety*

[2]*Department of Radioecology and Environmental monitoring*

[3]*Department of Nuclear Physics, Nuclear Research Centre of Algiers, Algeria*

[4]*Nuclear Research Centre of Birine, Algeria*

[@]f.belazreg@crna.dz

Background/Purpose: The GMSAS system (Gamma Monitoring Supervisory Algeria System) is a real-time data acquisition system for gamma dose rate ambient. It allows the measuring instruments of gamma dose rate ambient and early notification in case of nuclear or radiation accidents. It combines radiological monitoring by gamma detection with SCADA applications and automatic local stations network. The program for monitoring and controlling the national territory and nuclear facilities. It offers a clear and instantaneous view of instrument measurements on all nuclear sites and its neighboring environment. However, the program was developed under the LabVIEW environment with an ergonomic and interactive graphic screen for displaying gamma instrument measurement data and MySQL data information system to store and retrieve historical measurements. In conclusion, this software called "GMSAS Platform" allows the display of data with statistical calculation values and to detect an emergency situation if it occurs.

Materials & Methods: The development of supervisory Software was carried out using the LabVIEW environment applications and MySQL database. The special radiation supervisory computer system for radiation protection measuring system of national territory, which is used for centralized display management and control of various event of the gamma dose rate ambient environment system. In addition, it sends data from probe instrument to the computer and control system via communication protocol GSM/TCP to meet radiation measurements over the territory requirements under normal state and emergency condition.

Results: In this paper, we focused our work on the development Software and aspect of the radiation protection supervisory system for early detection response to nuclear and radiological accidents. The central unit performs data collection and alarm routines using MySQL and display data gamma dose rate measurements to the operators. The display programs allow the user to view the data in numerical or graphical format with alarm.

Conclusion: We have focused our study in the development of GMSAS Software of a SCADA environmental information system. Its main tasks are collecting measurement data, performing alarm checking routines and presenting the data to authorized users. In the future the collected gamma dose rate measurements will provide a basis for the use of dispersion models conducted by researcher that will help to estimate the degree of risk for the inhabitants in a given situation.

Keywords: Gamma Detection measurement, Supervisory control system; LabVIEW Datalogging Supervisory Control, Network Communication GSM/TCP.

T5-P16: Development of a Cost-Effective System for Environmental Radiation Monitoring and Mapping

H. Mekki[1@], A. Bourenane[1], K. Remita[1], B. Zahra[1], N. Hebboul [1]

[1] *Centre de recherche Nucléaire de Birine, CRNB, Ain Ouessera, Djelfa, Algeria.*
[@] *Corresponding author h.mekki@crnb.dz*

Background/Purpose: Radiation monitoring is essential for ensuring environmental safety, particularly in areas near nuclear facilities, medical institutions, or sites handling radioactive materials. Traditional radiation monitoring systems often involve high costs, limited portability, and complex deployment. To address these challenges, this study aims to develop a low-cost and efficient radiation detection and monitoring system.

Materials & Methods: The developed system includes radiation measurement stations for detection and data transmission, as well as a central collection station for data reception, visualization, analysis, and mapping. Each measurement station is equipped with a Geiger- Müller (GM) counter for radiation detection and low-cost electronics, such as microcontrollers, to process environmental radiation events [1]. Radiation data are transmitted in real time via the Global System for Mobile Communications (GSM) network using a short message service (SMS). A low-cost GSM electronic module bridges the microcontroller and the GSM network, enabling seamless transmission of environmental radiation data to a remote workstation that integrates software for processing, display, and mapping. Environmental radiation data are transmitted at regular intervals, which can be configured by the users. The system operates on a 12V DC power supply sourced from the electrical network, with a 12V battery integrated as a backup to ensure uninterrupted operation.

Results: The system was successfully tested under various radiation conditions. In addition to detecting environmental radiation in the test area, which ranged between 80 nSv/h and 150 nSv/h, the system was evaluated using Cs-137 gamma radiation source with an activity of approximately 24 kBq, at varying distances from the GM detector. All measurement demonstrated excellent agreement with those obtained using a standard dosimeter, with uncertainties not exceeding 20 nSv/h in the range of 80 nSv/h to 200 µSv/h.

Conclusion: A cost-effective and scalable system for monitoring and mapping environmental nuclear radiation, using open-source low-cost electronics was presented. Its low-cost and versatile design allows adaptation to diverse monitoring scenarios, providing a robust tool for effective radiation management and safety.

[1]. A. H. Zakaria, Y. M. Mustafah, J. Abdullah, N. Khair, and T. Abdullah, "Development of Autonomous Radiation Mapping Robot," Procedia Comput. Sci., vol. 105, pp. 81–86, 2017, doi: https://doi.org/10.1016/j.procs.2017.01.203.

Keywords: **Low cost electronics; radiation monitoring; mapping;**

T5-P17: Natural material treated by heat used to remove uranium from diluted solution

M. Bellaloui[1@], M. Bennemla[1], N. Bayou[1]

[1] *Nuclear Research Center of Draria*
[@] *Corresponding author: m-bellaloui@crnd.dz*

Background/Purpose: Marl, a carbonate clay of Plaisancian age, is the main constituent of our aquifer substratum. This material was taken from the watershed of wadi Al-Ghoula at the Draria site after drilling to depths of 30m.In other words, the impermeable lower part that retains groundwater. This material contains, in addition carbonates, clays whose retention toxics metals, is much known. A previous uranium retention studies have been investigated by using marl at raw state, gave a retention capacity of q_e=6.04 mg/g. [1]. The main aim of this work is to determine the influence of the marl heat treatment (300°C) to the retention capacity of uranium in solution.

Materials & Methods: The heat treatment, was made by using a muffle furnace heat at 300°C for four hours. The characterization work contains the particle size distribution, the determination of the specific surface area by Brunauer, Emmet and Teller theory, the functional analysis by Fourier Transform Infrared Spectroscopy, fluorescence analysis and finally Thermo-gravimetric/Derivative Thermo-gravimetric analysis. The in-batch uranium retention study using the treated marl sample as an adsorbent, will begin by optimizing the adsorption parameters. It will be followed by a kinetic and a diffusion study. Finally, the non- linear study of two- and three-parameter isotherms has been carried out.

Results: The particle size distribution of both samples is bimodal and the heat treatment applied did not modify its particle size. For the two samples, the adsorption and desorption isotherms and the pore size distribution indicate a predominance of the mesoporous character, with specific surface area values for raw and treated sample are respectively equal to 18.24 m2/g and 17.48 m2/g. The heat treatment caused a slight decrease in the mass contents for all elements and especially for major elements such as Si, Ca, Al, Fe and K and caused a slight progressive decrease in the intensity of the FTIR transmittance band signal. The optimal conditions of adsorption of uranium into treated marl was obtained. The kinetic study follows the pseudo-second order model and the diffusion process is controlled simultaneously by the intraparticle diffusion and the liquid film diffusion. The retention capacity obtained is q_e=3.90 mg/g and the non-linear data processing showed that this adsorption phenomenon follows the Sips isotherm

Conclusion: The heat treatment doesn't affect the raw marl in their physic-chemical proprieties but the value of retention capacity obtained (q_e=3.90 mg/g) is less than obtained by the raw form. So the treatment at 300°C is not a good opportunity to the adsorption of uranium.

References:

[1]. Mourad Bellaloui and al.. Marl collected from aquifer substratum of nuclear site used to remove uranium from solution. Journal of Radioanalytical and Nuclear Chemistry. 2024 doi.org/10.1007/s10967-024-09505-7

Keywords: Uranium; adsorption; marl; isotherms; heat treatment.

T5-P18: Application of environmental isotopes in the study of groundwater resources in arid zones.

D. Khous [a@], H. Chorfi [a], M. E. Cherchali[*], A.S. Moulla[*], S.A. Ouarezki[a]

[a] *Algiers Nuclear Research Centre, P.O. Box 399 Alger-RP, 16000 -Algiers – Algeria.*
[@] *Corresponding author d.khous@crna.dz*
[*] *retired scientist from the Algiers Nuclear Research Centre*

Background/Purpose: In Algeria, the issue of water availability is of a major concern for the water sector and great efforts are made in order to ensure water allocation to people as the resource becomes scarcer with time. In this socio-economic and climatic context, water resources in the Saharan Atlas (arid zones) remain poorly understood. Environmental isotopes (^{18}O,^{2}H,^{3}H) and Hydrochemical information are combined to determine the mechanism controlling chemistry and to identify natural or anthropogenic processes that control groundwater quality, as well as the source, the origin and the timing of recharge.

Materials & Methods: A field campaign has been carried out in the region of interest in October 2022. 23 sampling sites were visited, measured and collected for groundwater. Major elements were analyzed through high performance ion liquid chromatography (HPILC, Aquion). Stable isotope contents ($\delta^{18}O$, $\delta^{2}H$) were analyzed using a laser absorption spectrometer [1]. Tritium content was measured by liquid scintillations Spectrometry.

Results: The chemical compositions of the groundwaters show that the water samples fall into the Cl-SO4-Ca type. The $\delta^{18}O$ and $\delta^{2}H$ compositions of groundwater, for the present samples vary from -8.38 to -2.97‰ and from -58.7 to -28.8‰, respectively, with a mean value of -7.28‰ for $\delta^{18}O$ and -48.4‰ for $\delta^{2}H$. The majority of the samples values are distributed between the Meteoric Water Line for the western Mediterranean region where the deuterium excess is 14 per mil (WMWL: $\delta^{2}H = 8\ \delta^{18}O + 14$) [2] and the Global Meteoric Water Line (GMWL: $\delta^{2}H = 8\delta^{18}O + 10$) for precipitation of oceanic origin.

Conclusion: The mineralization of groundwater results from the dissolution of evaporates minerals (halite, anhydrite/gypsum) and ion-exchange processes. Environmental isotopes indicate that the aquifer recharge is a mixture of both old and recent waters. The excess deuterium in the groundwater suggests a predominant mixture of rainfall originating from the Atlantic and the western Mediterranean basin.

References:

[1]. Penna D, Stenni B, Sanda M, Wrede S, Bogaard TA, Gobbi A, Borga M, Fischer BMC, Bonazza M, Chárová Z.. On the reproducibility and repeatability of laser absorption spectroscopy

measurements for $\delta^{2}H$ and $\delta^{18}O$ isotopic analysis. Hydrol Earth Syst Sci.2010; 14(8):1551– 1566. doi. org/ 10. 5194/hess- 14- 1551.

[2].Celle-Jeanton H, Travi Y, Blavoux B.. Isotopic typology of theprecipitation in the western Mediterranean region at the three different time scales. Geophys Res Lett. 2001; 28:1215– 1218. https:// doi.org/ 10. 1029/ 2000g l012407.

Keywords: groundwater; arid zones; hydrochemistry; isotope;

T5-P19: Assessing Aquifer Recharge in the Southwestern Saharan Atlas: Insights from Isotopic and Precipitation Analysis

H. Chorfi[1@], D. Khous[1], M.S. Belksier[2], A. Zeddouri[2], S. Ouarezki[1], M.E. Cherchali[3]

[1] *Algiers Nuclear Research Centre, Department of Nuclear Technical Applications, 2, Bd Frantz Fanon, PO Box 399 Alger-RP, 16000, Algiers, Algeria.*

[2] *Oil Underground Reservoirs Laboratory, Gas and Aquifers, Hydrocarbons Faculty, Renewable Energies and Earth and Univers Sciences, Kasdi Merbah University, Ghardaïa road, BP. 511, 30000, Ouargla, Argelia.*

[3] *Retired scientists from Algiers Nuclear Research Centre*

[@] *Corresponding author h.chorfi@crna.dz*

Background/Purpose: Arid regions face critical water resource challenges due to scarce precipitation and high evaporation rates. This study evaluates aquifer recharge dynamics in the Abiodh Sidi Cheikh syncline in the South-Western Saharan Atlas using an integrated approach combining precipitation analysis and isotopic techniques. The objective is to assess groundwater recharge processes, residence times, and circulation patterns to ensure sustainable water management strategies in arid environments.

Materials & Methods: Stable isotopes ($\delta^{18}O$, $\delta^{2}H$) and radioactive tritium (^{3}H) were used to assess aquifer recharge. Stable isotopes, naturally present in precipitation, help trace groundwater's origin and mixing processes. Tritium, derived from atmospheric fallout, is a temporal tracer used to estimate the age of water and recharge periods. [1].

Results: The results indicate a dual recharge mechanism involving recent and ancient water sources. Shallow aquifers are influenced by contemporary precipitation with high tritium levels, while deeper aquifers contain older, slow-moving water. Groundwater residence times range from 13 to 32 years, with velocities of 0.91 to 9.95 m/year. Climatic factors like evaporation and precipitation intensity are key in isotopic fractionation and recharge processes. [2,3].

Conclusion: The study explores the recharging mechanisms of the Abiodh Sidi Cheikh syncline in the Southwestern Saharan Atlas, revealing a dual mechanism influenced by both modern and fossil water sources. The study also highlights the challenges of dry recharging procedures due to variations in residence times and groundwater flow rates.

References:

[1]. Zamora H.A.; and all. Evaluation of groundwater sources, flow paths, and residence time of the Gran Desierto Pozos, Sonora, Mexico. Geosciences 2019. doi:10.3390/geosciences9090378.

[2]. Hibbs B.J. Commentary and review of modern environmental problems linked to historic flow capacity in arid groundwater basins. Geosciences 2022;12:124

doi: 10.3390/geosciences9090378

[3]. Clark, I.D., & Fritz, P. Environmental Isotopes in Hydrogeology (1st ed.). CRC Press. 1997. doi:10.1201/9781482242911

Keywords: Aquifer recharge; Isotopic techniques; Arid regions; Tritium;

T5-P20: Effect of soil organic matter and clay content on activity concentrations of caesium-137 variations at the field scale.

A. Dilmi[1@], S. Benarousse[2], A. Azebouche[2], I. Chaibi[3], S. Radjemi[3], A. Arabi[2]

[1] National Forest Research Institute
[2]Algiers Nuclear Research Centre [3] Saad Dehleb University, Blida
[@] Corresponding author amal.dilmi@yahoo.fr

Purpose: The aim of this work was to demonstrate the existence of a close relationship between soil organic matter content, clay content and 137Cs concentration (widely used in the study of soil water erosion) at field scale.

Materials & Methods: The study site, which covers about 0.5 hectares, is located in the El Meurdja Arboretum, one of the northernmost foothills of the Blidean Atlas. It is located about 40 km south of the Algerian capital. Altitudes range from 850 to 1,000 m, with an average of 900 m, and slopes vary from 17% to 50%. The study area has a cool, humid Mediterranean climate, with rainfall ranging from 50 to 100 mm and temperatures ranging from 4 to 16°C in the cold season, rising to over 30°C in the summer.

Eleven soil samples were collected along a transect slope within the plot (0.5 ha). Four sampling points were selected to be representative of the topography, at soil depths of 0-5, 5-10 and 10-20 cm, with a distance of 20 m between two adjacent points [1]. After homogenisation of the soil samples, activity concentrations of 137Cs were determined by gamma spectrometry at the CRNA Nuclear Technology Laboratory. Clay and organic carbon contents were determined at the INRF Soil Science Laboratory using the Robinson pipette and the Anne method, respectively.

Results: The results obtained show that the organic matter content varies from 0.12% recorded in the 10-20 cm layer on the flat (zero slope) to 5.44% recorded in the 5-10 cm layer in the middle of the slope, with an average of 4.06%. Clay content ranged from 19.45% in the 0-5 cm layer at the centre of the slope to 32.3% in the 5-10 cm layer on the flat, with an average of 24.19%. 137Cs values ranged from 1.40 Bq/kg in the 0-5 cm layer at the top of the slope to 7.91 Bq/kg in the 5-10 cm layer at the bottom of the slope (accumulation site), with an average of 4.24 Bq/kg. Analysis of these results shows that the vertical and horizontal distribution of the parameters studied is variable due to disturbance of the surface layer of the soil by tillage on the one hand and by erosion on the other. There is a close relationship between clay content and 137Cs concentrations, but this proportionality varies according to the topography. However, a very weak relationship was observed between organic matter content and 137Cs concentrations. This latter finding contradicts the study by Ritchie and McCarty [2], which highlighted the existence of a relationship between caesium and organic matter.According to [3]. Dumat C., Staunton [3], the adsorption of caesium in soils, and therefore its mobility and availability, is largely determined by clay content and mineralogy. The presence of organic matter can lead to significant changes in the soil.

Conclusion: This work was carried out with the aim of demonstrating the existence of a relationship between organic matter content, clay content and 137Cs concentration within an agricultural field subjected to particle movement.

The results obtained show the existence of a proportional relationship between clay content and 137Cs concentration, a relationship consistent with several studies carried out worldwide. On the other hand, a weak relationship was observed between organic matter content and 137Cs concentrations. Most of the studies carried out in this context have demonstrated the existence of such a relationship. In the context of this study, topography, tillage and erosion are factors that

greatly influence the mobility of soil particles and their various components (clays, organic matter, minerals, etc.), both vertically and horizontally, which would explain the relationships highlighted. In order to obtain more accurate results, it is therefore important to carry out more detailed studies on the possible relationships between the different clay minerals, the humic fractions of the soils and caesium.

References:

[1]. Ksouri Y. Estimation de l'érosion hydrique à l'aide du 137 cs et de la variabilité de certains descripteurs de sol à l'échelle du champ. Mém. (M. Sc), Université Laval, Canada. 2004:70. https://www.collectionscanada.gc.ca/obj/s4/f2/dsk4/etd/MQ90777.PDF?is_thesis=1&oclc_number=60318553

[2]. Ritchie, J.C. and McCarty, G.W. ^{137}Cesium and soil carbon in a small agricultural watershed. Soil and Tillage Research. 2003;69: 45-51.

[3]. Dumat C., Staunton S.. Reduced adsorption of caesium on clay minerals caused by various humic substances. Journal of Environmental Radioactivity. 1999;46:187-200.

Keywords: soil; organic matter; clay; caesium ;

T5-P21: Radiological Scanning of the Environment around Draria site

A. Hammadi@, D.Taieb Errahmani, M.Maache, M.Boudria, M. Ziouche

Centre de Recherche Nucléaire d'Alger (CRNA)

a-hammadi@crna.dz

Background/Purpose: As part of the national radiological monitoring program, the CRNA initiated periodic monitoring around the Draria site using continuous radiological scanning. This monitoring involved mobile equipment (FHT 1376) and fixed stations (MFM-202 and MFM-203) units from the national early warning network. The data collected enabled the evaluation of both terrestrial and cosmic radiation contributions and the mapping of gamma dose rates using GIS tools. This quarterly monitoring is motivated by the presence of a 1 MW nuclear research reactor and recent urban expansion. The results show an average terrestrial gamma dose rate aligned with UNSCEAR guidelines, highlighting the need for a comprehensive approach to accurate radiological assessments.

Materials & Methods: The monitoring was conducted using a mobile system "MobiSys FHT 1376" which includes a 5-liter plastic scintillator detector coupled with a GPS and a portable computer. The software "Mobisys" is used for the data collection and treatment. This setup enabled the recording of both geographical coordinates and dose rates at each measurement point. With the use of Natural Background Rejection (NBR), the system could differentiate between natural and artificial radiation. After the field campaign, the raw data were processed using ArcGIS software within a Geographic Information System (GIS) to generate dose maps [1].

Results: The measurement routes for ambient gamma radiation using the FHT 1376 mobile unit were designed to cover the entire reactor security perimeter. A spatial distribution of the ambient gamma dose rate, generated using ArcGIS, showed an average dose rate of 25nSv/h, ranging from 13nSv/h to 50nSv/h, primarily reflecting terrestrial radiation, excluding cosmic contributions. The total gamma dose rate recorded by the MFM-202 and MFM-203 stations of the National Radiological Alarm Network was 98nSv/h, including cosmic radiation. According to UNSCEAR guidelines, cosmic radiation typically accounts for 30-40% of the total gamma dose rate at sea level [1]. For this study, a 40% contribution (39nSv/h) was assumed. After subtracting the cosmic component, the gamma dose rate attributed to terrestrial radiation measured by the MFM monitors was 59nSv/h, which aligns with the UNSCEAR 2008 report for Algeria, citing a terrestrial gamma dose rate of 54nGy/h [2].

Conclusion: The ambient gamma dose rate measurements, taken 1 meter above ground level, provide essential data for radiological monitoring around the NUR research reactor and establish a baseline for the CRND nuclear facility. The results emphasize the need to consider environmental and instrumentation factors in radiological assessments. The notable difference in air-absorbed dose values between the mobile system and MFM monitors is due to overestimation by the MFM monitors, caused by the inherent background of the detector and surrounding construction materials.

References:

[1] United Nations Scientific Committee on the Effects of Atomic Radiation (UNSCEAR). (2000). Sources and Effects of Ionizing Radiation. UNSCEAR 2000 Report to the General Assembly, with Scientific Annexes.

[2] United Nations Scientific Committee on the Effects of Atomic Radiation UNSCEAR. Sources and effects of ionizing radiation (2008). Report to the general assembly, Exposures from natural radiation sources.

Keywords: Scanning; MFM Monitor; ambient gamma dose rate ; cosmic contribution; national radiological alarm network.

T5-P22: Study of the head on collision of two dust acoustic solitary waves in a strongly coupled dusty plasma where the electrons and the ions are kappa-distributed

S. Kadi[2@],R.Annou[1],A.Tahraoui[2],A.Ferdi[1],W.Saddok[2]

[1] *Theoretical Physics Lab., Faculty of Physics, USTHB, Algiers, Algeria*
[2] *Quantum Electronics Lab, Faculty of Physics , USTHB, Algiers, Algeria*
[@] *Corresponding author* samirov_44@yahoo.fr

Background/Purpose The study of nonlinear phenomena, and in particular the head on collision of two oppositely propagating dust acoustic solitary waves (DA), in non-magnetized, strongly coupled dusty plasmas whose electrons and ions are kappa-distributed, taking into account the ion drag force. [1]. The characteristics of the wave, i.e. amplitude, width, phase velocity and phase shift after a collision, are established and evaluated numerically.

Materials & Methods: The Poincaré-Lighthill-Kuo technique PLK extended perturbation method is used to investigate the consequences of a head-on collision. Based on this method, we introduce the stretched coordinates [1-2] and analyze the low amplitude solitary waves. Is derived a couple of KdV equations governing the propagation of right and left solitary waves, which are solved and their solutions and phase shifts are found. We investigate the effect of the superthermality of electrons and ions (the spectral index ke, ki) on the characteristics of the waves, namely the amplitude, the wave speed, the phase shift and the wavelength

Results: The ion drag force has the effect of speeding gradually the propagation of two solitary waves, where the wave velocity is reduced when electrons and ions are taken to be supra-thermal. The coefficient "A" in the KdV equation is an important parameter that determines the amplitude, stability and interaction of solitary waves. The distribution of electrons and ions increases both speed and wavelength as the spectral index κi increases.

Conclusion: Two nonlinear Kortewege-de Vries equations (KdV) whose solutions make it possible to describe the characteristics and the propagation trajectories of the two colliding waves, are established by the Poincaré-Lighthill-Kuo technique.The resulting 3D surface diagram illustrates amplitude (Φ) visually as a function of spectral indices (κi, κe). This visualization allows us to understand the impact of changes in ion and electron distribution on amplitude during head-on collision, where the stability and interaction of solitary waves, it increases with increasing spectral index κi.

References:

[1]. S. Kadi, R. Annou, K. Annou, *Contrib Plasma Phys* **2023**, e202300004.
doi https://doi.org/10.1002/ctpp.202300004

[2]. Saini, N. S., and Kuldeep Singh. "Head-on collision of two dust ion acoustic solitary waves in a weakly relativistic multicomponent superthermal plasma." *Physics of Plasmas* 23.10 (2016).
doi: https://doi.org/10.1063/1.4963774

Keywords: Solitary waves; Ion drag force; KDV equation; PLK method; Spectral index

T5-P23: Influence of Carbonates on Radium Sorption in Soils: Distribution, Toxicity, and Environmental Risks

A. Kessab[1@], K. Guimeur[1], A. Mecelti[2], N. Mebriouk [3]

[1] *Department of Agronomy, Mohamed Khider University, Biskra*
[2] *Mohamed Chérif Messadia University, Souk Ahras*
[3] *Faculty of Technology, LMGHU Laboratory, 20 August 1955 University, Skikda, Algeria.*
***E-mail** : Kessab.amira@hotmail.fr*

Background/Purpose : This study evaluates the impact of carbonate-rich soils on the sorption and desorption behavior of radium, a radioactive element with significant environmental implications. Conducted in Djelfa, an area characterized by high limestone content, the research investigates how carbonate concentrations influence radium retention and its potential for environmental contamination.

Materials and Methods: Three soil types with varying carbonate content (low, medium, and high) were analyzed. Physicochemical characterization included pH, mineral composition, and organic matter content. Radium sorption experiments were conducted under controlled conditions, varying parameters such as contact time, pH, temperature, agitation speed, and initial radium concentration. Sorption capacity was evaluated using adsorption isotherms, and retention efficiency was compared across soil types.

Results: The study found that radium sorption followed a pseudo-second order kinetic model, indicating that the process is predominantly physico-chemical (R^2 = 0.995–0.990). Thermodynamic analysis confirmed that adsorption was spontaneous and exothermic, with Gibbs free energy values (ΔG^o) ranging between -8.2 and -10.3 kJ/mol and enthalpy changes (ΔH^o) between -12.4 and -14.2 kJ/mol. These findings suggest that sorption is more effective at lower temperatures. Furthermore, soils with higher carbonate content exhibited greater radium retention, reducing its mobility and potential groundwater contamination.

Conclusion: This study highlights the significant role of carbonates in influencing radium sorption, which in turn affects its environmental behavior and contamination risk. The findings suggest that carbonate-rich soils may help limit radium dispersion, reducing its bioavailability in groundwater and agricultural soils. Future research should explore additional factors affecting radium retention and investigate soil remediation strategies, including stabilization techniques and risk assessment models for radioactive pollutants.

References:

[1]. Smith J. et al. "Interaction of Radioactive Elements with Carbonates." Environmental Science and Technology, 2018.
[2]. Brown, R. et al. "Sorption and Desorption Processes of Radium in Contaminated Soils." Environmental Chemistry Journal, 2020.

Keywords: Radium sorption, carbonates, radioactive contamination, soil remediation, environmental management.

T5-P24: Development setup of low-level gamma-ray spectrometry using an MCNP – Gammavision combined method.

T. Azli[a@], S.Mazidi[a], S. Benbouzid[a], A. Hadri[a], Y. Amrane[a] M. Aliane[a]

[a]*Centre de Recherche Nucléaire de Draria*
[@]*Corresponding author t-azli@crnd.dz*

Background/Purpose: The Neutron Activation Analysis Laboratory at the Nuclear Research Centre of DRARIA has utilized an N-type High-Purity Germanium (HPGe) detector for the radioactivity measurement of highly activated small samples (mg-scale) for nearly two decades. To broaden the scope of this system, we aim to implement its use in environmental radioactivity monitoring. This requires the precise measurement of very low radioactivity levels in potentially complex matrices and large-volume samples (kg-scale). Achieving this represents a significant challenge with promising implications for future research. This study outlines the setup and optimization of the gamma-ray spectrometry laboratory, detailing the detector configuration and the experimental protocols designed for routine environmental monitoring. An optimized MCNP program was adapted to calculate the full energy peak efficiency for close-geometry measurements of voluminous radioactive sources.

Materials & Methods: A detailed Monte Carlo model of the N-type High-Purity Germanium (HPGe) detector was developed, incorporating a mono-energetic, multi-gamma source within a 450 cm^3 Marinelli beaker. This model was tailored for the analysis of large volume environmental samples and calibrated using experimental measurements.

Results: The computed efficiencies closely matched the experimental values, with a variance of only 5%. This agreement underscores the reliability of the method for environmental sample measurements.

Conclusion: The integration of MCNP calculations with the Gammavision-32 system demonstrates that an optimized HPGe detector model can accurately compute environmental sample activities for various geometries and matrices. This eliminates the need for costly calibration standards or corrections for coincidence summing once the detector geometry is well-characterized. The results offer a robust foundation for future applications in environmental dosimetry and radiological research.

Acknowledgments: The authors are very grateful to Dr Hakim MAZROU from the Nuclear Research Centre of Algiers (CRNA) for its precious help with regard to the MCNP software.

References:

[1]. Agarwal, C., Danu, L.S., Gathibandhe, M., Goswami, A., Biswas, D.C., 2014. nuclear Instruments and Methods in Physics Research A 763240-247.

[2]. Andreev, D.S., Erokhina K.I., Zvonov, V.S., Lemberg, I.Kh., 1972. Prib. Tekh. Eksp. 5, 63-65.

[3]. Andreev, D.S., Erokhina, K.I., Zvonov, V.S., Lemberg, I.Kh., 1973. Izv. Akad. Nauk SSSR. Ser. Fiz. 37 (8), 1609-1612.

Keywords: gamma spectrometry, MCNP , Gamma vision, efficiency, dosimetry

T5-P25: Natural radioactivity concentration measurement and the estimation of radiological impact in "ACHASTA" bentonite deposit by using γ-Ray Spectrometry technique.

S. Achour[1,*], S. Bouzid[1], T. Azli[1], D. Groune[1]

[1]*Draria Nuclear Nuclear Research Center, B.P.43, 16003, Sebala- El Achour-Draria, Algiers, Algeria;*
[*]*Corresponding author: S-ACHOUR@crnd.dz*

Background/Purpose: Bentonite is a clay commonly used in industry. Some bentonite deposits may contain concentrations of natural radionuclides such as uranium, thorium and their decay products, which may contribute to radiological exposure. Therefore, it is important to assess these exposures and implement appropriate radiation protection measures in order to limit the harmful effects of these radiations on the environment and workers' health.
The main purpose of this work is the radiological characterization of a bentonite sample collected from the "ACHASTA" bentonite deposit, one of the most economically important quarries in western Algeria, by measuring the concentration of natural radionuclide activities using gamma spectrometry, which offers a powerful analysis tool in this study.

Materials & Methods: The study sample was collected and prepared using several unit operations, and then it was sealed during 35 days for secular equilibrium before measurement. The spectra acquisition was carried out using a gamma spectrometry chain, equipped with high-resolution (FWHM) semi- conductor detector HPGe, of about 1.8 keV at 1332.5 keV γ-ray peak of 60Co. The spectra were analyzed using Gamma vision software dedicated to the gamma spectra processing. We specify that during the assessment of the radiological impact, the necessary radioprotection criteria were taken into account. The obtained results are discussed and compared according to the global average value, reported by UNSCEAR.

Results: The obtained results reveal the presence of natural radioactivity in the studied sample, which is mainly due to the presence of three series of long-lived natural radioelements namely: 238U, 332Th and their derivatives as well as the great affinity of K+ ions due to the presence of 40K, preferentially adsorbed in bentonite soils, which makes them highly radioactive. The values of activity concentrations are (26.715 ± 2.689), (34.415 ± 3.531), (4.576 ± 0.438), (22.584 ± 2.277) and (73,456 ± 3.703) (in Bq.kg -1) respectively, for 226Ra, 238U, 235U, 232Th and 40K radionuclides. The external doses rate of gamma radiation physically, absorbed by the deposit workers as well as the Annual Effective Dose Equivalent obtained are 41.39 nGy/h and 0.102 mSv/y respectively.

Conclusion: This study revealed that the presence of natural radioactivity in the ACHASTA deposit sample is mainly due to the decay series of U-238. The determination of the impact and the associated radiological risk recorded an exceedance on these sites due to the high concentration of radionuclides according to UNSCEAR. The nuclear technique of gamma spectrometry has proven to be a good tool for radiological characterizations of bentonite.

Keywords: Natural Radioactivity, Bentonite deposit, Radiological risk, γ-spectrometry, HPGe detector.

T5-P26: Application of Nuclear Techniques in the fight against desertification: Soil-to-Plant Transfer Factors as Indicators of Soil Degradation

H. Silhadi[1@], S. Benarous[1], A. Azbouche [*], A. Arabi[1], A. Dilmi[2], L. Boudraa[1].

[1]*Nulcear Research Center of Algiers, 02 Bd. Frantz Fanon, B.P. 399, Alger RP, Algiers, Algeria.*
[2]*National Institute for Forest Research, Bainem, Algiers, Algeria.*
[*]*Retired from Nuclear Research Center of Algiers, 02 Bd. Frantz Fanon, B.P. 399, Alger RP, Algiers, Algeria*

[@]*Corresponding author: h.silhadi@crna.dz*

Background/Purpose: To assess soil quality and potential contamination in El Meurdja Arboretum, ten soil and respective plant samples were collected and analysed in the laboratory. These analyses aimed to distinguish between natural soil and anthropogenic soil pollution. Additionally, the soil-to- plant transfer factor [1-2] was calculated to assess elemental accumulation in vegetation, providing valuable insights into nutrient dynamics, environmental risks, and the identification of potential candidates for phytoremediation.

Materials & Methods: Soil and plant samples were collected from five sites within the El Meurdja Arboretum, at an altitude of 600–1100 meters. After an appropriate samples preparation (air-dried, sieved, and homogenized), gamma spectrometry was used to detect and quantify radioactive elements, while ED-XRF analysis with calibration performed using certified reference materials, was used to evaluate the presence of heavy metals.

Results: Our investigation at the El Meurdja Arboretum has provided critical insights into soil degradation processes and contamination risks in the region. Gamma spectrometry confirmed expected levels of natural radioelements but also revealed localized Cs-137 accumulation, signalling potential erosion concerns. ED-XRF analyses highlighted a magnesium deficiency in plants and significant contamination by heavy metals. While the soil-to-plant transfer of radionuclides remains low, the selective accumulation of certain heavy metals-particularly specific plant species could be effective candidates for phytoremediation.

Conclusion: These findings underscore the need for continued environmental monitoring, targeted soil management strategies, and further research into the role of native vegetation in mitigating heavy metal pollution and enhancing soil resilience.

References:

[1] Vandenhove, H., et al. "Proposal for new best estimates of the soil-to-plant transfer factor of U, Th, Ra, Pb and Po." *Journal of Environmental Radioactivity* 100.9 (2009): 721-732.

[2] Mirecki, Nataša, et al. "Transfer factor as indicator of heavy metals content in plants." *Fresenius environmental bulletin* 24.11c (2015): 4212-4219.

Keywords: Soil erosion; ED-XRFs; Gamma-spectrometry; Cesium-137; heavy metal.

T5-P27: Radioactivity Evaluation of U-238, Th-232 and K-40 in Tea Samples

F. Kadem[1@], R. Bensedira[1], N. Belouadah[1] , L. Yettou[1]

[1 a] *USTHB, Faculté de Physique, Laboratoire SNIRM, B.P. 32, El-Alia, 16111, Bab Ezzouar, Algiers, Algeria*
[@] *Corresponding author kademassiae@gmail.com*

Background/Purpose: Tea is one of the most consumed beverages worldwide. Cultivated in many countries, including China, India, and Kenya, the tea plant produces various types of tea, with black and green tea being the most popular and widely marketed.
The quantification of naturally occurring radionuclides in the tea using gamma spectrometry is a methodology used to measure radiation levels in tea samples. This method relies on the detection of gamma radiation emitted by radioactive isotopes present in the tea, such as Uranium-238 (^{238}UU), Thorium-232(^{232}TTh) and Potassium-40 (^{40}KK). These samples were analysed using a gamma spectrometry system equiped with a HPGe detector.

Materials & Methods: For our study, we used marketed tea from different regions and of different colors. Three boxes of commercial tea, each weighing 125 g, were dried, ground, and sieved to obtain a uniform particle size of the samples. The samples were prepared and measured by a high resolution HPGe semi-conductor detector with (1.8 keV for Co-60 1332.5 keV Energy). The spectra were analyzed using the Genie 2000 software dedicated to the processing of gamma spectra. The efficiency calibration of the gamma spectrometry chain was obtained experimentally

Results: All analysed samples allowed to determine the activity concentrations of K-40, Th-232, and U-238 using high-resolution gamma spectrometry. The results were compared to those obtained by Roberto Cruz da Silva et al. [1]. The activity concentrations due to K-40 range from (568,110±45,658 to ($822{,}725 \pm 44{,}189$) Bq.kg^{-1}, and from ($15{,}353 \pm 6{,}646$) Bq.
Kg-1 to ($37{,}875 \pm 15{,}506$) Bq.kg-1 for Th-232. The highest activity concentrations were found for K-40. This can be explained by a high radionuclide transfer factor, linked to specific metabolic processes involving potassium in plants. Therefore, the quantification of other radionuclides shows lower concentrations than K-40. Traces of Cs-137 with low specific activity were detected in two samples.

Conclusion: The objective of the present study was to determine the natural radioactivity of the three most consumed and marketed tea samples. The activity concentrations for Ra- 226 were lower. The radium equivalent values are in accordance with international standards. Finally, the radiation dose was determined for the 3 radionuclides with range from 0.23 to 0.34 mSv/year and show the tea ingestion does not pose any significant radiological health risk to the population.

References:

[1] Roberto Cruz da Silva et al., Radiological evaluation of Ra-226, Ra-228 and K-40 in tea samples: A comparative study of effective dose and cancer risk, Applied Radiation and Isotopes 165 (2020) 109326

[2] Gökmen, I. G., Birgül, O., Kence, A., & Gökmen, A. Chernobyl radioactivity in Turkish tea and its possible health consequences. Journal of Radioanalytical and Nuclear Chemistry, 198, 1995,p487.

Keywords: Tea; Gamma spectrometry; natural radioactivity; Detector.

T5-P28: pH-Sensitive Alginate/PVP Matrix for Oral Delivery of Penicillin via Gamma Irradiation Crosslinking

D. Tahtat[a@], H. Bendjedda[b], S. Benamer[a], A. Nacer Khodja [A]

[1]*Algiers Center for Nuclear Research, BP-399 Algiers, Algeria*
[2]*Algiers university Benyoucef Benkhedda, 02 bd Didouche Mourad, Algiers, Algeria*

[@]*Corresponding author : djtahtat@crna.dz*

Background/Purpose : Penicillin G, a β-lactam antibiotic, suffers from instability under acidic conditions, requiring injectable administration [1]. This study investigates a polymeric hydrogel matrix combining alginate and polyvinylpyrrolidone (PVP) crosslinked by gamma irradiation to encapsulate penicillin. The objective is to protect the drug from gastric acidity and to achieve controlled release in the intestinal tract.

Materials & Methods: Alginate/PVP beads were synthesized via ionic gelation of alginate, followed by gamma irradiation to crosslink PVP. Characterization techniques included encapsulation efficiency by UV spectrophotometry, gel fraction determination, swelling behavior assessment in simulated gastric (FSG) and intestinal fluids (FSI) [2], and penicillin release kinetics. FTIR spectroscopy analyzed molecular interactions.

Results: Encapsulation efficiency was consistent across formulations, ranging from 37 to 46%. Gel fraction increased proportionally with alginate concentration and irradiation dose, reaching a maximum of 63% for beads irradiated at 10 kGy. Swelling behaviour was pH- sensitive, with minimal swelling in FSG and significant expansion in FSI. Beads irradiated at 10 kGy exhibited reduced swelling rates due to enhanced crosslinking. Penicillin release was gradual and dependent on bead composition and irradiation dose. Beads containing 3% alginate and 5% PVP reached 100% release within 3 hours in FSI, whereas beads containing 5% alginate and 5% PVP required up to 5 hours, with slower release observed at higher irradiation doses. In FSG, cumulative release was limited, ranging from 23 to 59%, confirming drug retention in acidic environments and targeted release in intestinal conditions. FTIR analysis revealed chemical interactions between alginate and PVP, with the formation of new bonds under irradiation, indicating structural synergy. These modifications contributed to the beads' stability and controlled release properties.

Conclusion: The alginate/PVP matrix demonstrated high potential for controlled-release applications, offering efficient encapsulation and tailored release profiles suitable for therapeutic use. The results support further development and evaluation in advanced biological models.

References:

[1] M.E. Pichichero (2005). A review of evidence supporting the American Academy of Pediatrics recommendation for prescribing cephalosporin antibiotics for penicillin-allergic patients. Pediatrics, 115(4), 1048-1057.DOI: 10.1542/peds.2004-1276.

[2] D. Tahtat, M. Mahlous, S. Benamer, A. Nacer Khodja. (2013). Oral delivery of insulin from alginate/chitosan crosslinked by glutaraldehyde. International Journal of Biological Macromolecules. 58 160-168.

Keywords: Penicillin encapsulation, Alginate-PVP matrix, Gamma irradiation, Controlled release, pH-sensitive hydrogel.

T5-P29: Study of the effect of solar radiation on Plants: a case study of the sunflower plant

M. Boukabcha[a, B] and K. El Miloudi[c]

[a] *Physics department, Faculty of Exact Sciences and Informatics, Hassiba BENBOUALI University of Chlef, Algeria*
[b] *Laboratory of Theoretical Physics and Physics of Materials, Hassiba BENBOUALI University of Chlef, Algeria*
[c] *Department of Sciences and Technology, Faculty of Technology, Hassiba BENBOUALI University of Chlef, CHLEF, Algeria*
[@] *Corresponding author: MAAMAR BOUKABCHA, Email: m.boukabcha@univ-chlef.dz*

Background/Purpose: This study aims to analyse the impact of solar radiation on human health, animals and plants as well as microorganisms in the Algerian coasts, focusing on sunflower plants. Solar radiation is essential for heating in humans and animals and photosynthetic activities in plants. However, excessive solar radiation can lead to harmful consequences for human, animals and plants as well as microorganisms.

Materials & Methods: In this study, we are using wavelet analysis for wavebands of sunlight on the sunflower plants inside a greenhouse place on the ground of Hassiba BEN BOUALI University of Chlef, Chlef, Algeria. The study examines patterns and trends in hourly solar radiation as ultraviolet radiation and light data from late February to early June 2016 for the sunflower plants.

Results: The results reveal important associations between solar radiation levels, particularly visible and ultraviolet radiation, and health outcomes for living organisms such as plants, and their effects on sunflower yield, growth and health in the study sites. Greenhouses also play an important role in reducing the impact of climate change and solar radiation dose, in addition to the biochemical reactions that occur internally and the absorption of solar energy by the sunflower plant, which results in the occurrence of photosynthesis, which is beneficial to plant life.

Conclusion: These results highlight the urgent need to contribute to health interventions and to carry out a specific and high-quality agricultural design related to the sunflower plants at all stages of its growth and development during its life cycle, which is approximately 100 days depending on the type of sunflower plants, in order to mitigate the negative effects of solar radiation in the selected sites, such as avoiding staying in the sun for a long time in the Chlef region and Algerian coasts, and using plastic houses for sunflower plants and other seasonal plants.

References:

1. Abdolahpour, M., M. Hambleton, and M. Ghisalberti. 2017. "The Wave-Driven Current in Coastal Canopies." Journal of Geophysical Research: Oceans 122, no. 5: 3660–3674.
2. Awal, M. A., Koshi, H. and Ikeda, T. (2006). Radiation interception and use maize/ peanut intercrop canopy. Agric. and Forest Meteorol. 139 : 74-83.
3. Adeyemi O, Awange JL, Agutu NO (2019) Spatial variability of solar radiation in Nigeria. RenewableEnergy 136:788–800

Keywords: Solar radiation; sunflower Plant; radiation Impact; plant growth; Plant

T5-P30: Assessment of Terrestrial Radiation Based on Ambient Gamma Dose Rates Measured by the National Radiological Early Warning System.

A. Hammadi[1], M. Boudria[1@], M.Maache[1], F. Belazreg[1]

Centre de Recherche Nucléaire d'Alger (CRNA)

m.boudria@crna.dz

Background/Purpose: For the majority of individuals, natural background radiation constitutes the largest portion of their overall radiation exposure. Among these sources, indoor radon (Rn) typically represents the most significant contribution to public radiation exposure, surpassing even other natural sources [1]. The main goal of this study is to develop a methodology for estimating the terrestrial component of the ambient dose equivalent rate using the ambient gamma dose rate measurements from the 21 radiological stations within the national radiological alarm network. This approach is supported by strong correlations reported between indoor radon concentrations and gamma dose rates [2], as well as between ^{222}Rn flux and terrestrial gamma dose rates (TGDR).

Materials & Methods: This study employed instant measurements of the ambient equivalent dose rate recorded between 2020 and 2024 by 21 monitoring stations within the Algerian network. The monitoring setup included the MFM-202 devices installed at 12 stations and the MFM- 203 devices installed at eight stations, ensuring extensive data coverage. The extensive availability of data, with an average of 90% of instantaneous data recorded across all Algerian stations over the four-year period, highlights the robustness of the monitoring network.

Results: In this study, the terrestrial gamma dose rate (TGDR) is estimated from the total gamma dose rate (γ-total). The measured γ-total consists of constant contributions, such as cosmic radiation, artificial ^{137}Cs from the Chernobyl accident, and terrestrial radiation (^{238}U, ^{235}U, ^{232}Th series, and ^{40}K), along with variable components. The study aims to estimate the mean terrestrial background by subtracting the cosmic contribution and radon-related peaks from the total dose rate. Artificial ^{137}Cs from the Chernobyl and Fukushima accidents are assumed to be negligible. Based on data from 20 stations of the National Radiological Alarm Network (2020-2024), cosmic doses range from 42 to 56 nSv/h (average 45 nSv/h), while terrestrial radiation varies between 22 and 84 nSv/h (average 46 nSv/h). Cosmic dose is consistent across most stations, with altitude influencing the dose.

Conclusion: The method needs improvement, particularly in specifying the monitor's location to avoid placement irregularities affecting dose rate measurements. However, the results showed that In–Amguel station, located at 990m with granite-type soil (HOGGAR), shows the highest natural background radiation due to enhanced radioactivity from U-238, Th-232, and K-40. In contrast, northern regions with sedimentary soils have lower terrestrial gamma doses.

References:

[1] UNSCEAR. Sources and effects of ionizing radiation (2008). Report to the general assembly, Exposures from natural radiation sources.

[2] García-Talavera, M., García- Pérez, A., Rey, C., Ramos, L, 2013. Mapping radon-prone areas using -radiation dose rate and geological information, Journal of Radiological Protection,33, 605–620. DOI: 10.1088/0952-4746/33/3/605

Keywords: natural radioactivity; the terrestrial component of the ambient dose equivalent rate, instant measurements of the ambient equivalent dose rate; cosmic contribution; national radiological alarm network.

T5-P31: Evaluation of an Agro Forest System to Control Erosion by Using Byrylium-7 in Semi-Arid Region of Northern Algeria

A. Kessaissia[1@], A. Azbouche[2], B. Morsli[3] and A.S. Moulla[2]

[1]*INRF Ténès Experimental Station for Watershed Protection of INRF , T, Chlef, Algeria*
[2]*Algiers Nuclear Research Centre, PO Box 399, Alger-RP, 16000, Algiers, Algeria*
[3]*INRF Tlemcen Experimental Station for Soil Conservation, Tlemcen, Algeria*
[@]*Corresponding author: kabderrahman2014@gmail.com*

Background/Purpose: The present study illustrates an application of the Berrylium-7 in the evaluation of new system of plantation (agro forest system) initiated in 2019 in an area of Tifiles watershed located in the province of Chlef (north western Algeria).

Materials & Methods: Two different investigation sites situated in slope area were used: The first one with a plantation of the agro forest type and a second one without plantation. In each site a reference area was selected for comparison purposes.

Results: The ^{7}Be activity in the reference planted site was estimated at 434±22.67 Bq·m^{-2} whereas in the unplanted reference site it was 497±25.61 Bq·m^{-2}. Nevertheless, the relaxation mass depth is equal to 8.33 kg·m^{-2}in the first site and 5.55 kg·m^{-2}in the second one.

Conclusion: The results show that the planted site is characterized by a lower amount of soil loss than the site without planting. This reflects the positive effect of the agro forest system in controlling erosion in slope area.

Author Index

Ü

Y

Z

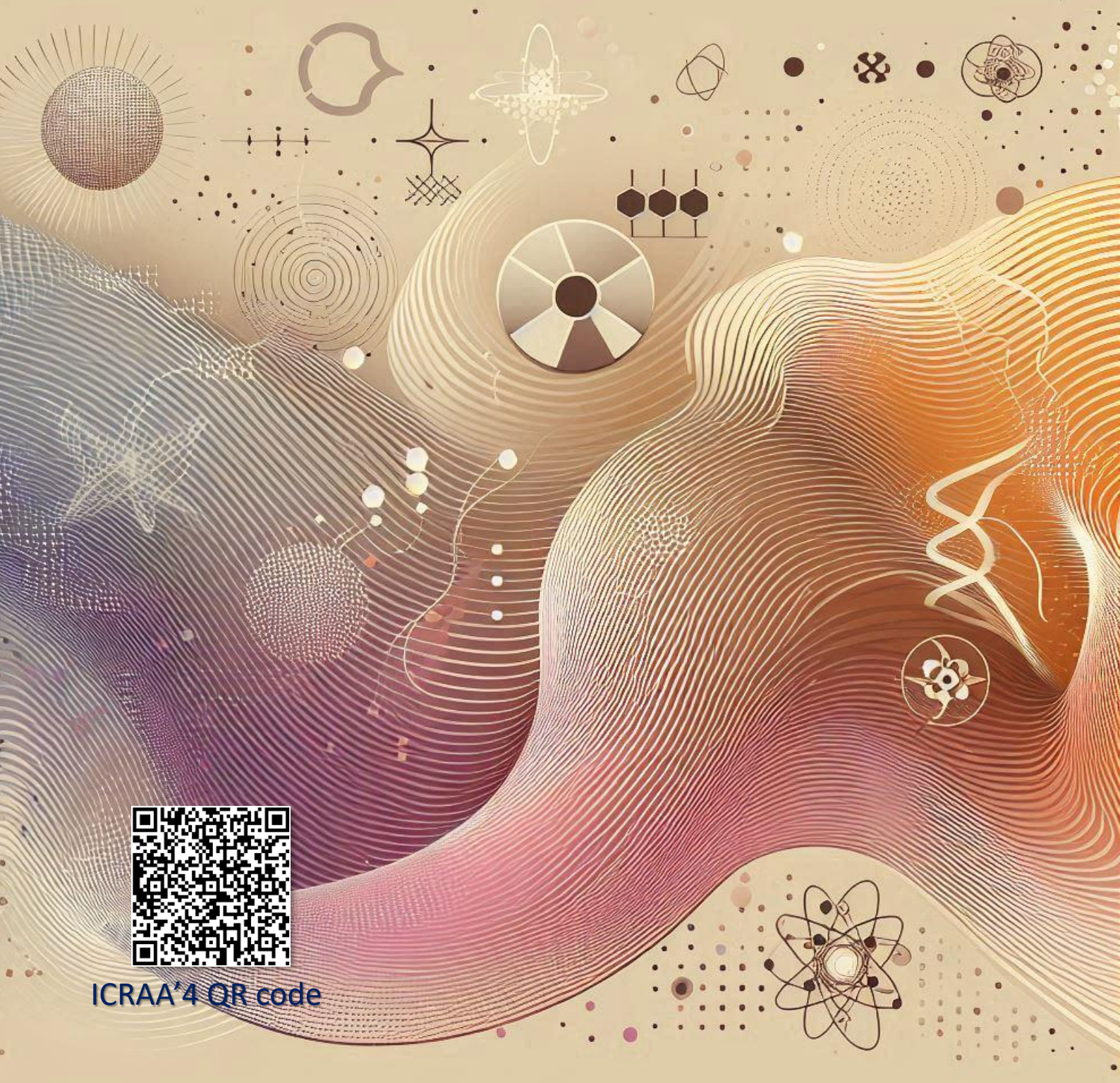

ICRAA’4 QR code